Hydrometeorology of large snowfall and snowmelt events in the Southern Alps of New Zealand

A thesis submitted for the degree of Doctor of Philosophy by

Rasool Porhemmat

School of Earth and Environment

University of Canterbury

"We go to the mountains to experience … how human beings must have felt a hundred thousand years ago, before civilization, governments, social structures, religions, and all the rules that you must follow to be a human." – ***Reinhold Messner***

UNIVERSITY OF CANTERBURY
Te Whare Wānanga o Waitaha
CHRISTCHURCH NEW ZEALAND

Deputy Vice-Chancellor's Office
Postgraduate Office

Co-Authorship Form

This form is to accompany the submission of any thesis that contains research reported in co-authored work that has been published, accepted for publication, or submitted for publication. A copy of this form should be included for each co-authored work that is included in the thesis. Completed forms should be included at the front (after the thesis abstract) of each copy of the thesis submitted for examination and library deposit.

Please indicate the chapter/section/pages of this thesis that are extracted from co-authored work and provide details of the publication or submission from the extract comes:

Chapter 2 is derived from Porhemmat R, Purdie H, Zawar-Reza, P, Zammit, C, and Kerr, T. 2020. The influence of atmospheric circulation patterns during large snowfall events in New Zealand's Southern Alps*. International Journal of Climatology.* DOI: 10.1002/joc.6966

Please detail the nature and extent (%) of contribution by the candidate:

The candidate was heavily involved in collecting data from different sources. He conducted the analysis, and led the publication of the results. All co-authors have given supervisory guidance and comments to improve the paper.

Candidate contribution ~90%

Certification by Co-authors:

If there is more than one co-author then a single co-author can sign on behalf of all

The undersigned certifies that:

- The above statement correctly reflects the nature and extent of the PhD candidate's contribution to this co-authored work
- In cases where the candidate was the lead author of the co-authored work he or she wrote the text

Name: Heather Purdie Signature: HPurdie Date: 28/08/2020

UNIVERSITY OF CANTERBURY
Te Whare Wānanga o Waitaha
CHRISTCHURCH NEW ZEALAND

Deputy Vice-Chancellor's Office
Postgraduate Office

Co-Authorship Form

This form is to accompany the submission of any thesis that contains research reported in co-authored work that has been published, accepted for publication, or submitted for publication. A copy of this form should be included for each co-authored work that is included in the thesis. Completed forms should be included at the front (after the thesis abstract) of each copy of the thesis submitted for examination and library deposit.

Please indicate the chapter/section/pages of this thesis that are extracted from co-authored work and provide details of the publication or submission from the extract comes:

Chapter 3 is derived from Porhemmat R, Purdie H, Zawar-Reza P, Zammit C., and Kerr T. 2020. Moisture transport during large snowfall events in the New Zealand Southern Alps: The role of atmospheric rivers. *Journal of Hydrometeorology*. DOI: 10.1175/JHM-D-20-0044.1

Please detail the nature and extent (%) of contribution by the candidate:

The candidate was heavily involved in collecting data from different sources. He conducted the analysis, and led the publication of the results. All co-authors have given supervisory guidance and comments to improve the paper.

Candidate contribution ~90%

Certification by Co-authors:

If there is more than one co-author then a single co-author can sign on behalf of all

The undersigned certifies that:

- The above statement correctly reflects the nature and extent of the PhD candidate's contribution to this co-authored work
  In cases where the candidate was the lead author of the co-authored work he or she wrote the text

Name: Heather Purdie Signature: HPurdie Date: 28/08/2020

Abstract

Seasonal snowpack is an important element of mountain cryosphere. In the New Zealand's Southern Alps/ Kā Tiritiri o te Moana, seasonal snow cover is of socio economic importance because of its key role in energy, agriculture and tourism sectors. Despite the extensive snow cover in such alpine regions, the knowledge of the snow processes such as large snowfall and snowmelt events is limited. Large snowfall and snowmelt events are a result of atmospheric circulation patterns that influence moisture transfers and surface climate in mountain regions. However, analysis of the relationship between large snowfall and snowmelt events and atmospheric forcing in alpine regions has remained a challenge mainly due to the scarcity of climate observations and snow measurements at higher altitudes. A better understanding of the synoptic-scale weather patterns can provide an insight into the distinct characteristics of atmospheric forcing impacting snow accumulation and snowmelt processes, especially in remote mountain regions. Therefore, the primary aim of this dissertation is to improve the understanding of synoptic-scale atmospheric forcing during large snowfall and snowmelt events in alpine regions.

The New Zealand Southern Alps, surrounded by the Pacific Ocean and in the path of the westerly air flows represent a typical maritime environment, making them an ideal location for the study of alpine snow processes. To explore the synoptic climatology of large snowfall and snowmelt events, the 90th percentile value of daily snowfall (snowmelt) from three automatic weather stations (AWS) across the Southern Alps was used. A composite anomaly approach using reanalysis atmospheric data (i.e. sea level pressure, temperature and geopotential heights) was applied to characterize the main synoptic-scale hydrometerological conditions associated with these events. Additionally, an analysis of integrated vapour transport (IVT) was conducted in order to learn more about the moisture transport characteristics of precipitation during large snowfall and major snowmelt events associated with rain on snow (ROS). The application of IVT fields allowed to identify the distinct characteristics of moisture transports and the potential role of atmospheric rivers (ARs) in transferring moisture across the Tasman Sea towards the Southern Alps.

Large snowfall events were found to account for 20-40% of total annual snow accumulation. Synoptic-scale atmospheric patterns influence the variability in timing and magnitude of large snowfall and snowmelt events. Weather patterns during large snowfall events in the Southern Alps are mainly characterised by strong negative anomalies of sea level pressure (SLP) and geopotential heights at 500 hPa (Z500) located over the southwest of New Zealand's South Island. However, over the New Zealand region, the days leading to large snowfall events experienced positive anomalies of Z500 accompanied by positive anomalies of low-tropospheric temperatures (850 hPa and 1000 hPa). These positive anomalies were associated with the passage of relatively warm airflows over the Tasman Sea and across the Southern Alps. Troughing regimes were

found to account for ~78% of large snowfall events. Large snowmelt events, however, were found to take place during both high pressure systems and troughing regimes, with the majority of rapid snowmelt events (~80%) occurring during high pressure systems with anomalously high temperatures. Observations of snowmelt at Mueller Hut revealed that even though snowmelt mostly occurs during spring, considerable melt (~300 mm day^{-1}) can also occur during winter month. These significant winter-melt events were found to be associated with rain-on-snow events. Anomalies of temperature revealed rising mid- and low-tropospheric temperatures (at 500, 700 and 850 hPa) during both high-pressure and troughing systems associated with large snowmelt events.

Atmospheric rivers making landfall in the Southern Alps were found to impact the seasonal snowpacks in two ways. Firstly, they produce large snowfall events and secondly, they generate major spring- and winter-time rain-on-snow (ROS) events. While ARs accounted for majority of large snowfall events across the Southern Alps (~70%), they were also responsible for nine out of ten largest ROS events identified at Mueller Hut station near the Main Divide of the Southern Alps. Similar hydrometeorological characteristics (e.g. duration and shape) were identified for both rain-producing and snow-generating ARs; however, in terms of strength, the former were found to contain higher IVT values over the Southern Alps (up to ~822 kg m^{-1} s^{-1}). AR-related ROS events were characterised by anomalously high temperatures, high advection of warm airflows and rising freezing level resulting in warm environments over the snowpacks, with air temperatures as high as ~10 °C, creating ideal conditions for rapid snowmelt at higher altitudes. The results of this study have improved the current knowledge of the hydrometeorological characteristics of snow processes in a mid-latitude maritime climate. Considering the high sensitivity of seasonal snowpacks in maritime environments to changes in atmospheric variables, the findings will contribute to the research into further quantifying the impacts of climate change on atmospheric circulation patterns as well as the timing and frequency of rain- and snow-producing ARs in such regions.

To my amazing family my parents, my brothers and my sister

دلم یک زمستان سخت میخواهد
یک برف
یک کولاک به وسعت تاریخ
که ببارد و تمام راهها بسته شوند
و توچاره ای جز ماندن نداشته باشی
و بمانی ...

Acknowledgement

A great number of people deserve my appreciation for their assistance in the completion of my thesis. My deep gratitude goes first to my supervisory team. I would like to gratefully acknowledge my primary supervisor Dr. Heather Purdie, who guided me through this PhD journey with continuing source of positive energy and enthusiasm. Her patience, motivation, and immense support helped me in all the time of research and writing of this thesis. Secondly, I am very much indebted to my co-supervisor, Professor Peyman Zawar-Reza for his valuable guidance, constructive recommendations and an open door policy. I thank Dr. Tim Kerr, with whom I had numerous dissuasions about various topics. Those conversations were vital in inspiring me to think outside the box. I would also like to thank Dr. Christin Zammit for providing constant help and support and being extremely critical at times, yet always available for advice.

This study was made possible by the financial support of UC Doctoral Scholarship. I am very grateful to the staff of the School of Earth and Environment for providing academic and technical support and amazing environment for post graduate studies. I would like to specifically thank John Thyne, Bridget Ginley, Kathy Hogarth, John Southward, Andrew Sturman, Marwan Katurji, Justin Harrison, Rob Spiers, Paul Bealing, NicK Key and Janet Warburton. I appreciate the provision of data by the National Institute of Water and Atmospheric Research (NIWA), the West Coast Regional Council and Meridian Energy. In particular, I am deeply thankful to Kathy Walter who has been always a great help providing data only minutes after receiving my requests.

I would like to express my sincere appreciation to my fellow PhD candidates who all have become close friends throughout my time in Christchurch. They introduced me to so many beautiful cultures from different parts of the world and surely proved friendship knows no borders. All those wonderful memories with many moments of laughter will stay with me forever. Kia ora koutou to all of you:

Dhan'yabāda **Wali** and **Rajeshwata**, Trimakasih the Indonesian gang **Trias**, **Berton**, **Aditya**, **Adam** and **Ririn**, Arigato **Daisuke**, Gua zhen che **Dorji**, Cam on **Huong**, Xie xie **Jaiwei**, **Anmeng** and **Ting Ting**, Danke **Benjamin**, Dhan'yavāda **Santosh**, Thank You **Romy, Nick, Sarah**, **Hamish**, **Jessie**, **Alison**, and **Levi**, Salamat **David**, Gracias **Julia**, **Rodrigo**, **Carlos, Pedro** and **Adlin**, Tashakor (تشکر) **Sulaiman jan** and Merci **Gilles** and **Arthur**.

Thank you to all my soccer teammates (UNISOL boys), climbing buddies and fellow mountain goats for their consistent companionship that helped me stay in good mental and physical health throughout the ups and downs of PhD. I especially thank my true friend, Arman, whose genuine friendship during the completion of my thesis was invaluable.

Most importantly, I would like to express my grateful thanks to my family for their continuous support and unparalleled love. There are no proper words to show how much I am grateful to my mother, Aghdas, whose endless kindness and prayers have been always with me despite the distance. My father, Jahangir, has been always a mentor and a close friend, whose value to me only grows with age. My brothers, Mojtaba and Mohammad Sadeq and my sister, Zahra, deserve my deepest appreciation for their love and support.

Table of Contents

Table of Contents

List of Figures

List of Tables

List of Symbols and Abbreviations

AR	atmospheric river
AWS	automatic weather stations
C	centigrade
CLWC	specific cloud liquid water content
cm	centimetre
ECMWF	European Centre for Medium-Range Weather Forecasts
g	gravitational acceleration
h	hours
hPa	hectopascal
IVT	integrated vapour transport
IWV	integrated water vapour
kg	kilogram
m	meter
mm	millimetre
MODIS	Moderate Resolution Imaging Spectroradiometer
MSLP	Mean Sea Level Pressure
NCAR	National Centre for Atmospheric Research
NCEP	National Centre for Environmental Prediction
NIWA	National Institute of Water & Atmospheric Research
NZST	New Zealand Standard Time
P	precipitation
q	specific humidity
ROS	rain-on-snow
s	second
SD	snow depth
SIN	Snow and Ice Monitoring Network
SLP	sea level pressure
SR50	Sonic Ranger 50
SWE	snow water equivalent
T1000	temperature at 1000 hPa
T850	temperature at 850 hPa
T700	temperature at 700 hPa
T500	temperature at 500 hPa
T_a	air temperature
T_s	snow temperature
u	zonal component of the wind speed
v	meridional component of the wind speed
VCSN	Virtual Climate Station Network
VICFWF	vertical integral of cloud frozen water flux
VICLWF	vertical integral of cloud liquid water flux

W	watt
Z500	geopotential heights at 500 hPa

1 Introduction

1.1 Background

Snow is an important component of the global freshwater supply in the mountain regions (Bales *et al.*, 2006; Fayad *et al.*, 2017; Hock *et al.*, 2019; Shaw *et al.*, 2020) providing water for more than one billion people across the globe (Barnett *et al.*, 2005; Mankin *et al.*, 2015). In the mid-latitude of New Zealand's Southern Alps, a large fraction of the winter precipitation falls in the form of snow, mainly from June to October (Fitzharris *et al.*, 1999). Seasonal snow cover in the Southern Alps directly impacts New Zealand's economy in hydro-electricity, agriculture and tourism sectors (Fitzharris *et al.*, 1999; Clark *et al.*, 2009; Sirguey, 2009; Hendrikx and Hreinsson, 2012; Kerr, 2013). The timing and magnitude of snow accumulation and subsequent melt events largely control hydrological processes in alpine catchments (Bales *et al.*, 2006; Romolo *et al.*, 2006a; Clark *et al.*, 2009; Safeeq *et al.*, 2016; Trubilowicz and Moore, 2017; Suriano, 2019). Among all processes in mountain hydrology, large snowfall and snowmelt events, are of special interest from hydrological and meteorological standpoints because of their impacts on snow-fed rivers with high socio-economic values (Serreze *et al.*, 2001). Large snowfall events increase the volume of snowpacks in a short period of time (Turner *et al.*, 2019). In addition, heavy snowfall events increase the risk of avalanches that can lead to disruptive consequences for people living in those regions (Birkeland and Mock, 1996; Mock and Birkeland, 2000; Esteban *et al.*, 2005; Hendrikx, 2005). Major snowmelt events, on the other hand, can cause flooding events as well as a sudden reduction in snowpack storage and water resource availability in alpine catchments (Bednorz, 2009; Semmens *et al.*, 2013; Guan *et al.*, 2016).

Mid-latitude seasonal snowpacks, such as those in the Southern Alps, are highly sensitive to climate variations (Beniston *et al.*, 2003; Nayak *et al.*, 2010; Gillies *et al.*, 2012; Fayad *et al.*, 2017). Rising global temperatures in a warming climate can bring about

significant changes in magnitude, extent and duration of seasonal snow cover resulting in a shift in hydrological regimes (Barnett *et al.*, 2005; Hendrikx and Hreinsson, 2012; Berghuijs *et al.*, 2014; Beniston *et al.*, 2018; Jobst *et al.*, 2018). Observations across the globe have shown that recent and projected changes in snow cover due to a warmer climate will impact water resources in mountain regions (Clow, 2010; Cohen *et al.*, 2015; Harpold and Brooks, 2018; Hock *et al.*, 2019).

Changes in seasonal cover are attributed to atmospheric conditions during snowfall and snowmelt events (Esteban *et al.*, 2005; Romolo *et al.*, 2006a, 2006b; Bednorz and Wibig, 2015). A number of processes control the atmospheric conditions of seasonal snowpacks at different scales ranging from micro scales to large scales (Figure 1.1) (Romolo *et al.*, 2006a, 2006b). Synoptic-scale weather patterns play a key role in shaping climatological characteristics of snowfall and snowmelt events (Birkeland and Mock, 1996; Neale and Fitzharris, 1997; Esteban *et al.*, 2005; Romolo *et al.*, 2006a; Bednorz, 2011) by controlling climatic parameters such as air temperature, humidity, cloudiness and moisture transport during the days leading to snowfall and snowmelt events. Therefore, synoptic analysis of climate variables has become a popular tool to study the hydrometeorology of mountain catchments (McGinnis, 2000; Yarnal *et al.*, 2001). As the Greek origin of the word “synoptic” meaning “seen together” implies, synoptic climatology aims to provide an overall view of climate conditions during environmental phenomena such as snowfall (Yarnal, 1993).

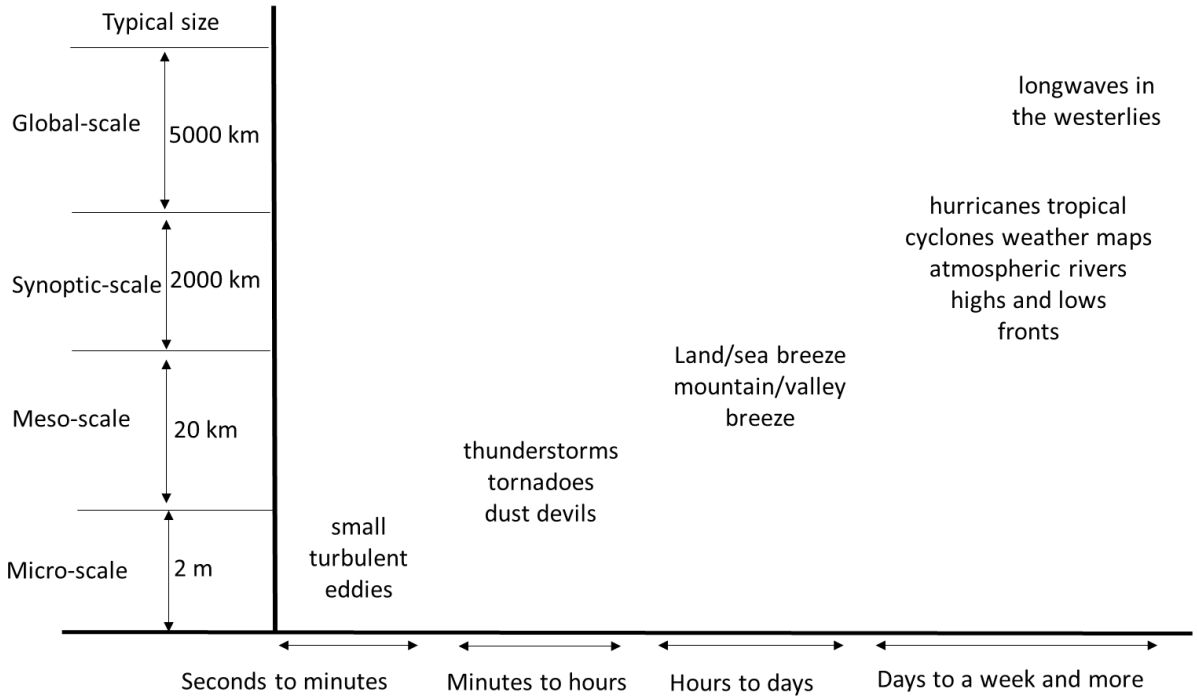

Figure 1.1 Time and space scales of atmospheric motion (reproduced from Sturman and Tapper (2006)).

Studies in snow-dominated regions have shown that the frequency and magnitude of snowfall and snowmelt events are generally concurrent with the occurrence of particular synoptic weather patterns that provide favourable meteorological conditions for such events to occur (Farukh and Yamada, 2014). These patterns have a direct link with temperature and moisture content characteristics in the atmosphere and energy flux over the snowpacks (Romolo *et al.*, 2006a, 2006b; Bednorz, 2013). Providing a thorough assessment of hydrometeorological conditions of snow processes has remained a challenge due to lack of snow observations in most mountain regions across the world. Therefore, regional studies with a focus on investigating the relationship between snow processes in mountain regions and synoptic-scale atmospheric conditions could provide valuable information for a better understanding of physical principles controlling such processes in mountain regions such as the Southern Alps.

In addition to the analysis of synoptic-scale weather patterns influencing snow processes in the mountains, it is important to improve the knowledge of atmospheric moisture flux and moisture pathways. Determination of moisture flux is necessary for

understanding how air characteristics change and how large-scale weather patterns translate to the amount and distribution of seasonal snowpacks (Cann and Friedrich, 2020). In the mid-latitude regions, a large portion of moisture is transported through narrow bands of strong moisture flux, known as atmospheric rivers (ARs), which are responsible for transferring water vapour from subtropics (Ralph *et al.*, 2004; Neiman *et al.*, 2008a; Gimeno *et al.*, 2014). Global studies have shown the frequent occurrence of ARs in the New Zealand region (Paltan *et al.*, 2017; Waliser and Guan, 2017). Yet the atmospheric conditions responsible for landfalling ARs in the Southern Alps remain poorly understood. Pioneering studies have recently highlighted the importance of ARs in major flooding events (Kingston *et al.*, 2016a) and glacier mass balance (Little *et al.*, 2019) across the alpine regions of the South Island. Recent work by Prince (2020) has documented a climatology of ARs in the New Zealand region suggesting a distinct seasonality in the occurrence of ARs controlled by seasonal variations in the mid-latitude jet streams.

Given the current knowledge of the impacts of ARs on seasonal snow cover in the Southern Alps, there is an opportunity to evaluate the role of ARs in moisture transport and energy transfers influencing the seasonal snowpacks in the Southern Alps. Atmospheric conditions associated with ARs can impact snow processes in two ways: firstly, by producing large snowfall events due to their high moisture flux (Guan *et al.*, 2010, 2012, 2013; Huning *et al.*, 2019), and secondly, because of their warmer temperatures resulting in more rain-on-snow events (ROS) compared to other winter storms (Rössler *et al.*, 2014; Guan *et al.*, 2016). Globally, research has focused on hydrological impacts of ARs with respect to heavy rain and flooding (see section 3.1 and 5.1), with less attention paid to the impacts of ARs on snow hydrology. The contributions of ARs to snowfall events has been documented in the mountain regions of North America (Guan *et al.*, 2010, 2013; Demaria *et al.*, 2017), Antarctica (Gorodetskaya *et al.*, 2014) and South American Andes (Viale *et al.*, 2018; Saavedra *et al.*, 2020). Considering the high

frequency of landfalling ARs at mid-latitudes between 38° and 50° (Saavedra *et al.*, 2020), it is, therefore, important to identify and understand their role in transferring moisture towards Southern Alps during the weather conditions impacting the seasonal snowpacks (e.g. snowfall and ROS).

1.2 The Southern Alps/ Kā Tiritiri o te Moana

The Southern Alps / Kā Tiritiri o te Moana are the highest mountain range in Australasia with the highest peak being Mount Cook / Aoraki (3724 m). With 26 mountain peaks over 3000 m in elevation, the Southern Alps (Figure 1.2a) extend along much of the length of New Zealand's South Island / Te Wai Pounamu (Figure 1.2b). The circumpolar westerly airflows are important factors in controlling the climate of the South Island (Sturman and Tapper, 2006). Perpendicular to the prevailing westerly air currents, the Southern Alps play an important role in perturbing airflows leading to blocking and rerouting of atmospheric flows and the formation of eddies and lee troughs (Sturman and Tapper, 2006). They are also main drivers of the characteristic synoptic features of the South Island (e.g. orographic precipitating enhancement, effects on weather fronts, etc.). Due to the proximity of the Southern Alps to the oceans, the regional climate of the Southern Alps has been characterized by a maritime-type climate (Sturman and Tapper, 2006) where the general circulation patterns over the South Pacific Ocean strongly influence the surface environmental events such as precipitation (Wratt *et al.*, 1996; Kingston and McMecking, 2015a). Average annual precipitation is highly variable across the South Island (Figure 1.2c) ranging from less than 1,000 mm $year^{-1}$ in the eastern parts to over 10,000 mm $year^{-1}$ near the Main Divide (Henderson and Thosmson, 1999; Kerr, 2011).

The Southern Alps' snowpacks provide an opportunity for studying snow processes in a typical maritime condition where snow usually covers 35% of the South Island before the beginning of the melt season (Fitzharris *et al.*, 1999). Similar to mid-latitude maritime environments such as western United States, Mediterranean regions, and Andes (Bales *et*

al., 2006; Viale and Nuñez, 2011; Fayad *et al.*, 2017), snowpacks in the Southern Alps experience frequent days with above freezing level temperatures and snow can accumulates at temperatures close to 0 °C (Purdie *et al.*, 2011). The frequent occurrence of rainfall events during the winter months is another important feature in characterizing the alpine hydrology of such environments (Prowse, 1981a; Moore and Owens, 1984).

New Zealand's South Island has around 40 major river systems, most of which originate from glaciated and snow-dominated terrains of the Southern Alps (Figure 1.2a). The role of seasonal snow cover in the economy of New Zealand has been recognized because of its important contribution to hydroelectricity schemes (Thompson, 2002) where snowmelt is estimated to account for up to 24% of the inflows to the major hydroelectricity lakes (McKerchar *et al.*, 1998). New Zealand relies heavily on hydropower which accounts for 60% of the total national electricity generation. On a national scale, approximately 65% of hydroelectricity is generated by South Island's hydroelectric plants highlighting the importance of rivers originating from the upper terrains of the Southern Alps. Alpine rivers of the Southern Alps are also water sources for irrigation schemes in the South Island. Meltwater from seasonal snowpacks can contribute up to 40-50% of the discharge in upper alpine catchments feeding major rivers in the Southern Alps (Fitzharris and Garr, 1995; Sirguey, 2009). Few studies documenting the importance of seasonal snow in the hydrology of the Southern Alps (McKerchar *et al.*, 1998; Sirguey, 2009; Kerr *et al.*, 2013; Jobst, 2016) have shown that even though the contribution of snowmelt to river flows is lower compared to alpine catchments in the European Alps (Penna *et al.*, 2016; Beniston *et al.*, 2018), western United States (Bales *et al.*, 2006) and Himalayan (Siderius *et al.*, 2013; Bharati *et al.*, 2014; Adnan *et al.*, 2017), the proportion of melt during spring is an important component of the water budget in alpine catchments. The seasonal contribution of snow to melt is expected to be a controlling factor especially during drought periods where the annual rain is below the normal values (Kerr, 2013; Sirguey, 2009).

Seasonal snow has also high economic significance for ski resorts in New Zealand making the Southern Alps a popular destination for winter sports tourism in the Southern Hemisphere (Hendrikx *et al.*, 2012, 2013). In 2017 alone, a record of 1.6 million skier days were observed in New Zealand ski fields (Ski Areas Association of New Zealand (SAANZ), 2018). Apart from playing a key role in water supply demands and tourism sectors, heavy snowfall events increase the risk of avalanches in the upper terrains of the Southern Alps (Hendrikx, 2005).

Despite the importance of the Southern Alps' seasonal snowpacks for New Zealand's economy, knowledge of atmospheric patterns associated with snow processes has been particularly limited (Neale and Fitzharris, 1997; Fitzharris *et al.*, 1999). The knowledge gap is in part attributable to a limited understanding of the physical processes controlling snow accumulation and snowmelt (Fitzharris *et al.*, 1999; Clark *et al.*, 2009) and a lack of adequately distributed observation networks (Hendrikx and Harper, 2013). Notwithstanding the extensive cover of seasonal snow in the Southern Alps (Clark *et al.*, 2009), prior to 2006, there did not exist a reliable monitoring network to systematically record and observe snow measurements (e.g. snow depth and snow water equivalent) and climate variables (e.g. temperature, humidity, wind etc.) at high altitudes of the Southern Alps.

A new network of high altitude automatic weather stations (AWS), the Snow and Ice Monitoring Network (SIN), was established across New Zealand by the National Institute of Water and Atmospheric Research (NIWA). In addition to typical climate variables recorded at weather stations, the network has been instrumented with ultrasonic depth sensors to monitor the snow depth throughout the year. There is, therefore, a new opportunity to study synoptic controls on snow processes using a larger dataset of snow measurements with a sufficient spatial distribution across the Southern Alps. Considering the importance of seasonal snowpacks in relation to electricity, agriculture and recreation, and the inevitable impacts of climate change on mountain water resources in

the Southern Alps (Poyck *et al.*, 2011; Hendrikx and Hreinsson, 2012; Hendrikx *et al.*, 2012; Jobst, 2016; Jobst *et al.*, 2018), it is, therefore, important to determine the atmospheric controls influencing physical dynamics of snow accumulation and snow ablation processes. The enhanced knowledge of atmospheric characteristics and moisture dynamics during such events will provide important implications for water management strategies in a typical maritime climate.

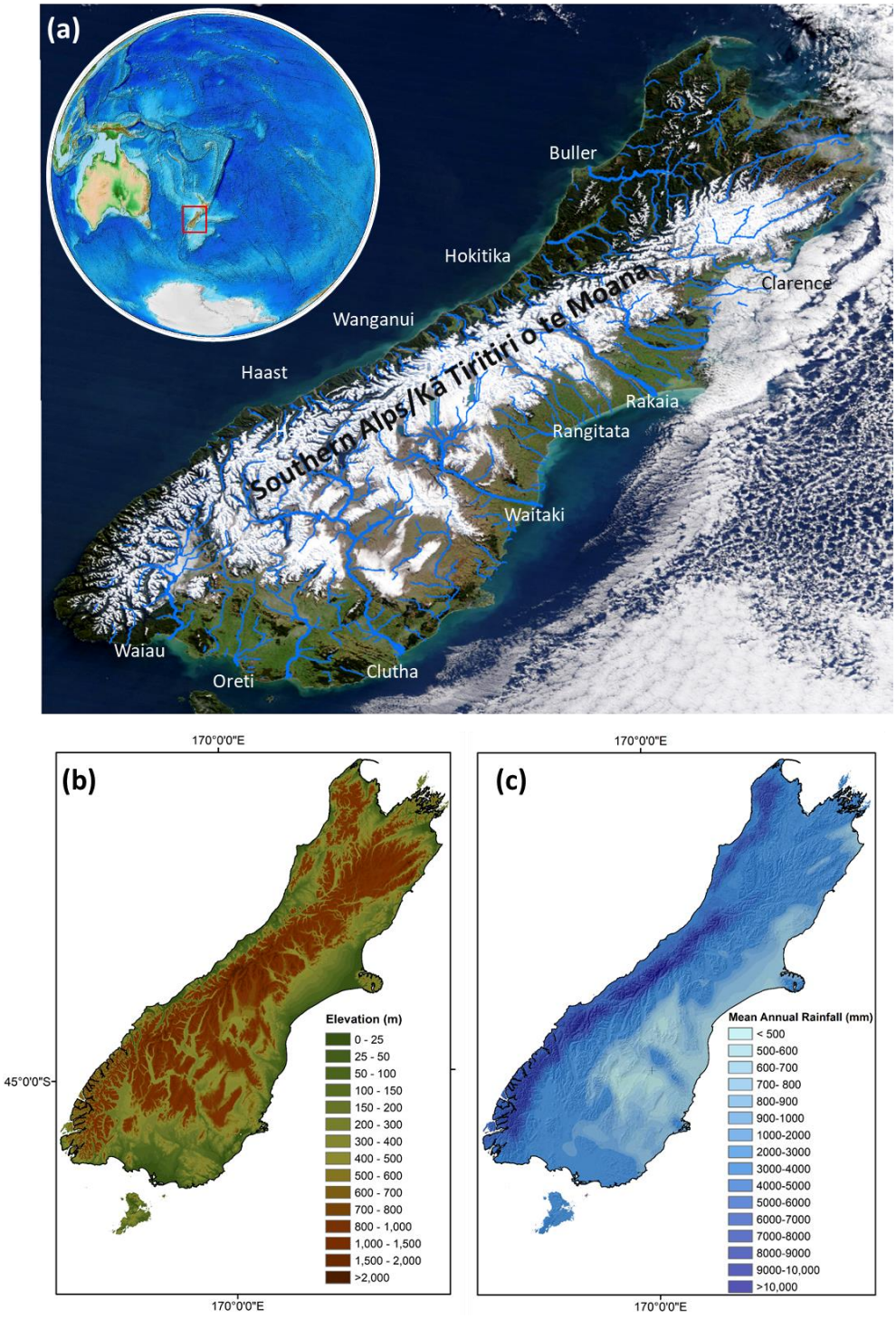

Figure 1.2 (a) Southern Alps / Kā Tiritiri o te Moana and its major rivers (The background image was captured by the Moderate Resolution Imaging Spectroradiometer (MODIS) on the Terra satellite on July 11, 2003), (b) elevation map of South Island, and (c) South Island's mean annual rainfall for years 1972-2016. Annual rainfall is estimated from the daily rainfall estimates of the NIWA's Virtual Climate Station Network (VCSN, Tait *et al.*, 2006).

1.3 Thesis aim

The aim of this thesis is to gain a better understanding of the atmospheric circulation patterns influencing snow processes in the maritime environment of the Southern Alps with a focus on large snowfall and snowmelt events. The specific research questions are:

1. What are the main characteristics of synoptic weather patterns during large snowfall events in the Southern Alps?
2. How does moisture flux change over the South Pacific Ocean across the Tasman Sea during large snowfall events in the Southern Alps?
3. What are the main synoptic weather patterns that influence large snowmelt events?
4. What are the distinctive synoptic-scale characteristics of moisture transport during major rain-on-snow (ROS) events in the Southern Alps?

1.4 Research methods

A full description of the methods utilised for this research can be found in each chapter (see section 2.2, 3.2, 4.2 and 5.2). Therefore, the focus of this section is to provide readers with a brief overview of the methods applied.

- **Identification of large snowfall and snowmelt events**

Firstly, direct observations of snow depth recorded at high altitude SIN weather stations across the Southern Alps are used to identify daily changes in snow depth. Increasing/decreasing values indicate snowfall/snowmelt events and the 90th percentile value of daily snowfall (snowmelt) is used to select days with large snowfall (snowmelt) events. For analysing snowfall events measurements from three SIN sites, namely Mahanga, Mueller Hut and Mt Larkins were used. These three sites are spatially distributed across the length of the Southern Alps. For snowmelt events the data recorded at Mueller Hut was used because of the consistency of a longer dataset of snowmelt events at this location.

- **Environment-to-circulation approach: Composite anomaly maps**

The second approach is based on an environment-to-circulation approach. An environment-to-circulation approach links surface environmental events to climate variables and atmospheric circulation patterns in contrast to a circulation-to-environment approach, in which specific atmospheric circulation patterns are related to an specific event (Yarnell *et al.*, 2010). Analysing the relationship between synoptic-scale atmospheric conditions and surface environmental events (e.g. droughts, cyclones, snowfall and snowmelt) has proven to be a useful tool in hydrometeorological studies (Dayan *et al.*, 2012; Schoof, 2013). Here synoptic-scale composite anomalies are used to learn more about atmospheric conditions during large snowfall and snowmelt events. Analysis of anomaly maps of mid- and low-tropospheric climate variables has a long history in identifying the meteorological and climatological characteristics of weather events (Yarnal, 1993; Yarnal *et al.*, 2001). In this research, climate variables during large snowfall and snowmelt events are compared to the 40-year average climatic normals (long-term average of 1979-2018). The atmospheric fields are ERA-Interim Reanalysis data from the European Centre for Medium-Range Weather Forecasts (ECMWF, Dee *et al.*, 2011). ERA-Interim provides global 6-hourly estimates of atmospheric variables with spatially and temporally complete dataset available back to 1979.

- **Moisture flux characterization**

The third methodology utilises the concept of integrated vapour transport (IVT) to quantify the magnitude of moisture flux from the Tasman Sea to the Southern Alps during large snowfall events and major ROS events. Integrated vapour transport is a measure of horizontal transport in the atmosphere (Rutz *et al.*, 2014b) and has a close link with precipitation in mountainous regions (Waliser and Guan, 2017; Young *et al.*, 2017). Using an AR identification method (3.2) IVT values are used to investigate the association of landfalling ARs and the selected snowfall and ROS events in the Southern Alps.

1.5 Thesis structure

This thesis is divided into 6 chapters. Following this introduction (chapter 1), chapters 2-5 each addresses one of the four main research questions. Summaries of the work packages that are required to address the main research questions are given in Figure 1.3 and Figure 1.4.

Chapter 2 tackles question 1 and begins with a review of synoptic climatology of snowfall events and introduces the methods used to identify large snowfall events at three weather stations (Mahanga, Mueller Hut and Mt Larkins). The synoptic characteristics of these events are identified using anomaly maps of sea level pressure, geopotential heights and temperature. The findings presented in this chapter have been published in International Journal of Climatology.

Porhemmat, R., Purdie, H., Zawar-Reza, P. Zammit, C., Kerr, T. (submitted). The influence of atmospheric circulation patterns during large snowfall events in New Zealand' Southern Alps, *International Journal of Climatology*. https://doi.org/10.1002/joc.6966.

Chapter 3 addresses the research question 2 by evaluating the moisture transport associated with large snowfall events with a primary focus on the role of ARs in producing large snowfall events in the Southern Alps. Following an introduction about the hydrometeorological impacts of ARs in mountain regions the characteristics of moisture transport during large snowfall events in the Southern Alps are explored using integrated vapour transport (IVT) fields. The findings presented in this chapter have been published in the Journal of Hydrometeorology:

Porhemmat, R., Purdie, H., Zawar-Reza, P. Zammit, C., Kerr, T. (submitted). Moisture transport during large snowfall events in the New Zealand Southern Alps: The role of atmospheric rivers, *Journal of Hydrometeorology*. *https://doi.org/10.1175/JHM-D-20-0044.1*.

Chapter 4 addresses the research question 3 by identifying the synoptic characteristics of the days with large snowmelt events near the Main Divide. Similar to the approach adopted in chapter 2, a synoptic-scale characterisation of atmospheric variables (sea level pressure and temperature) during snowmelt events are obtained by application of anomaly maps during the days with large snowmelt events relative to the long-term averages.

Chapter 5, analyses moisture transport during major rain-on-snow (ROS) events near the main Divide of the Southern Alps. Similar to the approach adopted in chapter 3, the IVT values are chosen to identify the relationship between ROS and ARs (5.2). Case studies are utilises to describe the main characteristics of moisture transport associated ROS over the seasonal snowpack.

Finally, chapter 6 revisits the research questions and demonstrates how they have been addressed. The main conclusions drawn from findings, their implications and a direction for future research are presented.

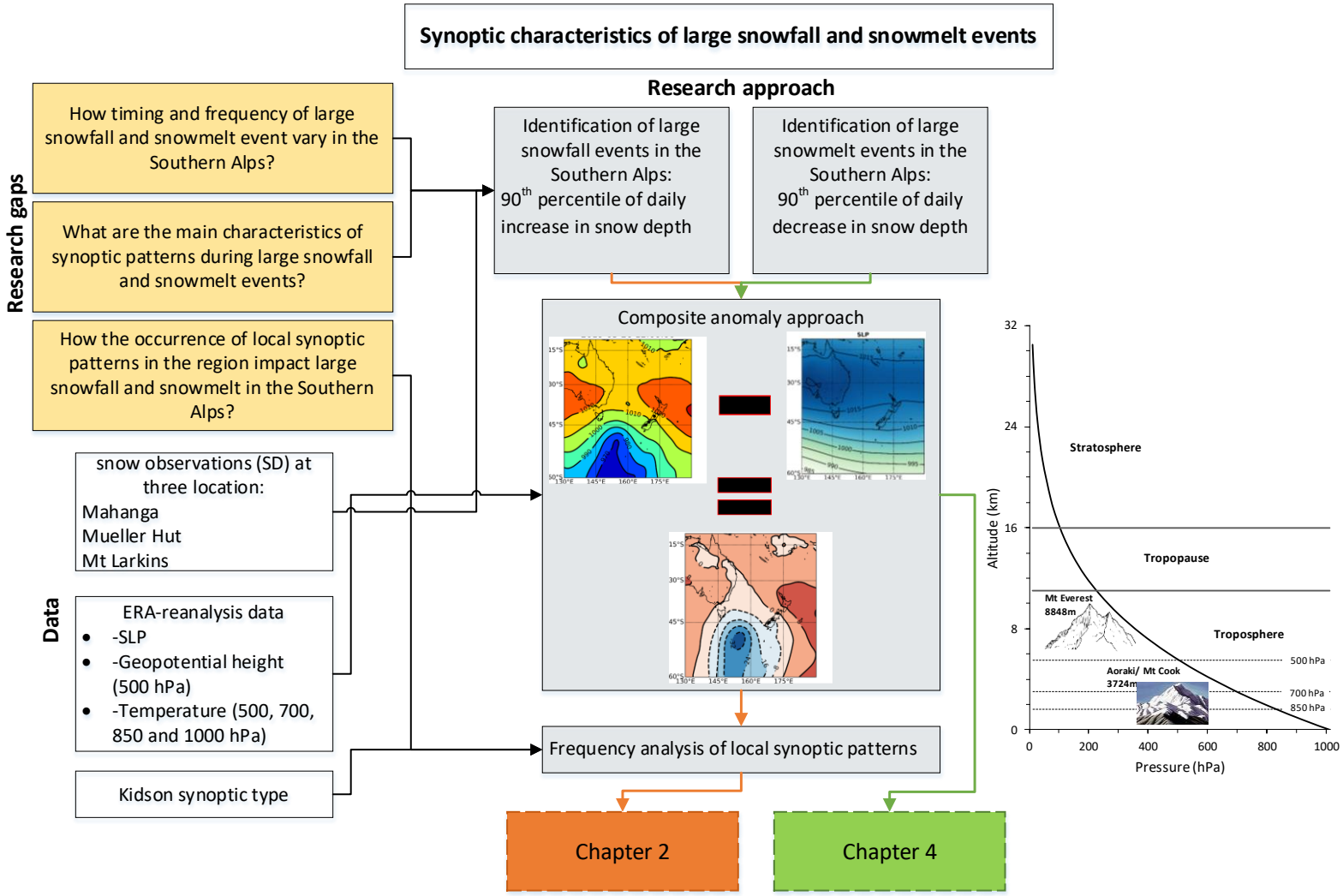

Figure 1.3 Synoptic climatology of large snowfall (Chapter 2) and snowmelt (Chapter 4) events.

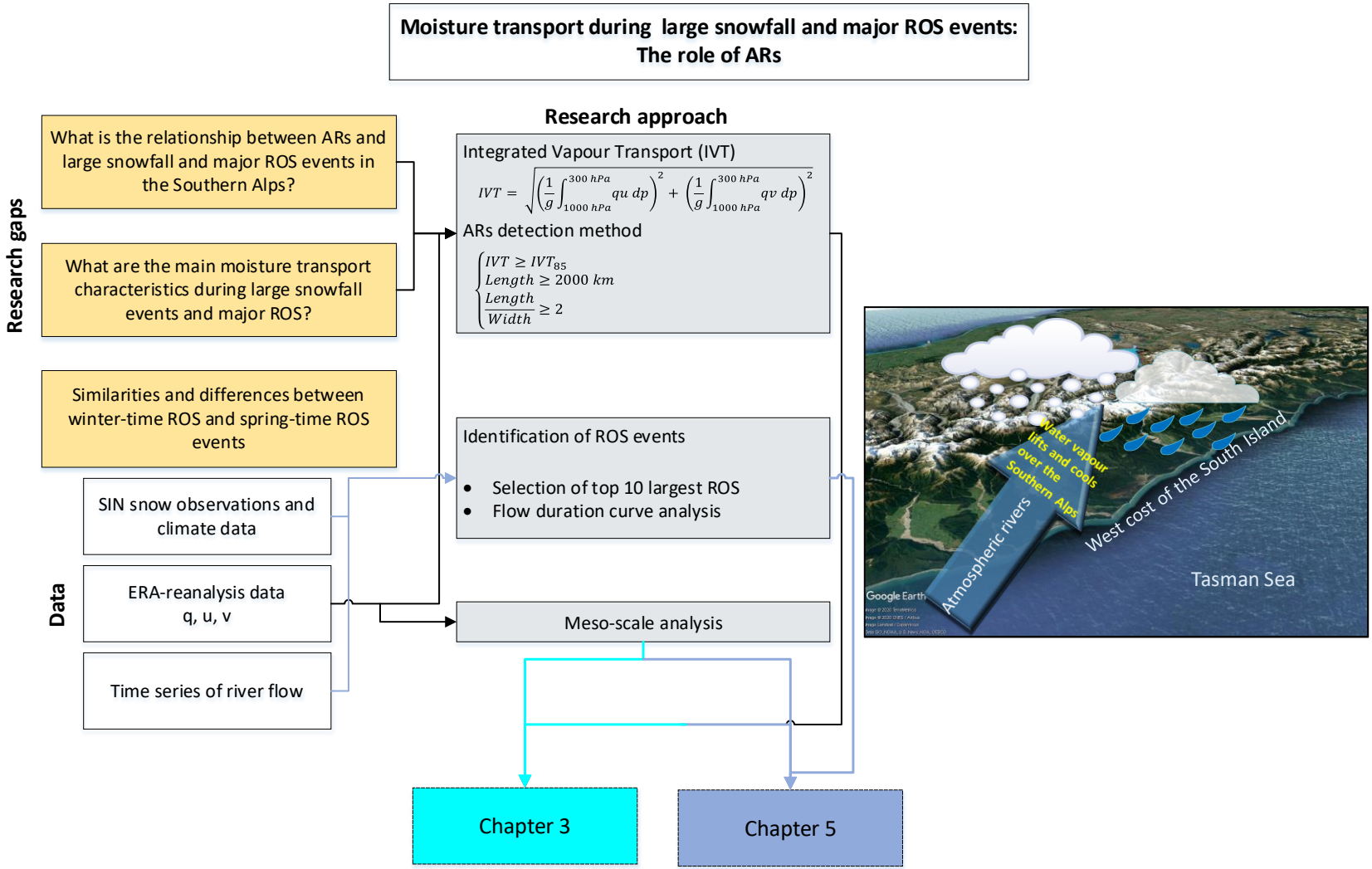

Figure 1.4 Moisture transport during large snowfall (Chapter 3) and ROS (Chapter 5) events.

2 The influence of atmospheric circulation patterns during large snowfall events in New Zealand's Southern Alps

Abstract

Large snowfall events contribute significantly to total annual snow accumulation across the maritime Southern Alps. However, the knowledge about atmospheric circulation patterns associated with large snowfall events over the New Zealand Southern Alps is very limited. In this chapter, Daily snow observation data from three automatic weather stations and ERA-Interim reanalysis data were used to investigate the relationship between atmospheric forcing and large snowfall events across the Southern Alps. To do so, analysis of composite anomaly maps during large snowfall events were carried out to identify the common features of the days with heavy snow accumulation. Large snowfall across the Southern Alps were mainly associated with strong negative anomalies of sea level pressure (SLP) located over the southwest of New Zealand's South Island. These conditions were concurrent with negative anomalies of geopotential heights at 500 (Z500) located in the centre of low pressure systems. However, over New Zealand, days leading to large snowfall events experience positive anomalies of Z500 showing a relatively warm environment during such events in the maritime Southern Alps. Positive anomalies of low-tropospheric temperatures (850 hPa and 1000 hPa) over the Tasman Sea and across the Southern Alps as well as high frequency of local synoptic patterns associated with troughing regimes (~78%) during large snowfall events provide more evidence of the important contribution of warm air flows originating from tropics.

2.1 Introduction

Snow in the mountains is a natural water reservoir providing water for over one billion people across the globe (Barnett, et al., 2005; Mankin et al., 2015). Winter precipitation in solid form is one of the main component of mountain climatology in alpine catchments. Numerous studies show that a small number of large (extreme) events can dominate the total seasonal snowpack in snowfall-dominated regions, leading to an increase of river flow during the melt season (Serreze *et al.*, 2001; Kumar *et al.*, 2012; Lute and Abatzoglou, 2014). For instance, in the western United States, large snowfall events have been found to account for up to 38% of annual snowfall water equivalent (Lute and Abatzoglou,

2014). New findings in Antarctica have revealed that the largest 10% of snowfall events contribute to 40-60% of annual snow accumulation (Turner *et al.*, 2019). Given the importance of large snowfall events in snow-dominated regions, it is, therefore, necessary to better understand the processes that lead to such events.

Daily snowfall characteristics and their associated conditions such as temperature, humidity and cloudiness are largely controlled by atmospheric circulation (Birkeland and Mock, 1996; Mock, 1996; Bednorz, 2011; Bednorz and Wibig, 2017). Also, in a warming climate, with a shift in precipitation form from snow-dominated to rain-dominated regimes (IPCC, 2013; Berghuijs *et al.*, 2014), a robust understanding of climate controls on snow accumulation in alpine catchments is necessary for quantifying ramifications of climate change. Exploring the relationship between climatological phenomena such as snowfall events and atmospheric circulation is, therefore, essential for identifying the current climate characteristics of large snowfall events and the potential impacts of climate change in the future.

A number of processes control the formation of snow in the atmosphere at a variety of scales of motion. Investigation of the processes at different scales from microscale to large scale has provided valuable insights on the climate forcing controlling snowfall events in different parts of the globe (Romolo *et al.*, 2006a). Synoptic patterns, which help identify relationships between the larger scale atmospheric circulation and the smaller scale surface environment, have been a popular tool to study the hydrometeorology of mountain catchments (McGinnis, 2000; Yarnal *et al.*, 2001). At synoptic scales, atmospheric processes (e.g. mid-latitude cyclones, hurricanes, frontal passage and the passage of upper-level disturbances) occur over areas in the order of 1000 km and last for several days. Such processes are typically associated with the horizontal scale of mid-latitude depressions.

Synoptic scale processes determine climatological and meteorological conditions at local and regional scales (Yarnal, 1993; Romolo *et al.*, 2006a; Sturman and Tapper, 2006). The relationship between synoptic scale processes and snowfall events have been well

documented in north America (Birkeland and Mock, 1996; Mock and Birkeland, 2000; Romolo et al., 2006), Japan (Tachibana, 1995; Ikeda *et al.*, 2009; Farukh and Yamada, 2014), European Alps (Spreitzhofer, 1999; Scherrer et al., 2004), central Europe (Bednorz, 2009, 2013; Putniković et al., 2016), the Iberian Peninsula (López-Moreno and Vicente-Serrano, 2007; García-Sellés *et al.*, 2010; Merino *et al.*, 2014; Mora *et al.*, 2016), Himalayas (Simon Wang *et al.*, 2015), the Antarctic continent (Gorodetskaya *et al.*, 2014) and Andes (Masiokas *et al.*, 2006; Garreaud, 2009; Viale and Nuñez, 2011; Stehr and Aguayo, 2017).

The inter-relationship of pressure and temperature fields is the main controlling factor of synoptic conditions during the snowfall. Most of these studies are based on an environment-to-circulation approach (Yarnal, 1993), where the atmospheric circulation patterns (e.g. pressure and temperature fields) controlling snowfall events are investigated (Esteban et al., 2005; Romoloet al., 2006). A popular tool to relate the surface environment and atmospheric circulation is the use of composite anomaly maps. The application of composite anomaly maps to investigate atmospheric trends and conditions during snowstorms is reasonably well documented. For example, in Bridger Bowl, located in Montana, United States, Birkeland and Mock (1996) used anomaly maps of 500 hPa heights to study the synoptic patterns associated with abnormal heavy snowfall events (daily snowfall events more than 32.8 cm). Analysis of composite anomaly maps of sea level pressure and temperature has been used to examine the circulation pattern leading to large snowfall events (e.g. Esteban et al., 2005; Bednorz, 2011; Farukh and Yamada, 2014; Bednorz and Wibig, 2017).

New Zealand Southern Alps' glaciers and snowfields are the largest in the Southern Hemisphere outside Antarctica and South America (Fitzharris et al., 1999). Estimations have shown that seasonal snow usually covers approximately 35% of the South Island in early spring (Fitzharris *et al.*, 1999; Clark *et al.*, 2009). The alpine rivers in the Southern Alps provide inflows to South Island largest lakes which are critical for power generation (Thompson, 2002). They also provide water for irrigation, especially during drought

periods (Kerr, 2013; Sirguey, 2009). The proximity of the Southern Alps to the oceans results in maritime conditions where winters are generally mild, so any increase in temperature due to climate change would impact the amount of water stored in the seasonal snowpack (Hendrikx et al., 2012; Hendrikx et al., 2013; Jobst et al., 2018; Jobst, 2016; Poyck et al., 2011).

Despite the essential role of seasonal snow as an important water reservoir in the region, less attention has been paid to atmospheric controls of seasonal snow accumulation. Synoptic climatology has been found to have a large impact on hydrometeorology of the Southern Alps (Neale and Fitzharris, 1997; Purdie *et al.*, 2011; Webster *et al.*, 2015; Little *et al.*, 2019). It is known that the north-westerly circulation is a key contributor for providing moisture and intense precipitation over the Southern Alps (Kingston & McMecking, 2015; Kingston et al., 2016; Little et al., 2019; Purdie et al., 2011; Salinger & Mullan, 1999). Studies on snow accumulation over glaciers on both west and east side of the Southern Alps (Franz Josef, Tasman and Brewster glaciers) highlighted the important role of local synoptic patterns during the snowfall events (Purdie *et al.*, 2011; Cullen *et al.*, 2019; Little *et al.*, 2019). The local synoptic types in New Zealand known as Kidson types (Kidson, 1994, 2000; Renwick, 2011), have been used to describe the synoptic-scale atmospheric patterns associated with snow accumulation over glaciers. Findings of these studies show that the majority of winter snowfall events coincide with troughing regimes (Purdie *et al.*, 2011; Cullen *et al.*, 2019). Despite short-term observations, these site-specific studies have provided basic knowledge about general weather patterns of snowfall accumulation in the Southern Alps. The information about characteristics of atmospheric circulation prior and during large snowfall events is believed to provide new insights into the climatology of large snowfall events in the region.

The aim of this chapter is to provide further knowledge of large scale circulation that defines atmospheric conditions associated with large snowfall events in the maritime Southern Alps. Snow observations from three automatic weather stations (AWS) across

the Southern Alps (Mahanga, Mueller Hut and Mount Larkins) are used to identify large snowfall events (Figure 2.1). To analyse the synoptic conditions leading to these large events, anomaly maps of sea level pressure (SLP), geopotential height at 500 hPa (Z500), and temperatures at 500, 850 and 1000 hPa (T500, T850 and T1000) are examined prior and during the snowfall days. In order to find the dominant weather types associated with large snowfall events across the Southern Alps analysis of relationships between the events and the frequency of local synoptic patterns (Kidson, 2000) will be conducted.

2.2 Data and Methodology

2.2.1 Study Site

The South Island of New Zealand spans latitudes 41° S to 47° S and is dominated by the Southern Alps (Figure 2.1). The Southern Alps are a northeast to southwest-trending mountain range along much of the South Island rising to over 3000 m a.s.l. with distinctive maritime influence. The circumpolar westerly flow is the dominant feature of the Southern Hemisphere meteorology which significantly influence New Zealand weather and climate (Sturman and Tapper, 2006; Ummenhofer and England, 2007). The distribution of precipitation in the South Island of New Zealand is influenced by the presence of the Southern Alps. Precipitation of the South Island shows a significant spatial variation from 4000 mm $year^{-1}$ on the west coast, up to 15000 mm $year^{-1}$ to 500 mm $year^{-1}$ in the rain shadow regions to the east (Kerr, 2011).

Snow hydrology processes (e.g. snow accumulation and snowmelt) are important hydrological processes in alpine catchments of the Southern Alps. A seasonal snowline of 1000 m has been reported for different parts of the South Island (Fitzharris *et al.*, 1999). However, because of the maritime characteristics of the Southern Alps, winter rain frequently occurs above this line. The mean duration of seasonal snow coverage in the Southern Alps is from May to October while the period of snowmelt is very short mainly during November and December (Fitzharris *et al.,* 1999). Compared to the Western United States (Bales *et al.*, 2006; Li *et al.*, 2017; Zheng *et al.*, 2018), European Alps (Penna

et al., 2016; Beniston *et al.*, 2018) and Himalayan catchments (Siderius *et al.*, 2013; Bharati *et al.*, 2014; Adnan *et al.*, 2017) where snowmelt is a large fraction of water supplies, the contribution of meltwater to runoff in the Southern Alps catchments is lower but still influences the management of irrigation and hydro-electricity schemes in South Island, New Zealand (McKerchar *et al.,* 1998; Kerr, 2013). Previous estimations have shown that the contribution of snowmelt from seasonal snowpacks to river flows in the upper terrains of the Southern Alps can reach up to 40% (Sirguey, 2009).

The main challenge to fully understand the hydrometeorology in the mountain catchments of the Southern Alps has stemmed from lack of systematic snow observations. Unlike the long-term snow observations in western United States, Canada and European Alps, the snow measurements in the mountain catchments of the Southern Alps are very limited. Improved success in snow measurement however, has been recently gained by establishing a network of high altitude automatic weather stations (AWS) by the National Institute of Water and Atmospheric Research (NIWA) (Hendrikx & Harper, 2013). The new network has provided an opportunity to collect climate variables and snow observations close to the Main Divide of the Southern Alps.

2.2.2 Datasets

2.2.2.1 Snow and Ice Monitoring Network (SIN)

This study utilises snow depth data recorded at three NIWA's AWS sites, namely Mahanga, Mueller Hut, and Mt Larkins (Figure 2.1, Table 2.1). At these stations, snow depth is recorded by ultrasonic sensors (SR50) at hourly resolution alongside climate variables such as air temperature, wind direction and speed, precipitation, humidity, and incoming solar radiation. Data are available since 2009 at Mahanga, 2010 at Mueller Hut and 2014 at Mt Larkins.

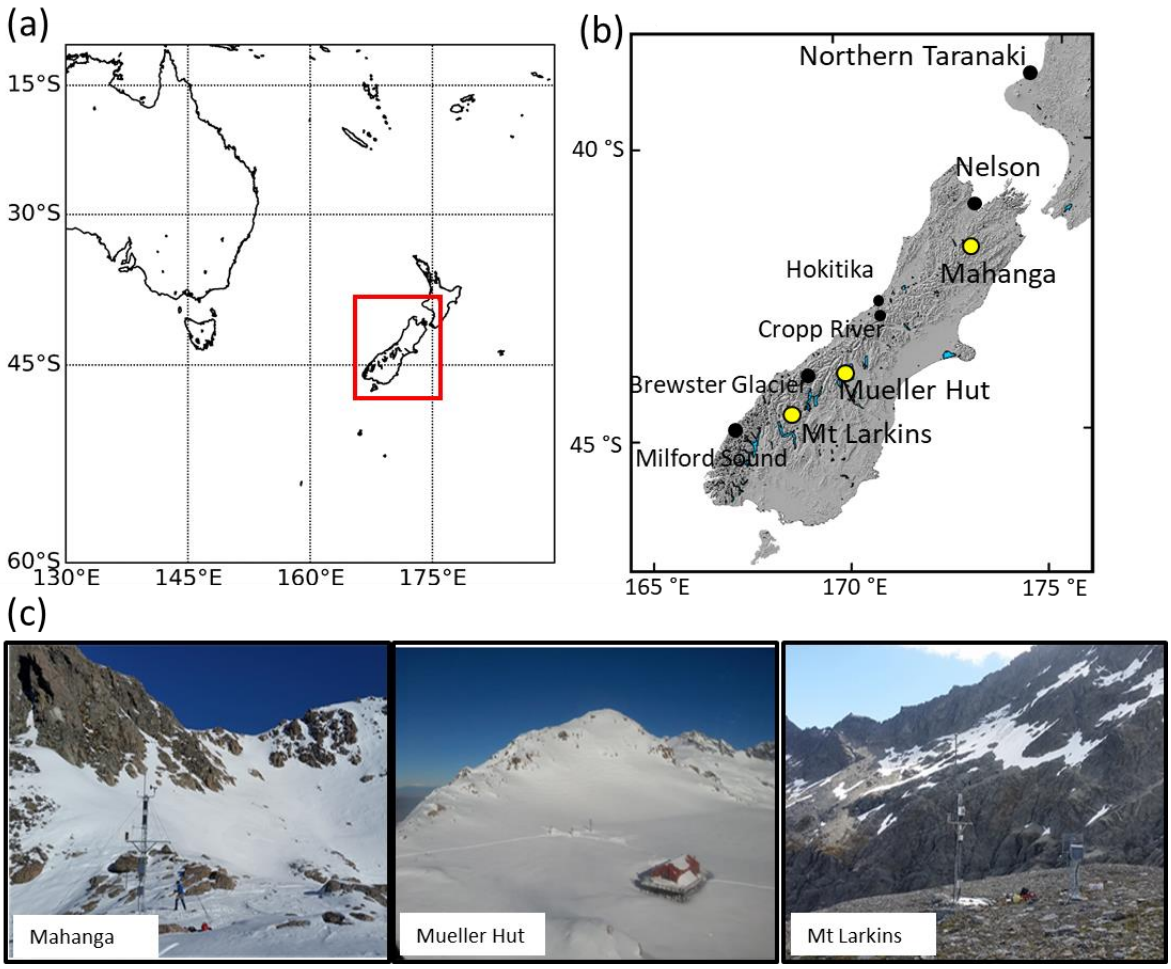

Figure 2.1 (a) Synoptic window over South Pacific region used in this study (red box: 10°-60° S and 130° E-160° W), (b) locations of automatic snow observation sites in the Southern Alps (yellow dots), and (c) photos of three study sites. Photo credits: NIWA's field team.

Table 2.1 Details of three SIN study sites.

Site	Elevation (m)	National Park	Average temperature (°C)	Latitude Longitude (NZTM)	Proximity to the Main Divide (km)	Open date
Mahanga	1940	Nelson Lakes	2.6	1570754.0 5348190.0	On the Main divide	March 2009
Mueller Hut	1818	Aoraki/Mt Cook	2.3	1363581.0 5154867.0	2.5 km east of Main Divide	April 2010
Mt Larkins	1900	-	0.3	1243078.0 5019851.0	25 km east of Main Divide	June 2013

The first step in examining the climatology of large snowfall events is to define what constitutes a large event. To identify daily snowfall events, snow depth observations recorded by ultrasonic depth gauge (SR50) were used. Only daily snowfall events with depths greater than 2.5 mm, which is the precision of the recorded data, were considered

at each station. Different thresholds of daily snowfall ranging from 5 cm to 33 cm of daily snow depth increase have been used in previous studies to determine large snowfall events Most of these thresholds are based on climatology and topography of the region of interest. For example, Birkeland and Mock (Birkeland and Mock, 1996) used a daily threshold of 32.8 cm of snow accumulation in their investigation of the relationship between atmospheric circulation and heavy snowfalls. This threshold characterises the heavy snowfall conditions that could lead to hazardous avalanches in the region. An increase in snow accumulation of more than 5 cm was used in Russian Arctic and Iberian Peninsula to identify large events (Merino *et al.*, 2014; Bednorz and Wibig, 2016). In northern Japan, Farukh and Yamada (2014) selected the topmost 100 snowstorms in order to explore the synoptic climatology related to heavy snowfalls. Bednorz (2013) defined days with more than 20 cm of daily snow accumulation as extreme events.

Because characteristics differ at each of the three sites, an absolute number cannot be solely used as an event threshold. Hydrological studies often define a large or extreme events such as precipitation, or flooding using percentile-based indices, for example using the percentile values of >90th, >95th, >99th and >99.9th (Coles, 2001; Lute and Abatzoglou, 2014; Vicente-Serrano *et al.*, 2017). The cumulative distribution function of daily snowfall events at Mahanga, Mueller Hut and Mt Larkins is shown in Figure 2.2. The threshold values for three percentile values (95th, 90th and 85th) have been summarised in Table 2.2. Applying different percentiles results in different thresholds and different numbers of events. For example, at Muller Hut a percentile of 95th lead to a threshold of 36 cm and only 9 large snowfall events. However, by selecting percentiles 90th and 85th the threshold will be 31 cm and 24 cm and the number of identified events will be 18 and 26, respectively. This shows that changing the percentile values by 5 percent could result in a difference in the threshold (and number of events). Because of relatively short-time measurements of snow in the Southern Alps, choosing a threshold based on 95th or 99th percentiles would result in a small sample of events. Considering the focus of this study

is on the extreme snowfall events and also because of the large variability in the snow distribution across the Southern Alps, the heaviest 10% of daily solid precipitation was defined as a large snowfall events. This method followed similar approach used in other snow-dominated regions across the globe (Moberg *et al.*, 2006; Kanada *et al.*, 2010; Orlowsky and Seneviratne, 2012; Turner *et al.*, 2019). The advantage of selecting the 90th percentile value is that a unique value can be chosen for each site. Also, given the relatively short data set, using a 90th percentile allows for a large enough sample size from which to conduct the analysis. A percentile value of 95th, for instance, would result in choosing a limited number of events in the Southern Alps.

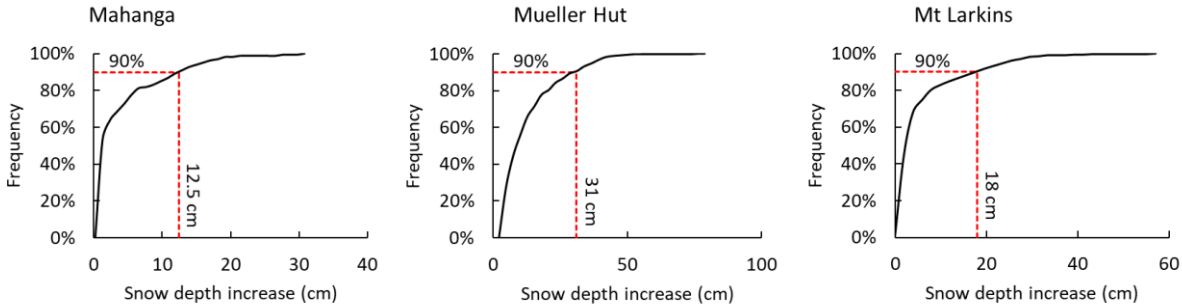

Figure 2.2 Cumulative distribution function of daily snowfall events at three sites. The red line marks the 90th percentile used in this study to identify large snowfall events.

Table 2.2 Percentile values (95th, 90th and 85th) and number of events identified at three sites based on the thresholds.

Site	Mahanga		Mueller Hut		Mt Larkins	
Percentile	Threshold (cm)	Number of events	Threshold (cm)	Number of events	Threshold (cm)	Number of events
95th	16	15	36	9	23	8
90th	12.5	23	31	18	18	17
85th	9.7	28	24	26	12	25

2.2.2.2 ERA-Interim reanalysis data

Different meteorological fields including sea level pressure (SLP), geopotential height at 500hPa (Z500) and temperature at 500, 850 and 1000 hPa (T500, T850 and T1000)

were retrieved from the European Centre for Medium-Range Weather Forecasts (ECMWF) ERA-Interim reanalysis data (Dee *et al.*, 2011) at a 0.5° × 0.5° resolution. The data was obtained at 6-hourly intervals for the synoptic window of 10°-60° S and 130° E-160° W (Figure 2.1). Vertical pressure gradient has a non-linear distribution in the atmosphere with a rapid decrease in the lower atmosphere (Figure 2.3). In terms of altitude, 500 hPa is approximately at 5500 m a.s.l. and is therefore located above the friction of the highest peaks in the Southern Alps (Aoraki / Mt Cook: 3724 m a.s.l.). The 500 hPa geopotential height is used by meteorologists and climatologists because it determines the surface weather (Kidson, 1994; Yarnal *et al.*, 2001). The 850 hPa pressure level lies below 2000 m a.s.l. which is potentially an important pressure level over the Southern Alps for investigating circulation patterns and meteorological patterns for mountain hydrometeorology controlling the formation of snow in the lower troposphere (Sailor and Li, 1999; Mora *et al.*, 2016).

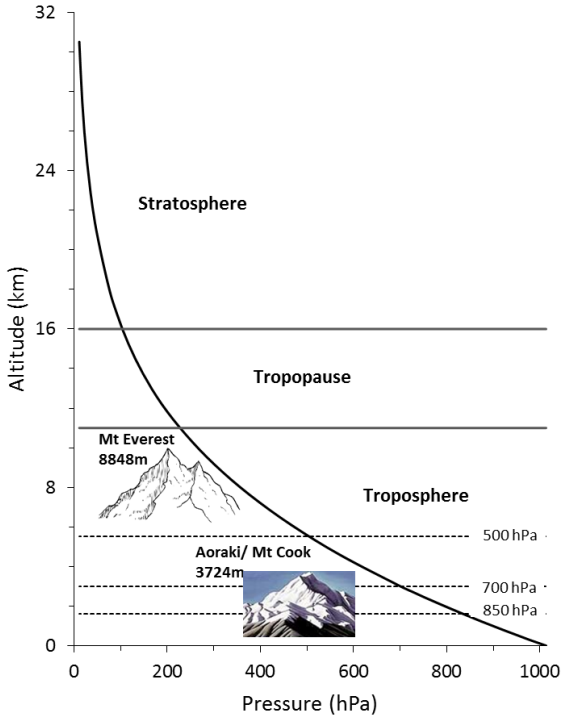

Figure 2.3 Vertical profile of pressure in the lower atmosphere, reproduced from Sturman & Tapper (2006). The dashed lines show the approximate altitude of 500, 700 and 850 hPa pressure levels in the Southern Alps.

2.2.3 Composite anomaly approach

Understanding the atmospheric drivers of large snowfall events requires a comprehensive analysis of large-scale climate conditions. The climate of New Zealand is largely influenced by the hemispheric-scale westerly circulation (Salinger and Mullan, 1999; Kingston *et al.*, 2016b). In the Southern Alps, composite anomaly analysis has been found a simple but useful tool to identify the atmospheric circulation patterns associated with hydrological processes (Kingston and McMecking, 2015b; Kingston *et al.*, 2016b). Composite analysis is commonly used to identify the basic structure and characteristics of climatological phenomena as well as exploring the impacts of large scale atmospheric patterns on weather and climate events. A composite anomaly approach was conducted in order to identify the relationship between atmospheric circulation patterns and snow accumulation. Several studies have used the composite anomaly approach to explore the influence of the atmospheric circulation pattern on snowfall events (Mock, 1996; Mock and Birkeland, 2000; Bednorz, 2011, 2013; Farukh and Yamada, 2014; Bednorz and Wibig, 2016; Mora *et al.*, 2016). This approach explains the differences between averaged values of a selected atmospheric variable and climatic normals. The intensity of the weather systems and climatology of New Zealand is influenced largely by the position of upper-level jet streams (Cullen *et al.*, 2019). Even though the analysis of high level jet streams provides important details about the nature of atmospheric circulation especially in association with cyclonic activities and their moisture transport mechanisms (Sodemann and Stohl, 2013), this study mainly focuses on the low- and mid-level tropospheric activities (below 500 hPa) where the major mechanisms of atmospheric moisture transport and their interaction with orography occur during the extreme precipitation events (Gimeno *et al.*, 2014, 2016). Seasonal climatological means of T500, T850, Z500 and SLP for 1979-2018 period were calculated for the cold months of June to October and were used as the climatic normal (Figure 2.4). Anomaly maps of T500, T850, Z500 and SLP were then computed as the difference between the average

value of these variables during the snowfall events and the 40-year cold months averages. The choice of using the 5-month average maps as the basis of the analysis is mainly because of the general snow patterns in the region. The maximum snow depth is usually between September and October. A statistical comparison between the 4-month temperature averages (June to September) and the 5-month temperature averages (June to October) shows that the difference between the two fields are not statistically significant (p-value < 0.01). As a result, the average climatic normals have been calculated for the whole snow accumulation rather than solely three so called "winter months" in the Southern Alps (June-August). Additionally, difference maps of the above mentioned values for the day prior to the snowfall events were constructed by subtracting the values of the day before from the snowfall days. These maps can describe the atmospheric conditions conducive to heavy snow accumulation and help identify the upper level disturbance patterns (shortwaves) that are superimposed in larger patterns (Birkeland and Mock, 1996; Sturman and Tapper, 2006). Most of the moisture in the mid-latitudes is carried by fast flowing extratropical cyclones and jet streams (Ralph *et al.,* 2004; Neiman *et al.*, 2008; Rutz *et al.,* 2014); therefore, the pace of these changes in flow regimes can be drawn by looking at a difference map of climate conditions during the day prior to the snowstorms.

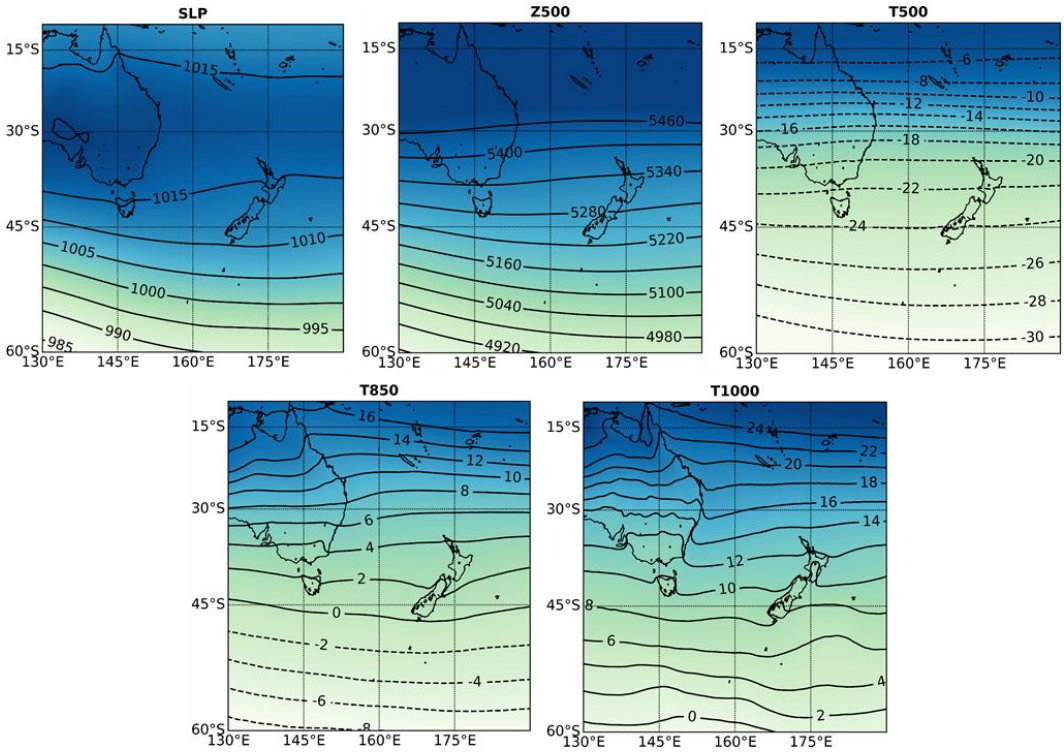

Figure 2.4 Average SLP (hPa, contour intervals: 5 hPa), Z500 (meters, contour intervals: 60 meters), T500 (°C, contour intervals: 2 °C), T850 (°C, contour intervals: 2 °C) and T1000 (°C, contour intervals: 2 °C) (1979-2018) over New Zealand during the cold months (June, July, August, September and October).

2.2.4 Local synoptic patterns

Synoptic classification is a useful tool to identify the characteristics of climatic variables (Barry and Perry, 1973; Smithson, 1986; Harman and Winkler, 1991; Yarnal, 1993; Yarnal *et al.*, 2001). The analysis of atmospheric circulation over New Zealand (Trenberth, 1976; Sturman *et al.*, 1984; Trenberth and Mo, 1985; Kidson, 1994, 2000) provided information about large scale synoptic patterns and indicated the biennial, annual and semi-annual variations. An early study investigated the atmospheric circulation patterns over the South Island of New Zealand and grouped the daily surface synoptic charts from 1961 to 1980 (Sturman *et al.*, 1984). The results indicated the dominance of anticyclonic circulation and westerly flows with anticyclonic south-westerly being the most frequent in all seasons. Kidson (1994, 2000) developed a set of daily weather types for New Zealand using 40 years of NCEP/NCAR analysis data (National Centre for Environmental Prediction/National Centre for Atmospheric

Research). The twice-daily fields of 1000 hPa geopotential height were used to define twelve synoptic types. These types have been grouped into three regimes, namely troughing, zonal and blocking (Figure 2.5). Troughing regimes, which are frequent troughs and frontal systems, consist of four synoptic types designated T, SW, TNW and TSW. These generally bring wetter, colder and cloudier conditions to the entire country. They are less frequent in autumn, and are linked to below-normal temperatures in the south and above-normal precipitation over the entire country.

Zonal regimes (H, HNW and W) represent the dominant west-east wind flows over New Zealand and are typically associated with below-normal precipitation in the north and east of the country. However, they can bring milder conditions in the South Island and potentially lead to precipitation due to westerly flow and showers resulted from HNW and W types. Blocking patterns with highs are more frequent in summer and autumn, stalling or slowing the passage of approaching weather systems. The blocking regimes (HSE, HE, NE, HW and R) are linked to a southwest-northeast contrast in precipitation and above normal temperatures, except on the east coast of both north and south islands. The blocking group are often associated with anomalous northerly flow across much of the country. However, NE and R classes could lead to precipitation in the northern and eastern parts of the North Island. Kidson types have been widely used by researchers to investigate the synoptic climatology of different hydrometeorological phenomena in New Zealand (Smart and McKerchar, 2010; Griffiths, 2011; Renwick, 2011; Parsons *et al.*, 2014). Here, the frequency of the Kidson synoptic types during the large snowfall events over the Southern Alps was examined. It is worth noting that the Kidson types do not provide a quantitative analysis of climate variables during large snowfall events; however, the classification accompanied by anomaly maps could lead to identifying further details of the processes involved in atmospheric circulation patterns associated with such events in the Southern Alps.

2.3 Results and Discussion

2.3.1 Snowfall events

Snow accumulation is spatially and temporally variable across the Southern Alps due to latitude difference, topographic characteristics, proximity to the Main Divide and exposure to wind (Kerr et al., 2013; Webster et al., 2015). Measurements of snow depth during the period of this study show that at Mueller Hut and Mt Larkins sites snow mainly accumulates from June to October, peaking between mid-September to early October (Figure 2.6). At the most northern station (Mahanga), the snow accumulation season is slightly shorter, ending in September. In the case of seasonal snowpacks, snowmelt occurs over a relatively short period in the Southern Alps. At Mueller Hut and Mt Larkins the snowmelt period is usually between mid-October and mid-December, while at Mahanaga snow depth reduces from approximately late September to mid-November. The total annual snow accumulation at Mueller Hut site is noticeably larger than the other two sites. This is likely due to the location of the site (near the Main Divide of the Southern Alps) which is largely influenced by the spillover effect on the lee side of the Southern Alps during the prevailing westerly and north-westerly precipitation patterns (Neale and Fitzharris, 1997). The spatially variable snow accumulation may also be a result of station location with respect to local topography such as elevation and wind exposure that could lead to a strong inter-annual variation of snow depth in different parts of the Southern Alps (Clark *et al.*, 2011; Kerr *et al.*, 2013; Webster *et al.*, 2015).

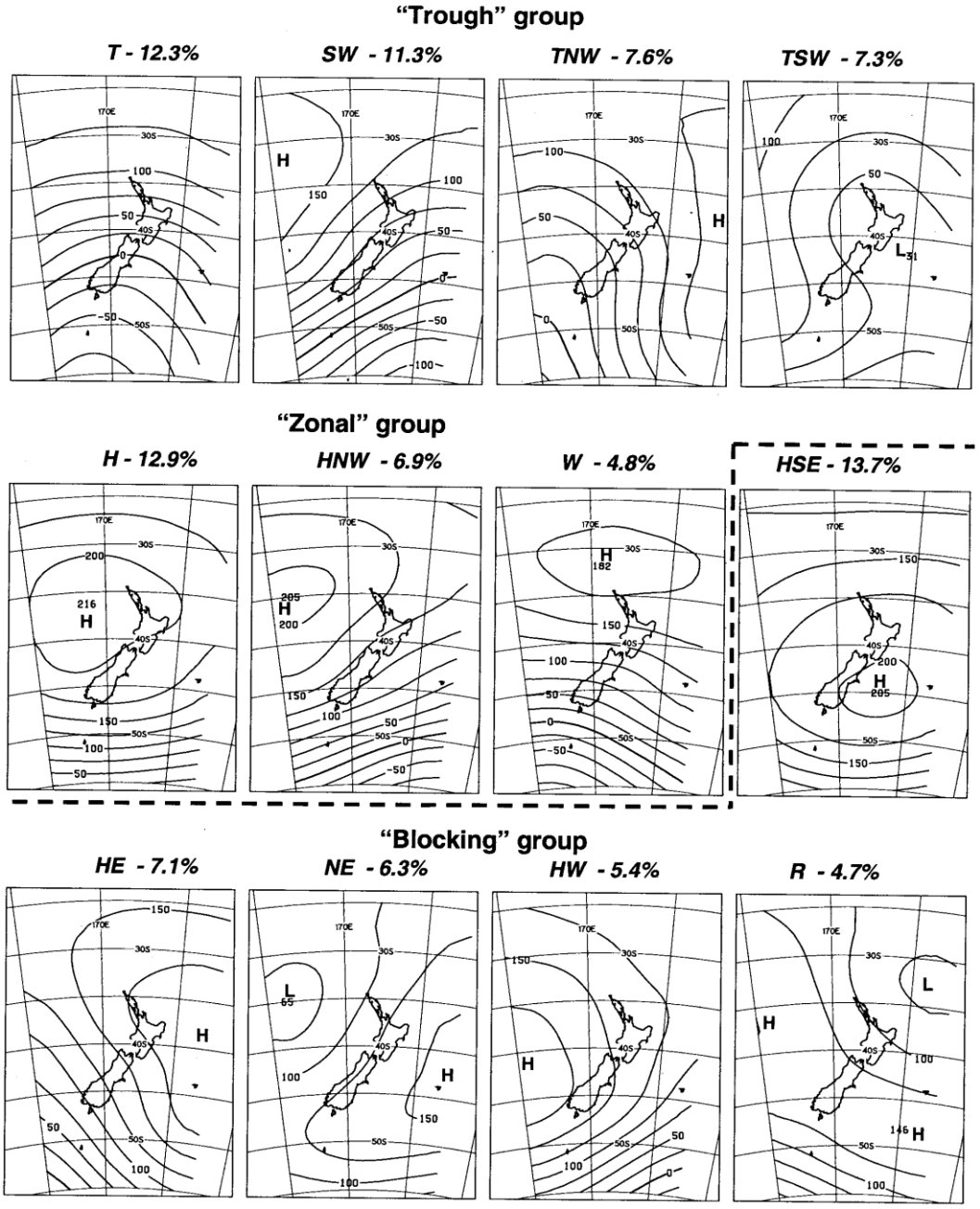

Figure 2.5 The Kidson Types, Trough (T), South Westerly (SW), Trough North West (TNW), Trough South West (TSW), High (H), High North West (HNW), Westerly (W), High South East (HSE), High East (HE), North Easterly (NE), High West (HW) and Ridge (R). From Kidson (2000). The contours are 1000 hPa geopotential heights (meters).

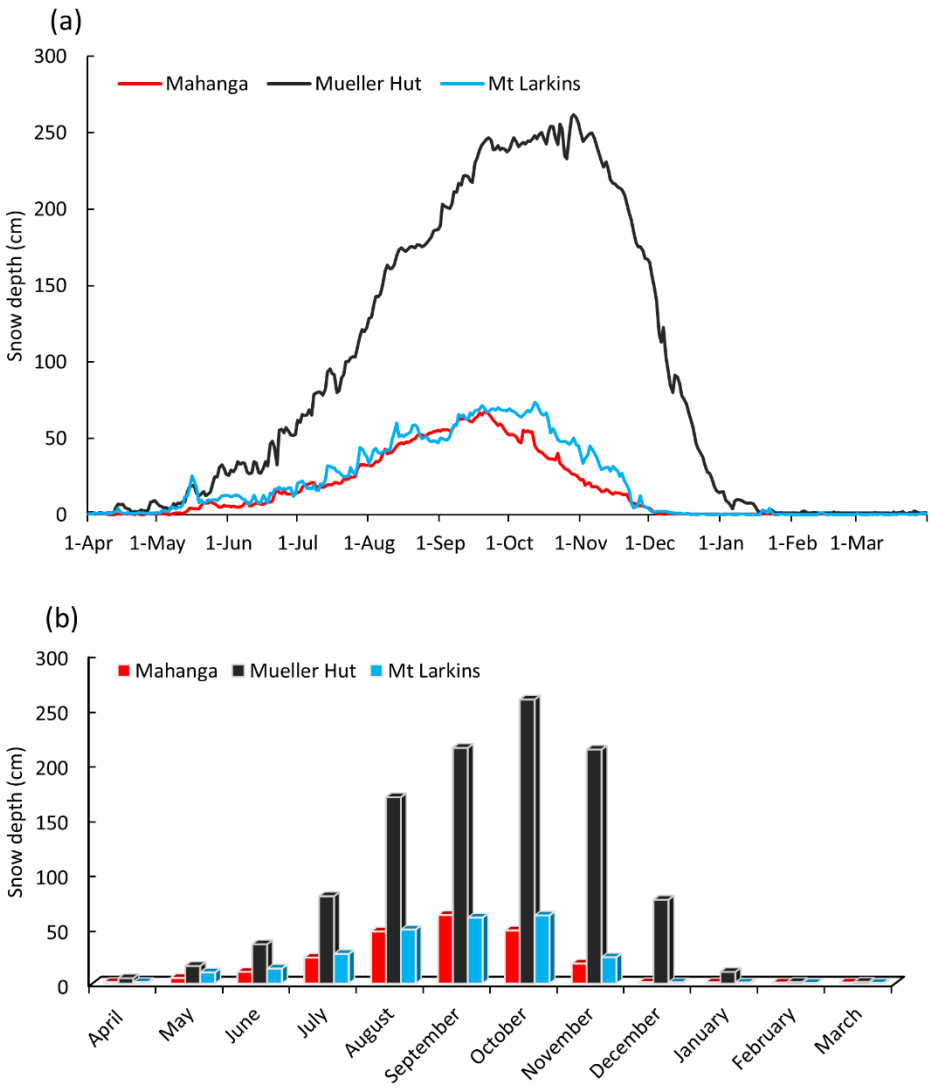

Figure 2.6 Average daily and (b) average monthly snow depth data measured by SR50 at Mahanga (2010-2018), Mueller Hut (2010-2018) and Mt. Larkins (2014-2018).

Applying the 90th percentile of daily snow depth to identify the large snow fall events led to selecting a threshold of 12.5 cm of daily snow for Mahanga, 18 cm for Mt. Larkins and 31 cm for Mueller Hut (Table 2.3). During the study period, 23 large snowfall events (days) at Mahanga, 18 at Mueller Hut and 17 at Mt. Larkins were recorded. These large events play a vital role in the hydrology of the Southern Alps by contributing to a sizeable fraction of the total snow accumulation. Up to 35-40% of annual snow accumulation recorded at Mueller Hut (2016/17) was received during these large events. The timing of the events show that the month of July has highest number of large snowfall events (14 days) (Figure 2.7). August and September ranked equally with 10 snowfall events. The

frequent occurrence of large snowfall events during spring-melt season (6 events in October and 7 events in November) demonstrates that they are not limited exclusively to winter months (June to September).

Table 2.3 A summary of snowfall events at the three SIN sites investigated in this study.

Site name	Number of snowfall days	Snowfall (cm) based on 90th percentile value	Average annual snow accumulation (cm)	Range of maximum snow depth (cm)	Average contribution of large snowfall events to annual accumulation (%)
Mahanga	195	12.5	241	56 (2013/14)-125.4 (2017/18)	22
Mueller Hut	310	31	632.7	212.4(2016/17)-364.2 (2012/13)	32
Mt Larkins	114	18	395.9	79(2014/15)-147.5(2017/18)	25

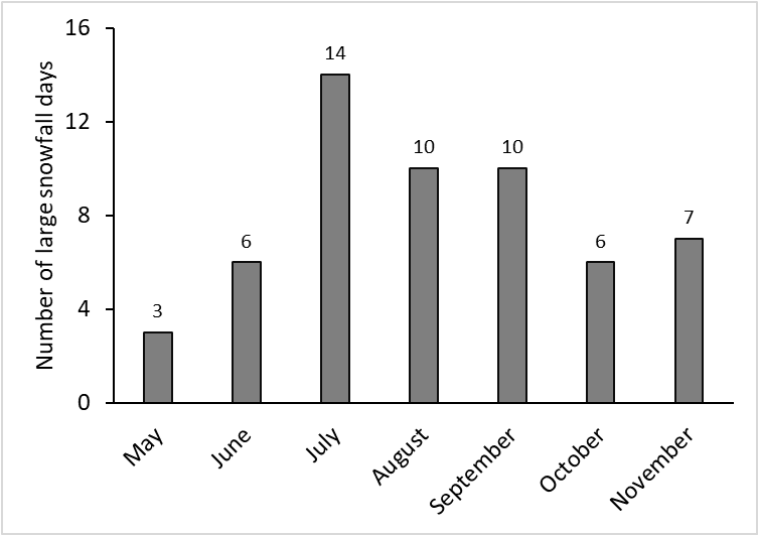

Figure 2.7 Total number of large snowfall days from June to November at three sites.

2.3.2 Composite and anomaly maps of atmospheric fields during the snowfall events

The average values of atmospheric variables from ERA-reanalysis data during the snowfall events including sea level pressure and geopotential height at 500 hPa, and temperature at 500 hPa, 850 hPa are shown in Figure 2.8 and Figure 2.9. A summary of these variables is given in Table 2.4. The average SLP differs from 998.5 hPa at Mueller

Hut site to 1005 hPa at Mahanga site. The magnitude of mean temperature at different pressure levels shows relatively similar values for three sites. However, cooler temperatures at 850 hPa were found at Mt Larkins (1.1 °C) compared to other two locations (Mueller Hut: 2.2 °C, Mahanga: 2.1 °C). The Geopotential heights at 500 hPa are slightly higher during large snowfall events in the north of the Southern Alps at Mahanga site compared to events occurring further south at Mt Larkins and Mueller Hut.

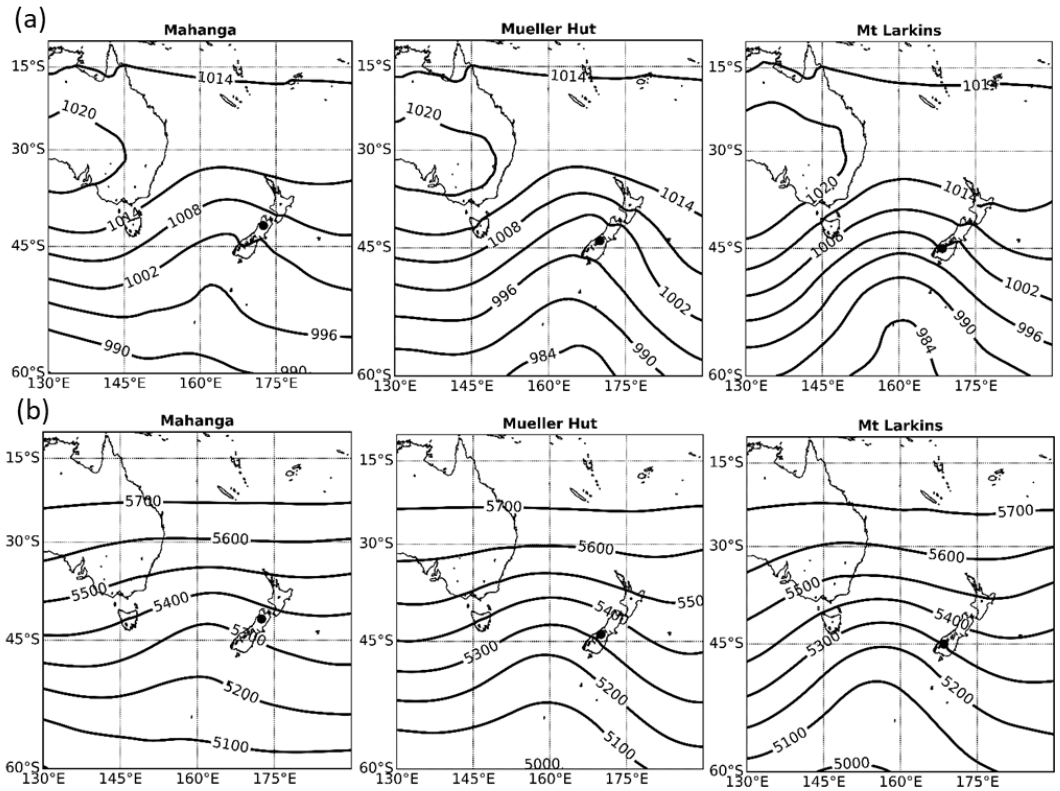

Figure 2.8 (a) Average SLP (hPa, contour intervals: 6 hPa) during large snowfall events, and (b) average Z500 (meters, contour intervals: 100 meters) during large snowfall events. The black dots show the locations of the sites.

The analysis of composite anomaly maps reveals important information about large snowfall events. The events are always associated with distinctive negative anomalies of SLP in the Southern Alps (Figure 2.10a). The negative anomalies are centred over the Tasman Sea mainly to the south west of New Zealand's South Island (near 46-48° S and 160-165° E). Even though the overall patterns of SLP anomalies are very similar during the days with large snowfall events in the region, stronger anomalies are evident for Southern locations (Mueller Hut and Mt Larkins). The SLP at the centre of the lows during

the events at Mahanga, Mueller Hut and Mt Larkins decreased by 12.3 hPa, 15.5 hPa and 18.4 hPa relative to long-term winter averages, respectively. These patterns are similar to those identified by Hendrikx (2007) for the historic 12 June 2006 snow storm in Canterbury region where a pressure depression of 24 hPa combined with a very cold front from the southwest lead to an exceptional snow storm with a record snow accumulation in some parts of the Canterbury region.

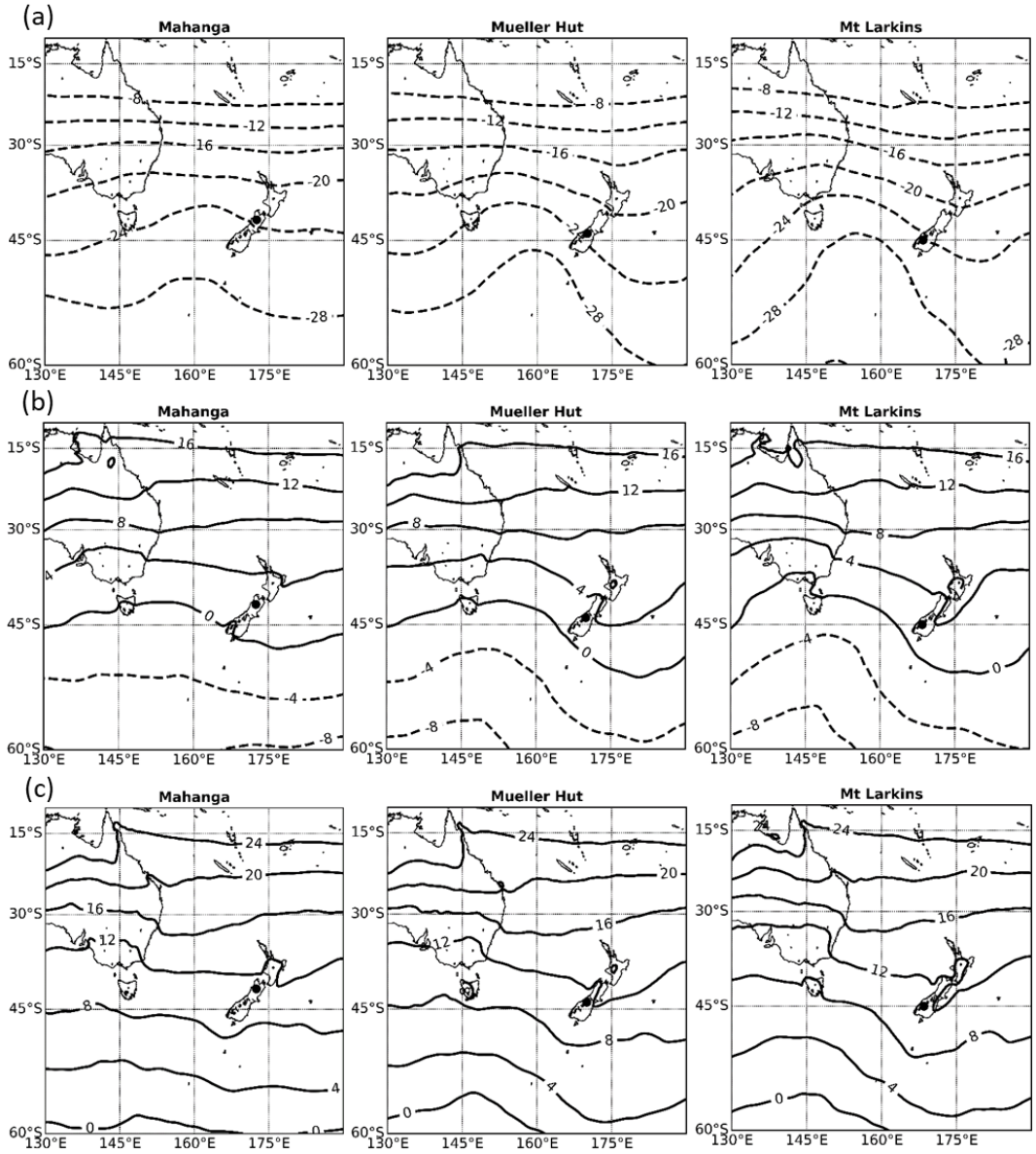

Figure 2.9 Average T500 during large snowfall events (°C), (b) average T850 (°C) during large snowfall events, and (c) average T1000 (°C) during large snowfall events. The black dots show the locations of the sites.

The geopotential heights at 500 hPa (Z500) during the snowfall events are above the normal winter values (Figure 2.10b); however, depressions with lower values are formed in the centres close to the centres of SLP anomalies. Geopotential height represents the actual height of a pressure surface above mean sea level. Generally, heights are lower in colder air masses and higher in warmer air masses. This is due to cold mass being denser than warm air which result in a lower pressure surface in cold air masses and a higher pressure surface in warm air masses.

The Z500 patterns observed here differs from those reported in other parts of the world (e.g. northern Japan, United States and Central Europe). In northern Japan, Farukh and Yamada (2014) reported negative anomalies of geopotential height at 500 hPa caused by cold air masses originating from eastern Siberia during extreme snowfall episodes. Birkeland and Mock (1996) also noted heavy snowfall events in the Bridger Range of Montana, United states are related to cold north-westerly airflows leading to strong negative anomalies of geopotential height at 500 hPa. The positive anomaly of geopotential height can be related to warmer airmass between 1000 hPa and 500 hPa pressure levels at mid and lower troposphere. However, anomaly maps of temperature during the snowfall events revealed that it is highly probable that the warmer temperatures occur mostly in the lower troposphere. In the mid troposphere (500 hPa) weak negative anomalies of temperature with values between -1 and 0 °C are seen (Figure 2.11a). However, the temperature patterns at 850 hPa show positive anomalies with values between above 0 °C and 1 °C over the Southern Alps (Figure 2.11b). The temperature anomalies at 1000 hPa seem to be slightly stronger at lower pressure levels (at 1000 hPa, Figure 2.11c).

These anomaly patterns of temperature are evident of the influence of north-westerly airflows with warmer temperatures during the large snowfall events at lower troposphere relative to long-term winter average. The positive anomalies of temperature at lower troposphere are somewhat similar to the findings of previous studies in other

maritime environments of the eastern Russian Arctic and the western United states. Bednorz and Wibig (2016) reported strong positive anomalies of temperature during snowfall events over the eastern Russian Arctic due to the warm cyclonic airflows from Pacific Ocean. Similarly, above-normal temperatures (at 925 hPa) related to heavy winter precipitation has been reported over the western United States (latitudes north of 37° N) where the majority of heavy winter precipitation is associated with cyclonic activities and atmospheric rivers in the region (Neiman *et al.*, 2008). Conversely, in continental Europe, strong negative anomalies of temperature have been reported during heavy snowfall episodes due to the impacts of polar continental anticyclones over eastern Europe (Bednorz, 2013). Findings from solid winter precipitation in mid-latitude Chilean and Argentinian Andes (32.5°-34° S) found negative temperature anomalies during large snowfall events (Viale and Nuñez, 2011). This cooler than average environment in the Andes is attributed to the influence of cold fronts approaching the west coast of South America and replacing warmer anti-cyclonic patterns over the region during intense and extreme snowfall events.

A comparison between temperature anomalies during large snowfall events in the Southern Alps and South American Andes suggests that despite the different patterns of temperature anomalies (below average temperatures for the Andes and above average temperatures for the Southern Alps) the anomalies at these two mid-latitude maritime environments are not as significant as those in high latitude maritime environments (e.g. Arctic regions). This can be explained by the higher temperature difference between warmer cyclonic systems responsible for winter precipitation and climatic normals at higher latitudes while in mid-latitude maritime regions differences between the weather systems resulting in snowfall events and climatic normals are not significantly distinctive during winter solid precipitation.

Table 2.4 A summary of basic statistics of meteorological fields during snowfall events.

Meteorological fields	Minimum			Maximum			Mean		
	Mahanga	Mueller Hut	Mt Larkins	Mahanga	Mueller Hut	Mt Larkins	Mahanga	Mueller Hut	Mt Larkins
SLP (hPa)	989.8	983	985.5	1024	1012.5	1018.9	1005	998.5	1001.4
Z500 hPa (m)	5219	5171.3	5140	56150	5555.8	5465.1	5357.8	5321.3	5302
T500 (°C)	-29.9	-28.91	-29.94	-16.39	-15.14	-14.91	-23.3	-23	-24.5
T850 (°C)	-5.7	-1.65	-1.27	6.54	6	4.1	2.2	2.1	1.11
T1000 (°C)	2.7	6.8	5.7	13.5	13.7	13.2	9.8	9.8	9.5

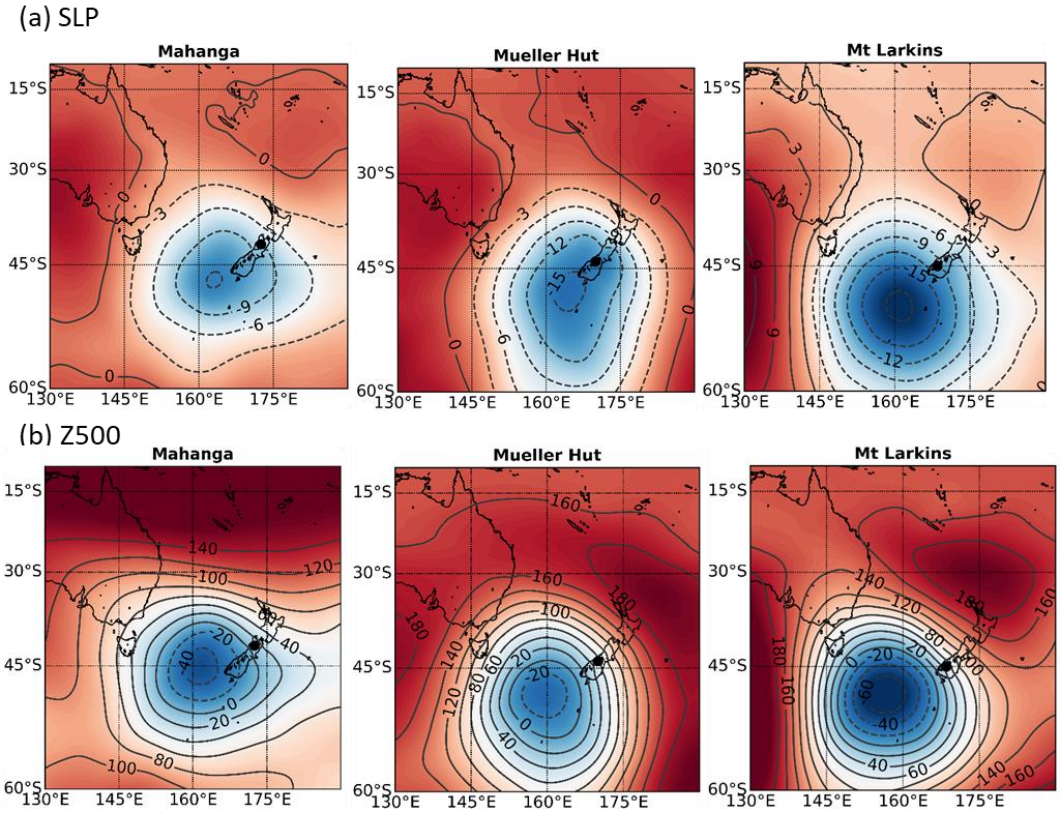

Figure 2.10 (a) Anomalies of SLP (hPa, contour intervals: 3 hPa) during the days of large snowfall. Solid lines indicate positive anomaly and dashed lines indicate negative anomalies. (b) Anomalies of Z500 (meters, contour intervals: 20 meters) during the days of large snowfall. The dashed lines show negative values.

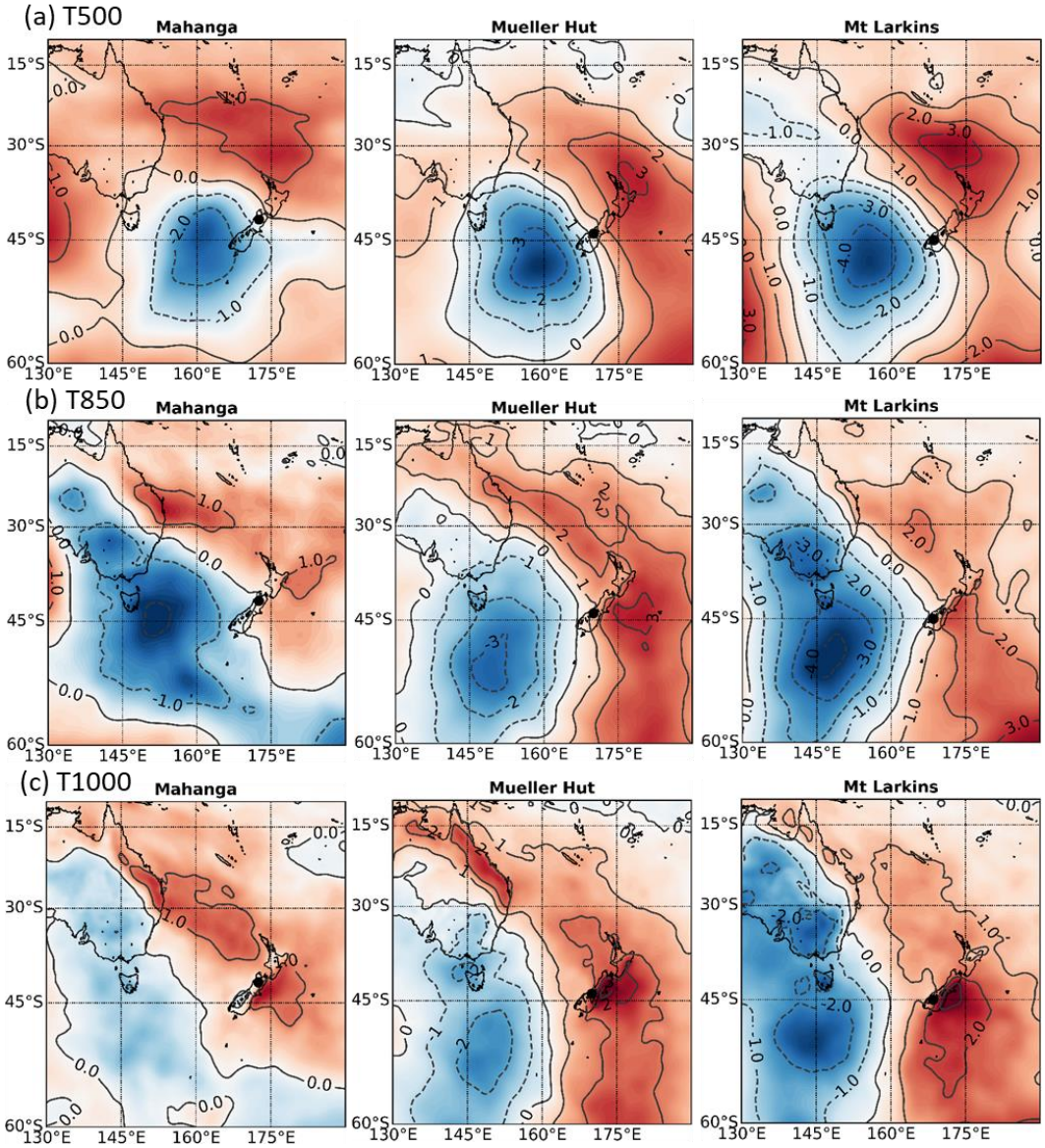

Figure 2.11 Anomalies of temperature (°C, contour intervals: 1 °C) during the days of large snowfall (a) at 500 hPa, (b) 850 hP, and (c) 1000 hPa. The dashed lines show negative values.

To investigate the conditions leading to large snowfall events, the difference between the atmospheric fields (SLP and Z500) of snowfall days and the day prior to the events were calculated. On average SLP drops by 4 to 8 hPa on the day of snowfall compared to the day prior. A depression system extending over the Southern Alps is noticeable during the large snowfall events (Figure 2.12a). Similarly, 500 hPa geopotential patterns indicate a large difference between the days of snowfall and the day prior to snowfall with values up to 75 m (Figure 2.12b). This provides evidence about rapid changes in sea level pressure and geopotential heights across the Tasman Sea and the Southern Alps over a

period of 24 hours. Rapid airflows with an eastward direction towards the Southern Alps resembles the rapidly changing conditions reported in the western United States (Birkeland and Mock, 1996) where intensified troughs are developed alongside the west coast and helps develop heavy snowfall events in the high altitudes. Maps of air temperature anomalies at 500 hPa show a negative anomaly (Figure 2.13a). This is an indicator of the slightly colder air masses at upper levels of airflows responsible for moisture transport during the snow events compared to the day prior to the snowfall event. Unlike the conspicuous temperature anomaly at higher elevations there are no distinctive temperature differences at lower elevations. The zero line (no difference between the snowfall day and the day before) is located close to the locations of the sites indicating the temperature during the day of snowfall and the day prior to the event does not vary significantly at 1000 and 850 hPa pressure levels (Figure 2.13b and Figure 2.13c).

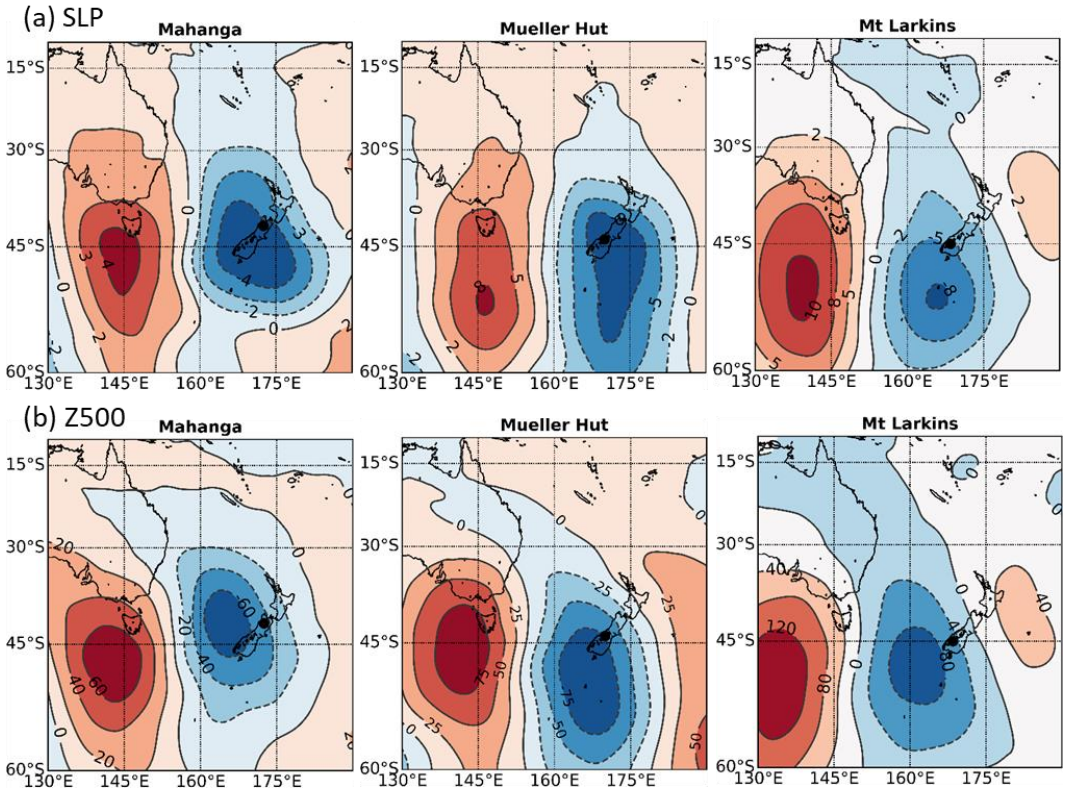

Figure 2.12 (a) Difference maps of SLP (hPa) between the day of the snowfall events and the day prior to the snowfall events, and (b) difference maps of Z500 (meters) between the day of the snowfall events and the day prior to the snowfall events. The dashed lines show negative values.

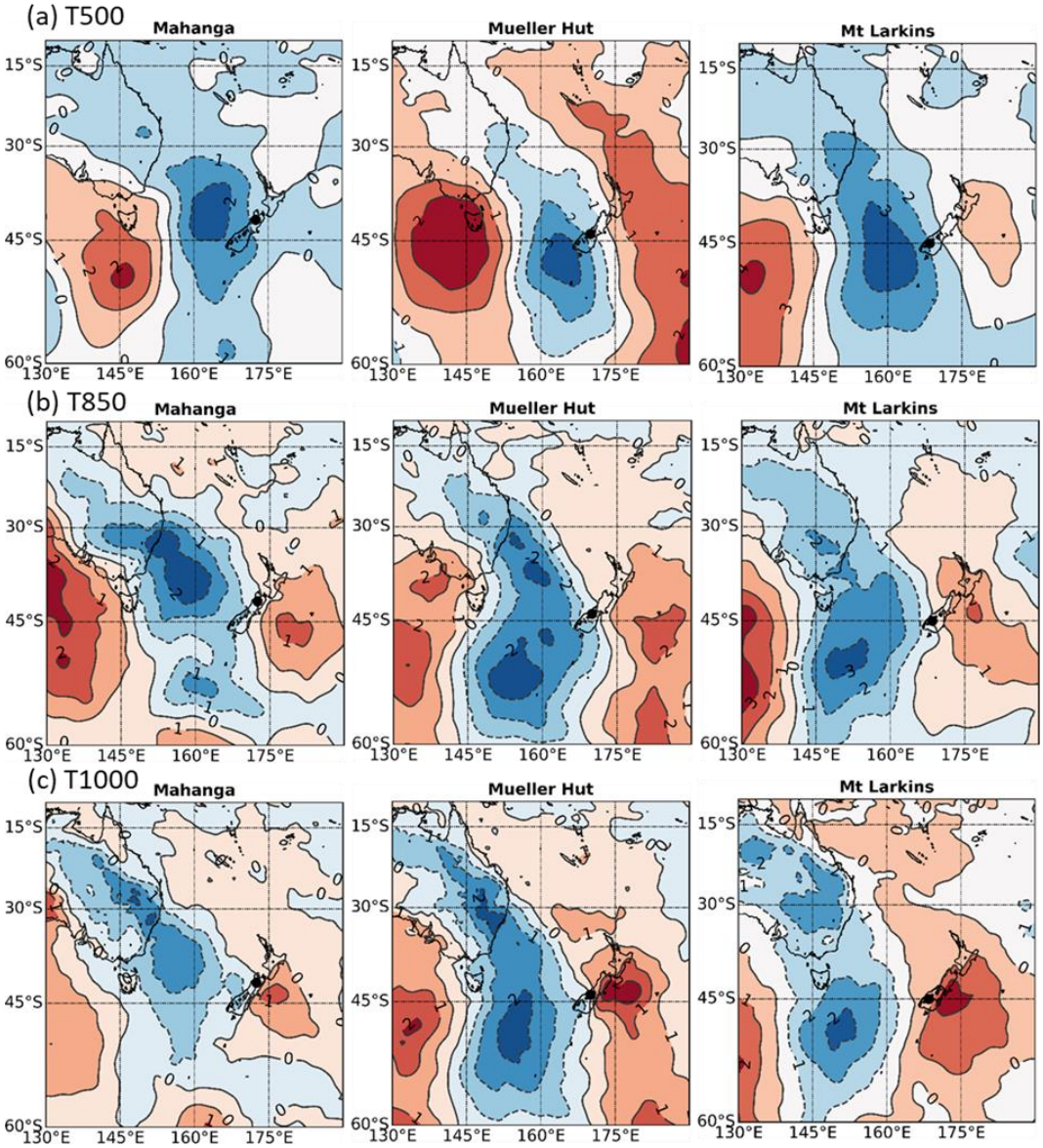

Figure 2.13 (a) Difference maps of T500 (°C) between the day of the snowfall and the day prior, (b) difference maps of T850 (°C) between the day of the snowfall and the day prior, and (c) difference maps of T1000 (°C) between the day of the snowfall and the day prior. The dashed lines show negative values.

2.3.3 Local synoptic patterns associated with heavy snowfall

The trough regime accounts for most of the snow accumulation in the Southern Alps. All three sites receive the majority of their snow during days with a trough regime, 74 % at Mahanga, 88% at Mueller Hut and 70.5% at Mt Larkins (Figure 2.14 and Table 2.5). All four Kidson types belonging to the troughing regime contribute to snow accumulation, however, the T type contributes more than any other types to the large snowfall events

in the Southern Alps. Type T accounts for ~34%, 66% and 58% of observed snow accumulation at Mahanga, Mueller Hut and Mt. Larkins sites, respectively. Zonal group types (W and HNW) account for 15% of large snow fall events at all three sites. Zonal patterns are generally associated with anticyclones in the north, but they can have a different influence in the South Island due to westerly flows and moisture carried by HNW and W types. Mt Larkins (29.5%) and Mahanga (13%) received more of their large snowfall events during zonal conditions compared to Mueller Hut (5.5%).

The most important zonal weather type associated with snowfall occurrence is the W type responsible for 9 large events during the study period. Four snowfall events took place during blocking conditions (HE type) accounting for about 8 % of snowfall events. In the Southern Hemisphere, high pressure systems generally result in warmer than average temperatures across New Zealand. In such systems the high pressure builds and persists in place for a prolonged period of time. Even though the HE type generally coincides with high pressure conditions in the north east and anomalous northerly flow across the country (Kidson, 2000; Renwick, 2011) observations show that the formation of a low system on the west coast over the Tasman Sea could bring about a condition favourable for precipitation over the Southern Alps. The stationary blocking highs slow down the low pressure system moving towards New Zealand and the solid precipitation falls on the edge of the two systems (Figure 2.15).

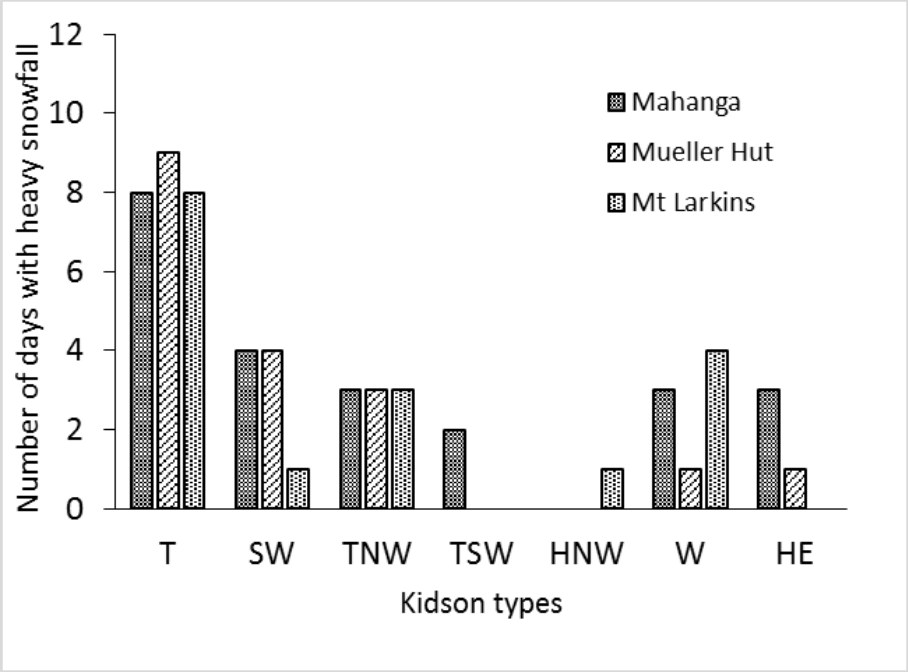

Figure 2.14 The frequency of Kidson types during large snowfall events at three sites.

Table 2.5 The frequency of synoptic regimes and Kidson types during large snowfall events.

		Frequency of large snowfall events (%)			
Synoptic Regime	**Kidson types**	**Mahanga**	**Mueller Hut**	**Mt Larkins**	**% Total**
Troughing	T	34.8	66.6	58.8	77.8
	SW	17.4	22.2	5.8	
	TNW	13	_	5.8	
	TSW	8.7	_	_	
% Total		**74**	**88.8**	**70.5**	
Zonal	HNW	_	5.5	11.8	16
	W	13	_	17.6	
% Total		**13**	**5.5**	**29.4**	
Blocking	HE	13	5.5	_	16.2
% Total		**13**	**5.5**	_	

Our results support the findings on Franz Josef and Tasman glaciers where approximately 75% of the winter snowfall was found to coincide with troughing regimes (Purdie et al., 2011). Likewise, analysis of data associated with Brewster Glacier (a

mountain glacier on the west side of the Main Divide, Figure 2.1c) has shown that the largest snowfall events occur during troughing regimes (mainly TNW type) with strong west to north-west airflows (Little *et al.*, 2019). However, recent studies on Brewster Glacier by Cullen *et al.* (2019) concluded that the W type during zonal conditions are the main contributor to total snow accumulation on Brewster glacier. It is not clear how such synoptic types influence snow accumulation in other parts of the Southern Alps.

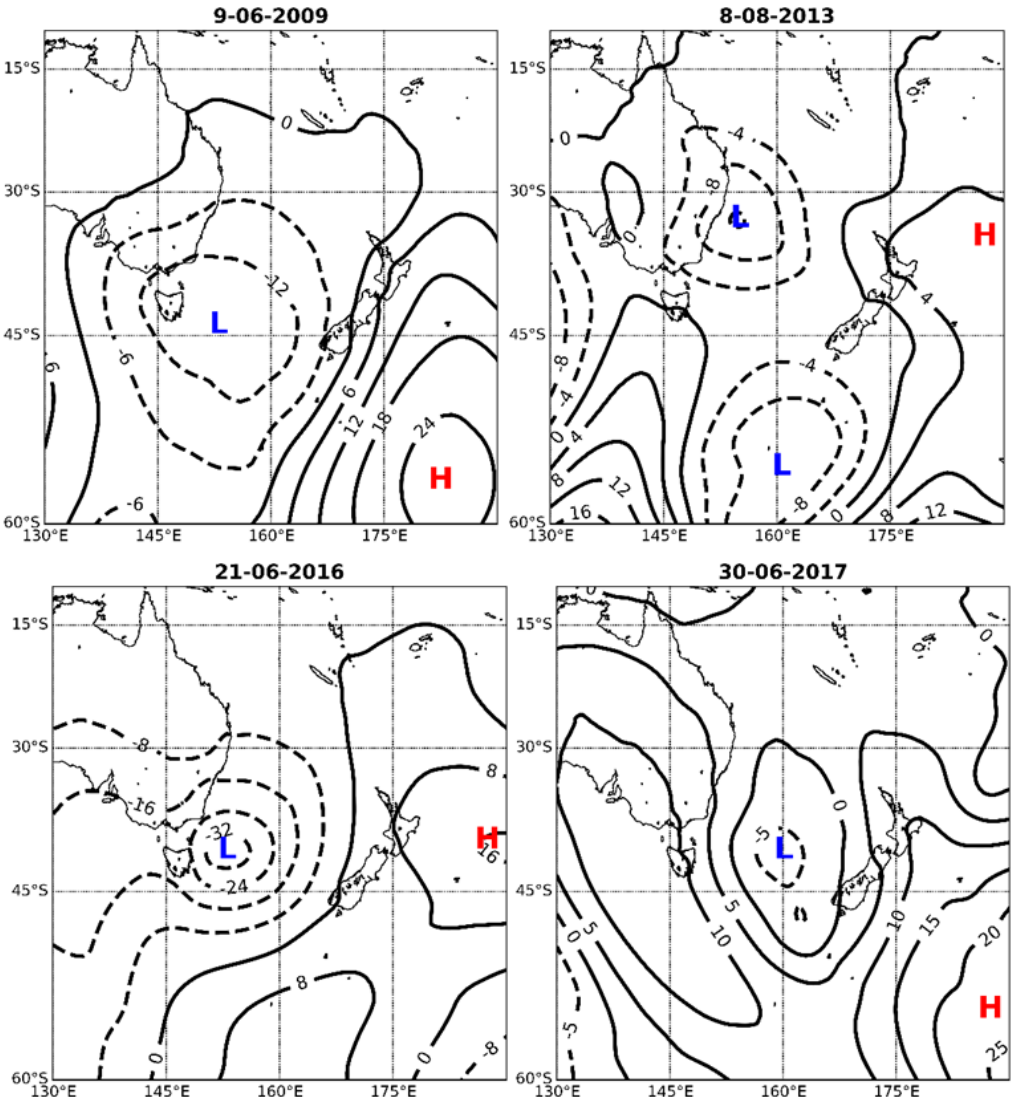

Figure 2.15 MSLP anomaly maps of snow events during the days with blocking regime (HE Kidson type) showing low pressure system west of the South Island and high pressure system on the east; blocking systems slow down the low pressure system and result in snow fall events on the western side of blocking anticyclones.

2.4 Summary and conclusions

The importance of large snowfall events in the Southern Alps of New Zealand has not previously been documented. This study found that up to 35-40% of annual snow accumulation was received during the large snowfall events highlighting the vital contribution of these events to the snow hydrology of the alpine catchments in the region. Frequency of snowfall events in the Southern Alps indicated that even though the majority of large snowfall events mainly occur in cold months (from July to September) the Southern Alps also receive noticeable numbers of snowfall events during spring months (October and November). The interaction of large scale atmospheric circulation and local environment result in conditions favourable for large snowfall events in alpine catchments. Using three locations across the Southern Alps provided an opportunity to investigate the large-scale weather patterns over a larger domain. It is evident that general synoptic conditions during large snowfall events follow somewhat similar patterns at three locations in north, middle and south of the Southern Alps. However, due to different characteristics such as proximity to moisture source and the Main Divide of the Southern Alps, latitude difference, and other topographic features they receive different amount of snow during the accumulation season.

Using a composite anomaly approach, it was found that low pressure systems with deep centres formed in the southwest of New Zealand's South Island are the common features of large snowfall events. A depression of geopotential heights at 500 hPa with centres located at relatively similar locations with the centre of low pressure systems is also evident during snowstorms in the Southern Alps. However, perhaps the most interesting patterns associated with large snowfall events were the temperature anomalies that create a unique condition with different characteristics from other maritime conditions. Despite higher temperatures relative to the long-term averages of cold months' temperatures, no significant divergence has been found between the temperature at different pressure levels during the snowfall events and the long-term

average temperatures. This highlights the important role of the Southern Alps in producing the orographic winter precipitation by cooling down adiabatically the warmer air masses coming from Pacific Ocean when they make landfall over the Southern Alps. This situation can result in conditions with temperature not far from the freezing level across the vast areas of the Southern Alps where the majority of large snowfall events can occur at temperature close to the freezing level. Additional information on synoptic conditions of snowfall events was achieved by computing difference maps of the day with snowfall compared to the day prior. A typical characteristics of synoptic climatology is the short-lived duration and fast moving weather patterns during most snowstorms where a substantial rapid change in the atmospheric fields occurs in the 24 hours leading to the snowfall events.

Analysing local synoptic patterns during snowfall events allows to gain further knowledge about snow accumulation in the region. Using a longer dataset, results supports previous findings on both east and west flanks of the Main Divide highlighting the importance of a troughing regime in the Southern Alps's snowstorms. It was found that across the Southern Alps about 78 % of the large snowfall events were related to a troughing regime. Why the majority of snowfall events are associated with trough systems can be explained by the amount of moisture brought by these weather patterns through extratropical cyclones and jet streams. In addition to the fast moving weather types associated with troughing regimes, zonal regimes also contribute to large snowfall events to a lesser extent (16%). Southern Alps can also receive large snowfall events during blocking regimes formed on the east of the New Zealand region. These high pressure systems provide conditions favourable for solid precipitation by slowing down low pressure systems over the Tasman Sea moving towards the Southern Alps and resulting in snowfall on the edge of low pressure and high pressure systems.

Results from this research have provided an overall view on climate controls of large snowfall events in the maritime alpine regions of the Southern Alps which can be used to

improve forecasting models for predicting large snowfall events and avalanche hazard forecasting. The composite anomaly approach used here provides useful information on how the meteorological fields change during snow storms. They anomaly maps helped identify the areas in the composites that departs significantly from the background variability. However, they might not be able to describe the individual events. One way to tackle this in future work is to compute the daily/hourly anomalies first and then produce composites. Daily/hourly anomalies should be accomplished by subtracting the 10-year normal for each variable from the value from a particular day and hour. In addition, the anomaly maps presented here do not explain categorically the potential moisture sources and moisture transport pathways. This will be further investigated in the next chapter (chapter 3) by improved understanding of the position and characteristics of the jet streams responsible for transferring moisture across the South Pacific Ocean over Tasman Sea towards the Southern Alps during large snowfall events. Also, there is currently a gap in knowledge regarding the temperature characteristics of snowfall events in the Southern Alps. In particular, the role of rain/snow temperature threshold during snowfall events is largely unknown. Through the analysis of temperature anomalies this study has shown that large snowfall events can occur at temperatures close to the freezing level. This means changes in climate related to global warming can have significant impacts on the timing and magnitude of the winter snow accumulation in the upper terrains of alpine catchments in the region. Future work will focus on understanding the temperature characteristics of snowfall events in the maritime Southern Alps.

3 Moisture transport during large snowfall events in the Southern Alps: The role of atmospheric rivers

Abstract

Synoptic-scale moisture transport during large snowfall events in the New Zealand Southern Alps is largely unknown due to a lack of long-term snow observations. In this study, records from three recently developed automatic weather stations (Mahanga, Mueller Hut and Mt Larkins) near the Main Divide of the Southern Alps were used to identify large snowfall events. The large snowfall events are defined as those events with daily snow depth increase by greater than the 90th percentile at each site. ERA-Interim reanalysis data were used to characterize the hydrometeorological features of the selected events. Findings show that large snowfall events in the Southern Alps generally coincide with strong fields of integrated vapour transport (IVT) within a north-westerly airflow and concomitant deepening low pressure systems. Considering the frequency of large snowfall events, approximately 61% of such events at Mahanga (13 out of 21 events) were associated with narrow corridors of strong water vapour flux, known as atmospheric rivers (ARs). The contributions of ARs to the large snowfall events at Mueller Hut and Mt Larkins were 70% (12 out of 17 events) and 71% (10 out of 14), respectively. Meso-scale analysis of the moisture transport dynamics during the passage of landfalling ARs revealed the key characteristics of a snow-generating AR in the Southern Alps. An enhanced presence of low and mid-level moisture between 700-850 hPa and pronounced increases of wind velocities (more than 30 m s^{-1}) with high values of the meridional component between 750-850 hPa were identified over the Southern Alps during these events.

3.1 Introduction

In mid-latitudes a sizeable fraction of moisture is transported through atmospheric rivers (AR) (Ralph *et al.*, 2004; Neiman *et al.*, 2008a). ARs are narrow channels of enhanced water vapour within the atmosphere that are responsible for most horizontal transport of moisture outside of the tropics (Zhu and Newell, 1998; Ralph *et al.*, 2019). In the hydrometeorological literature, other terms such as warm conveyor belt (WCB) and Tropical Moisture Exports (TMEs) are also used to define similar meso-scale and synoptic-scale features with high water vapour content impacting the hydrological cycle

in many parts of the world (Gimeno *et al.*, 2014; Ralph *et al.*, 2017). However, TMEs are characterized by high horizontal export of tropical moisture content to higher latitudes (Lu and Lall, 2016) , and WCB are defined as cyclonic-relative airflows as strongly ascending in the vicinity of extratropical cyclones and their fronts (Eckhardt *et al.*, 2004). Although the term "atmospheric rivers" was first used by Zhu and Newell (1998), knowledge about these filamentary plumes of enhanced moisture in the lower troposphere has been known for a while (Gimeno *et al.*, 2014). The word "rivers" was used as an analogy of the filamentary water flux to that within the world's largest rivers (Newell *et al.*, 1992; Gimeno *et al.*, 2014). Non-technical terms such as "Pineapple Express", "Hawaiian fire hose" and "Maya Express" are commonly synonymous to this phenomenon in North America (Lackmann and Gyakum, 1999; Dirmeyer and Kinter, 2009). More than 90% of total water vapour flux at mid-latitudes is found to be associated with ARs (Zhu and Newell, 1998; Neiman *et al.*, 2008a). The two main sources of moisture in ARs are local moisture convergence along the cold front of an extratropical cyclone and the direct poleward transport of tropical moisture (Bao *et al.*, 2006).

The high moisture content and strong wind velocities associated with ARs usually bring about heavy precipitation, especially when they intercept mountain terrains (Ralph *et al.*, 2004; Junker *et al.*, 2008; Guan *et al.*, 2010; Neiman *et al.*, 2013; Rutz *et al.*, 2014b). Strong relationships have been found between ARs and hydrological processes such as precipitation, streamflow and flooding events in the mid-latitudes of western North America (Neiman *et al.*, 2008b, 2008a; Leung and Qian, 2009; Guan *et al.*, 2010; Dettinger *et al.*, 2011; Ralph *et al.*, 2016), South America (Viale and Nuñez, 2011; Viale *et al.*, 2018; Molero and Novelli, 2019) and Europe (Stohl *et al.*, 2008; Lavers *et al.*, 2012; Lavers and Villarini, 2013a; Benedict *et al.*, 2019; Whan *et al.*, 2020). In the western US, for example, it is estimated that 25-50% of the total water supply in California is due to the landfall of ARs (Guan *et al.*, 2010; Dettinger *et al.*, 2011). One of the reasons ARs has recently gained more attention in regions such as western United States is their potential to put an end

to long term droughts. About 33-40% of the drought breaks in California are related to the landfall of atmospheric rivers (Dettinger, 2013).

At higher altitudes, ARs have been found to be an important source of solid precipitation in the Sierra Nevada mountains, Andes and Antarctica (Guan *et al.*, 2010, 2012, 2013; Hansen *et al.*, 2013; Demaria *et al.*, 2017; Huning *et al.*, 2017, 2019). Satellite measurements and in situ observations in the western United States show that up to 40% of seasonal snow water equivalent are the result of ARs (Guan *et al.*, 2010). Frequent landfalls of ARs accompanied by the negative phases of the Arctic Oscillation (AO) and the Pacific-North American (PNA) atmospheric circulation indices provide conditions favourable for anomalously high snow accumulation across the Sierra Nevada (Guan *et al.*, 2013). The penetration of ARs to the inland semiarid Southwest of the United States can lead to a contribution of more than 25% of winter precipitation (Demaria *et al.*, 2017). The analyses of three historic snowstorms during the past 60 years on Mt. Shasta, in California, United States demonstrated a clear link between large snowfall events and ARs (Hansen, 2016). Investigation of climatology of winter precipitation over the subtropical Central Andes indicates that strong water vapour transport from the Pacific Ocean largely modulates heavy snowfall events in the region (Viale and Nuñez, 2011). Similarly, Gorodetskaya et al. (2014) reported a close connection between extreme snowfall events and strong moisture fluxes associated with ARs in East Antarctica where a large portion of annual snow accumulation is found to be linked to few extreme snowfall events.

Moisture transport in the South Pacific region across the Tasman Sea enhanced by regional orographic influence is a typical feature of winter precipitation in the Southern Alps (Cullen *et al.*, 2019; Little *et al.*, 2019). However, the contribution of ARs in climate and hydrometeorology of the Southern Alps is limited. This is surprising given that recent global studies have shown that a considerable number of ARs occur in the New Zealand region (Guan and Waliser, 2015; Waliser and Guan, 2017). Recently Kingston et al. (2016a) investigated the impact of ARs on extreme flooding events at the Waitaki River

between1972-2012, finding that all major flooding events were associated with ARs. Their study highlighted the need for further investigation to better understand the role of ARs in the region. More recently, Little et al., (2019) documented the role of ARs on glacier mass balance at Brewster glacier, located on the west side of the Main Divide of the Southern Alps, showing significant relationship between ARs and glacier mass gain and loss by influencing snow accumulation and snow ablation. It is, therefore, important to examine the role of ARs on large snowfall events at a greater spatial scale across the Southern Alps.

Given the importance of westerly and north-westerly airflow for Southern Alps precipitation (Griffiths and Mcsaveney, 1983; Henderson and Thosmson, 1999; Purdie *et al.*, 2011; Little *et al.*, 2019), of particular interest is the analysis of moisture transport in the South Pacific region over the Tasman Sea and its relationship with large snowfall events in the Southern Alps. Large snowfall events are a critical source of water in mountain catchments by increasing total snow water equivalent (SWE). The Southern Alps form the headwaters of most of the rivers in the South Island. Seasonal snow is an important element of water resources in the Southern Alps by influencing the timing and magnitude of the discharge of alpine rivers (Clark *et al.*, 2009; Kerr, 2013). Meltwater from seasonal snowpacks can contribute up to 40-50% of the discharge in upper alpine catchments which in turn feed major rivers in the Southern Alps (Fitzharris and Garr, 1995; Sirguey, 2009). This contribution impacts the hydroelectricity generation capability and sustainable irrigation during summer (McKerchar *et al.*, 1998; Thompson, 2002; Hendrikx *et al.*, 2012). However, climate change is expected to substantially impact the seasonal snowpacks in the Southern Alps (Poyck *et al.*, 2011; Hendrikx *et al.*, 2012; Jobst *et al.*, 2018).

Regional climate models currently suggest that the maximum daily temperatures in the Southern Alps of New Zealand could rise by more than 4 °C by the end of this century (Dean *et al.*, 2006). Improved understanding of the atmospheric dynamics and moisture

transport controlling the timing and magnitude of snowfall will provide important information for water management policies in the region, given the potential impact of climate change on the distribution and duration of seasonal snowpacks in the Southern Alps. The main aim of chapter 3 is to explore the key characteristics of moisture flux during large snowfall events in the region (question 2). Gridded atmospheric reanalysis data and daily snow observations across the Southern Alps are used to assess the contribution of ARs to such events by analysing the magnitudes of integrated vapour transport (IVT) during snowstorms.

3.2 Data and Methodology

3.2.1 Data sources

Similar to chapter 2, snow observations were obtained from the Snow and Ice Monitoring Network (SIN, Figure 2.1). The large snowfall events have been identified using the 90th percentile value of daily snowfall increase (see section 2.2.2.1). For the purpose of this chapter, the selection of large events were based on 24-hour snow depth increase by greater than the 90th percentile at each site over the period of observation. In the case where large snowfall events were associated with snowstorms longer than 24 hours, analysis was conducted for the total period of the storm rather than individual snowfall days.

The meteorological fields were obtained from the Interim European Centre for Medium-Range Weather Forecasts (ECMWF) reanalysis data (Dee *et al.*, 2011). Meteorological observations on land and ocean are assimilated into numerical weather predication models to produce atmospheric reanalysis data (Lavers *et al.*, 2012). ECMWF ERA-Interim data were retrieved at 6-hourly temporal resolution and 0.5° × 0.5° spatial resolution for a geographic window spanning of 10°-60°S and 130°E-160°W (see Figure 2.1b). The data used in this study includes sea level pressure (SLP, hPa), geopotential height at 500 hPa (Z500, m), temperature (T, °C), specific humidity (q, g kg^{-1}), specific cloud ice water content (g kg^{-1}), zonal and meridional wind fields (u and v, m s^{-1}), vertical

integral of cloud frozen water flux (VICFWF, kg m^{-1} s^{-1}) and vertical integral of cloud liquid water flux (VICLWF, kg m^{-1} s^{-1}).

3.2.2 Synoptic patterns associated with large snowfall events: Composite anomaly approach

Composite anomaly maps have been found to be a useful tool to assess the atmospheric patterns during large snowfall events (Mock and Birkeland, 2000; Esteban *et al.*, 2005; Bednorz, 2013). In order to determine the synoptic patterns related to large snowfall an anomaly approach is applied using the sea level pressure fields. The difference between the gridded values of SLP during the days of large snowfall events and 40-year winter average SLP (Figure 3.1) were used to produce surface pressure anomaly maps.

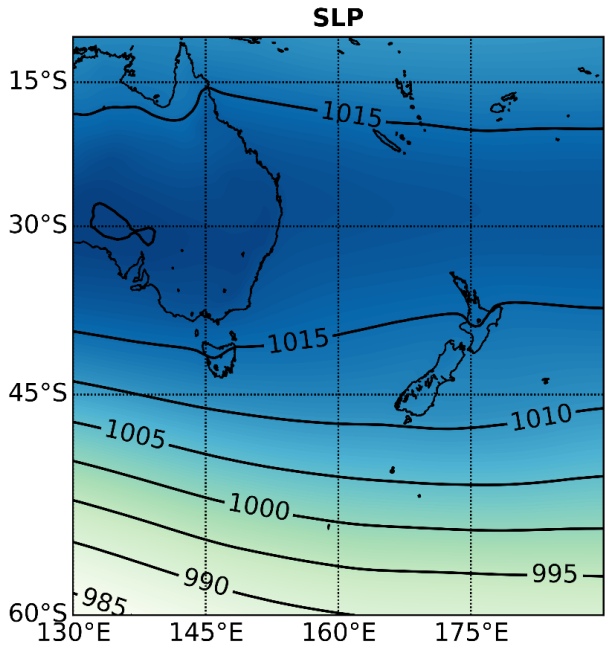

Figure 3.1 40-year average mean sea level pressure during the cold months (June-October).

3.2.3 Moisture transport: Identification of ARs

The total amount of water in the atmosphere provides critical information about moisture transport from tropics to mid-latitudes (Dettinger *et al.*, 2011; Lavers *et al.*, 2012; Rutz *et al.*, 2014b; Schumacher *et al.*, 2020). There are two commonly used methods to quantify intense lower-tropospheric moisture. The first approach measures

the integrated vapour transport (IVT, kg m^{-1} s^{-1}) and the second approach measures integrated water vapour (IWV, cm). IVT defines as:

$$IVT = \sqrt{\left(\frac{1}{g}\int_{1000\ hPa}^{300\ hPa} qu\ dp\right)^2 + \left(\frac{1}{g}\int_{1000\ hPa}^{300\ hPa} qv\ dp\right)^2} \quad (3.1)$$

where g (m s^{-2}) is the gravitational acceleration, q (g Kg^{-1}) is the specific humidity, u (m s^{-1}) is the zonal component of the wind, v (m s^{-1}) is the meridional component of the wind, and p is the pressure. IWV is defined as:

$$IWV = \frac{1}{g}\int_{1000\ hPa}^{300\ hPa} q\ dp \quad (3.2)$$

where g (m s^{-2}) is the gravitational acceleration and q (g Kg^{-1}) is the specific humidity. The merit of the use of AR detection algorithms to study the moisture transport is the relative simplicity of finding the filamentary patterns of water vapour associated with this phenomenon as well as simple identification of the role of ARs in the hydrological cycle at a regional and global scale (Gimeno *et al.*, 2014; Hansen, 2016; Rutz *et al.*, 2019). In most recent hydrometeorological studies IVT is preferred over IWV for identifying ARs (Cordeira *et al.*, 2017; Waliser and Guan, 2017; Young *et al.*, 2017; Ralph *et al.*, 2019). This is mainly because IVT has a better relationship with precipitation over mountainous terrains (Junker *et al.*, 2008; Guan *et al.*, 2013), and a stronger correlation with winter precipitation (Guan *et al.*, 2010, 2013, 2016; Rutz *et al.*, 2014b). The IVT prior and during the snowfall events was computed for the synoptic window of 10°-60°S and 130°E-160°W (Figure 2.1a). The integration was conducted on specific humidity and u and v components of the wind for 50 hPa intervals between 300 and 1000 hPa using equation (3.1).

This study followed the approach taken by Rutz et al. (2014) where areas with IVT greater than a specific threshold (e.g. 100 or 250 kg m^{-1} s^{-1}), longer than 2000 km in length, and with length/width ratio of greater than 2 are identified as ARs. Most AR detection algorithms are based on employing IVT thresholds (e.g. Neiman *et al.*, 2008;

Dettinger *et al.*, 2011; Gimeno *et al.*, 2014). The 85th percentile of IVT values have been used in several studies conducted in mid-latitudes of Europe and North America (Lavers *et al.*, 2012; Guan and Waliser, 2015; Shields *et al.*, 2018; Rutz *et al.*, 2019), and this is the approach used here. The 6-hourly IVT values were calculated for a grid point located on the west coast of South Island approximately between 40.5 °S and 46 °S (Figure 3.2) during the main snow accumulation months in the Southern Alps (June to October 2009-2017). The monthly average of IVT and IVT_{85th} has been calculated for each month (June-October, Figure 3.3 and Table 3.1). The monthly average IVT varies from 103 (kg m^{-1} s^{-1}) in August to 153 (kg m^{-1} s^{-1}) in October. IVT_{85th} values range from 179 (kg m^{-1} s^{-1}) in August to 254 (kg m^{-1} s^{-1}) in October and the value for the whole period between June to October is 232 kg m^{-1} s^{-1}. The selection of IVT threshold during snow accumulation months is because considerable differences in the values of IVT have been reported for different seasons in mid-latitude regions (Lavers *et al.*, 2012; Guan and Waliser, 2015). Here, the IVT_{85th} for the whole period is used as the threshold (232 kg m^{-1} s^{-1}) as the analyses are based on the whole period when the large snowfall events occur rather than monthly analysis. The range of the IVT values during winter and spring months shows that a threshold of 232 is a reasonable point at which to identify the ARs in the South Island of New Zealand. Next the average IVT was calculated over the course of each snowfall event on the west coast of South Island at the closest gird point to each snow observation (Mahanga: -41.5 °S and 171 °E , Mueller Hut: -43.5 °S and 169 °E, Mt Larkins: -44.5 °S and 167 °E). If the average IVT during each snowfall event exceeds the threshold, the moisture flux will be checked for the shape requirements (L ≥2000 km and L/W ≥2).

In addition to analysis of IVT, in order to obtain more information about the moisture transport during the days leading to the snowfall events, the average values of ERA-Interim vertical integral of cloud frozen and liquid water fluxes (VICFWF and VICLWF, kg m^{-1} s^{-1}) are calculated. These two variables reveal the relative amounts of

solid or liquid water in the clouds (Daniel *et al.*, 2002) which largely influences precipitation in mountainous regions by impacting the seeder-feeder phenomenon (Khain and Pinsky, 2018).

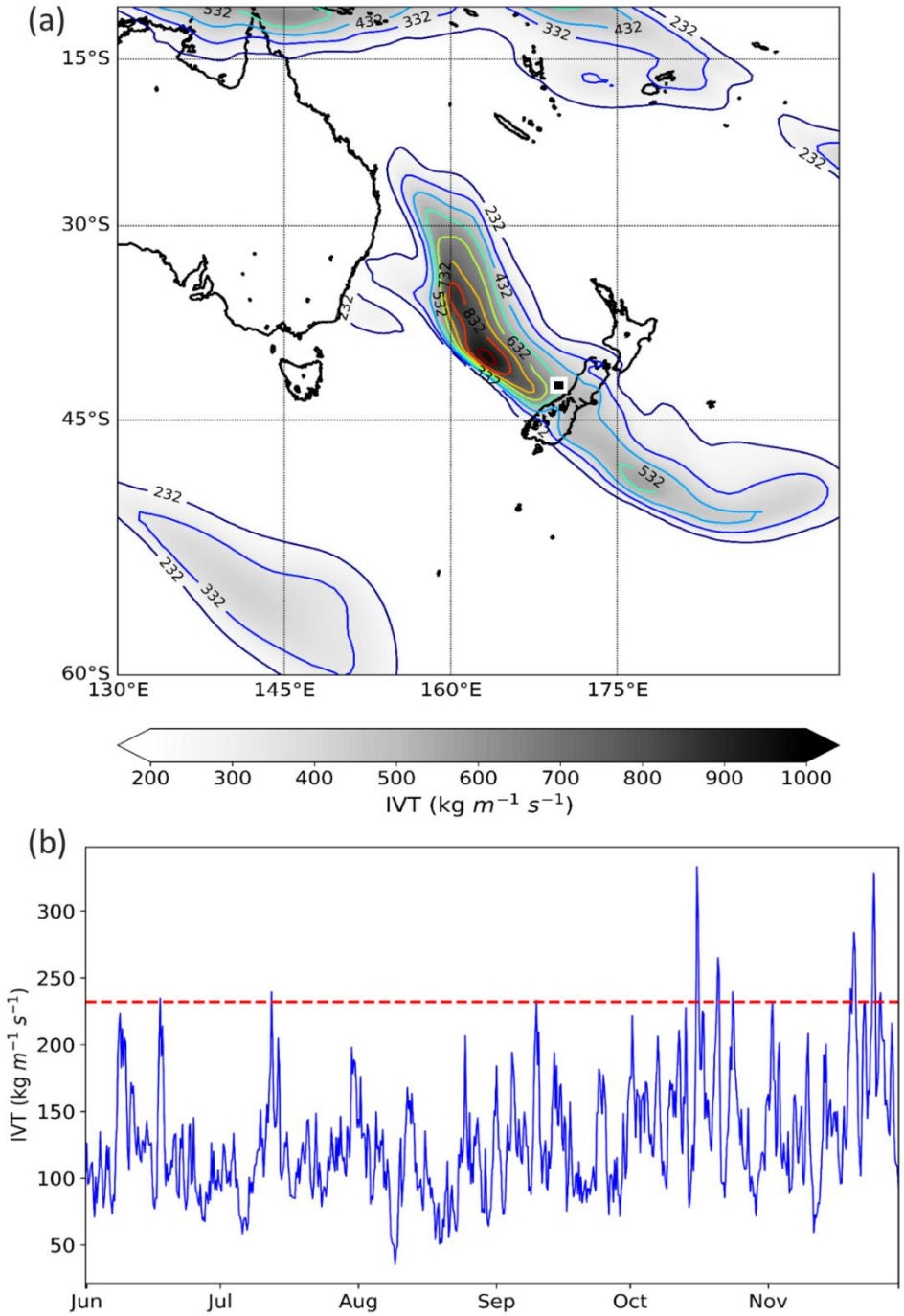

Figure 3.2 A detected AR over South Island of New Zealand. The black square mark the location of the gird point at which the 85th percentile IVT was calculated. (b) Time series of average IVT for the period of 2009-2017 along the west coast of New Zealand South Island (43 °S and 170.5 °E). The red dashed line represents the 85th percentile of IVT value (232 kg m^{-1} s^{-1}).

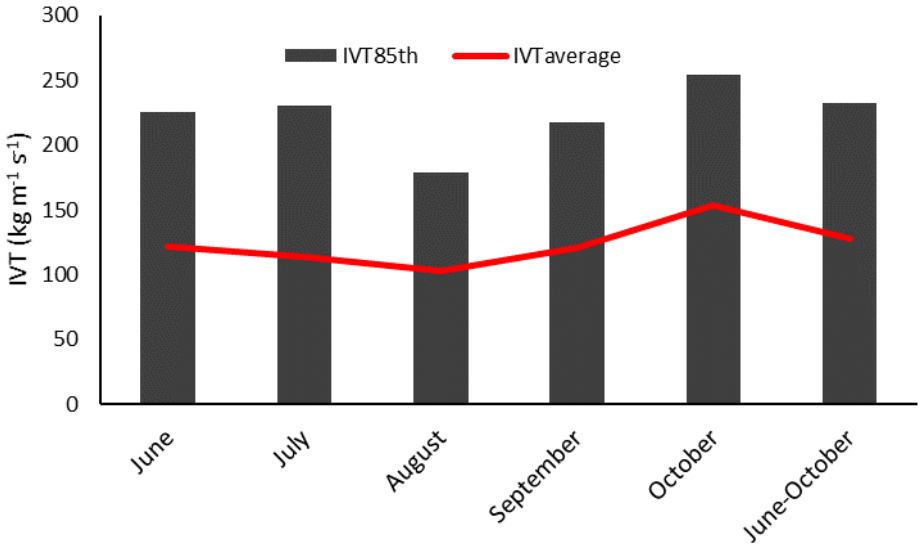

Figure 3.3. Average monthly IVT (kg m^{-1} s^{-1}) and IVT_{85th} between June to October.

Table 3.1 A summary of average IVT (kg m^{-1} s^{-1}) and IVT_{85th} between June to October.

Months	June	July	August	September	October	June-October
$IVT_{average}$	122	114	103	121	153	128
IVT_{85th} (kg m^{-1} s^{-1})	225	230.5	179	218	254	232

In order to relate the intensity of ARs to hydrological events, Ralph *et al.* (2019) introduced a scale to categorize ARs based on the maximum instantaneous IVT and the duration of the events during the landfall of ARs at a given location (Figure 3.4). Weather events associated with ARs are ranked based on categories from 1 (weak storms) to 5 (exceptional storms). This scale can be used to communicate more objectively what impacts an atmospheric river will have on weather and water resources in a region. It indicates the likelihood of beneficial results (e.g. rain after a long period of drought, snowfall in the mountains) as well as the hazardous consequences (e.g. flooding events) of AR-related events. The scale will be used to evaluate the strength and influence of ARs associated with large snowfall across the Southern Alps.

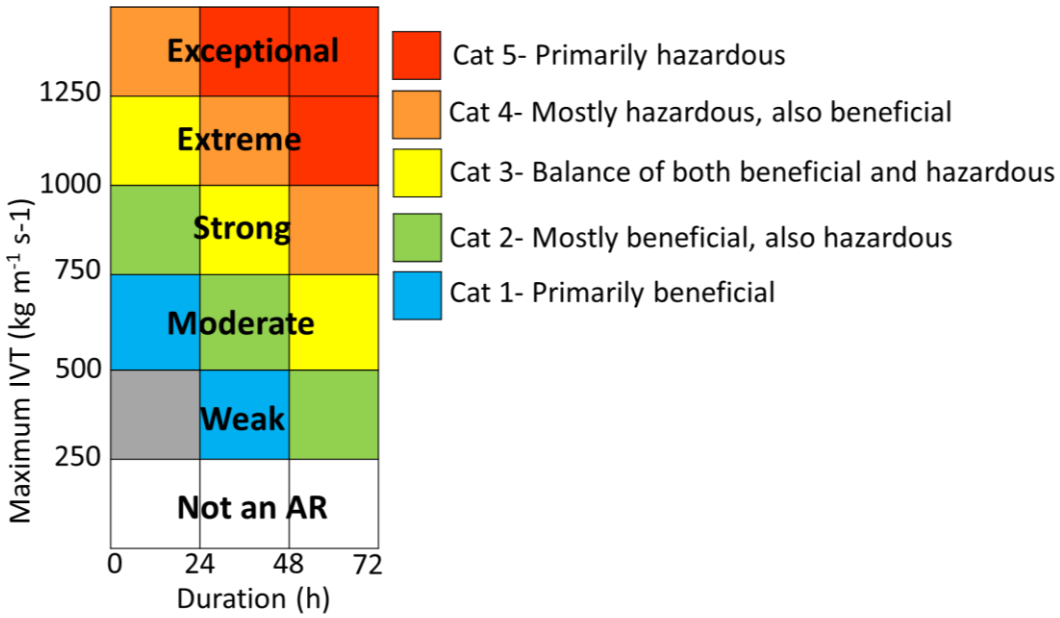

Figure 3.4 ARs scale based on the maximum IVT and the duration of the landfall at a given location (from Ralph *et al.*, 2019).

3.2.4 The 1000-500 hPa thickness line: the rain/snow boundary line

The thickness line represents the vertical measurement in meters between two different pressure levels. The most commonly used thickness values for atmospheric analysis and forecasting are 1000-500 hPa, 1000-850 hPa, 1000-700 hPa, 850-700 hPa, and 700-500 hPa. These thickness values are associated with air density and temperature. As warmer air is less dense, the distance between the pressure level heights is larger. Conversely, the cold air is denser, and the distance between the two pressure level heights decreases (Figure 3.5). Thickness values, therefore, provide a useful tool to determine cold fronts in air masses. The 1000-500 hPa thickness value of 5400 m (also known as 540 line) is the line commonly used to identify the partitioning of rain from snow (Esteban *et al.*, 2005). Rain and snow are equally likely when the 1000-500 hPa thickness is about 5225 m. Rain rarely occurs when the 1000-500 hPa thickness is less than 5190 m. Snow, on the other hand, is unlikely when the 1000-500 hPa thickness is more than 5395 m. In this study, the 1000-500 hPa thickness line was used to identify the boundary between the cold and warm air masses inside atmospheric rivers during snowstorms.

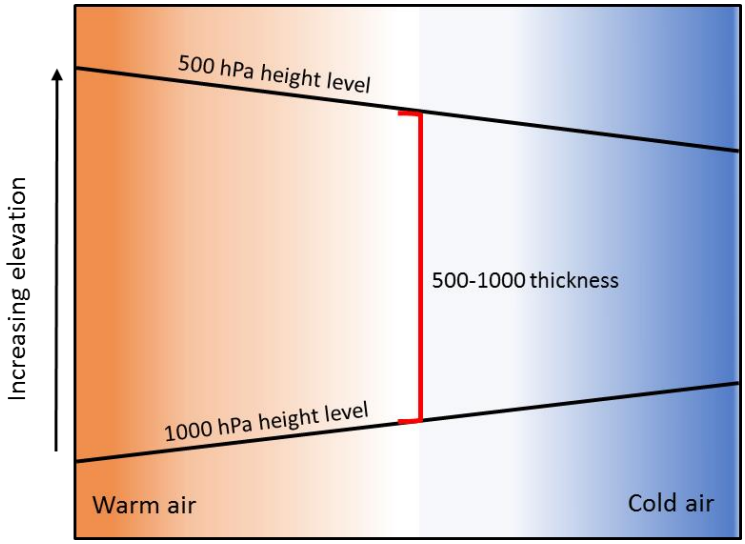

Figure 3.5 1000-500 thickness line (5400 m line) indicating the approximate boundary between rain and snow.

3.2.5 Mesoscale plan-view analysis

Even though ARs are generally considered synoptic scale phenomena (Mahoney *et al.*, 2016), taking a mesoscale approach is essential in order to characterize the dynamics of moisture transport leading to intense precipitation (Ralph *et al.*, 2004; Neiman *et al.*, 2013). The mesoscale analysis is conducted to shed more light on the physical processes lying between the synoptic and local scales (Sturman and Tapper, 2006). Mesoscale factors such as specific humidity, wind speed and temperature are strongly controlled by synoptic-scale processes. On the other hand, mesoscale phenomena act as a link to connect the features at smaller scales (orographic controls in the mountains, surface roughness, etc.) to the synoptic and larger scale weather patterns. In order to examine the dynamics of ARs associated with large snowfall events, the vertical structure of the zonal and meridional components of the wind (u and v, m s^{-1}) and specific cloud ice water content (g kg^{-1}) is analysed during the snowstorms at the locations of snow observations. These analyses will be used to characterize the individual AR-related snowstorms and find the key signatures of such events in the Southern Alps.

3.3 Results

3.3.1 Large snowfall events in the Southern Alps

The 90th percentile of daily snow depth led to selecting a threshold of 12.5 cm of daily snow for Mahanga, 18 cm for Mt Larkins and 31 cm for Mueller Hut for detecting large snowfall events (see section 2.3.1 and Table 2.3). This amounted to 21 events at Mahanga, 17 events at Mueller Hut and 14 events at Mt Larkins (Table 3.2). The proportion of the average annual sum of large snowfall events relative to the total snow accumulation indicates that an average of 26% (Mahanga), 32% (Mueller Hut) and 28% (Mt Larkins) of the interannual variability in snow depth were associated with these events.

Table 3.2 Snow depth observations and IVT magnitudes during large snowfall events at three SIN sites (Mahanga, Mueller Hut and Mt Larkins).

Event	Duration (hours)	SD (cm)	Max IVT alongside west coast	Average IVT alongside west coast	Max IVT at SIN sites	L/W ≥2	AR: Yes/No
Mahanga							
9/06/2009	12	14.1	390	170.7	242.2	✓	No
3/07/2009	18	12.7	363.8	187.9	194.9	✓	No
23-24/07/2009	22	42.0	476	314.4	362.7	✓	Yes
31/08/2009	16	12.7	600.6	410.7	443.3	✓	Yes
8/06/2010	22	18.8	540.9	322.6	369.1	✓	Yes
9-10/10/2010	24	16.7	359.5	247.3	265.9	✓	Yes
20/10/2010	13	13.8	225.8	176.9	195.0	×	No
18/06/2012	19	15.0	402.1	288.3	324.1	✓	Yes
9/09/2012	34	18.2	664.9	403.3	487.7	✓	Yes
8/08/2013	14	14.2	319.8	245.5	263.2	✓	Yes
12-13/08/2014	18	29.0	461.8	261.9	353.4	✓	Yes
16-17/09/2014	28	17.1	289.1	179.2	198.3	×	No
20/09/2014	18	17.0	273.9	199.3	225.9	✓	No
12/11/2014	25	14.0	392.8	254.7	329.8	✓	Yes
19/11/2014	18	14.3	309.3	222.9	251.6	✓	No
20/05/2016	21	14.6	464.6	281.8	326.1	×	No
21/06/2016	24	31.9	513.2	382.8	263.6	✓	Yes
3/07/2016	19	13.7	310.4	221.1	146.1	×	No
26-27/07/2016	37	27.0	403.6	245.1	276.9	✓	Yes
14/08/2017	12	21.3	360.2	284.4	297.5	✓	Yes
7/09/2017	16	26.9	320.19	242.2	265.5	✓	Yes
Contribution of large snowfall events to the total annual snow accumulation: 26%							
Contribution of ARs to large snowfall events: 61% (13 events)							
Mueller Hut							
25/09/2010	19	30.3	377.7	307.7	338.8	✓	Yes
18-19/10/2011	32	49.5	321.8	245.2	356.6	✓	Yes
2-3/08/2014	29	74.7	441.7	269.9	424.9	✓	Yes
12-13/08/2014	18	32.5	269.3	203.1	340.9	×	No
15-16/09/2014	24	35.2	177.6	150.9	178.8	×	No

19-20/11/2014	27	32.4	362.1	254.8	294.6	✓	Yes
1-2/09/2015	26	32.3	435.0	345.1	296.2	✓	Yes
13-14/07/2016	28	99.0	542.2	366.3	556.8	✓	Yes
24/07/2016	21	32.8	525.4	299.9	511.0	✓	Yes
28-29/07/2016	34	31.1	238.2	152.5	189.8	×	No
11-12/10/2016	18	70.0	485.9	355	478.0	✓	Yes
12/11/2016	22	30.9	88.5	65.7	79.5	×	No
26_27/11/2016	46	35.5	332.0	269.2	274.0	✓	Yes
1-2/07/2017	32	81.3	368.1	237.4	366.6	✓	Yes
22/07/2017	26	51.4	369.4	319.9	452.7	✓	Yes
13-14/08/2017	32	33.0	330.2	236.6	240.1	×	No
5-6/09/2017	34	63.0	280.0	237.0	276.9	✓	Yes
Contribution of large snowfall events to the total annual snow accumulation: 32%							
Contribution of ARs to large snowfall events: 70% (12 events)							
Mt Larkins							
1/07/2014	20	34.0	520.4	319.0	425.9	✓	Yes
11/08/2014	18	29.9	410.8	231.6	78.4	×	No
14-15/05/2015	32	46.5	360.3	262.8	286.9	×	No
15/06/2015	22	33.9	317.3	281.0	273.7	✓	Yes
18/06/2015	18	24.6	508.3	326.0	404.5	✓	Yes
19/08/2015	19	19.6	367.2	268.4	269.8	✓	Yes
13-14/07/2016	34	67.0	541.0	301.1	398.6	✓	Yes
27-28/07/2016	34	59.5	302.4	264.0	271.3	×	No
11-12/10/2016	24	108.0	570.8	374.6	495.4	✓	Yes
26-27/11/2016	24	27.0	504.3	276.9	325.1	✓	Yes
13/08/2017	22	29.5	372.2	258.1	256.3	✓	Yes
5-6/09/2017	28	23.8	355.5	264.5	245.9	✓	Yes
9/09/2017	18	32.7	242.2	153.9	218.1	×	No
5/11/2017	14	25.9	366.4	280.3	255.8	✓	Yes
Contribution of large snowfall events to the total annual snow accumulation: 28%							
Contribution of ARs to large snowfall events: 71% (10 events)							

3.3.2 Association of ARs with large snowfall events

Figure 3.6 shows the average values of six-hourly integrated vapour transport (IVT), vertical integral of cloud frozen water flux (VICFWF) and vertical integral of cloud liquid water flux (VICLWF) during the large snowfall events. The mean estimates of VICFWF and VICLWF during the snowfall events were used to diagnose the importance of the moisture content in the clouds during the snowfall events. Figure 3.6b reveals that over the period of snowstorms VICFWF increased towards the Southern Alps where the highest values of VICFWF were calculated for the grid points of three snow observation sites near the Main Divide (2.8 kg m^{-1} s^{-1} at Mahanga, 3.4 kg m^{-1} s^{-1} at Mueller Hut and 3.3 kg m^{-1} s^{-1} at Mt Larkins). The average values of VICLWF shows a similar pattern to VICFWF; however, the liquid water flux decreases from the west coast towards the Southern Alps with the higher values recorded on the west coast of the South Island (3.9

kg m^{-1} s^{-1} at Mahanga, 5.4 kg m^{-1} s^{-1} at Mueller Hut and 4.7 kg m^{-1} s^{-1} at Mt Larkins). Depicting the average values of 6-hourly IVT during the large snowfall, Figure 3.7c shows relatively high moisture flux (greater than IVT 85th percentile: 232 kg m^{-1} s^{-1}) along the west coast of South Island. The average IVT is within the range of 260-300 kg m^{-1} s^{-1} over the period of the snowstorms (260 kg m^{-1} s^{-1} at Mahanga 290 kg m^{-1} s^{-1} at Mueller Hut and 275 kg m^{-1} s^{-1} at Mt Larkins).

As the main focus of this study is the assessment of moisture transport for each individual storm, the key characteristics of moisture flux during the identified large snowfall events have been explored. Table 3.2 summarizes the details of IVT calculations, the requirements for AR identification as well as duration and total accumulated snow depth during the events. Three examples of identified landfalling ARs responsible for large snowfall events at the three locations are shown in Figure 3.7. These three ARs resulted in the largest snowfall event recorded at each location (see Table 3.2).

In terms of magnitude, the analysis of IVT during the landfall of ARs alongside the west coast of the south Island reveals maximum instantaneous values greater than 500 kg m^{-1} s^{-1} during the snowstorms over the Southern Alps (e.g. 9th September 2012 event at Mahanga, 13-14th July 2016 event at Mueller Hut, and 11-12th October at Mt Larkins). However, the average values of IVT over the period of each snowstorm remains mainly below 300 kg m^{-1} s^{-1}. Also, near the Main Divide of the Southern Alps, where the snow observation sites are located, rarely does the maximum IVT exceed 500 kg m^{-1} s^{-1}. Our results show that, considering the frequency of large snowfall events reported in Table 3.2, approximately 61% of large snowfall events at Mahanga (13 out of 21 events) were associated with ARs. The contributions of ARs to the large snowfall events at Mueller Hut and Mt Larkins were 70% (12 out of 17 events) and 71% (10 out of 14), respectively. However, based on the snow depth increase these proportions are 71%, 80% and 70% for Mahanga, Mueller Hut and Mt Larkins, respectively. It is worth noting that from a hydrological perspective it would have been desirable to calculate these contributions

based on snow water equivalent rather than snow depth. However, due to lack of reliable and consistent snow water equivalent data during all snowfall events our analysis was limited to snow depth observations. These findings still provide some insight into the potential importance of such narrow channels of moisture to large snow events in the maritime Southern Alps, where up to 40% the total snow accumulation could results from several snowfall events.

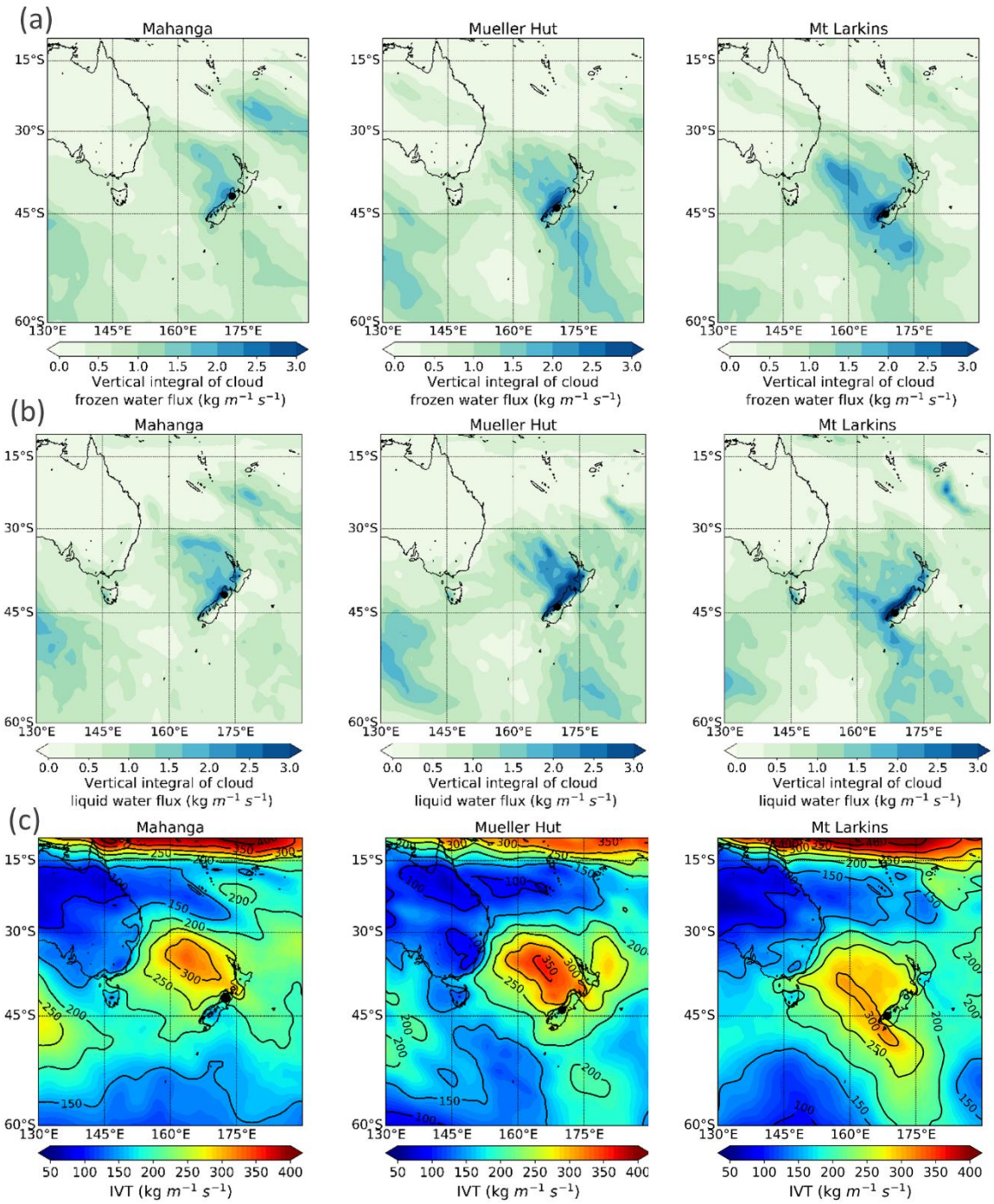

Figure 3.6 Average vertical integral of cloud frozen water flux (VICFWF, kg m^{-1} s^{-1}), (b) average vertical integral of cloud liquid water flux (VICLWF, kg m^{-1} s^{-1}), and (c) average integrated vapour transport (IVT, kg m^{-1} s^{-1}). The average values are calculated during large snowfall events at Mahanga (2009-2017), Mueller Hut (2010-17) and Mt Larkins (2014-2017).

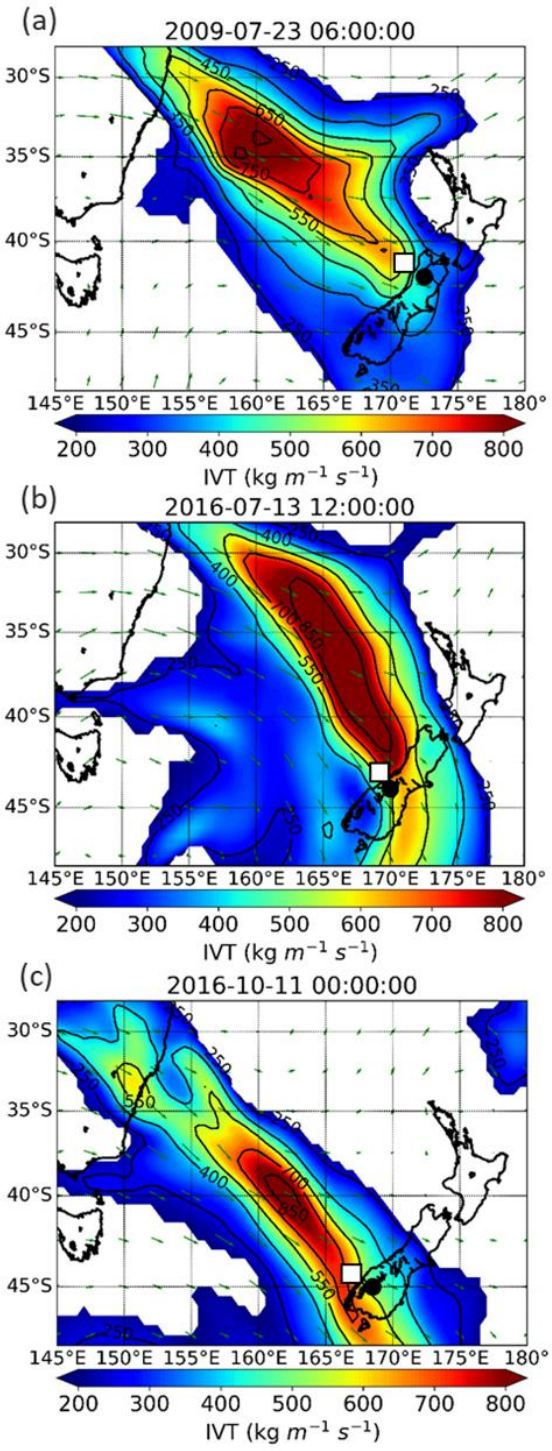

Figure 3.7 Examples of ARs during large snowfall events at (a) Mahanga, (b) Mueller Hut, and (c) Mt Larkins. The black dots mark the locations of snow observation sites, and the white squares mark the locations of the closest grid point on the west coast of New Zealand South Island to each snow observation site. Green arrows indicate the wind vectors at 850 hPa.

3.3.3 Case studies of large snowfall events in the Southern Alps

To further analyse the relationship between snowfall events and ARs three case studies were selected for further investigation. The case studies are the July 2009 snowfall event at Mahanga, the July 2016 snowfall event at Mueller Hut and the October 2016 snowfall event at Mt Larkins. Even though these events were selected based on daily snowfall events at each location the storms associated with these events were usually lasted for more than 24 hours in the Southern Alps.

3.3.3.1 Case study 1: July 2009 snow event

The largest snowstorm recorded at Mahanga station during the study period occurred 23-34 July. The data at Mueller Hut and Mt Larkins were not available at the time of this event. A total amount of 42 cm of snow depth (SD) with an increase of ~8 cm in snow water equivalent (SWE) was recorded at Mahanga over a period of 25 hours between 23-07-2009 06:00 (NZST) and 24-07-2009 07:00 (NZST) (Figure 3.8). The SLP anomalies were computed for the days leading to the event with respect to the 40-year average of cold months (June, July and August). The SLP anomaly patterns reveal a low-pressure system moving eastwards over the Tasman Sea and crossing New Zealand during the snowstorm. The pressure at the centre of the low-pressure system dropped by more than 30 hPa during the snowstorm (Figure 3.9).

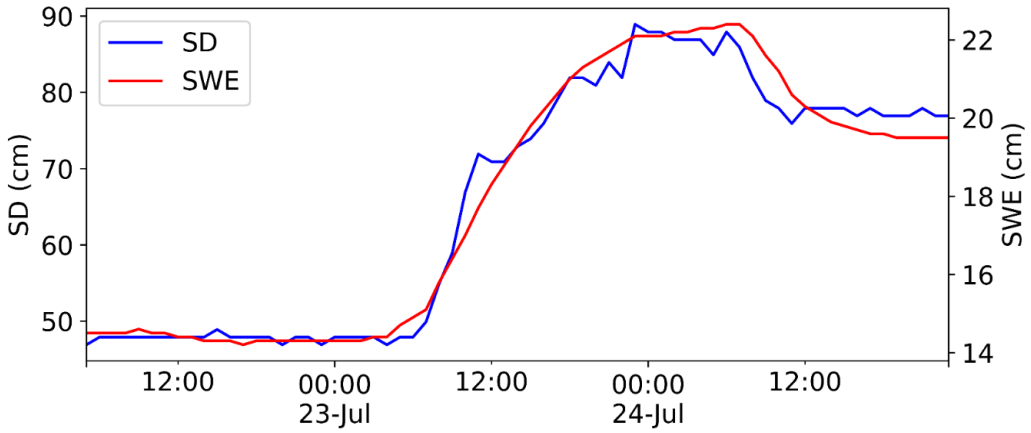

Figure 3.8 Hourly snow depth (SD, cm) and snow water equivalent (SWE, cm) records at Mahanga site during July 2009 snow event.

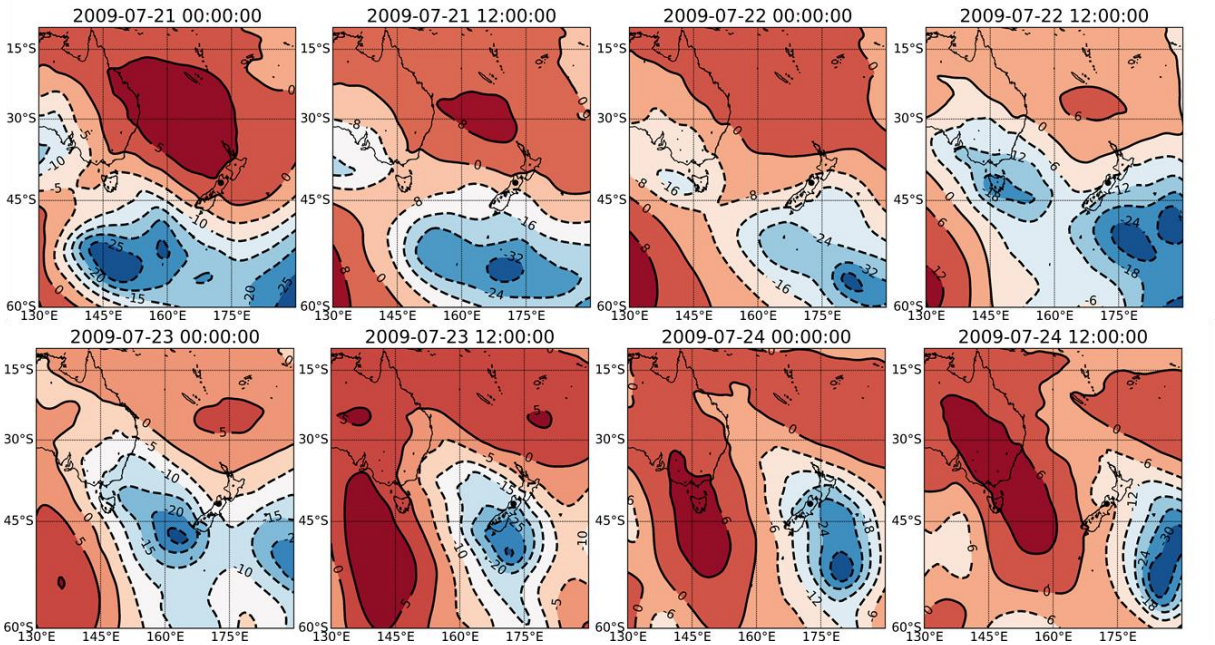

Figure 3.9 SLP (hPa) anomalies from 21st July 2009 to 24th July 2009 (NZST).

3.3.3.2 IVT fields during July 2009 snow event

The six-hourly IVT fields during July 2009 snowfall event are shown in Figure 3.10. The snowfall event was associated with an atmospheric river which made landfall over the Southern Alps on 23 July 2009. IVT values exceeded 900 kg m^{-1} s^{-1} inside the AR over the Tasman Sea. At the location of Mahanga station, the IVT magnitude reached a maximum of 368.8 kg m^{-1} s^{-1} on 2009-07-23 06:00 (NZST); likewise, the calculated IWV shows a fairly high value of 24.5 cm (Figure 3.11). According to the classification scale (Figure 3.4), the AR at Mahanga site is categorized as weak Cat 1 (primarily beneficial). However, along the west coast of South Island, where the AR first made a landfall, the AR reached a maximum of IVT≥500 kg m^{-1} s^{-1} and <750 kg m^{-1} s^{-1} with a duration of approximately 24 h and it AR is, therefore, classified as moderate Cat 2 (mostly beneficial, also hazardous).

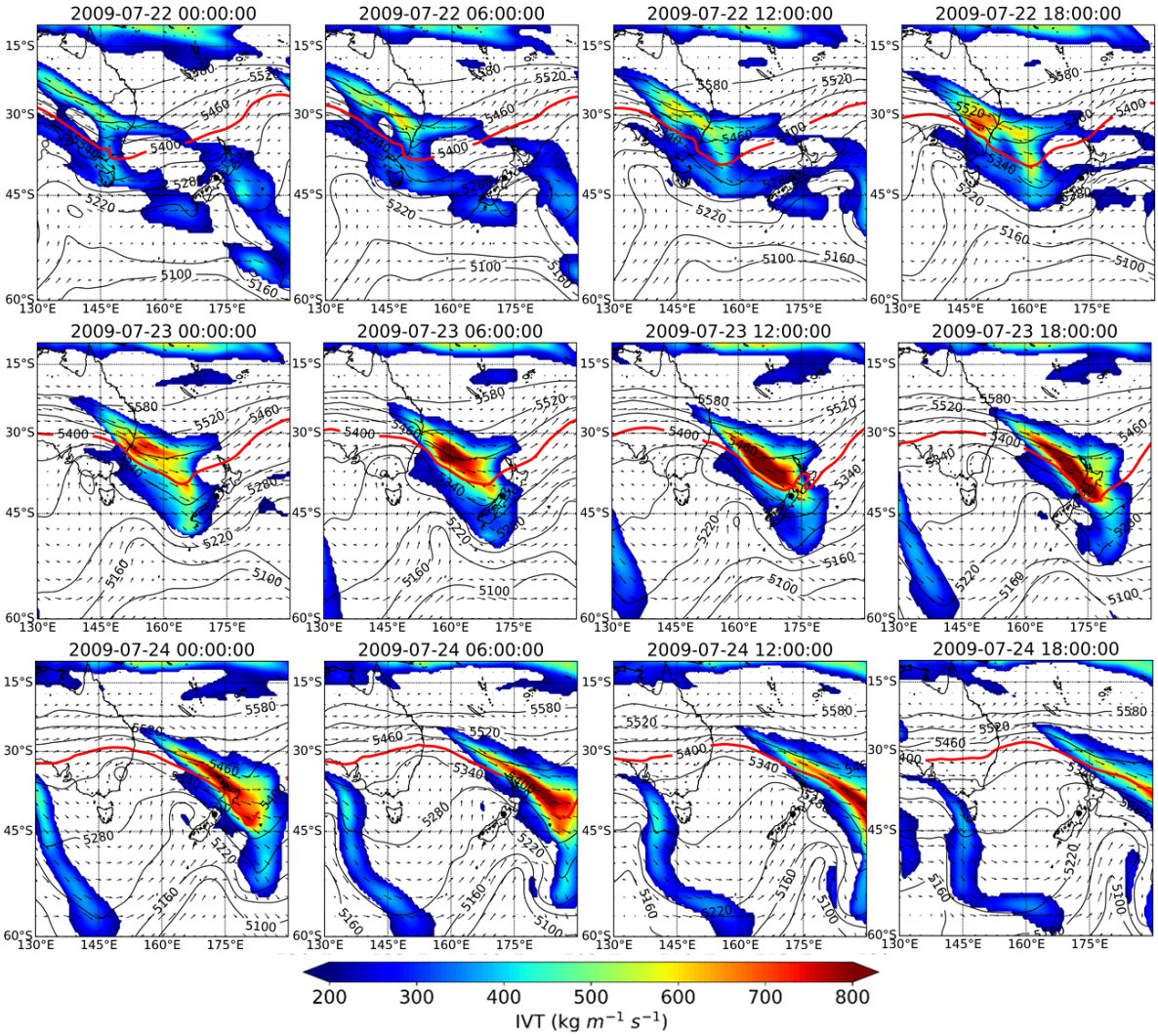

Figure 3.10 Six-hourly IVT and 1000-500 thickness line from 22nd July 2009 to 25th July 2009 (NZST). Contours are the 1000-500 thickness line. The red contour is the 5400 m thickness line showing the boundary between warm and cold air masses.

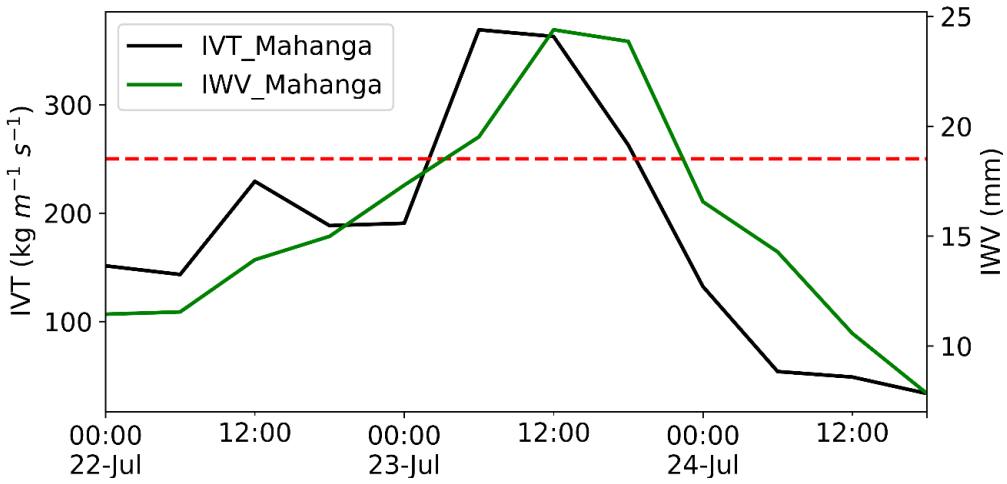

Figure 3.11 IVT and IWV during the 23-24th July 2009 (NZST) snowstorm at Mahanga. The red dashed line is the 232 kg m^{-1} s^{-1} IVT.

3.3.3.3 Profile analysis of July 2009 snowfall event

A mesoscale depiction of the IVT fields from the AR approaching the South Island at 2009-07-23 06:00 (NZST) is shown Figure 3.12a. The IVT values reached magnitudes of 700 kg m^{-1} s^{-1} in the northwest of the South Island. The vertical structure of the AR was examined to identify the positions of moisture plume in the clouds. Figure 3.12b shows the distribution of the specific cloud liquid water content (CLWC) between 1000 and 300 hPa revealing the highest magnitude of the CLWC at 750 hPa (0.07 g Kg^{-1}) at the location of Mahanga site during the event. The vertical profile of the zonal and meridional components of the wind (u and v) during the snowstorm reveals interesting information about the distribution of the wind at different heights. While the zonal component of the wind decreases gradually from 650 hPa (mid-level and low-level jets) the meridional component of the wind (v) show a significant increase with a maximum value of ~19 m s^{-1} at 800 hPa.

One of the important features of AR-related snowstorms is the position of the rain/snow boundary line (5400 m line). The position of rain/snow line or 1000-500 hPa thickness line (red line, Figure 3.12a) marks the boundary between the warm tongue of the air mass and the cold part. Figure 3.12a shows that the southern limit of the

rain/snow line is located at 40° S and 168° E on 2009-07-23 06:00 (NZST) leading to a cold environment favourable for snow precipitation at high altitudes in the north of the South Island. The change in the shape of the thickness line reveals the orographic role of Southern Alps in adiabatic cooling of the warm system approaching the mountain terrains (Figure 3.13).

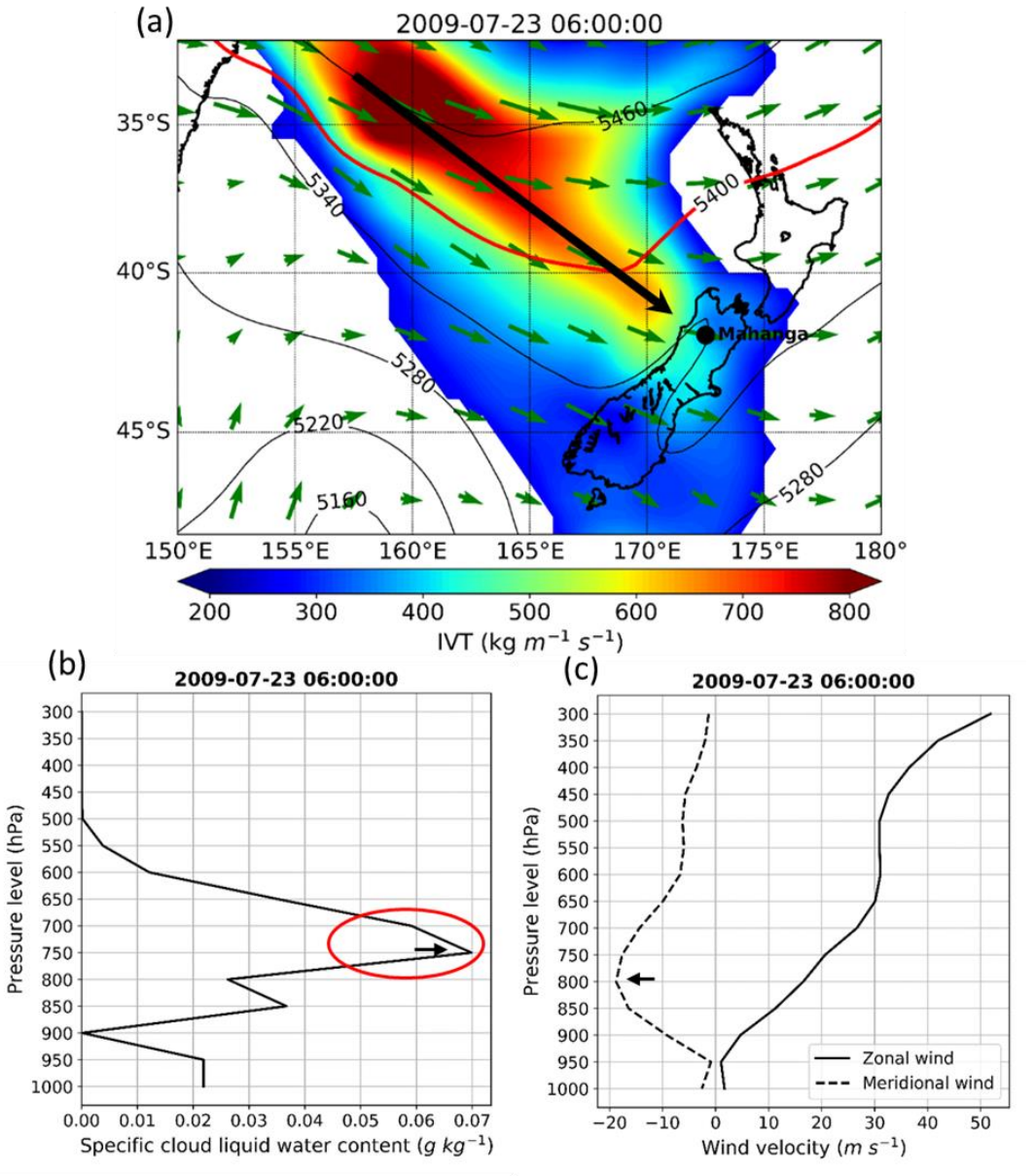

Figure 3.12 (a) Mesoscale plan-view of IVT fields on 2009-07-23 06:00 (NZST). The black arrow show the main direction of the AR approaching the Southern Alps. Green arrows indicate the wind vectors at 850 hPa (b) vertical profile of specific cloud liquid water content (CLWC) at Mahanga, and (c) vertical profile of zonal and meridional wind components at Mahanga.

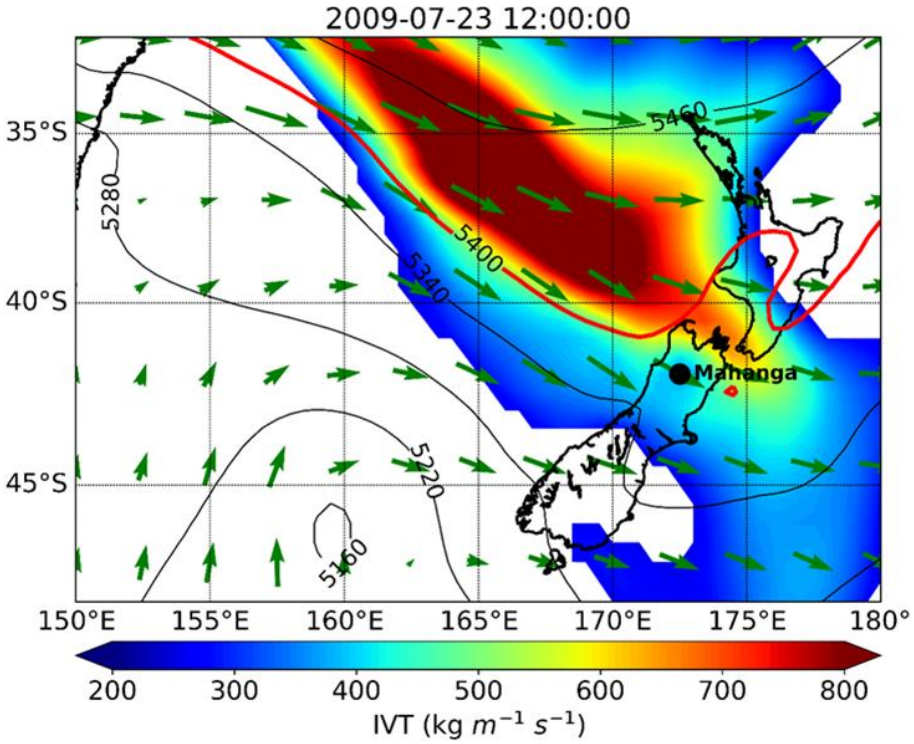

Figure 3.13 Mesoscale plan-view of IVT fields on 2009-07-23 00:12 (NZST). The black dot is the location of Mahanga station.

3.3.3.4 Case study 2: July 2016 snow event

The July 2016 snowstorm is the largest snowfall observed at Mueller Hut during the period of this study. However, the snow accumulated across the Southern Alps between 13th to 15th July (NZST). Figure 3.14 shows the snow depth (SD) and snow water equivalent (SWE) at the three sites. Both Mueller Hut and Mt Larkins received a considerable amount of snow during the event (99 cm at Mueller Hut and 67 cm at Mt Larkins). The observed SWE at Mueller Hut and Mt Larkins reached to 36.2 cm and 14 cm, respectively. At Mahanga an increase of ~10 cm in snow depth and 4.7 cm in SWE was recorded. A lag in snow pillow response to the added weight can be seen during the event compared to the snow depth sensor. A deepening depression moving across the South Pacific Ocean towards the Southern Alps was the dominant synoptic feature of this storm (Figure 3.15). The central pressure plummeted by 40 hPa relative to the 40-year average pressure. Another synoptic feature associated with this event is the presence of a blocking system over eastern New Zealand before the low-pressure system moved

towards the region. The high pressure associated with the blocking system can potentially cause the low-pressure system to move fairly slowly over the Southern Alps and increase the duration of the snowfall event.

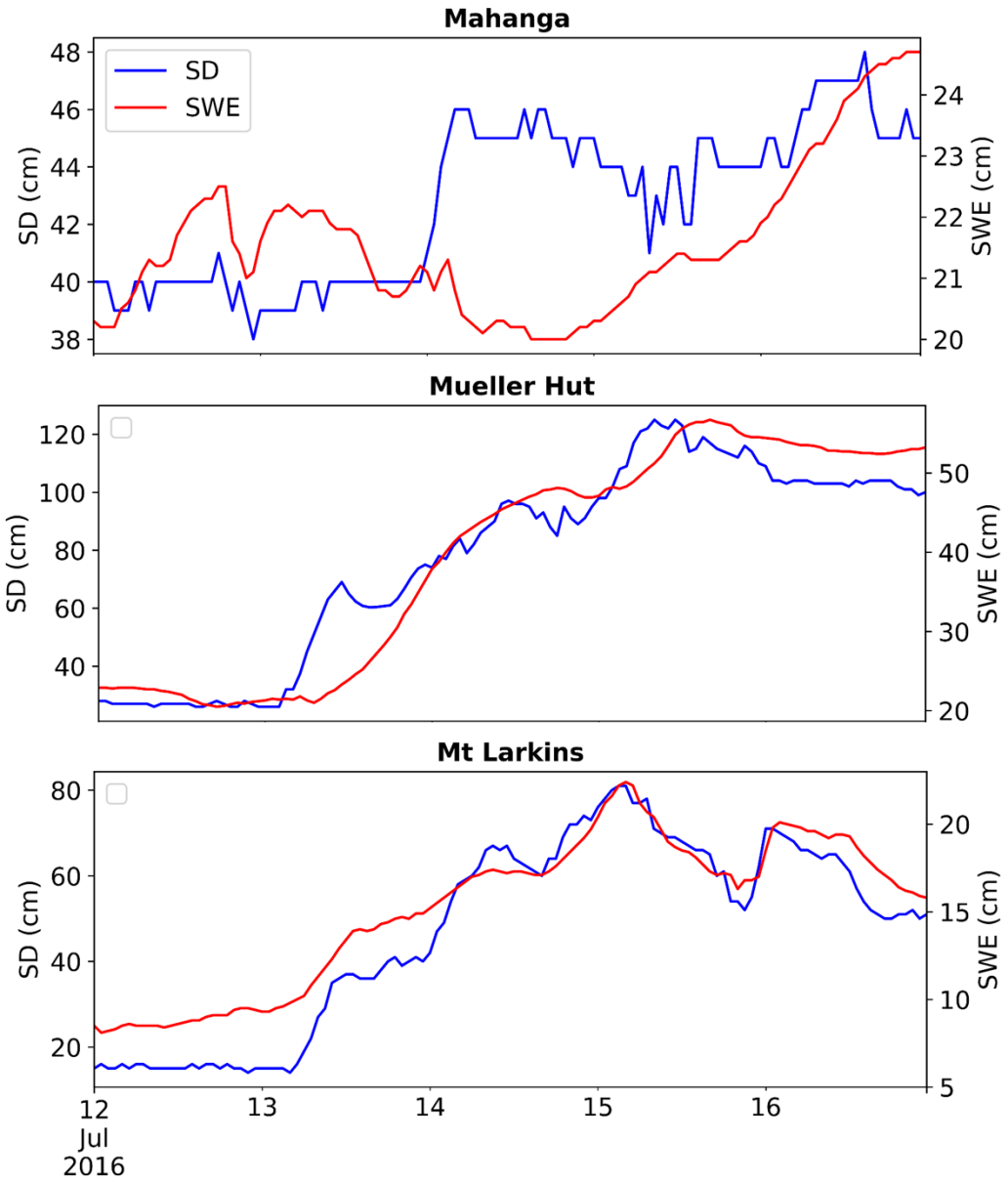

Figure 3.14 Snow depth during the July 2016 snowstorm at three locations (Mahanga, Mueller Hut and Mt Larkins).

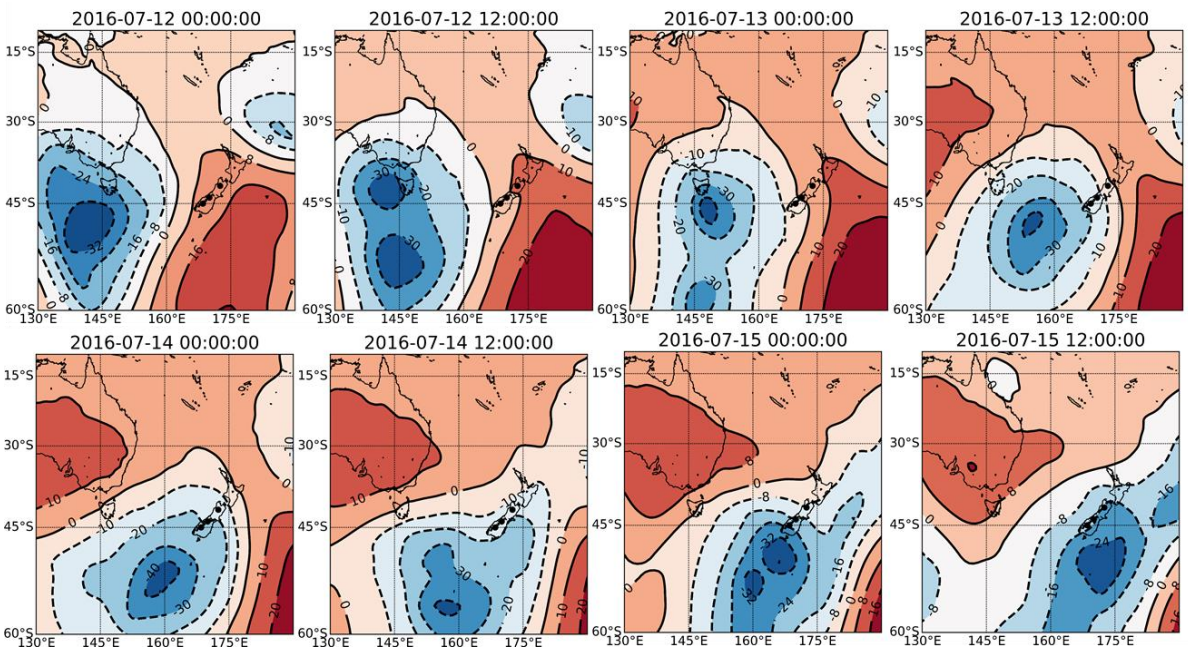

Figure 3.15 SLP (hPa) anomalies from 12th July 2016 to 16th July 2016 (NZST).

In terms of moisture transport during the snowstorm, the six-hourly IVT fields reveal that the landfall of two ARs with distinctive characteristics resulted in a significant snowstorm across the Southern Alps (Figure 3.16). The first atmospheric river is a relatively warmer south-eastward air mass moving towards South Island and making landfall in the Southern Alps on 2016-07-12 00:00 (NZST) and slid towards north-east before leaving the country. The second AR was a colder moisture plume which approached the south-west of the South Island and made landfall over the Southern Alps at 2016-07-14 18:00 (NZST). During the first phase, the maximum IVT in the plume exceeded the magnitude of 1000 kg m^{-1} s^{-1} over the Tasman Sea with a maximum of 1035 kg m^{-1} s^{-1}. Along the west coast of the South Island the IVT values vary within the range of 750-1000 kg m^{-1} s^{-1}. Given the duration of the AR along the west coast (~24 h), the AR is classified as a strong Cat 3 (balance of beneficial and hazardous). Across the Southern Alps the IVT and IWV values show a distinctive spatial distribution (Figure 3.17). Higher values were computed at Mueller Hut (middle of the Southern Alps) and Mahanga (north of the Southern Alps) compared to Mt Larkins (south of the Southern Alps). The maximum 6-hourly IVT and IWV values at the Mueller Hut location reached 556.8 kg m^{-1} s^{-1} and 25 cm, respectively. The AR is regarded as a moderate Cat 2 AR (maximum IVT ≥500

kg m^{-1} s^{-1} and <750 kg m^{-1} s^{-1}, duration ~24 h) at Mueller Hut (mostly beneficial, also hazardous). The second AR associated with the snowstorm river is classified as moderate Cat 1 AR when it reached the west coast of the South Island (maximum IVT ≥500 kg m^{-1} s^{-1} and <750 kg m^{-1} s^{-1}, duration ~18 h). A maximum IVT of ~300 kg m^{-1} s^{-1} with a duration of less than 24h was computed at Mueller Hut; therefore, the AR is categorised a weak Cat 1 AR (primarily beneficial). It is worth noting that even though the landfall of ARs produced large snowfall events at the high altitudes of the Southern Alps, the moisture plumes were also responsible for considerable rainfall events at lower elevations across the west coasts of New Zealand. In a particular case at North Egmont (southwest of North Island) the highest one-day rainfall for the month of July (225 mm) was recorded during the passage of this system.

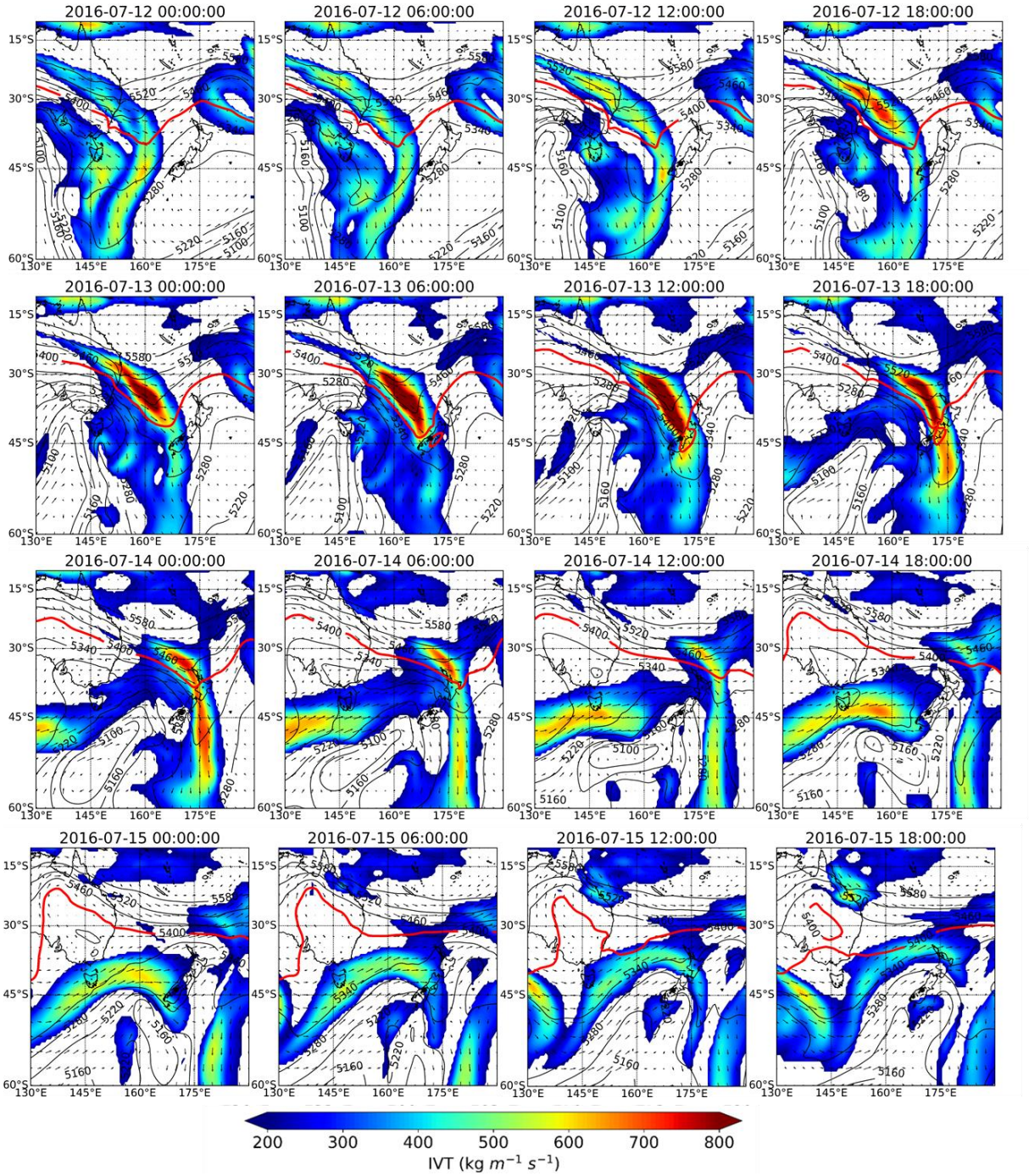

Figure 3.16 Six-hourly IVT (kg m^{-1} s^{-1}) and 1000-500 thickness line from 12th July 2016 to 16th July 2016 (NZST). Contours are the 1000-500 thickness line. The red contour is the 5400 m thickness line showing the boundary between warm and cold airmasses.

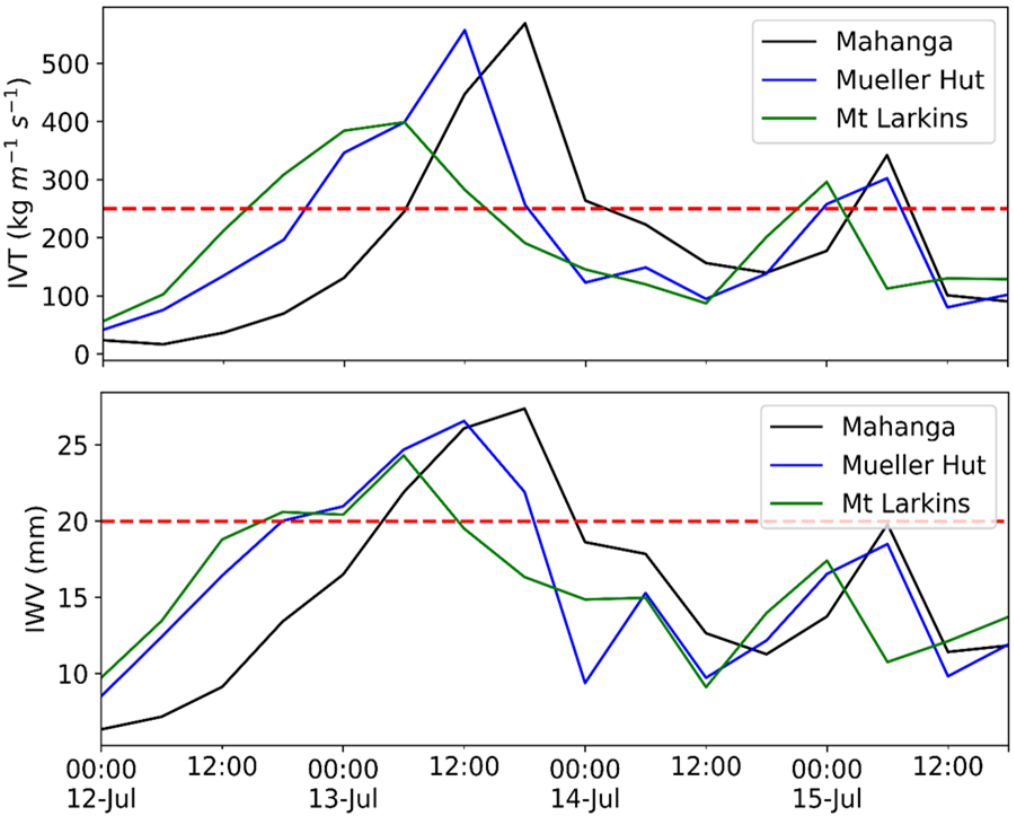

Figure 3.17 IVT (kg m^{-1} s^{-1}) and IWV (mm) during July 2016 snow storm at three locations (Mahanga, Mueller Hut and Mt Larkins).

3.3.3.5 Profile analysis of July 2016 snowfall event

A mesoscale depiction of the moisture plume associated with the July 2016 at 2016-07-13 12:00 (NZST) is shown in Figure 3.18. The noteworthy feature of the AR is the influence of Southern Alps topography in altering the position of the rain/snow boundary line (5400 m line). The vertical distribution of the specific cloud liquid water content (CLWC) indicates a very distinctive higher magnitude of moisture in the clouds in the low- and mid-level troposphere (between 700 and 850 hPa) over the Southern Alps (Figure 3.18b). The highest liquid content of the cloud (~0.65 g Kg^{-1}) was observed at Mueller Hut between 700-750 hPa. The cross section of wind components at three locations are shown in Figure 3.18c. Strengthening meridional wind speeds are distinctively identifiable between 750-800 hPa. The meridional wind speed fields show a surge with a value of ~28-30 m s^{-1} between 750-800 hPa at the location of Mueller Hut.

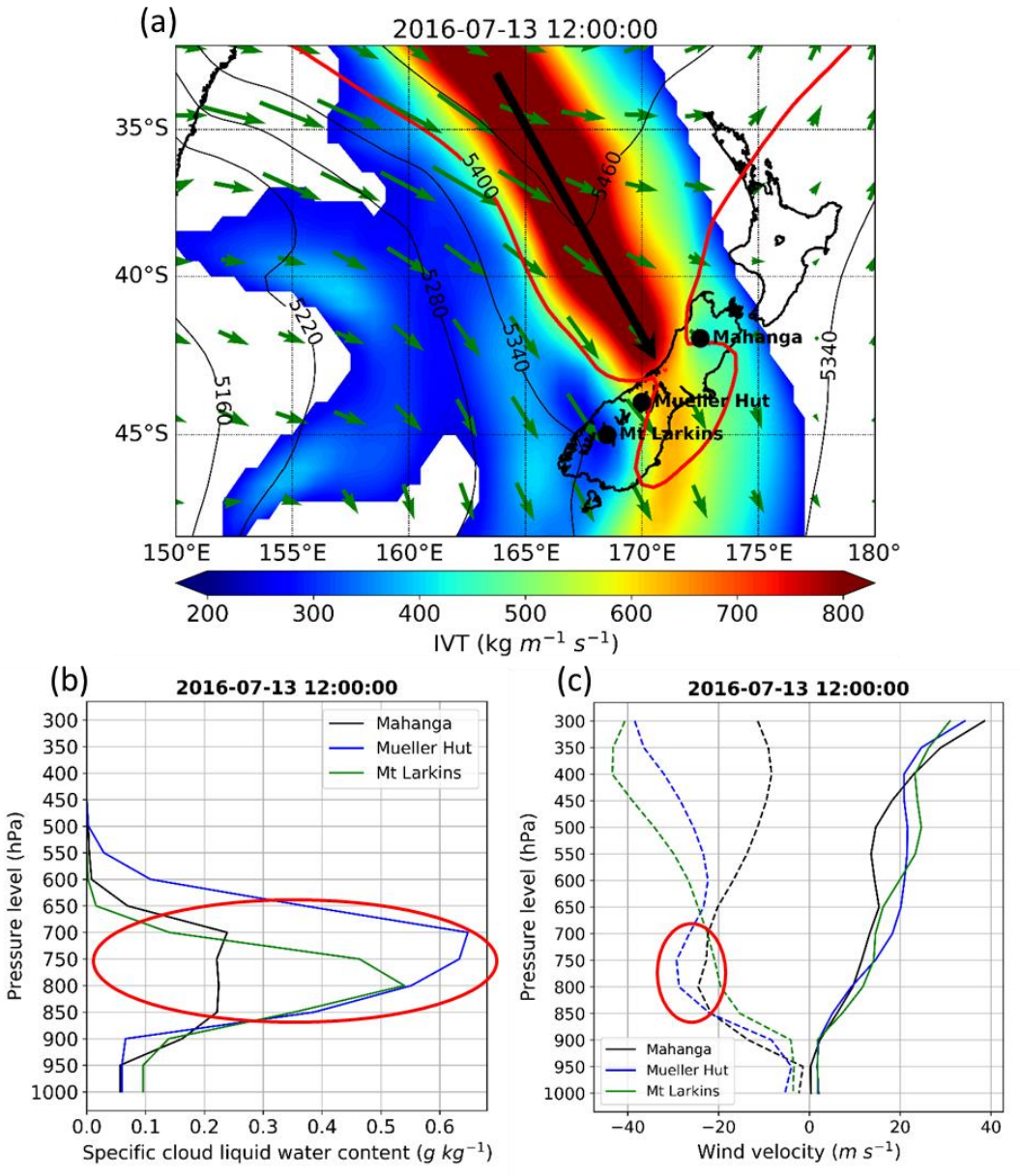

Figure 3.18 (a) Mesoscale plan-view of IVT (kg m^{-1} s^{-1}) on 2016-07-13 12:00 (NZST), (b) vertical profile of specific cloud liquid water content (g kg^{-1}) at three locations (Mahnaga, Mueller Hut and Mt Larkins), and (c) vertical profile of zonal and meridional wind components (m s^{-1}) at three locations.

The strong northwesterly flow was followed by a weaker moisture flux (IVT <300 kg m^{-1} s^{-1}) but colder (the thickness line between 5280-5340 m over the Southern Alps) water vapour plume (Figure 3.19a). However, similar to the first phase, there seems to be high concentration of moisture at lower troposphere (800 hPa) (see Figure 3.19b). Also, lower meridional wind velocities (less than 15 m s^{-1}) and stronger

zonal wind velocities (~20 m s^{-1}) compared to first phase of the snowstorm were identified at 800 hPa (Figure 3.19c).

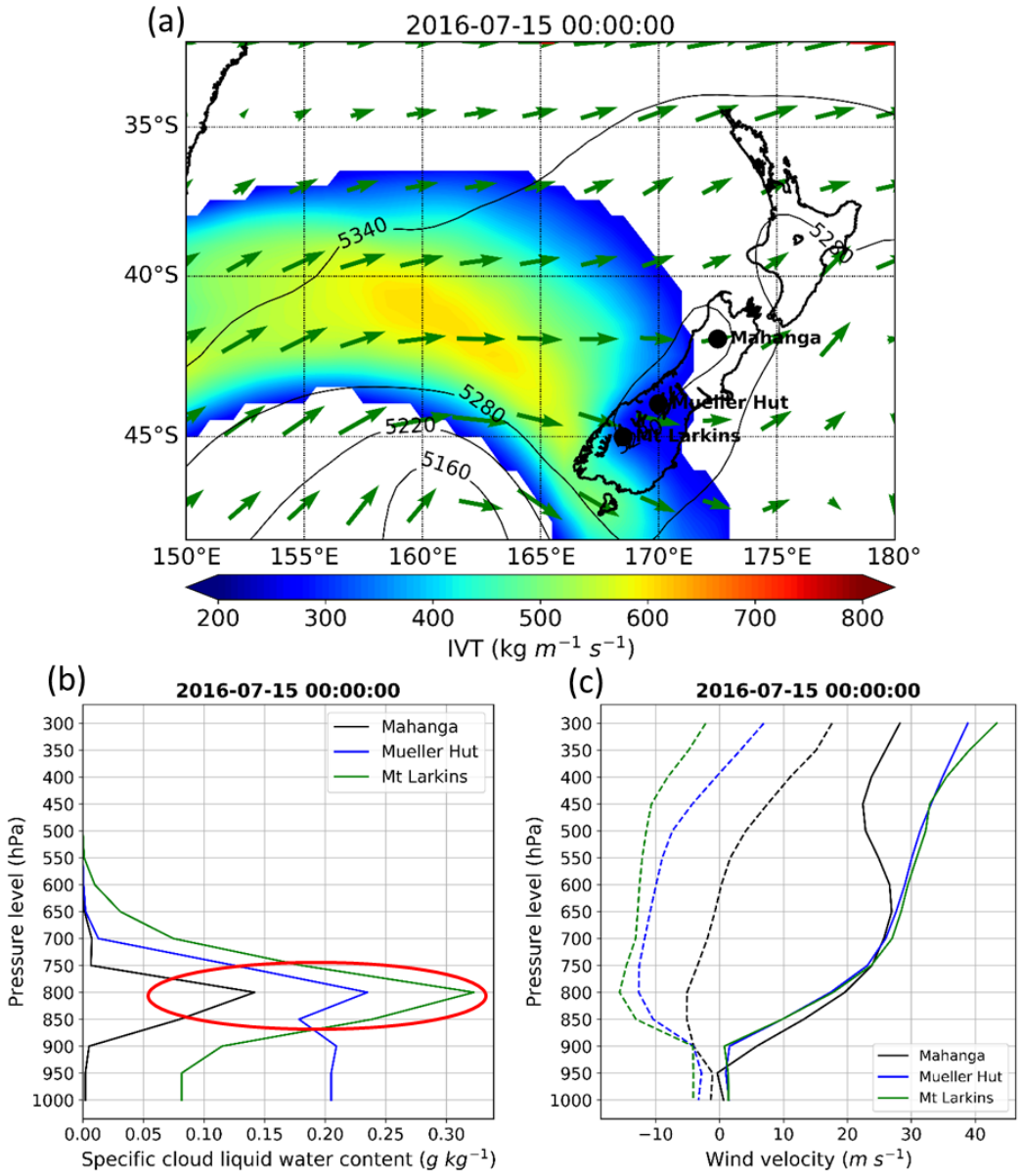

Figure 3.19 (a) Mesoscale plan-view of IVT (kg m^{-1} s^{-1}) on 2016-07-15 00:00 (NZST), (b) vertical profile of specific cloud liquid water content (g kg^{-1}) at three locations (Mahanga, Mueller Hut and Mt Larkins), and (c) vertical profile of zonal and meridional (dashed lines) wind components (m s^{-1}).

3.3.3.6 Case study 3: October 2016 snowfall event

The October 2016 snowstorm brought considerable snow to the Southern Alps. Figure 3.20 shows the snow depth (SD) and snow water equivalent (SWE) observations during the event at the three study locations. The snowfall event is the largest snowfall event

recorded at Mt Larkins with a total snow accumulation of 108 cm and a 17.2 cm increase in snow water equivalent. Also, the Mueller Hut site received significant snow with ~70 cm increase in SD and ~8 cm in SWE. Despite considerable snow accumulation at Mt Larkins and Mueller Hut, the AR led to rainfall events farther north at the location of Mahanga site. Rain-on-snow (ROS) processes resulted in a positive change of SWE with decreasing snow depth at Mahanga. Afterwards, a decrease in SWE due to rapid snowmelt began in the following days after the ROS event.

The event was the result of a low-pressure system with a very deep centre at which the pressure was more than 40 hPa below the long term average (Figure 3.21). The depression moved southeast from south of the Tasman Sea towards the New Zealand region. Figure 3.22 shows the track of IVT fields prior and during the snowfall events. An AR with an exceptionally high moisture flux (core IVT values exceeding 1900 kg m^{-1} s^{-1}) travelled rapidly south-eastward from the south of Australia. Interestingly, unlike the ARs associated with July 2009 and July 2016 snowfall events, this AR did not initially cross the west cost of the South Island. The spatial distribution and transport of moisture during the days prior to the snowstorm shows the passage of the AR at lower latitudes as it passed the south of the South Island. Afterwards, the intense water vapour plume moved north-eastward and made landfall over the Southern Alps leading to considerable snow accumulation in the high altitudes of southern and central terrains of the Southern Alps. The AR is categorized a strong Cat 3 AR (maximum IVT ≥750 kg m^{-1} s^{-1} and <1000 kg m^{-1} s^{-1}, duration of ~24 h) along the southwest coast of the South Island. The values of IVT and IWV during the passage of the atmospheric river over the region at three sites are shown in Figure 3.23. A maximum IVT of 500 kg m^{-1} s^{-1} was calculated at Mt Larkins on 11-10-2016 00:00 (NZST). A similar value of IVT (480 kg m^{-1} s^{-1}) was recorded at the Mueller Hut location on 11-10-2016 12:00 (NZST). Based on the duration and maximum IVT values, the AR was categorized as moderate Cat 2 at Mt Larkins and weak Cat 1 at Mueller Hut.

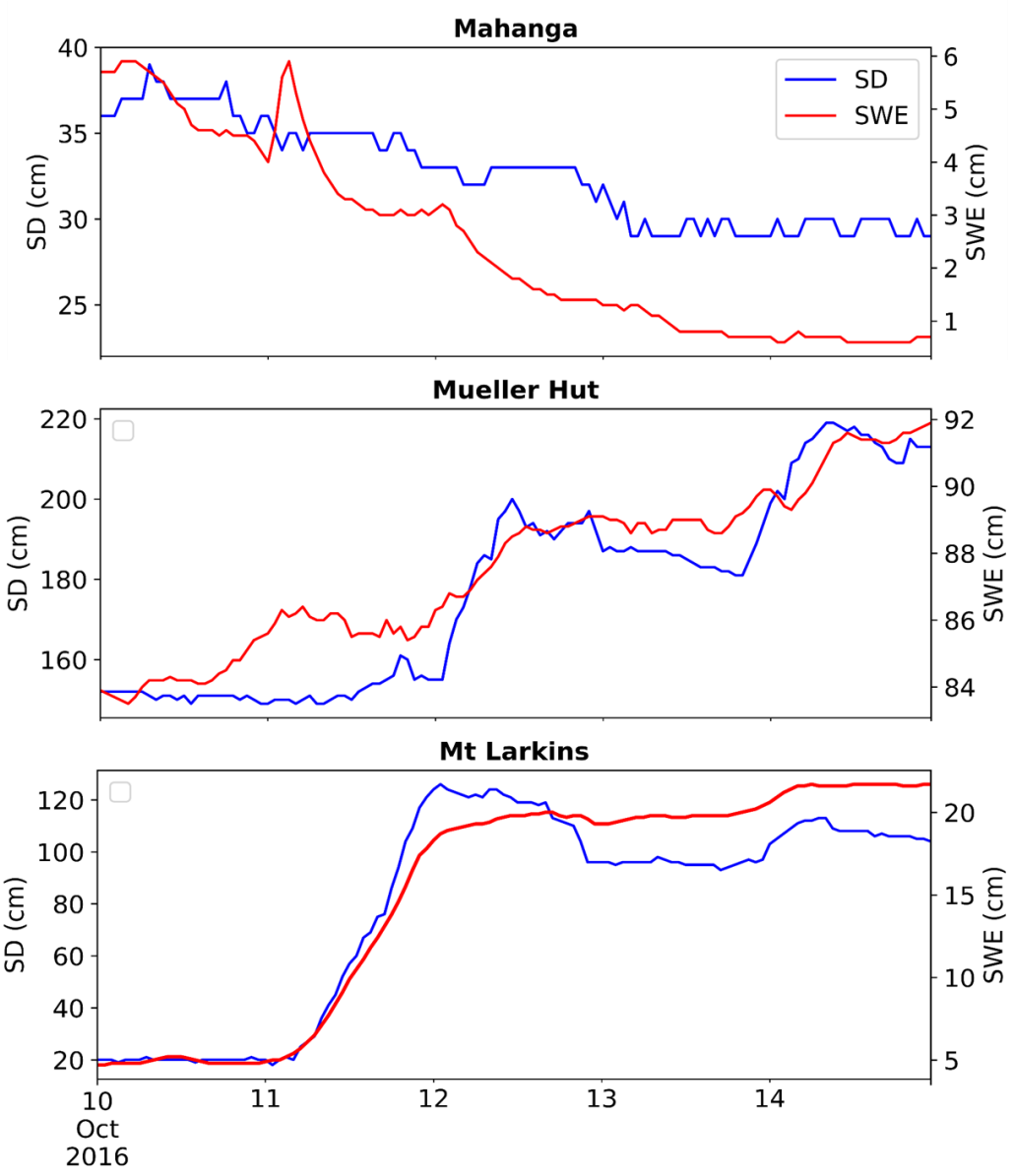

Figure 3.20 Snow depth (cm) and snow water equivalent (cm) during October 2016 snowstorm at three locations (Mahanga, Mueller Hut and Mt Larkins).

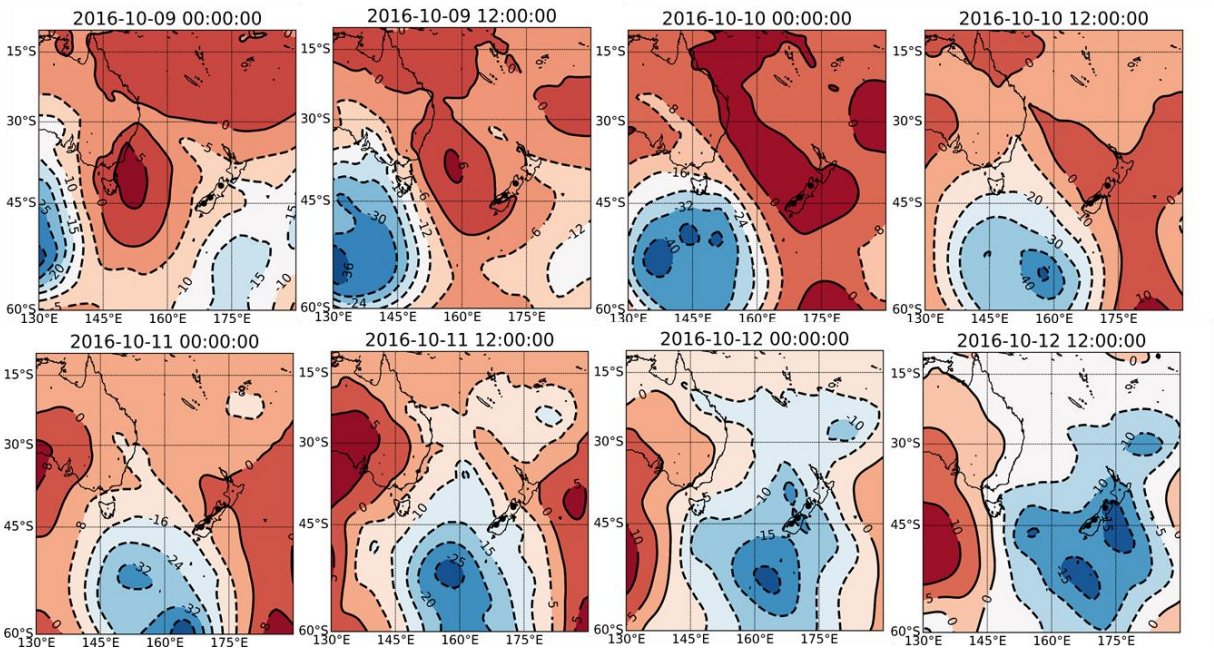

Figure 3.21 SLP (hPa) anomalies from 9th October 2016 to 13th October 2016 (NZST) showing the low pressure system during the storm.

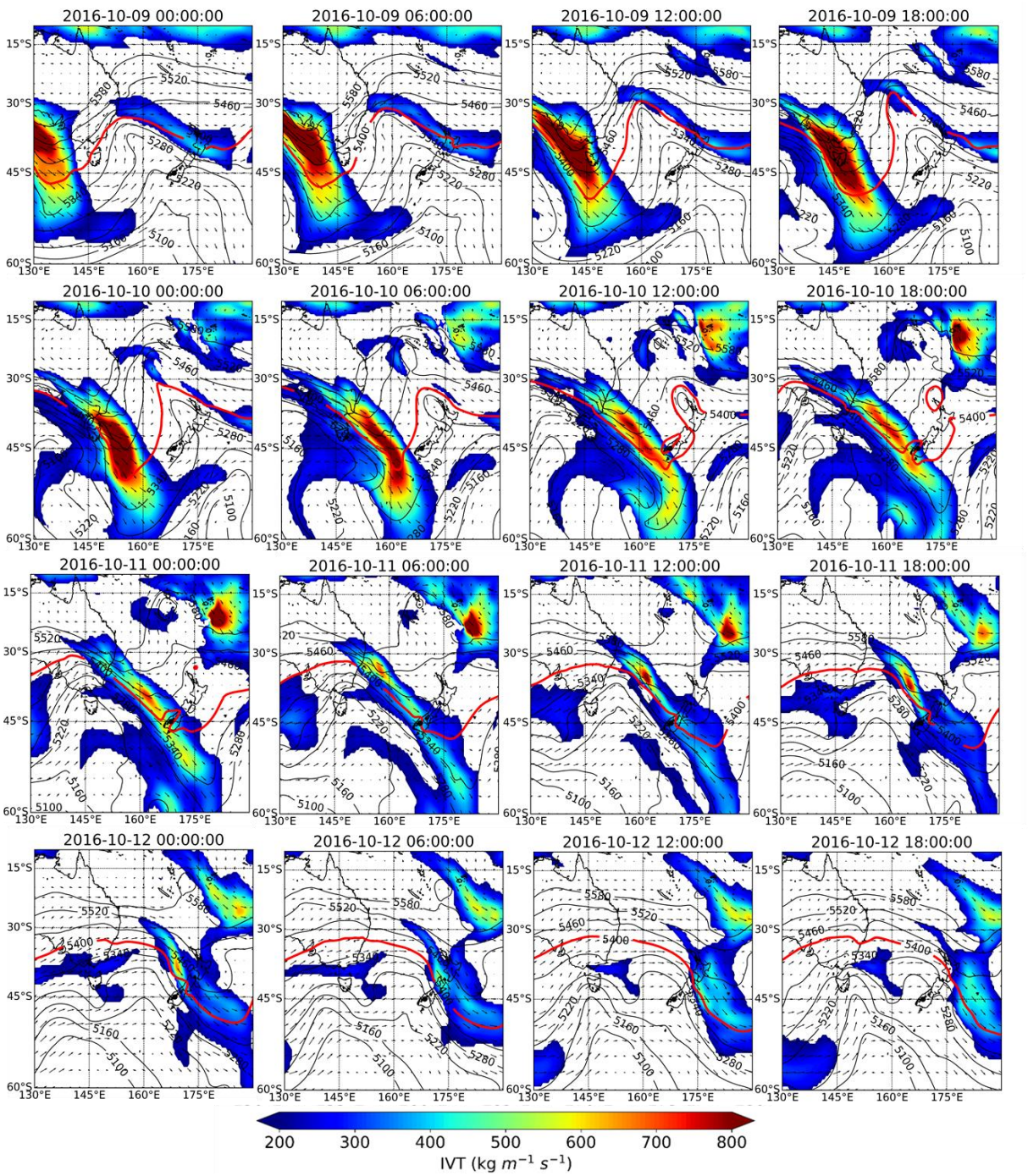

Figure 3.22 IVT (kg m^{-1} s^{-1}) and 1000-500 thickness line from 9th October 2016 to 13th October 2016 (NZST).

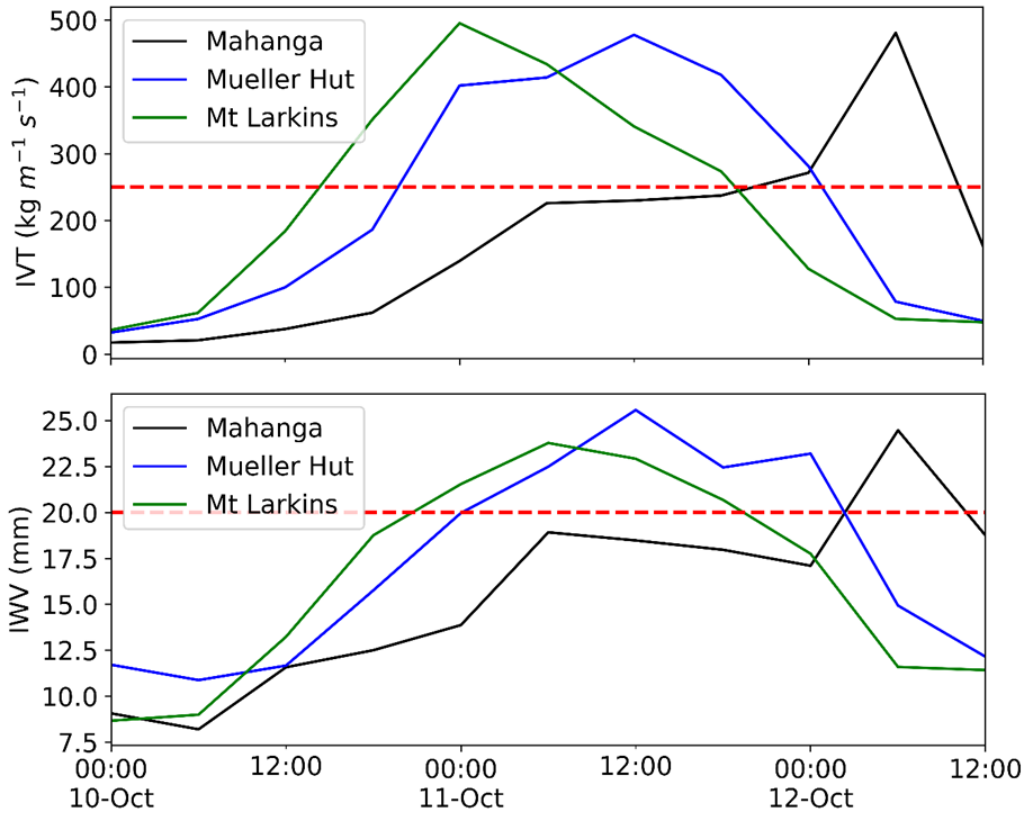

Figure 3.23 IVT (kg m^{-1} s^{-1}) and IWV (mm) at three locations (Mahanga, Mueller Hut and Mt Larkins) during October 2016 event.

3.3.3.7 Profile analysis of October 2016 snowfall event

A meso-scale view of the AR associated with the snowfall event at 11-10-2016 00:00 is shown in Figure 3.24 as the ARs crossing the Southern Alps. Figure 3.24a shows the changes in the shape and position of the 1000-500 hPa line (5400 m line) dictated by the topography of the Southern Alps. The position of the 5400 m line is an important feature of ARs during cold months determining the melting level in the atmosphere. During the October 2016 event the 5400 m line lies at lower latitudes of the Southern Alps. This condition explains why high altitudes at farther north latitudes receive liquid precipitation during the event (e.g. Mahanga: ~50 mm).

Similar to July 2006 and July 2016 snowfall events, a key feature of the AR associated with the October event is the accumulated water content of the clouds between 700-850 hPa (Figure 3.24b), further highlighting the importance of mid-level jet streams in transporting moisture across the Southern Alps during precipitation. Strengthening

values of meridional wind components between 750-800 hPa is another characteristic of the AR. At this level the meridional component of the wind (v) of the wind rose up to a value of ~26 m s^{-1} at the location of Mt Larkins during the passage of the moisture plume on 11-10-2016 00:00 (Figure 3.24c).

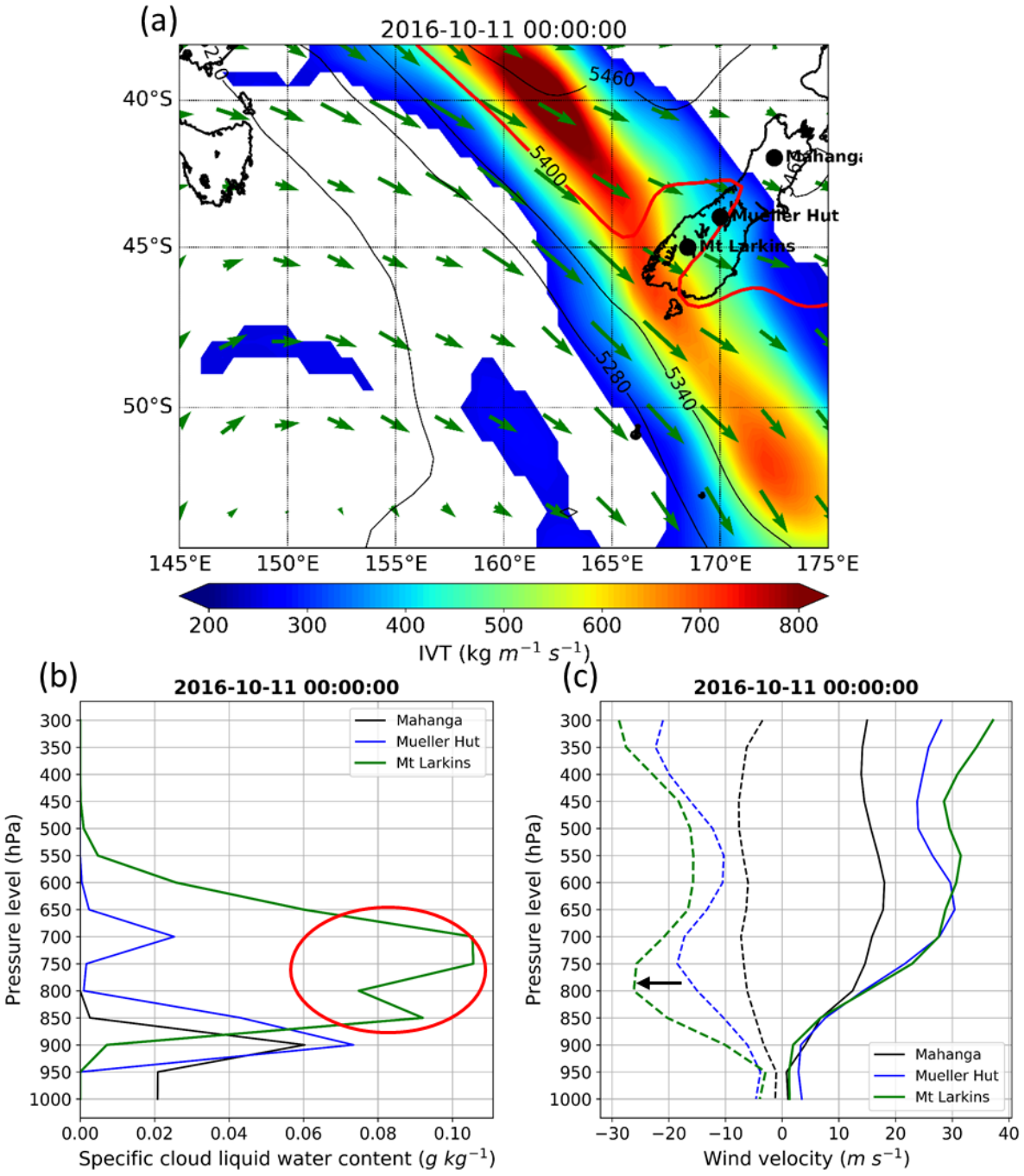

Figure 3.24 Mesoscale plan-view of IVT (kg m^{-1} s^{-1}) on 2016-10-11 00:00 (NZST), (b) vertical profile of specific cloud liquid water content (g kg^{-1}) at three locations, and (c) vertical profile of zonal and meridional (dashed lines) wind components(m s^{-1}).

3.4 Discussion

The characteristics of moisture transport during the large snowfall events (90th percentile value of daily snowfalls) across the Southern Alps was explored. Data from three Snow and Ice Monitoring Network (SIN) sites spatially distributed along the length of the Southern Alps have provided valuable observations of the seasonal snow across the region. The strengthening fields of the vertical integral of eastward cloud water flux during the large snowfall events (Figure 3.6) supports the findings in previous studies (Griffiths and Mcsaveney, 1983; Henderson and Thosmson, 1999; Little *et al.*, 2019) that north-westerly and westerly air masses are the main source of water vapour during winter precipitation. The majority of daily snowfall events in the Southern Alps (~70%) are associated with ARs and their large-scale water vapour transport across the Tasman Sea. The key role of ARs in winter precipitation of the Southern Alps are in line with previous studies in other parts of the world such as Eastern Antarctica (Gorodetskaya *et al.*, 2014), western United states (Guan *et al.*, 2013; Backes *et al.*, 2015; Hansen, 2016) and South American Andes (Viale and Nuñez, 2011) where a large fraction of total annual snow accumulation is received amidst the landfall of several ARs during a snow year. The magnitude of maximum IVT during the snowstorms rarely exceeds 1000 kg m^{-1} s^{-1} along the west coast of the South Island. The majority of the maximum IVT remains just below 500 kg m^{-1} s^{-1} at the locations of the snow observations across the Southern Alps. These results are in broad consistency with a recent study on Brewster glacier, located on the west flank of the Main Divide of the Southern Alps. Little *et al.* (Little *et al.*, 2019) showed that the IVT magnitude during the 5 most extreme snowfall events at Brewster glacier between October 2010 to September 2012 were within 250-500 kg m^{-1} s^{-1}.

Synoptic and meso-scale analyses of atmospheric conditions during three specific case studies found that strong fields of IVT within a north-westerly airflow and concomitant low pressure systems provide favourable conditions for large snowfall events in the Southern Alps. The formation of deep lows over the southwest of the South Island has

similar characteristics during the large snowfall events (Figure 3.9, Figure 3.15, Figure 3.21). Additionally, analyses of vertical structure of moisture transport provide a new framework to enhance our understanding of hydrometeorological attributes of ARs in the Southern Alps. The consistency of presence of moisture at low and mid-level jet streams (700-850 hPa) were identified during three case studies. Also, a distinctive increase of meridional winds between 750-850 hPa was found across the Southern Alps during the large snowfall events (Figure 3.12c, Figure 3.19c, and Figure 3.24c). The enhanced fields of meridional winds (up to 30 m s^{-1}) revealed that they are a main driver responsible for transporting moisture across the South Pacific Ocean towards the Southern Alps. These characteristics of AR-associated snowfall events in the Southern Alps are generally similar to those findings reported from different locations of the world such as Mount Shasta and Sierra Nevada in California, United States (Backes *et al.*, 2015; Hansen, 2016), and Central Andes (Viale and Nuñez, 2011) where the low-level tropospheric water transport with a strong component of the meridional wind were found during large snowfall events. These findings can be used for predicting extreme snowfall events in similar maritime environments.

ARs at mid-latitudes of the Southern Alps are transient features with a typical life-span of less than 36 hours. However, the existence of a high-pressure system over and to the east of New Zealand can slow down the low-pressure system and its associated AR as it travels southeast (e.g. July 2016 snowfall event). This, consequently, increased the duration of the weather system over the region compared to the two other cases (July 2009 and October 2016). The duration of the AR at a given location combined with the intensity of the IVT values is the controlling factor in classifying ARs. According to the classification scale of Ralph *et al.* (2019), the ARs associated with large snowfall events were Cat 2 (July 2009) and Cat 3 (July 2016 and October 2016) along the west coast of the South Island. However, they were categorised as weak and moderate Cat 1 (July 2009) and Cat 2 (July 2016 and October 2016) at the location of the weather stations suggesting

that these ARs are mainly beneficial in terms of hydrological impacts in alpine catchments by providing solid precipitation at high altitudes.

However, it is worth noting that they could also result in flooding events at lower altitudes and along the coast where the majority of winter precipitation falls in liquid form. Ralph *et al.*, (2019) highlighted the fact that the position of rain/snow line can influence the classification scheme. The position of the rain/snow line is a key feature during the winter precipitation in the maritime Southern Alps because of the proximity of the mountains to the ocean due to the narrow length of the South Island.

Perhaps the most noticeable characteristics of ARs when travelling over the Southern Alps is the position and shape of the 1000-500 hPa thickness line (5400 m line). A striking similarity can be seen during the large snowfall events (July 2009: Figure 3.13, July 2006: Figure 3.18a, October2016: Figure 3.24). The shape of the rain/snow line is dictated by the Southern Alps topography and the snowfall events occur in the cold side of the boundary line. The maritime characteristics of weather patterns in New Zealand's South Island results in a condition where the position of the 1000-500 thickness line during snowfall events is significantly sensitive to temperature variations. Even though the majority of AR-related winter storms studies here produced large snowfall events at higher altitudes of the Southern Alps, the same weather systems concurrently led to intense rainfall events on the adjacent coastal regions on the west coast.

Also, at high altitudes, the phase of the winter precipitation is largely influenced by the position of the rain/snow line. During October 2016 event, when the AR first made landfall in the southwest of the South Island and then moved north, the position of the rain/snow line made a large distinction between phases of the precipitation (solid or liquid). Despite the fact that all three locations are located at somewhat similar altitudes Mt Larkins and Mueller Hut sites received a considerable amount of snow during this event while the precipitation mainly fell in the liquid form at Mahanga site resulting in a rain-on-snow (ROS) condition. This highlight the importance of an accurate assessment

of rain/snow line during winter and spring precipitation in the maritime environments such as Southern Alps where the majority of large snowfall events occur at temperature near 0 °C.

This condition can potentially result in more rainfall events above the snowline in the region especially during winter and spring compared to continental environments providing conditions susceptible for intense flooding events due to ROS at higher altitudes. Even though, previous studies have shown the frequent occurrence of winter ROS in the Southern Alps (Moore and Owens, 1984); knowledge gaps have remained regarding the impacts of such events on alpine hydrology of the Southern Alps. Several studies have predicted significant changes across the globe in the trend and frequency of ARs due to a warming climate (Lavers *et al.*, 2013, 2015; Espinoza *et al.*, 2018). The sensitivity of AR-related snowfall events to small changes in temperature in the Southern Alps shown in this study provides evidence that a warming climate can pose a major threat to the future of seasonal snowpacks as more AR-related snowfall events will turn into rain events.

3.5 Summary and conclusions

It is generally understood that ARs are important in hydrological events in the mid-latitude regions. In this study, the focus was placed on recognizing the role of ARs in solid precipitation of the Southern Alps. Daily snow observations from three locations across the Southern Alps were combined with atmospheric variables from ERA-Interim reanalysis data to investigate the moisture transport during large snowfall events. Comparing the average annual sum of large snow events with the total annual snow accumulation indicates that such events could account for up to 40% of the total snow accumulation throughout a snow year highlighting their relative importance in winter precipitation over the Southern Alps. The occurrence of snow events in the Southern Alps is significantly influenced by atmospheric forcing over the Tasman Sea. Strong fields of IVT responsible for moisture transport, accompanied by low pressure systems centred in

west and southwest of the New Zealand's South Island are the main driver of large snowfall events over the Southern Alps. Findings provided further evidence about the strong connection between winter-time large snowfall events and landfalling ARs in the Southern Alps, where a majority of such large snowfall events were resulted from narrow and strong moisture flux traveling across the Tasman Sea toward the Southern Alps. The frequent occurrence of ARs during large snow events across the Southern Alps indicates the key role of meridional water transport for precipitation. The moisture transport within a predominantly north-westerly airflow is a significant contributing component during large snowfall events. Meso-scale analysis shows that low and mid-level jet streams play a critical role in transferring moisture across the South Pacific Ocean over Tasman Sea prior to large snowfall events in the Southern Alps. The close relationship between ARs and large snowfall events has implications on predictability of extreme winter precipitation in the Southern Alps. Since the position and strength of water vapour flux inside an AR impact the magnitude of incoming moisture available for precipitation, the findings of this study can be used to complement operational forecasting models for predicting large snow events in the maritime conditions.

One of the main features of AR-related snow storms is their relatively warmer nature in comparison to the non-AR counterparts (Guan *et al.*, 2016) which explains their temperature being close to the freezing/melting line. The results presented here focused exclusively on large snowfall events. Our analysis of an AR-related storm indicated the sensitivity of such events to small changes in temperature in the maritime Southern Alps. Future work would address the frequency of winter-time ARs making landfall in the region and their potential role in producing rain rather than snow at higher altitudes. Investigating the rain/snow threshold temperature could provide a robust understanding of the dynamic behaviour of freezing/melting transition in such temperate environments where seasonal snowpacks are under a serious threat due to projected climate change.

4 The influence of synoptic-scale atmospheric forcing on snowmelt in the Southern Alps

Abstract

Large snowmelt events play an important role in controlling hydrological processes of alpine catchments. Variability in timing and magnitude of such events is largely influenced by synoptic-scale atmospheric patterns. In the New Zealand Southern Alps, large snowmelt rates (greater than 90th percentile of daily snowmelt) are observed during both typical spring-melt and winter-melt events. Using a composite anomaly approach, this study has identified the atmospheric circulation patterns during large snowmelt events in the Southern Alps. Findings show that while days with above normal pressures associated with anticyclonic systems account for the majority of snowmelt events, the highest winter-melt and spring-melt rates (up to 330 mm day^{-1}) occurred mainly during troughing regimes with below normal pressure. Anomaly analysis of temperature of the atmospheric column shows rising mid- and low-tropospheric temperatures (at 500, 700 and 850 hPa) during both high-pressure and troughing systems associated with large snowmelt in the Southern Alps.

4.1 Introduction

The Southern Alps of New Zealand host the largest snow and ice fields in the Southern Hemisphere outside the Antarctic and South America (Fitzharris *et al.*, 1999). Even though the contribution of snowmelt to river flows in the Southern Alps is lower compared to other typical alpine catchments such as European Alps (Penna *et al.*, 2016; Beniston *et al.*, 2018), western United States (Bales *et al.*, 2006) and Himalayan catchments (Siderius *et al.*, 2013; Bharati *et al.*, 2014; Adnan *et al.*, 2017) meltwater from seasonal snowpacks can contribute up to 40-50% of the discharge in upper alpine catchments which in turn feed major rivers in the Southern Alps (Fitzharris and Garr, 1995; Sirguey, 2009). This contribution has been found to play an important role in water supply for hydroelectricity and agriculture schemes in the Southern Alps (Neale and Fitzharris, 1997; Clark *et al.*, 2009; Poyck *et al.*, 2011; Kerr, 2013). Surrounded by the Pacific Ocean, upper terrains of the Southern Alps have provided a unique opportunity to

investigate the snow hydrology processes in a typical maritime condition. One of the most important aspects of snow hydrology is the basic knowledge of climate controls affecting snowmelt processes (DeWalle and Rango, 2008). Maritime snow-dominated regions are strongly influenced by ocean-atmosphere interactions resulting in warmer and moister snowpacks compared to continental regions (Fitzharris *et al.*, 1999; Cohen *et al.*, 2015; Cullen and Conway, 2015; Fayad *et al.*, 2017; Pall *et al.*, 2019). A small change in temperatures could render the snow patterns in such areas, with a high likelihood of snow accumulation and more episodes of winter melt. With the projection of more episodes of winter melt and early snowmelt associated with climate warming (Stone *et al.*, 2002; Barnett *et al.*, 2005; Knowles *et al.*, 2006; Clow, 2010; Nayak *et al.*, 2010; Hendrikx and Hreinsson, 2012; Ministry for the Environment, 2016; Hock *et al.*, 2019), a robust understanding of weather patterns influencing snowmelt processes is therefore essential. Rapid snowmelt episodes, in particular, have considerable economic impacts in snow-dominated regions through increasing the risk of winter and spring flood events and/or reducing sustainable river flows in spring and summer months (Fitzharris *et al.*, 1980; Grundstein and Leathers, 1998; Guan *et al.*, 2016).

Snowmelt processes are generally controlled by the exchange of energy between snowpack and its surrounding environment. The transfer of energy from synoptic-scale processes in the atmosphere to the land surface has been found to be an important source of energy for snowmelt (Grundstein and Leathers, 1998, 1999; Romolo *et al.*, 2006a; López-Moreno and Vicente-Serrano, 2007). Such large-scale characteristics of the weather systems can be predicted more accurately compared to local point-scale factors such as wind speed, temperature, radiation and humidity especially for remote mountainous areas without observations (Moore and Owens, 1984). Therefore, enhanced understanding of how synoptic weather patterns influence intense snowmelt processes will provide useful information about the snow-surface energy interactions.

Approximately 75% of the variance associated with turbulent fluxes (sensible and heat fluxes) during spring-melt in the Southern Alps has been attributed to air mass and regional circulation patterns (Moore and Owens, 1984). McKerchar *et al.*, (1998) have shown that there is significant correlation between snowmelt increases and La Niña years because of increasing temperatures during these years. A few studies explored atmospheric circulation patterns associated with snowmelt (Hay and Fitzharris, 1988; Fitzharris *et al.*, 1997; Cullen and Conway, 2015), but they tended to be of short duration and mainly focused on ablation processes over glaciers in summer months. A 38-day measurement of snowmelt at Mueller Hut by Neale *et al.,* (1997) was the only attempt to investigate the synoptic climatology of seasonal snow cover in the Southern Alps. They documented the close connection between large-scale circulation patterns and energy balance of the melt events. They also found that melt events were mostly attributed to troughs and anticyclones. These studies in the Southern Alps have proven that synoptic patterns can play an important role in partitioning energy balance during ablation season over glacier and spring melt from the seasonal snow cover.

This chapter further investigates the synoptic-scale characteristics of atmospheric forcing during large snowmelt events in spring and winter. It should be noted that the efforts to explore the atmospheric forcing controlling winter-melt at higher altitudes of the Southern Alps have been hindered mainly due to the lack of observational measurements of snow throughout the year (Cullen and Conway, 2015). As a result, the timing and the rate of intense snowmelt episodes especially those occurring in winter months are poorly understood. Given the current gap in the knowledge of large snowmelt processes of the Southern Alps, the main objectives of chapter four is to: (1) determine the frequency and intensity of large snowmelt events during winter and spring (2) investigate the relationship between atmospheric circulation patterns and large snowmelt events. A synoptic-scale characterisation of atmospheric variables (sea level pressure and temperature) during snowmelt events are obtained by adopting a

composite anomaly approach during the days with large snowmelt events relative to the long-term averages.

4.2 Data and Methods

This study utilised the daily snow observations from Mueller Hut automatic weather station (1818 m a.s.l), near the Main Divide of the Southern Alps over a course of 8 years (2010-2018). The Main Divide plays a key role in characterizing river flow regimes of many alpine catchments in the Southern Alps. Mueller Hut site is located on the upper terrains of the Hooker River, a tributary of the Lake Pukaki catchment. The Pukaki catchment in turn yields water to seven major hydroelectric power plants. These power plants account for approximately 35-40% of New Zealand's electricity capacity (Cutler and Fitzharris, 2005; Purdie and Bardsley, 2010). Sub-catchments of the Lake Pukaki plus Lake Ohau and Lake Tekapo are the main sources (~80%) of the inflow to the Waitaki River where snowmelt is estimated to contribute to 26-30% of the annual discharge in catchments of these three lakes (Sirguey, 2009).

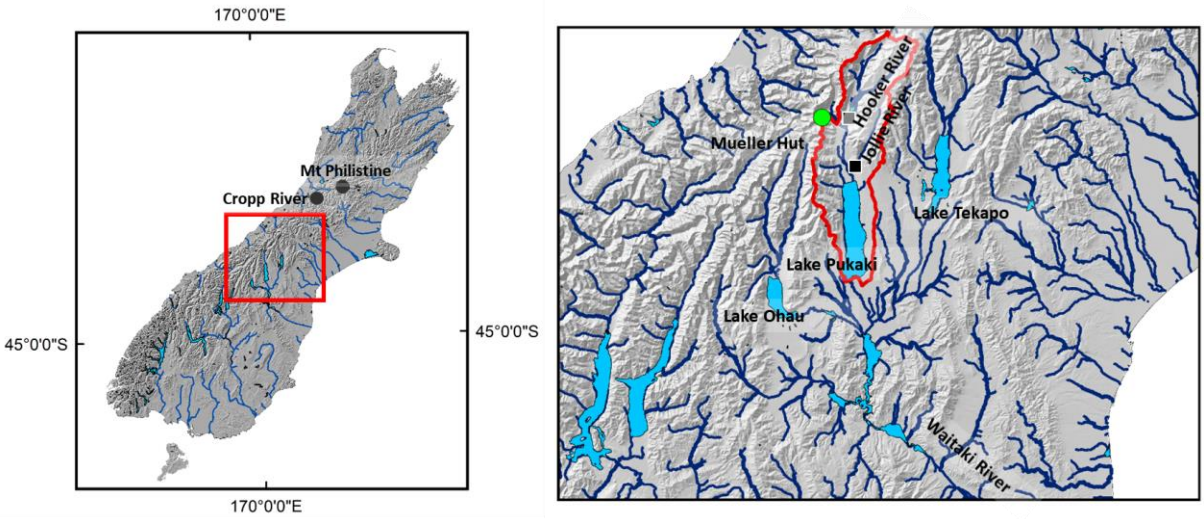

Figure 4.1 Location of Mueller Hut station (green dot) in the upper terrains of Pukaki catchment.

Snow depth is measured using an ultrasonic snow depth sensor (SR50). Similar to previous studies (e.g. Suriano 2019; Grundstein and Leathers 1998; Suriano and Leathers 2017), a decrease in daily snow depth was used as a proxy for snowmelt. Snowmelt

events were divided into two categories: winter-melt during the accumulation months (1st June to 30th September) and spring-melt during the melting months (1st October to 31st December). Previous studies have used different thresholds to identify large snowmelt episodes. For example, in the Central Europe, Bednorz (2009, 2012) define days with snow decrease greater than 5 cm day^{-1} as rapid snowmelt episodes. Over the northern Great Plains of the USA, a threshold of snowmelt greater than 2.54 cm was selected to determine the large snowmelt events (Grundstein and Leathers, 1999). Here, a large snowmelt event was defined based on the value of 90th percentile of daily snowmelt; consequently, days with snowmelt greater than or equal to the value of 90th percentile were defined as large snowmelt episodes.

In order to analyse the synoptic-scale conditions during melt episodes, the meteorological variables were obtained from the European Centre for Medium-Range Weather Forecasts (ECMWF) re-analysis data (Dee *et al.*, 2011). ECMWF's ERA-Interim data including sea level pressure (SLP) and temperature at 500, 700 and 850 hPa (T500, T700 and T850) were retrieved at 6-hourly temporal resolution and 0.5° × 0.5° spatial resolution for a synoptic window of 10°-60° S and 130° E-160° W (Figure 4.1).

The selection of pressure levels depends upon many factors including the objectives of the study and characteristics of the region. The pressure levels used in this work (500, 700 and 850 hPa) provide a good representation of mid- and low-tropospheric attributes (Kidson, 1994; Yarnal *et al.*, 2001; Farukh and Yamada, 2014). In terms of altitude, 500 hPa is approximately at 5500 m a.s.l., located above the friction of the highest peaks in the Southern Alps (Aoraki/Mt Cook: 3724 m a.s.l., Figure 2.3). The 700 hPa atmospheric pressure surface is about 3000 m a.sl. The 850 hPa pressure level lies below 2000 m a.s.l. which is an important pressure level over the Southern Alps for investigating circulation patterns and meteorological patterns for mountain hydrometeorology controlling the surface weather situations in the lower troposphere (Sailor and Li, 1999; Mora *et al.*, 2016).

4.2.1 Composite anomaly approach

To characterize the influence of atmospheric controls on snowmelt episodes, a composite anomaly approach was carried out. Composite anomaly approach is a simple synoptic-climatological technique that paints a physically reasonable picture of atmospheric variations (Yarnal *et al.*, 2001; Bednorz, 2009). Based on this approach, the differences between average values of atmospheric variables for a particular phenomenon (e.g. snowmelt episodes) and climatic normal are computed. A long-term average of meteorological variables (1979-2018) during the accumulation months (June to September) and melting months (October to November) were used as climatic normals (Figure 4.2 and Figure 4.3).

From the preliminary analysis of the local synoptic pattern (Kidson, 2000), the days with large melt events were found to be associated with two main regimes: troughs and highs. In order to avert producing an erroneous picture of the mixed conditions, these two regimes were used to categorize the synoptic patterns. Thus days with similar synoptic regimes were grouped together and the composite anomaly analyses were constructed for each regime separately.

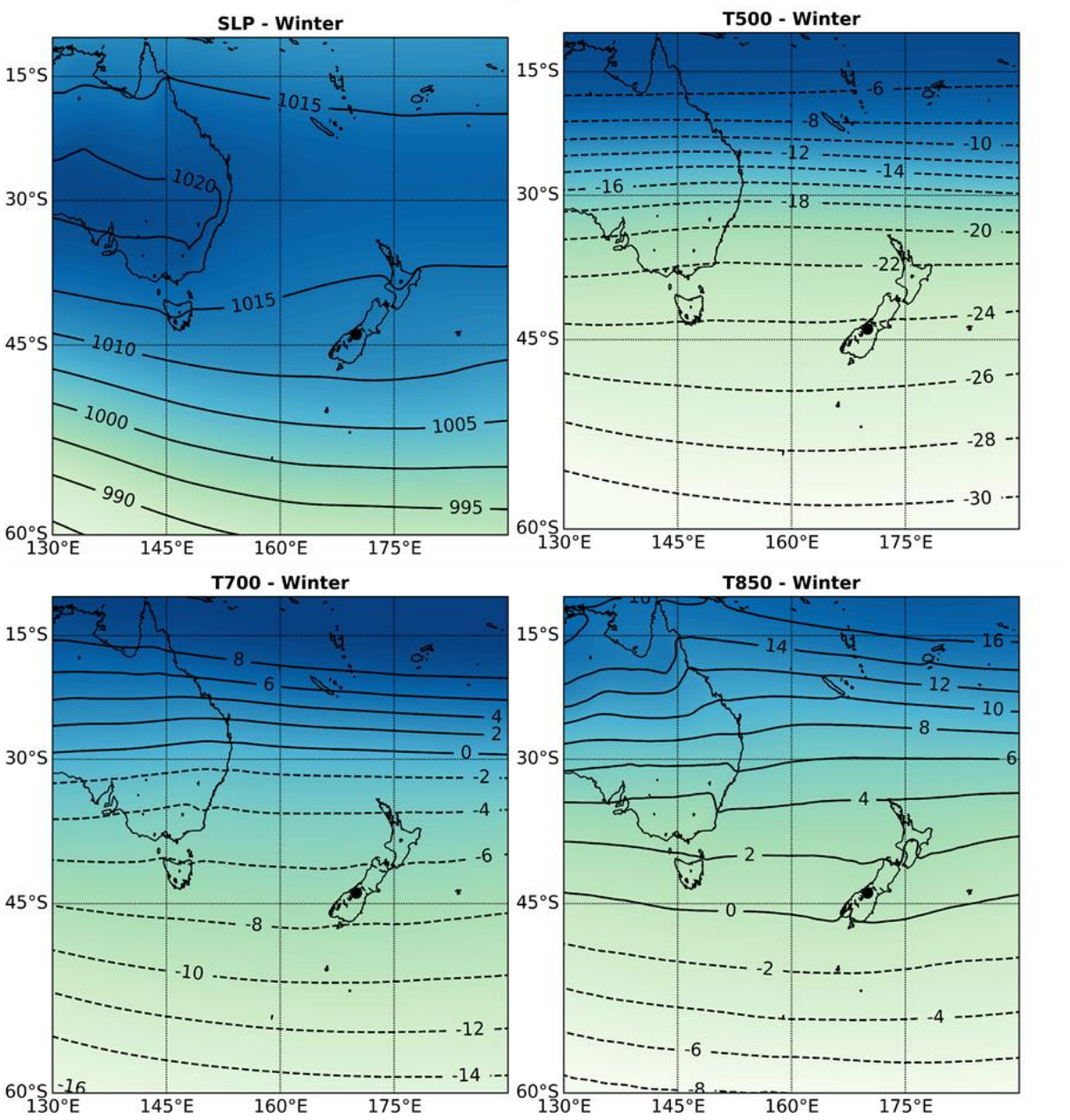

Figure 4.2 40-year average of SLP (hPa), T500 (°C), T700 (°C), T850 (°C) and T1000 (°C) during the cold months (June to September).

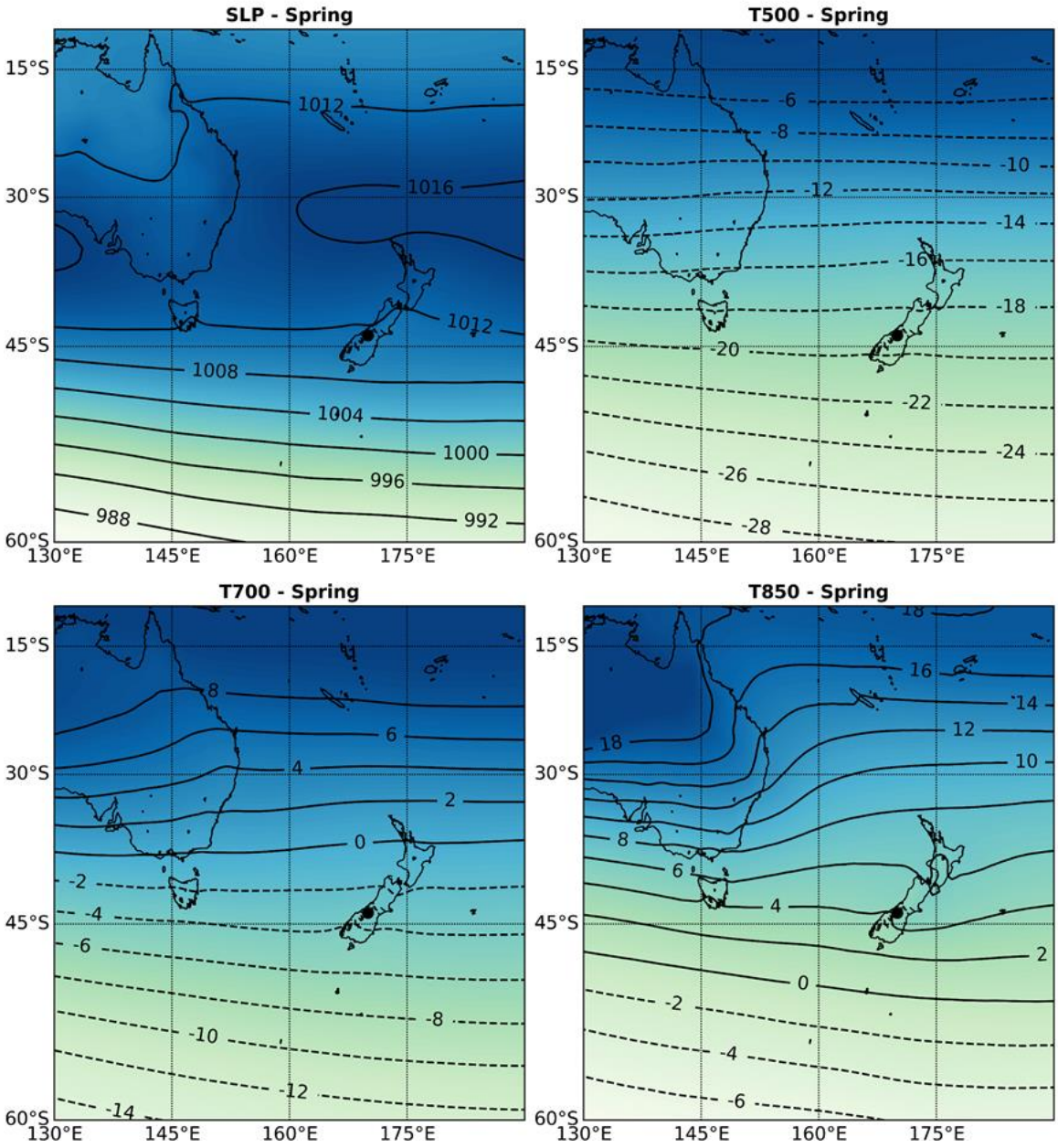

Figure 4.3 40-year average of SLP (hPa), T500 (°C), T700 (°C), T850 (°C) and T1000 (°C) during the melting months (October to December).

4.3 Results

Observations at Mueller Hut station show that snowmelt during winter months varies from less than 1 mm day^{-1} to 299 mm day^{-1} averaging 12 mm day^{-1}. During spring months decrease in snow depth changes from less than 1 mm day^{-1} to 330 mm day^{-1} with an average of 46 mm day^{-1}. The 90th percentile threshold for daily melt is approximately 75 mm day^{-1} leading to the identification of 221 daily melt events between 2010 and 2018 at Mueller Hut (Figure 4.4a). Results reveals that out of 221 days with large

snowmelt, ~80% (178) occurred in spring (October: 22 days, November: 69 days, December: 87 days); however, the ablation events are not exclusively limited to spring months (Figure 4.4b). Melt values for 95th, 90th and 85th percentiles (Table 4.1) show that the values vary from 100 mm/day (95th) to 53 mm/day (85th). This shows that by increasing/decreasing percentile by 5 percent, the threshold approximately changed by 2.5 mm/day. Using the 90th percentile (75 mm/day) during winter (June to September), 43 days were identified as having large melt events. The frequency of days with large melt during winter months shows that 14 events occurred during early winter (June). A similar number of events was recorded during July (11 events) and September (10 events) while August experienced only 8 events.

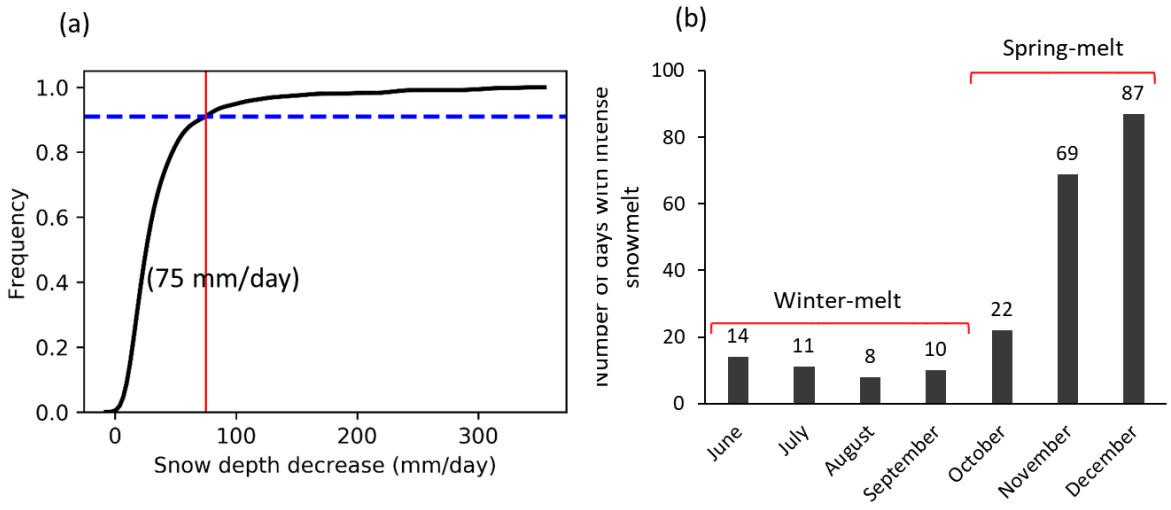

Figure 4.4 (a) Frequency of melt events at Mueller Hut. The red line marks the 90th percentile (75 mm day^{-1}), and (b) number of days with large snowmelt during accumulation season (June to September) and melt season (October to December) from 2010/11 to 2017/18.

Table 4.1 Percentile values and corresponding thresholds for daily snowmelt at Mueller Hut

Percentile	Threshold (mm/day)
95th	100
90th	75
85th	53

4.3.1 Climatology of winter snowmelt: anomalies of SLP, T500, T750 and T850

In order to assess the influence of synoptic patterns during large snowmelt episodes anomaly maps of sea level pressure (SLP) and temperature at 500 hPa, 700 hPa and 850 hPa were constructed. According to Kidson weather types (see section 2.2.4, Figure 2.5) the winter-melt events are associated with two major synoptic groups, high synoptic regimes and troughing synoptic regimes, with high weather types accounting for 18 events and troughing types accounting for 25 events. Anomaly maps of SLP during large snowmelt events with high-pressure regimes indicates that such events are associated with above-normal SLP over the New Zealand region with a centre formed west of New Zealand over Tasman Sea (Figure 4.5). The pressure at the centre of the high is ~7.6 hPa higher than the SLP average during cold months (1010.5 hPa). Composite anomaly of temperature reveals higher than normal temperatures at different pressure levels (Figure 4.5). Long-term averages of temperature during winter months vary from -23.4 °C at 500 hPa to 1.2 °C at 850 hPa, with -6.5 °C at 700 hPa. Positive anomalies of temperature are evident near the Main Divide, at the grid point of Mueller Hut location, suggesting enhanced temperature at mid and lower troposphere during the melt episodes (500 hPa: 1.4 °C, 700 hPa: 1.7 °C and 850 hPa: 1.4 °C).

Anomalies of SLP during snowmelt associated with troughing regimes in winter months show distinctive patterns. The spatial extent of low pressure systems are present over a large area of South Pacific Ocean surrounding New Zealand (Figure 4.6). The atmospheric patterns feature negative anomalies of SLP with a deep centre located in the southwest to south of New Zealand South Island. The pressure at the centre of low pressure dropped by more 8 hPa during the melting events. However, similar to snowmelt days during high regimes, positive anomalies of temperature during troughing regimes were identified. Increasing temperatures relative to long-term averages at 500 hPa (by 2.13 °C), 700 hPa (by 1.03 °C) and 850 hPa (by 0.69 °C) indicates that melt events

during troughing regimes are characterized by stronger anomalies at higher levels (mid troposphere) compared to lower troposphere.

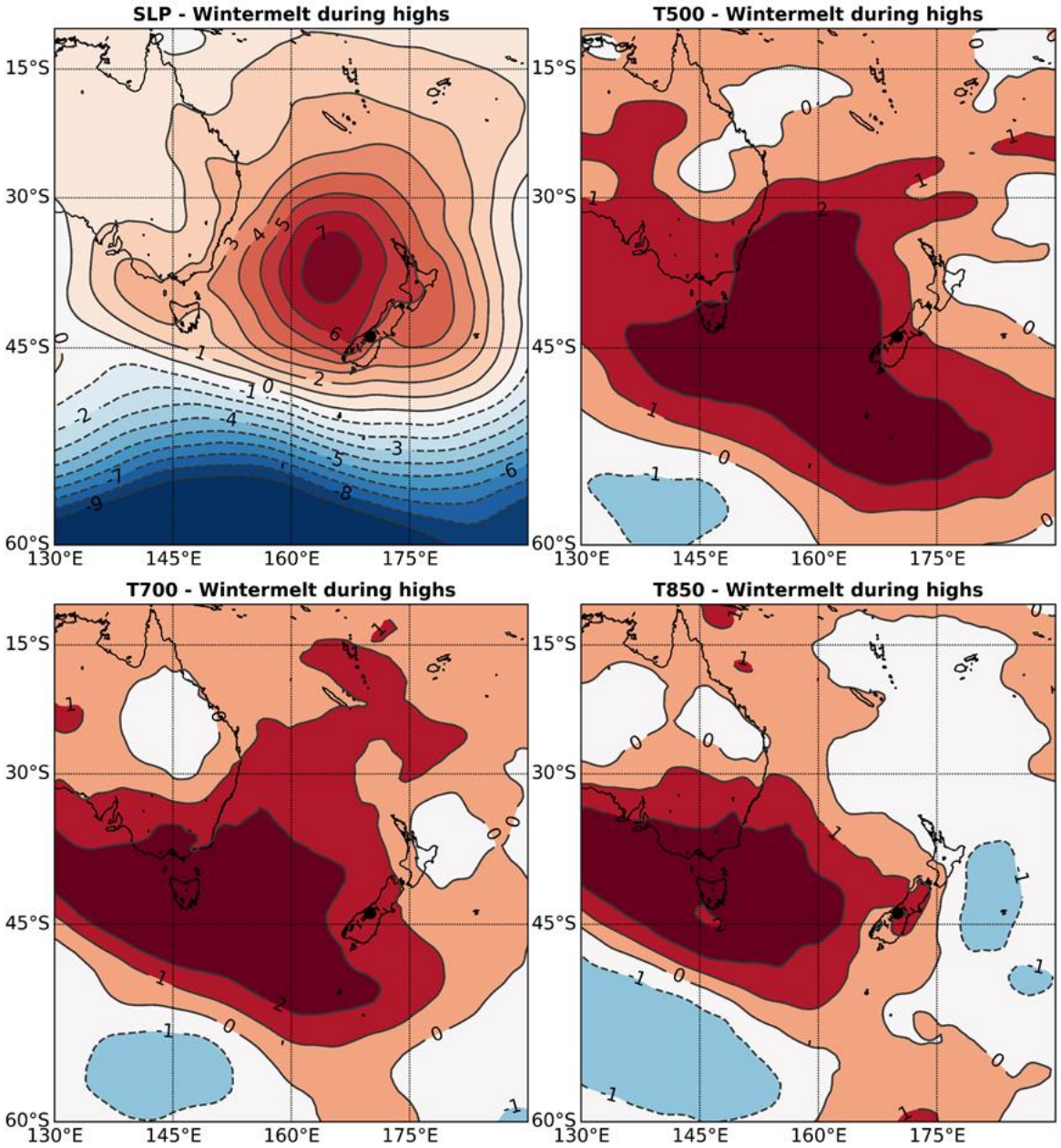

Figure 4.5 Anomaly maps of atmospheric variables for winter-melt event during highs.

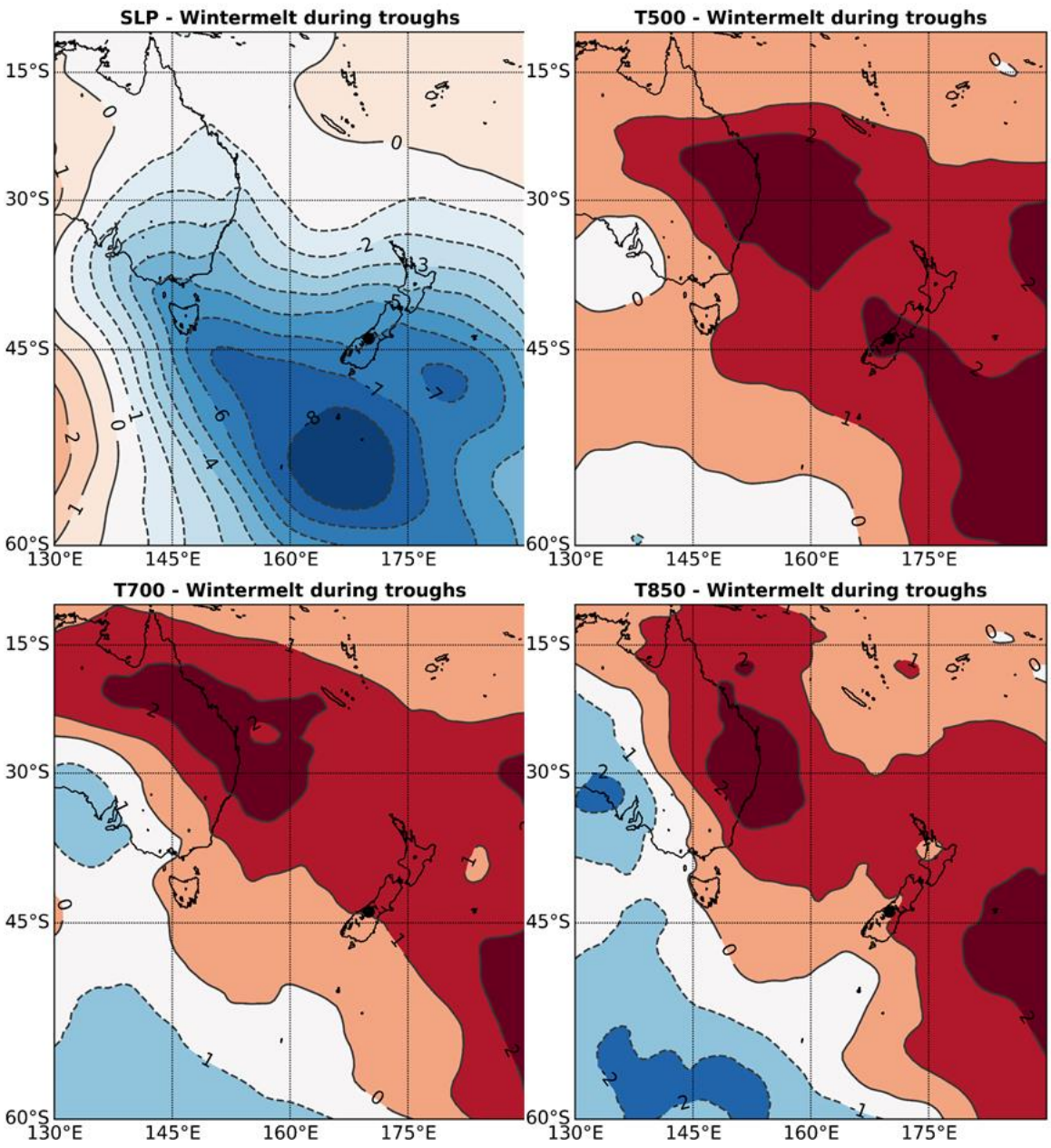

Figure 4.6 Anomaly maps of atmospheric variables for winter-melt during troughs.

4.3.2 Climatology of spring snowmelt: anomalies of SLP, T500, T750 and T850

Similar to winter-melt, the large spring-melt events (1st October to 31st December) are associated with two major synoptic regimes: highs and troughs. However, a larger number of melt events are the result of high pressure systems over the region. Anomaly maps of SLP revealed that the majority of snowmelt episodes are associated with high pressure systems with centres formed near the Main Divide and east of South Island (Figure 4.7). The pressure at the centre of highs increases by more than ~8 hPa relative

to long-term October-to-December averages (1014.5 hPa). In terms of temperature, the events during high regimes were characterized by strong positive temperatures anomalies. The average temperatures of spring months at 500 hPa, 700 hPa and 850 hPa are -17.1 °C, -0.3 °C and 7.5 °C, respectively As shown in (Figure 4.7), well above average temperatures were evident across the region during melt events. Over the Southern Alps at the location of Mueller Hut, increases in temperatures by 3.56 °C, 3.36 °C and 4.1 °C were recorded at 500, 700 and 850 pressure levels, respectively.

Similar to winter-melt episodes, days with troughing regimes can be responsible for rapid snowmelt during spring-melt in the Southern Alps. Composite anomalies of SLP reveal that days with rapid snowmelt during troughs are associated with low pressure systems cantered over southwest of the New Zealand's South Island (Figure 4.8). Such weather patterns resulted in higher than normal temperatures at mid and lower troposphere where strong positive anomalies of temperature are evident at 500 hPa (3.1 °C), 700 hPa (2.4 °C) and 850 hPa (2.5 °C) (see Figure 4.8).

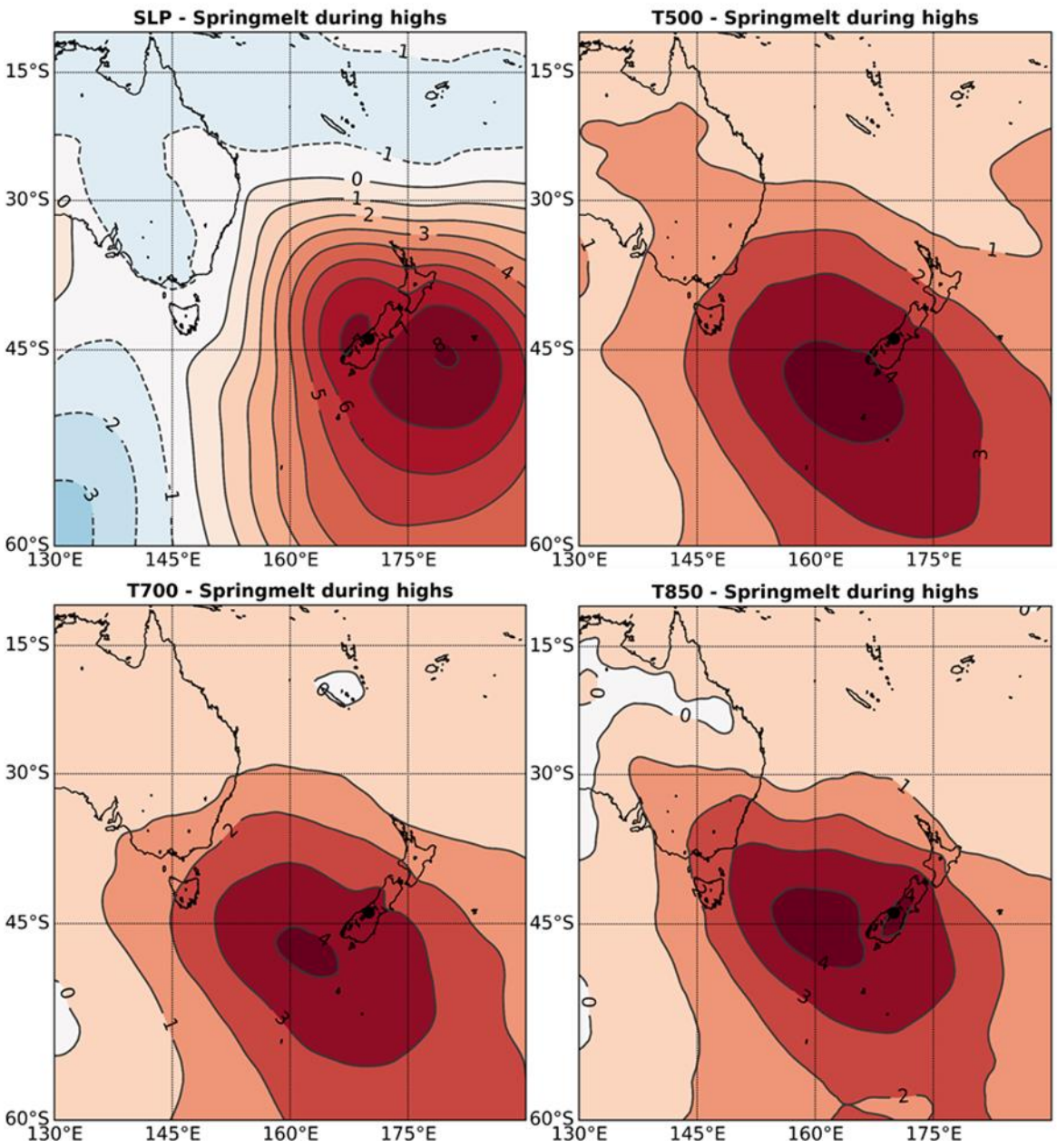

Figure 4.7 Anomalies of atmospheric variables during melt season (1st October to 31st December) during highs.

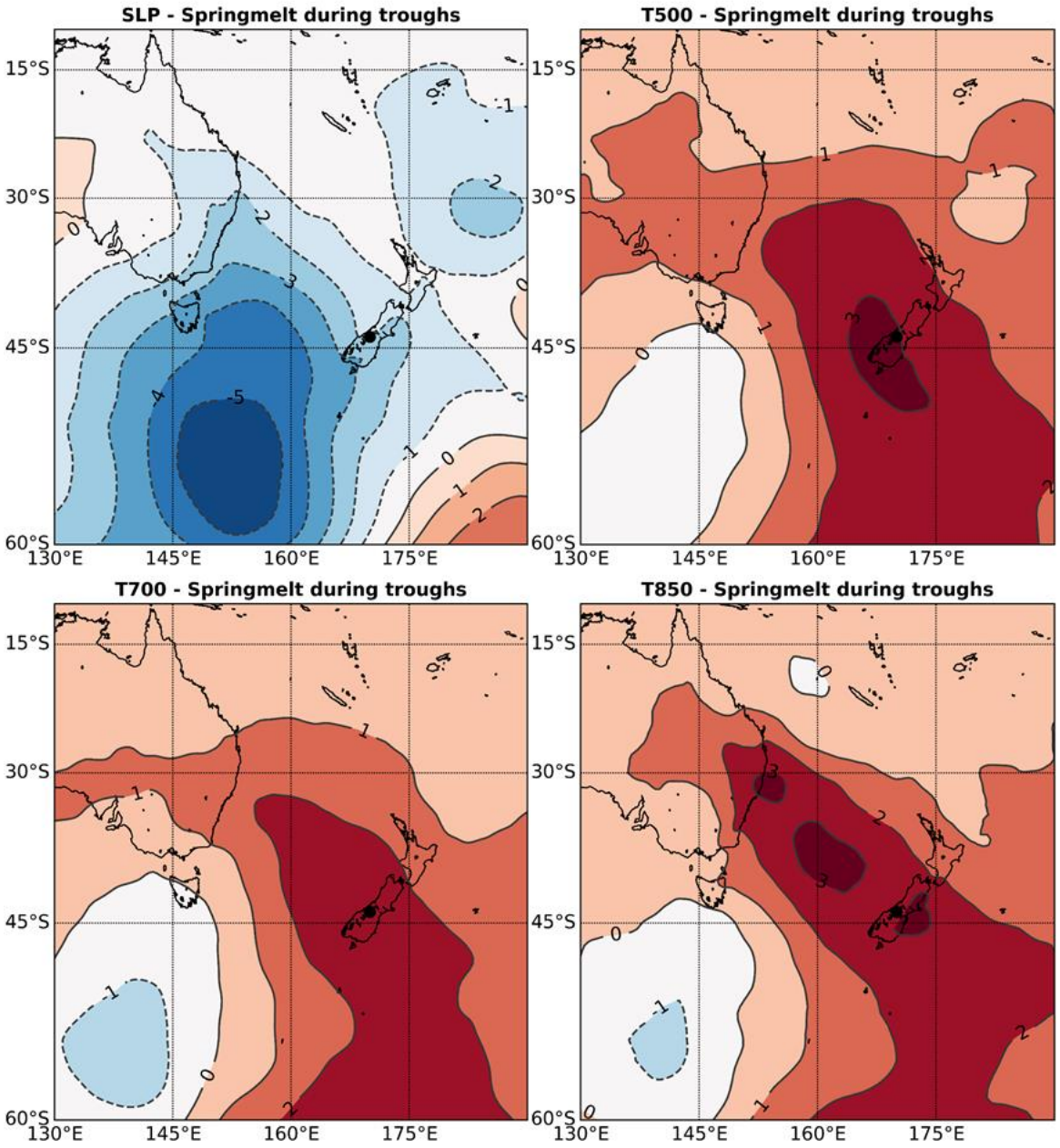

Figure 4.8 Anomalies of atmospheric variables during melt season (1st October to 31st December) during troughs.

4.4 Discussion and conclusions

Snowmelt serves as a fundamental source of water in the alpine catchments of the Southern Alps where the timing and magnitude of water released from seasonal snowpack plays a critical role in hydro power generation and irrigation management. Given the important influence of atmospheric circulation on snowmelt processes, the primary purpose of this research was to evaluate the main characteristics of synoptic patterns associated with large snowmelt from seasonal snowpack near the Main Divide

of the Southern Alps. Unlike previous studies which rely on short-term datasets during melting months, this study utilises a period of eight years to determine the large snowmelt episodes in the Southern Alps. The seasonal snowpack at Mueller Hut usually lasts for 5 to 6 months (June to December) where snow mainly accumulates from June to October, peaking between mid-September and early October. The snowmelt period usually starts in October and the seasonal snowpack is gone by the end of December. The majority of high (≥75 mm day^{-1}) ablation events at Mueller Hut occur during spring months (November to December) but some do occur in winter.

Following previous research in other snow-dominated regions (e.g. Grundstein and Leathers, 1999; Grundstein, 2003; Romolo *et al.*, 2006; Bednorz, 2009; Suriano, 2019), findings in this study show that synoptic-scale circulation patterns can be a key element in determining the hydrometerological characteristics of large snowmelt events. The role of high pressure system in rapid snowmelt events in the Southern Alps are similar to previous findings in regions such as Polish-German lowlands (Bednorz, 2009) and North America (Grundstein and Leathers, 1998; Romolo *et al.*, 2006a; Suriano, 2019) highlighting the prevailing influence of anticyclones that result in clear skies and therefore higher rates of net radiation as being a main source of energy for large snowmelt episodes. Further analysis of anomaly maps of SLP and temperature indicated that changes in mid- and low-tropospheric conditions are important factors in rapid snowmelt episodes in the Southern Alps. During high pressure systems in both winter and spring, rising temperatures at mid- and low-troposphere accompanied with positive anomalies of SLP are the main driver of large snowmelt events. Anomaly maps of SLP shows that the centre of the related high pressure systems during winter-melt and spring-melt contain different patterns. Large snowmelt events are associated with high-pressure systems with centres located over the Southern Alps and east of South Island during spring months while during winter-melt the centre of high-pressure systems are mainly located at west of New Zealand over Tasman Sea. Exploring temperature patterns

indicates higher than normal temperatures at Mueller Hut during snowmelt events on days with high pressure weather patterns in the region in winter and spring (Figure 4.5 and Figure 4.8). Temperature anomalies during high pressure systems in winter showed stronger anomalies of temperature at 500, 700 and 850 hPa pressure levels with values up to 4 °C greater than long-term average, while weather patterns associated with large spring melt episodes had positive anomalies up to 2 °C.

Findings also show that large snowmelt events can occur during trough regimes associated with warm and humid advection of airflow across the Tasman Sea. Even though the frequency of such events is lower than their high pressure counterparts, they largely influence snowmelt processes in the maritime Southern Alps, so that the highest snowmelt rates over winter months (299 mm day^{-1}) and spring months (330 mm day^{-1}) both occur during troughing regimes. Both these two melt episodes were associated with trough north-westerly (TNW) type. Such high rates of melt can be a result of warm extratropical cyclones and warm conveyor belts originating from tropics and bringing warm and humid airmasses to mid-latitudes of New Zealand. Atmospheric circulation patterns associated with troughing regimes indicates that low-pressure weather patterns accompanied with anomalously rising temperatures in mid and lower troposphere are the main driver of high snowmelt rates during winter and spring months. These patterns are similar to those weather patterns previously reported in Northern Hemisphere (Grundstein and Leathers, 1998; Grundstein, 2003; Romolo *et al.*, 2006a; Suriano, 2019) highlighting the importance of troughing regimes in ablation events by increasing the chance of rain-on-snow events (ROS). Currently the knowledge about the role of ROS events on snowmelt and as result on hydrological processes in alpine catchments of the Southern Alps is very limited. The next chapter (chapter 5) makes an effort to investigate the hydrometeorological characteristics of ROS and their impacts on snowpacks in the Southern Alps.

This chapter has demonstrated that in the Southern Alps' maritime climate, snowpacks are vulnerable to melting throughout the whole snow season. Given the rates of projected climate warming it could be expected that winter melt events become an increasingly important component of alpine hydrology. Further research to better understand changes in timing and magnitude of snowmelt will be crucial for watershed management in the region.

5 Rain-on-snow events in the Southern Alps: The role of atmospheric rivers

Abstract

A better understanding of hydrometeorological characteristics of rain-on-snow (ROS) events is required because of their significant impacts on hydrological processes in snow-dominated regions. This chapter examined the relationship between atmospheric rivers (ARs) and ROS events over seasonal snowpacks in the maritime Southern Alps. Results show that ARs are the main driver of warm water vapour transport in the region during ROS events leading to large winter- and spring-time rainfall events at higher altitudes of the Southern Alps. Detailed analysis of case studies revealed an increase in vertical integral of heat flux during AR-related ROS events. This condition led to anomalously warm temperatures at mid and lower troposphere with a rise in freezing level to ~725-650 hPa as well as rapid increases in air temperature with values up to 10 °C near the Main Divide of the Southern Alps. High snowmelt rates (up to 20 cm day^{-1}) due to increased temperature during AR-related ROS events was observed. The flow rate data from alpine rivers show that a combination of high melt rates and intense rainfall associated with AR-related ROS events can lead to major flooding events in upper terrains of the Southern Alps during both winter and spring months. The connection between ROS events and floods highlights the importance of a better understanding of hydrological processes controlling snowmelt runoff during ROS which is currently lacking in the maritime environments.

5.1 Introduction

Rain-on-snow (ROS) events are important hydrometeorological phenomenon in alpine catchments. A combination of snowmelt and heavy rainfall can result in a rapid hydrological response and bring about significant flooding events. Major floods in the western United Stated (Marks *et al.*, 1998; Guan *et al.*, 2016; Li *et al.*, 2019), Canadian British Columbia and Rocky mountains (Loukas *et al.*, 2000; Pomeroy *et al.*, 2016), the European Alps (Merz and Blöschl, 2003; Rössler *et al.*, 2014) and Arctic regions (Cohen *et al.*, 2015) have been found to be associated with ROS events. Several studies have shown that increasing frequency of ROS events brings about significant impacts on water

resources by reducing the snow water equivalent (SWE) stored in seasonal snowpacks in the upper terrains of alpine catchments (Jeong *et al.*, 2017; Jeong and Sushama, 2018). A number of authors have also documented the role of ROS events in triggering winter avalanches in snow-dominated regions (e.g. Conway and Raymond, 1993; Stimberis and Rubin, 2011; Abermann *et al.*, 2019).

The Southern Alps of New Zealand are influenced by maritime weather conditions with mountainous regions regularly experiencing temperatures above 0 °C in winter months (Fitzharris *et al.*, 1999). Consequently, seasonal snowpacks in the Southern Alps can experience successive periods of accumulation and melt during winter, as shown in chapter 4, with conditions susceptible to frequent ROS events over the snowpack (Moore and Owens, 1984; Cullen and Conway, 2015). Similar to other maritime snow-dominated regions, the seasonal snowpacks of the Southern Alps have been found to be highly sensitive to small changes in temperature (Poyck *et al.*, 2011; Hendrikx and Hreinsson, 2012; Hendrikx *et al.*, 2013). A higher frequency of ROS events is projected in a warming climate where a shift from snow-dominated patterns to rain-dominated patterns is inevitable (Barnett *et al.*, 2005). More frequent episodes of ROS events during winter and spring would largely impact the hydrological cycle by melting snow cover at higher rates resulting in the reduction of stream flow during spring (Surfleet and Tullos, 2013; Cohen *et al.*, 2015). Fitzharris *et al.* (1980) attributed the October 1978 flood in Central Otago to a ROS event where snowmelt accounted for over 30% of the river flow in the upper terrains of the Fraser River catchment. At lower elevation, where snow covered only 10% of the catchments during the event, the contribution of the snowmelt was estimated to be ~10%. This suggests that snowmelt during ROS events could have an important contribution during periods with existing snow coverage in the upper terrains of the alpine catchments. Enhanced knowledge of the hydrometeorological processes related to ROS events is therefore necessary in water management strategies of snow-dominated regions. Despite the frequent occurrence of ROS events in the Southern Alps (Prowse,

1981a; Moore and Owens, 1984; Cullen and Conway, 2015), little is known about the hydrometeorological characteristics (e.g. water vapour transport, synoptic controls and temperature variations).

Recent studies have shown that atmospheric rivers (ARs) play an important role in transferring water vapour in the South Pacific Ocean across the Tasman Sea (Kingston *et al.*, 2016a; Little *et al.*, 2019). ARs are narrow corridors of enhanced water vapour in mid and lower troposphere responsible for more than 90% of the total mid-latitude vertically integrated water vapour transport (Zhu and Newell, 1998; Neiman *et al.*, 2008a). The hydrometeorological impacts of ARs especially during major precipitation and flooding events have been well documented in many parts of the world (Neiman *et al.*, 2008, 2013; Stohl, Forster and Sodemann, 2008; Leung and Qian, 2009; Guan *et al.*, 2010; Dettinger *et al.*, 2011; Viale and Nuñez, 2011; Lavers *et al.*, 2012; Lavers and Villarini, 2013; Ralph *et al.*, 2016; Cordeira *et al.*, 2017). The role of ARs in ROS events, however, is still largely unknown. The typical warm nature of ARs can result in liquid precipitation at high altitudes. In the western United States, Guan *et al.* (2016) reported that 50% of ROS events are related to ARs. Rössler *et al*. (2014) showed that passage of a warm and moist AR over Swiss Alps resulted in a major ROS flooding event in October 2011. A recent study on Brewster Glacier, a mountain glacier located on the west flank of the Main Divide of the Southern Alps highlighted the important role of ARs in anomalously high ablation rate during summer melt in the Southern Alps' glaciers (Little *et al.*, 2019). There appear to be a seasonal variation of energy balance components during storms in the Southern Alps. Anderton *et al.* (1978) found that during spring months storms (November) on Ivory Glacier, the energy flux from rainfall was responsible for approximately 45% of the melt. However, during the summer months ablation, the heat content from rain was found to be the fourth most important component of the energy balance (16%) while combined sensible and latent heat fluxes accounted for 60% and net radiation accounted for 24% of the total energy balance. A similar contribution of rain heat flux was reported by Little

et al (2019) on Brewster Glacier during ablation period. These findings suggest that the rain heat flux due to ROS events occurring during colder months account for a larger portion of energy required for snowmelt compared to rain events during summer months where other components of energy flux are more significant.

Considering the influence of ROS on the energy balance of mountain regions, it is important to identify the large-scale hydrometeorological characteristics of such event over Southern Alps' seasonal snowpacks. Of particular interest is the role of ARs in producing ROS events over the seasonal snowpack in the Southern Alps. Owing to the warm air temperature associated with ARs (Guan *et al.*, 2016), intense precipitation caused by ARs could potentially lead to warm ROS events during colder months of winter and spring across the Southern Alps. Given the current gap in the knowledge of hydrometeorology of ROS events in the Southern Alps, the primary aim of chapter 5 is to explore the mechanisms of moisture transport during ROS event (question 4). More specifically, this chapter intends to: (1) identify the role of ARs in producing winter- and spring-time major ROS events by analysing the integrated vapour transport (IVT), (2) investigate atmospheric conditions and snowpack response of two major ROS events during winter (June 2016) and spring (November 2018) in order to provide a better understanding of hydrometeorological characteristics of ROS events in the maritime Southern Alps, and (3) to evaluate the hydrological effect of ROS events by analysing the hourly and daily flow rates of two alpine rivers in the upper terrains of the region during the storms.

5.2 Data and methodology

5.2.1 Data sources

In order to characterize the ROS events, this study obtains continuous records of snow observations and climate variables from Mueller Hut station over a course of 8 years (2010-2018). Mueller Hut is located near the Main Divide of the Southern Alps (1818 m a.s.l., 43.72° S, 170.06° E, Figure 4.1) in the upper terrains of the Hooker River, a

tributary of the Lake Pukaki catchment. Being close to the freezing level in the Southern Alps, Mueller Hut is an ideal site to capture rainfall and snowfall events during the snow accumulation and snow ablation periods. The data used here include precipitation (P, mm), snow depth (SD, cm), snow water equivalent (SWE, cm), air temperature (T_a, °C) and snow temperature (T_s, °C).

To analyse the characteristics of atmospheric circulation during ROS events, the ERA-Interim Reanalysis data from the European Centre for Medium-Range Weather Forecasts (ECMWF) (Dee *et al.*, 2011) were used. Data retrieved for the purpose of this study include specific humidity (q, g kg^{-1}), zonal and meridional wind components (u and v, m s^{-1}), vertical integral of heat flux (W m^{-2}), temperatures at 500 hPa, 700 hPa and 850 hPa (T500, T700, and T 850, °C), and geopotential heights at 1000 hPa and 500 hPa (Z1000 and Z500, m). The data were obtained for the synoptic window of 10°-60° S and 130° E-160° W at a 6-hourly temporal resolution and 0.5° × 0.5° spatial resolution (Figure 2.1). Even though the main focus of this study was to explore atmospheric conditions (e.g. moisture transport characteristics and synoptic conditions) associated with ROS events, consideration is also given to the hydrological response of stream flows in upper reaches of Lake Pukaki catchment. Hourly and daily discharge series from Jollie River and Hooker River at Ball Hut Road Bridge, were used to characterise stream flows during the ROS events.

5.2.2 Identification of rain-on-snow (ROS) events

A measurable liquid precipitation falling on existing snowpack on the ground is defined as a ROS event (Trubilowicz and Moore, 2017; Li *et al.*, 2019). The focus of this study is large events that could potentially result in rapid changes in snowpack and streamflow. Previous studies have used different thresholds of accumulated precipitation during ROS events (Lundquist *et al.*, 2008; Trubilowicz and Moore, 2017; Würzer and Jonas, 2018). A threshold of 1 cm day^{-1} accumulating rainfall with reduction in snow water equivalent or snow depth is the most commonly used method to identify ROS

events (Cohen *et al.*, 2015; Guan *et al.*, 2016). For the purpose of this study, daily rainfall records from the tipping bucket rain gauge at Mueller Hut station were used. In order to characterise the general patterns of moisture transport during major ROS events the 10 topmost ROS events with the highest daily accumulated rain were selected during the periods when snow was on the ground, the temperature was above freezing level, and a decrease in snow depth occurred.

5.2.3 Identification of atmospheric rivers (ARs)

In order to analyse the moisture transport characteristics of selected ROS events the integrated horizontal water vapour transport (IVT) was calculated (see section 3.2.3, equation (3.1)). An AR detection method the same as the one applied in chapter 3 ($L \geq 2000$ km, $L/W \geq 2$, and $IVT \geq IVT^{85th}$) was used to identify the relationship between moisture flux and ARs during ROS events.

5.2.4 Case studies: Hydrometeorological characteristics of two rain-on-snow events

To provide a clear picture of hydrometeorological characteristics of ROS events two major ROS events were selected, one occurring in winter and the other in spring. The total accumulated rainfall was used to identify the largest winter-time and spring-time ROS events during the study period. The impacts of these two events on snowpack (e.g. snow depth and snow water equivalent) were evaluated using snow observations recorded at Mueller Hut. In order to examine the atmospheric circulation patterns responsible for ROS events a more comprehensive analysis of synoptic conditions was carried out. It is well documented that the application of composite anomaly approach provides valuable information about atmospheric conditions associated with a phenomenon (Yarnal, 1993; Birkeland and Mock, 1996). Since temperature is a critical controlling factor during ROS events (Cohen *et al.*, 2015; Guan *et al.*, 2016; Pall *et al.*, 2019), anomalies of temperatures at different pressure levels (500 hPa, 850 hPa and 1000 hPa) relative to the 40-year averages (1978-2018) data were constructed during the ROS events.

Additionally, vertical temperature profiles (from 300 hPa to 1000 hPa) were computed in order to characterize the temperature changes in the lower troposphere during ROS events. The 1000-500 hPa thickness line (the differences of geopotential heights at 1000 hPa and 500 hPa) was used to identify the boundary between the cold and warm air masses during the storms. Analyses of the thickness line can provide additional information about temperature characteristics of airflows when travelling across the South Pacific Ocean over the Tasman Sea. Also, vertical integral of heat flux were used to help better understand the source of warm advection in the atmosphere during ROS events.

Finally, because of the strong association between rapid runoff rates and major ROS events found in previous studies (Marks *et al.*, 1998; Rössler *et al.*, 2014; Pomeroy *et al.*, 2016), analyses of hourly and daily streamflow rates during these ROS events were done in order to assess the hydrological conditions during ROS events in upper terrains of the Southern Alps. To do so, the increase in discharge in relation to the long-term average of the daily discharge was examined in two alpine rivers in the region, namely Hooker River and Jollie River. These two rivers are located in the upper terrains of Lake Pukaki catchment and are the closest to the snow observation site. Flow duration curves for these two rivers were produced to assess the frequency and magnitude of river flows during ROS events through a simple graphical representation of stream flow. In a flow duration curve the flow discharge is plotted against percentage of exceedance that indicates the percentage of time when the flow equalled or greater for that specific period of time (Vogel and Fennessey, 1995). The exceedance probability is calculated by:

$$P = 100 * [M / (n + 1)] \quad (5.1)$$

where P is the probability that a given discharge is equalled or exceeded (% of time). M is the rank of the discharge and n is the number of events during the period of record.

5.3 Results

5.3.1 Meteorological observations

Figure 5.1 shows the total accumulated rain and mean daily and maximum temperatures recorded at Mueller Hut station during the 10 topmost identified ROS events. Note that even though these events are selected based on accumulated daily rain, they are mainly related to storms lasting for more than 24 hours in the region. Timing of the occurrence of ROS events revealed that the majority (8 out of 10) occurred during warmer months of October and November. Intense ROS events are less frequent in the colder months compared to spring months, with two events taking place in June 2016 and September 2010. In terms of total accumulated rain, the events are the results of heavy rainfall ranging from 144.5 mm (6-9th September 2010 (NZST)) to 366 mm (7-9th November (NZST)). The mean daily temperature during the ROS events ranges from -0.3 °C (during 6-9th September 2010 event) to 4.9 °C (during 9-10th June 2016 event). The maximum temperature recorded during the events varies between 3.2 °C during 6-9th September 2010 event to 10.1 °C during 7-9th November 2018 event (Figure 5.1).

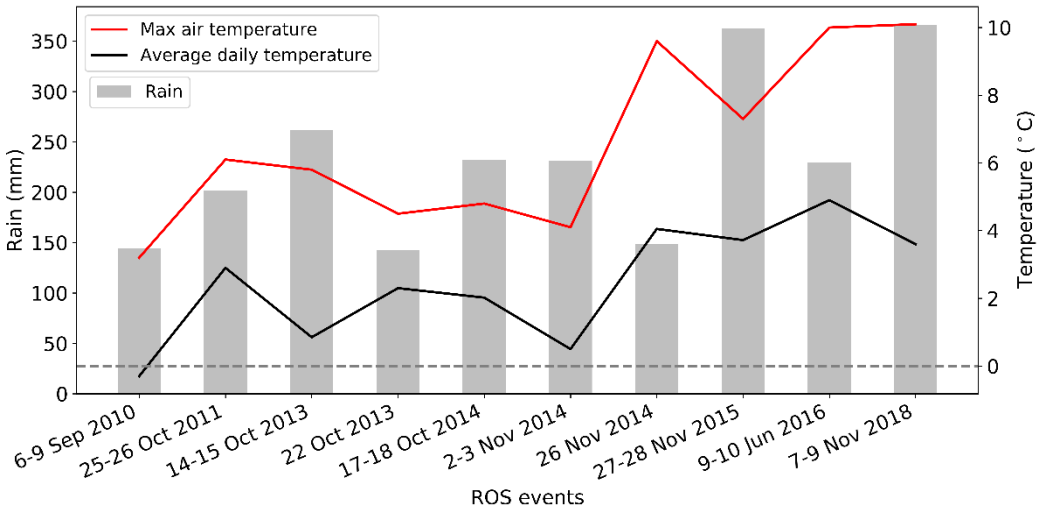

Figure 5.1 Total accumulated rain (mm) and temperature (°C) during selected ROS events between 2010 and 2018. The red line is the maximum temperature recorded during the ROS event. The black line is the average daily temperature during the events. The grey dashed line marks the 0 °C line.

Analysis of water vapour changes provides new information regarding moisture transport during the ROS events in the Southern Alps. Regions of strong water vapour transport are evident during the ROS events. According to the definition of ARs used in this study, all but one event (26th November 2014) are associated with narrow filamentary water vapour bands in the form of ARs. Despite similar meteorological characteristics with ARs (high water vapour content and strong low level winds), the 26th November 2014 event was not categorized as an AR since the shape of the moisture band did not fulfil the requirements of an AR (i.e. length/width >2). This event was associated with warm cyclonic activities over the Tasman Sea to the west of New Zealand resulting in high values of IVT (up to 1245.4 kg m^{-1} s^{-1} over the Tasman Sea) with consequent heavy precipitation across the South Island of New Zealand.

Table 5.1 Characteristics of moisture flux during selected ROS events.

Date (NZST)	Max IVT over the Tasman Sea (kg m^{-1} s^{-1})	Max IVT at West Coast grid point (kg m^{-1} s^{-1})	Max IVT at Mueller Hut grid point (kg m^{-1} s^{-1})	Duration at Mueller Hut (hours)	AR: YES ✓ NO ✖
06-09-2010	1241	664.2	531.7	30	✓
26-11-2011	1052.8	388.4	326.7	24	✓
15-10-2013	1701	979.7	760.7	30	✓
22-10-2013	1701.17	720	688.7	36	✓
17-10-2014	1009.8	559.6	474	>24	✓
03-11-2014	1265.6	670.6	560.4	>36	✓
26-11-2014	1245.4	874.8	733.4	24	✖
27-11-2015	1522	849.2	780.4	>24	✓
09-06-2016	1513.1	547.2	467.2	42	✓
08-11-2018	1494.1	1157.5	822.02	42	✓

It is evident that the intense ROS events are mainly associated with warm north-westerly airflows. The location of thickness line mirrors an increase in temperature over New Zealand region during the passage of moisture plumes leading to ROS events. The

5400 m thickness line, which is traditionally used in meteorological maps to approximate the transient line between warm and cold airflows, is mostly located far south of the New Zealand's South Island during these events (red line, Figure 5.2).

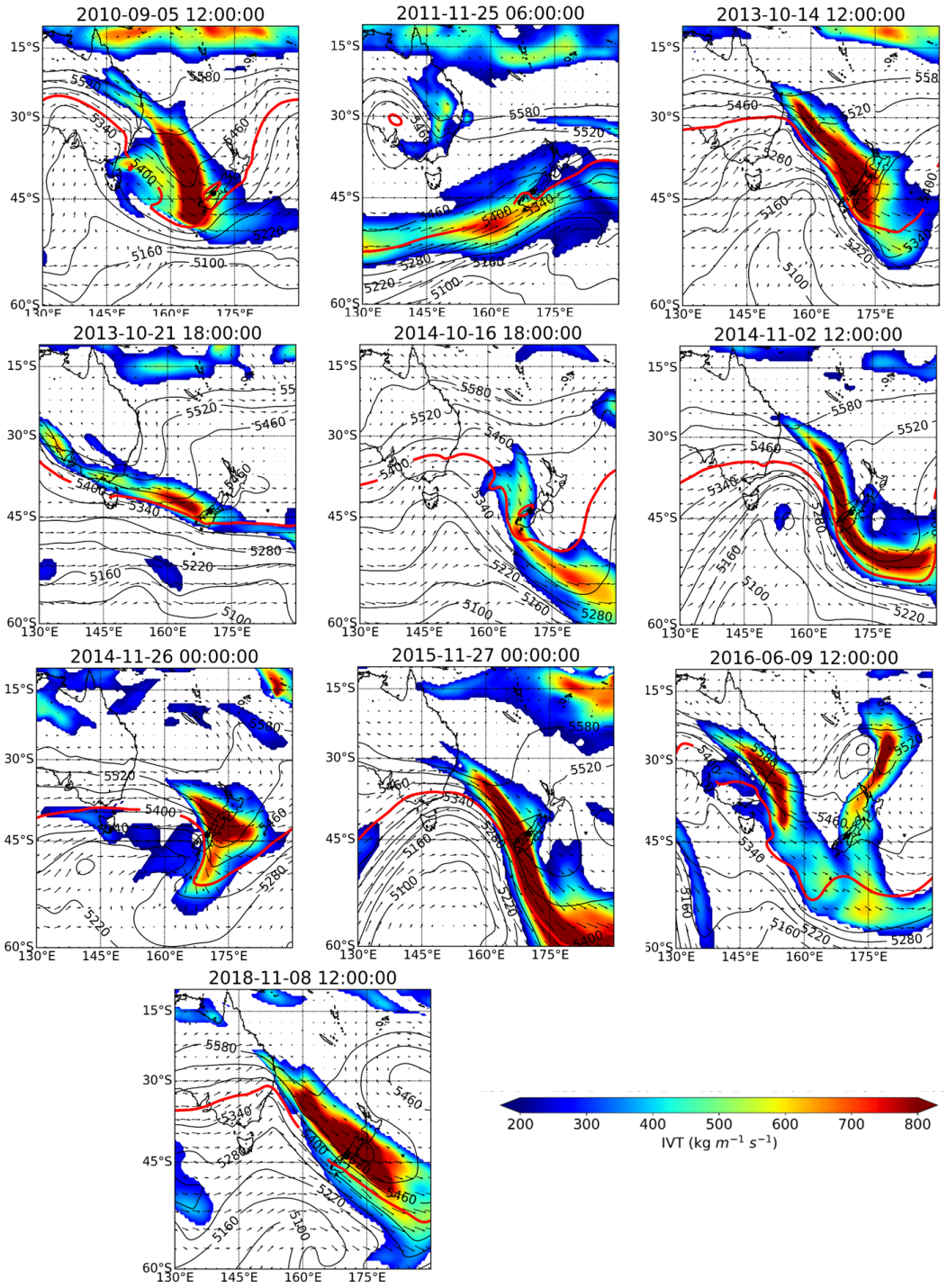

Figure 5.2 Integrated vapour transport (IVT, kg m^{-1} s^{-1}) associated with the 10 topmost ROS at Mueller Hut. The red line is the 5400 m thickness line showing the boundary between cold and warm airflows.

Analysis of maximum integrated vapour transport (IVT) and persistence at a given location provides a clear picture of intensities of such events. Table 5.1 shows the maximum values of IVT over the Tasman Sea while systems moving towards the Southern Alps and also at the west coast of the Southern Alps when they made landfall. Also, the maximum IVT and the persistence of the systems (IVT ≥232 kg m^{-1} s^{-1}) at the location of Mueller Hut are presented. Results revealed that the maximum values of IVT always exceeded 1000 kg m^{-1} s^{-1} over the Tasman Sea, with a maximum of 1700 kg m^{-1} s^{-1} during two events in October 2013. The maximum magnitude over the Southern Alps (at the grid point of Mueller Hut) varies between 326.7 kg m^{-1} s^{-1} (10th August 2010) to 822 kg m^{-1} s^{-1} (8th November 2018). Applying a threshold of 232 kg m^{-1} s^{-1} (see section 3.2.3, Figure 3.2) revealed that the duration of ARs near the Main Divide ranges from less than 24 hours to ~42 hours.

In order to better understand the hydrometeorological characteristics of ROS events two case studies of AR-related ROS events are analysed in more detail. The following sections present a comprehensive analysis of atmospheric circulation conducive to these events and their impacts on snowmelt processes and river discharge in the region.

5.3.2 Case study 1: Winter ROS (June 2016)

The first case study was a rainstorm event that occurred between 9th and 10th June 2016 (NZST). Meteorological and snow observations from the Mueller Hut AWS indicate that the storm resulted in a ROS event (Figure 5.3). The rain gauge at Mueller Hut recorded a total of 229.5 mm precipitation. Precipitation began at 09-06-2016 05:00 (NZST) and continued over a course of 45 hours. The air temperature rose up to a maximum of 7.37 °C at 09-06-2016 00:00 (NZST). The temperature sensor at 10cm-depth showed that the rain event caused an increase in temperature within the snowpack (from – 0.16 °C to 2.98 °C). This high temperature can be related to percolation of rain water through the snowpack. The rising air temperature and increase in snowpack temperature led to a rapid decrease in snow depth (ΔSD = ~30 cm) during the event. Even though SWE

was not available for this event, previous knowledge of typical snow densities of approximately 400 kg m^{-3} in the Southern Alps (e.g. Heine, 1962; Fitzharris et al., 1999; Purdie et al., 2015) means that it is reasonable to expect that snow depth change due to compaction, account for only approximately 2 cm, and so the majority of snow depth change is attributed (10-12 cm) to snow melt.

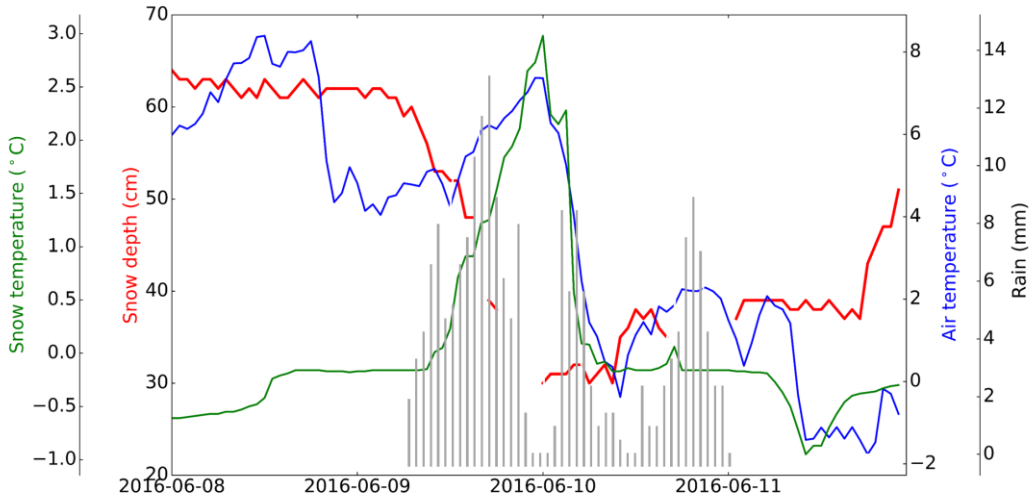

Figure 5.3 Meteorological observations during the June 2016 ROS event.

During the June event, the combination of rapid snowmelt and rainfall resulted in rapidly increasing flow rates in upper terrains of the region. The streamflow data from Hooker River at Ball Hut Road Bridge and Jollie River (Figure 4.1) indicate a significant increase in flow rates during the event (Figure 5.4). The Hooker River gauge recorded a maximum daily flow of 68.7 $m^3 s^{-1}$ on 11th June (NZST). At Jollie River the daily flow rate reached a maximum daily of 21.4 $m^3 s^{-1}$ on 10th June (NZST). These flow rates are approximately three times greater than the long-term average flow rates (Hooker River: 24 $m^3 s^{-1}$, and Jollie River: 7.5 $m^3 s^{-1}$). Figure 5.4 revealed that hourly river flow rates reached a peak flow rate of 82.2 $m^3 s^{-1}$ at 2016-06-11 15:00 at Hooker River and 31.57 $m^3 s^{-1}$ at 2016-06-10 18:00 at Jollie River.

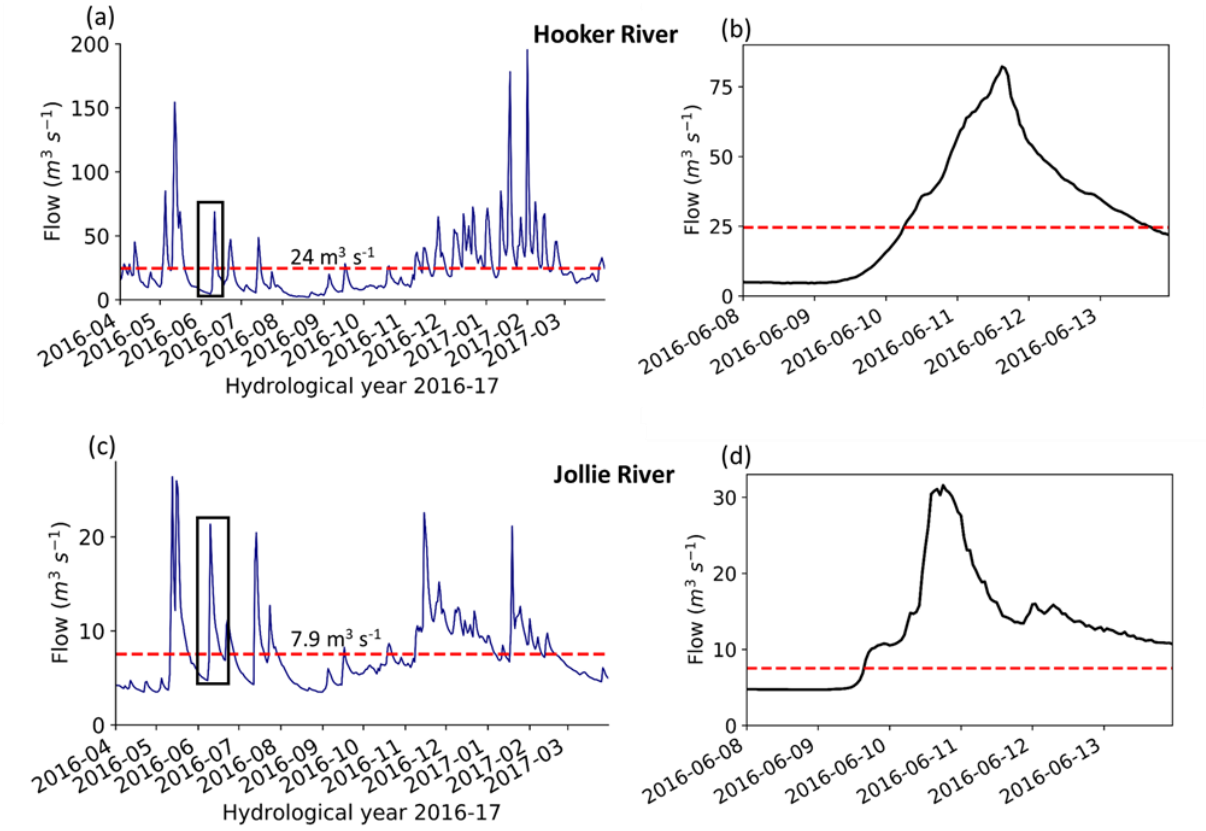

Figure 5.4 (a) Time series of average daily flow during water year 2016-17 at Hooker River, (b) hourly flow during the June ROS event at Hooker River, (c) is similar to (a) but for Jollie River, and (d) is similar to (b) but for Jollie River. The black box shows runoff associated with ROS events. The red dashed line is the long-term average of daily discharge.

5.3.2.1 Meteorological characteristics of June 2016 ROS event

Synoptic analysis of surface maps for the day prior and during the ROS event indicate that the event was the result of a strong low-pressure system with a central pressure of ~982 hPa at 09-06-2016 12:00 (NZST) (Figure 5.5) associated with a troughing synoptic regime approaching the South Island.

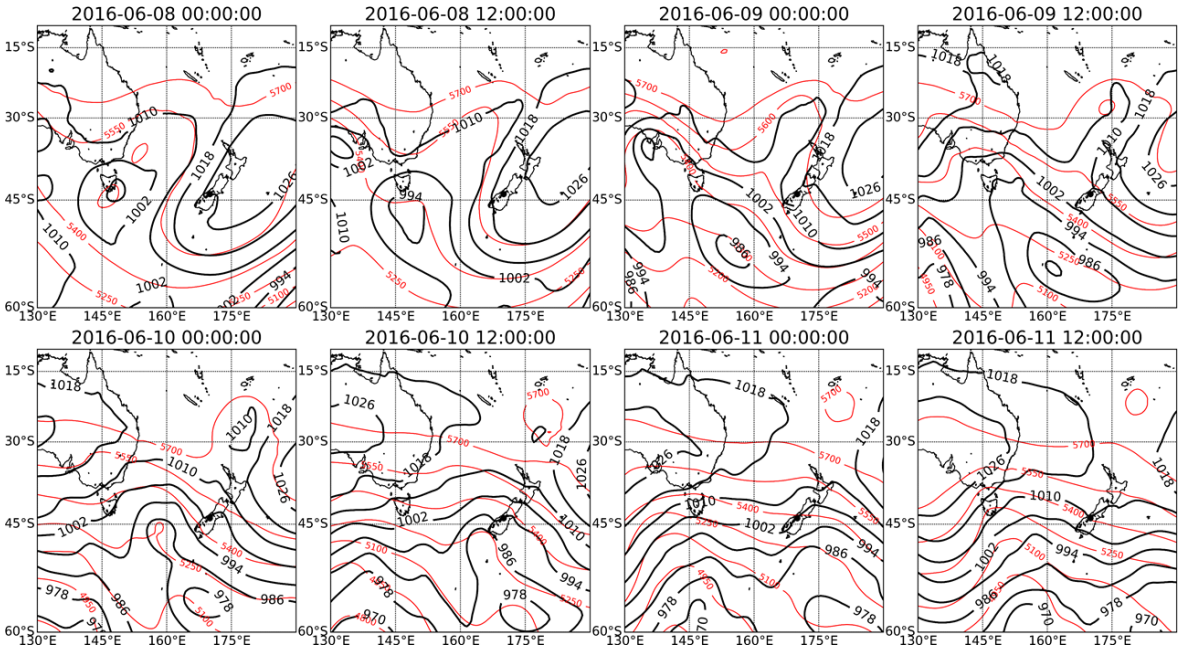

Figure 5.5 SLP (hPa) and Z500 (m) during June 2016 ROS event.

Six-hourly IVT values prior and during the event showed that the event was related to two separate moisture plumes in the Tasman Sea (Figure 5.6). IVT values increased to a maximum of ~550 kg m^{-1} s^{-1} along the West Coast of South Island (at 42.7° S and 170.9° E, Figure 5.6 and Figure 5.7). This condition produced significant precipitation along the West Coast, with up to 456 mm recorded at Cropp River rain gauge (Figure 4.1). Over the Southern Alps, the IVT magnitude exceeded the value of 232 kg m^{-1} s^{-1} over a period of 48 hours reaching a maximum of ~467 kg m^{-1} s^{-1} at 09-06-2016 12:00 (NZST).

Temperature is a key element of ARs. AR-related storms are warm by nature due to warmer vapour airflows originating from tropics (Neiman *et al.*, 2008a; Rössler *et al.*, 2014; Guan *et al.*, 2016). Determining the temperature characteristics of ARs is therefore critical for assessing their impacts on snowpacks during ROS events. In evaluating the heat flux during the ROS event, the vertical integral of heat flux was constructed through the atmospheric column. Figure 5.8a shows that the vertical integral of heat flux rose up to 10.2 $\times 10^9$ W m^{-2} when the moisture plume travelling over the Tasman sea at 09-06-2016 12:00 (NZST). This increase in heat flux is due to advection of moist and warm airflow carried by ARs and leading to an increase in temperature at mid and lower troposphere. The 5400 thickness line (red line, Figure 5.6) was located in the south of the

South Island during most of the storm. This condition results in liquid precipitation at high altitudes of the Southern Alps. However, at the last stage of the storm, the 5400 thickness line moved northward after 10-06-2016 06:00 (NZST) leading to a transition from rain to snow at Mueller Hut for a short period of time (see Figure 5.3).

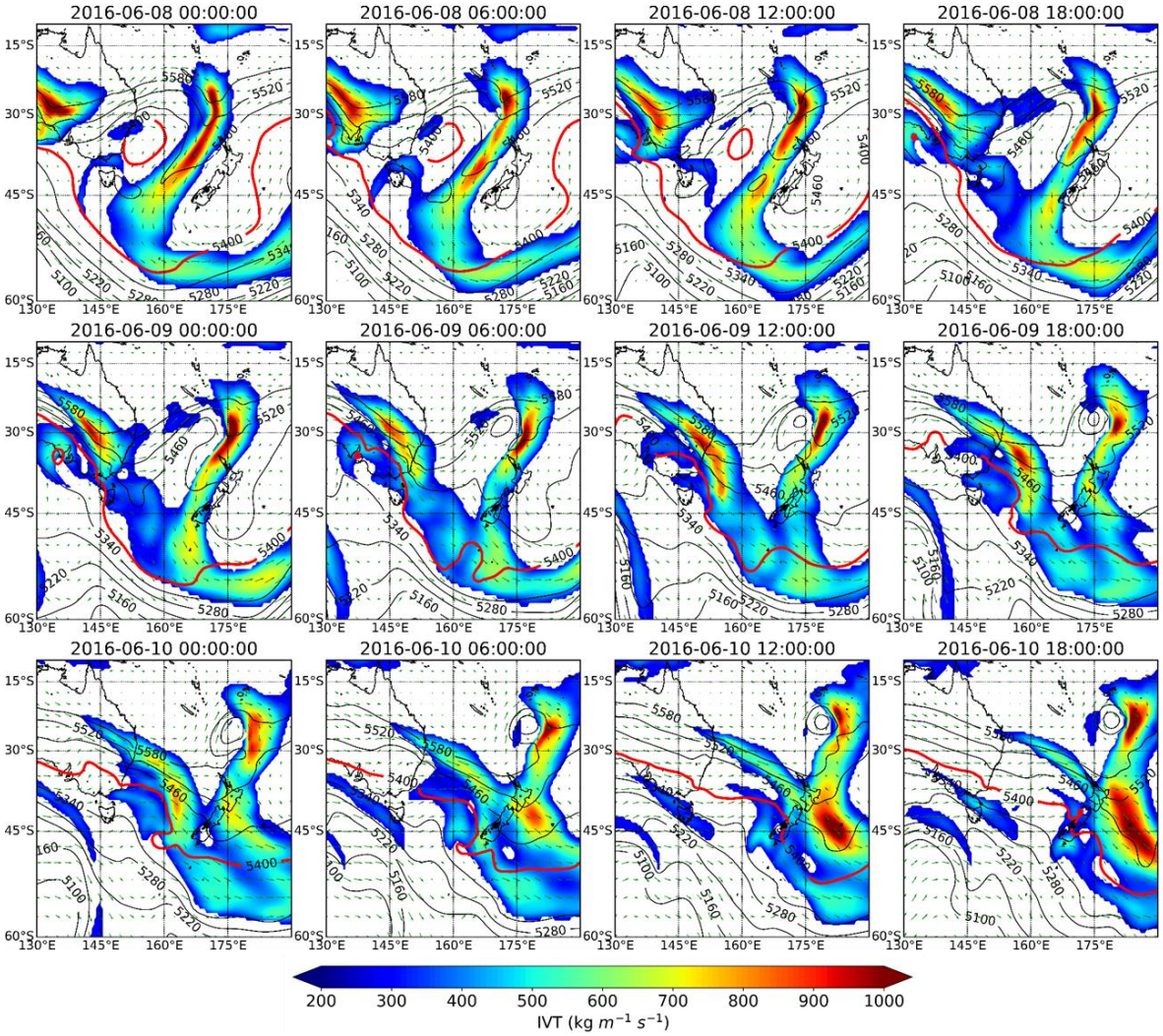

Figure 5.6 Six hourly IVT (kg m^{-1} s^{-1}) values during June 2016 ROS event. Red line is the 5400 m thickness line determining the boundary between warm and cold airmasses.

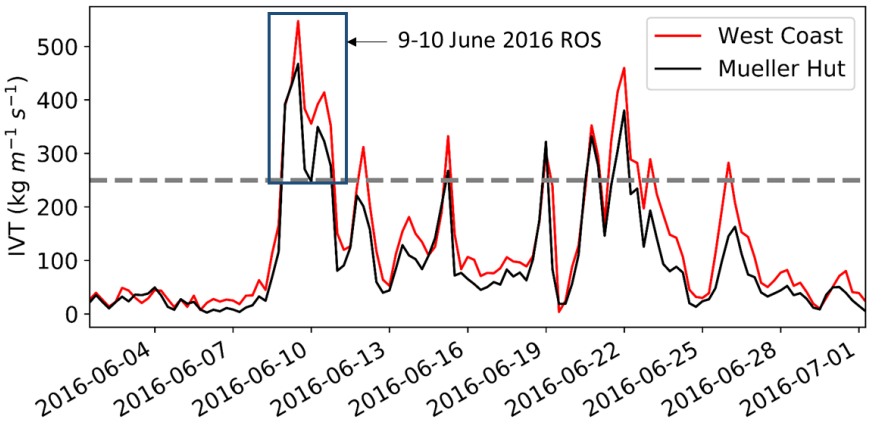

Figure 5.7 Six-hourly time series of IVT values (kg m^{-1} s^{-1}) during June 2018 alongside the West Coast of New Zealand and near the Main Divide (Mueller Hut). The dashed line indicates the 232 kg m^{-1} s^{-1} value.

The temperature profile between 300 and 1000 hPa (Figure 5.8b) reveals that temperatures at pressure levels lower than 725 hPa were above freezing level, ranging from 0 °C at 725 hPa to 15.8 °C at 1000 hPa, at 09-06-2016 12:00 (NZST). The freezing level is way higher than the height of the mountain ranges in the region. A depiction of temperature anomalies at three pressure levels (500 hPa, 850 hPa and 1000 hPa) shows a significant increase of temperature during the passage of the ARs across the region (Figure 5.8c). While the overall patterns of temperature anomalies at three pressure levels are similar, the anomalies are stronger at higher levels (~9 °C above average at 500 hPa and ~10.5 °C above average at 850 hPa) compared to the surface level (~5.6 °C above average at 1000 hPa).

5.3.3 Case study 2: Spring ROS (November 2018)

The November 2018 ROS was associated with heavy rainfall that affected many parts of the South Island. The Cropp River rain gauge on the West side of the Southern Alps, for example, recorded a cumulative rainfall of 670.2 mm. Similarly, Mt. Philistine AWS, located at 1655 m (~145 km north east of Mueller Hut, Figure 4.1) recorded 541 mm of rain during the storm. Figure 5.9 shows meteorological observations recorded at Mueller Hut during the event. Although a total cumulative rainfall of 366 mm was recorded over a period of ~88 hours, much of the rain (299 mm) fell on 8th November (NZST) at Mueller

Hut. Air temperature reached a maximum of 10 °C at 08-11-2018 18:00 (NZST). Similar to the June ROS event, the warm temperatures led to rapid snowmelt at Mueller Hut. Snow depth decreased by ~40cm between 7th November and 9th November. Unlike June 2016 event, SWE data were available for this event showing substantial snow loss (ΔSWE=20 cm). The temperature sensor at 10cm into the snowpack shows that temperature reached a maximum of 1 °C at 08-11-2018 7:00 during the event.

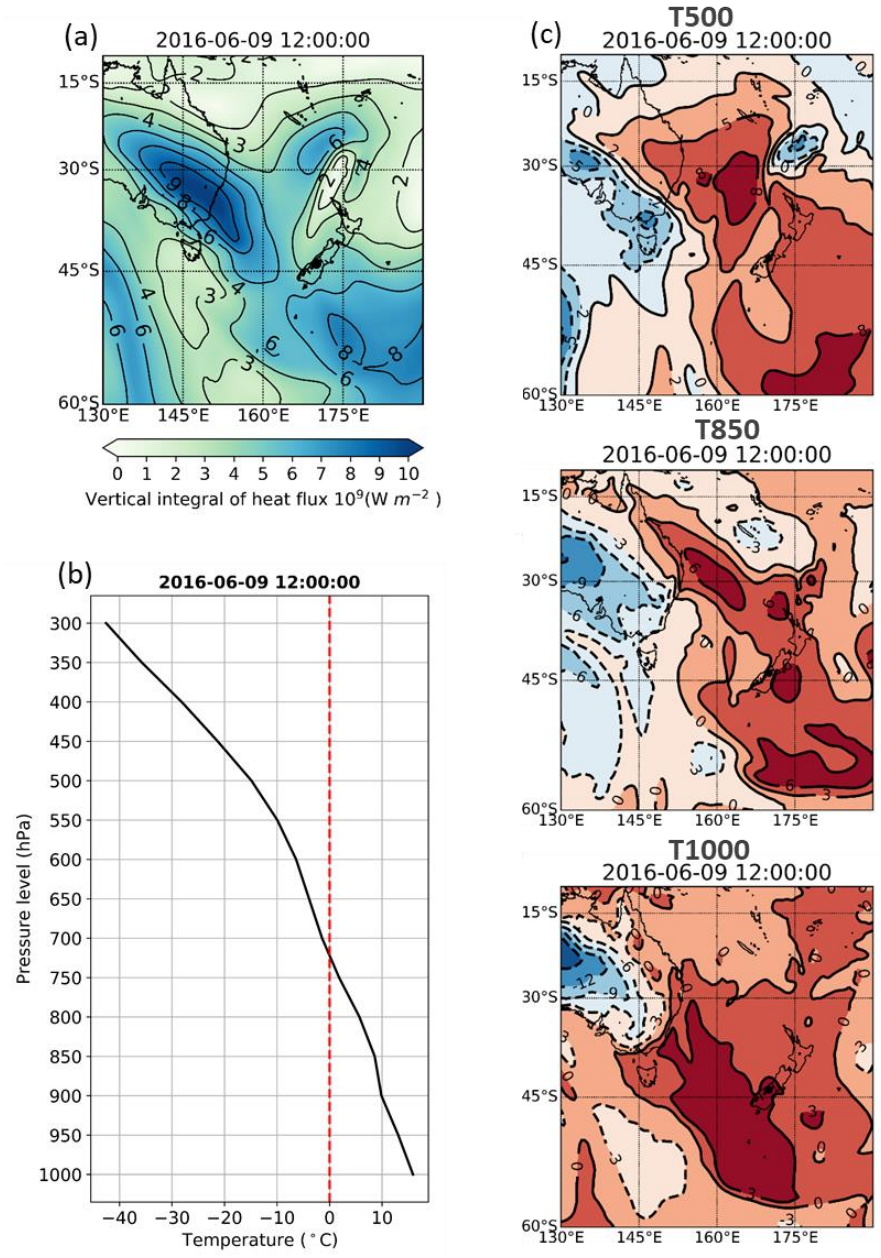

Figure 5.8 (a) The vertical integral of heat flux 09-06-2016 12:00 (NZST) (b) temperature profile at 09-06-2016 12:00 (NZST), and (c) anomalies of temperature during June 2016 ROS event at three pressure levels. The red dashed line defines the 0 °C line.

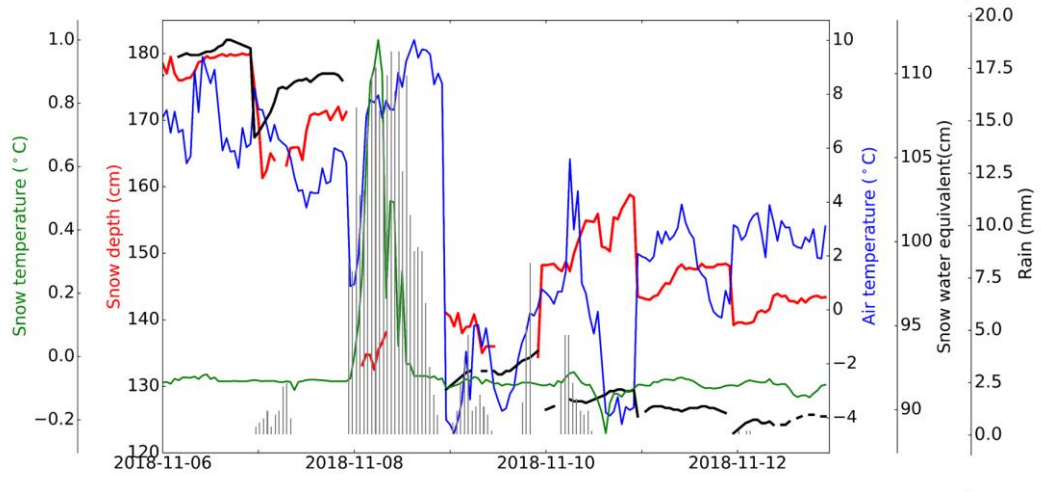

Figure 5.9 Meteorological data during November 2018 ROS event.

During the November rainstorm, a combination of heavy rain and snowmelt caused stream flow rates to increase rapidly in alpine catchments of the Southern Alps. Major flooding events caused significant damage to roads and bridges in Canterbury, Otago and West Coast regions of South Island (NZHERALD, 2018). Peak flow rates during this event were at least three times greater than those of June 2016 event due to both more intense rainfall and higher snowmelt rates. The Jollie River flow gauge recorded its highest daily flow rate of water year 2018/19 reaching ~64 $m^3 s^{-1}$ on 9th November (Figure 5.10). The instantaneous peak flow reached a maximum of 72.8 $m^3 s^{-1}$ at 09-11-2018 04:00 (NZST). Likewise, a major increase in river flow rate was recorded at Hooker River. Hooker River had its third highest daily flow rate in water year 2018/19 with 254 $m^3 s^{-1}$ during this event with a maximum hourly flow of 374 of $m^3 s^{-1}$ at 09-11-2018 05:00 (NZST).

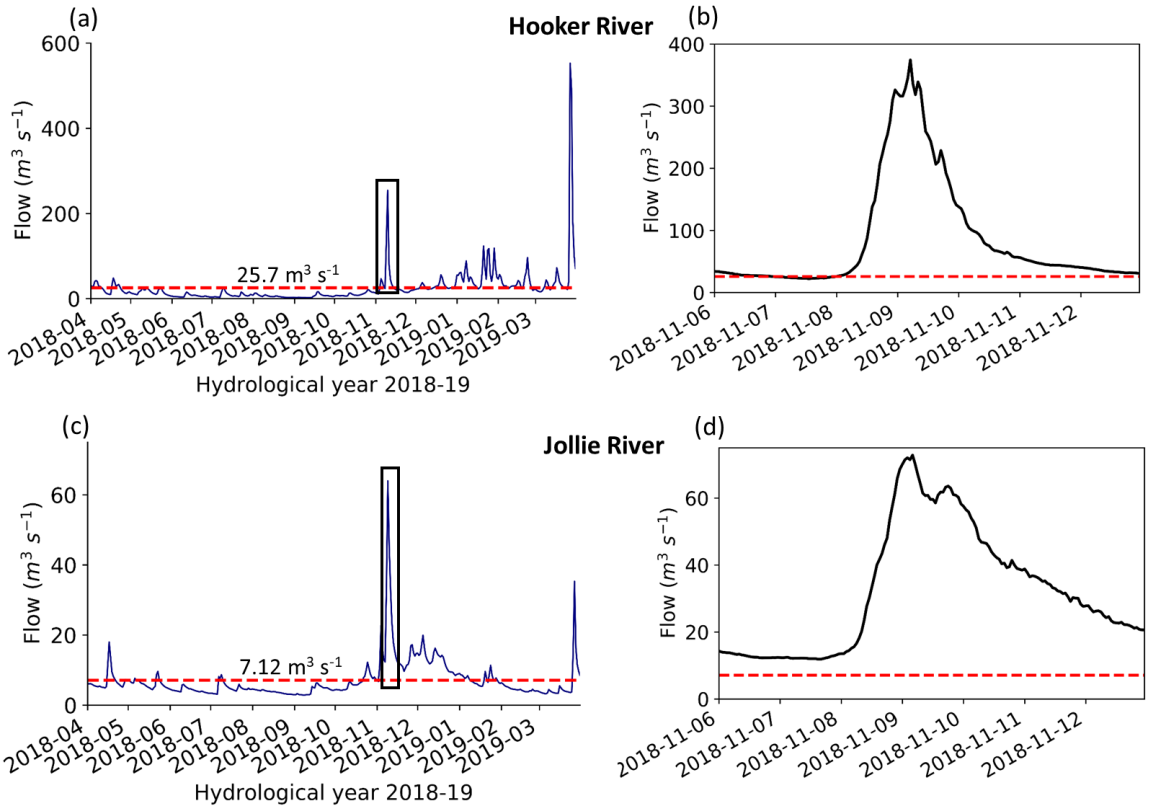

Figure 5.10 (a) Time series of average daily flow during water year 2017-18 at Hooker River, (b) hourly flow during the November ROS event at Hooker River, (c) is similar to (a) but for Jollie River, and (d) is similar to (b) but for Jollie River. The black box shows runoff associated with ROS events. The red dashed line is the long-term average daily flow.

5.3.3.1 Meteorological characteristics of November 2018 ROS event

Analysis of SLP during the storm indicates that the November 2018 ROS event was associated with a rapidly deepening low pressure system over Tasman Sea travelling towards New Zealand region (Figure 5.11). The sea level pressure with a low centre (~970 hPa) formed in the southwest of South Island. Analysis of six-hourly IVT fields illustrates the passage of an AR over the South Island of New Zealand during the event (Figure 5.12). The time series of IVT values (Figure 5.13) indicates that the IVT values along the West Coast reached a maximum of ~1158 kg m^{-1} s^{-1} at 08-11-2018 12:00 (NZST), while the Main Divide (at the grid point of Mueller Hut) experienced a maximum IVT of 822 kg m^{-1} s^{-1} at 08-11-2018 12:00 (NZST). The threshold of IVT ≥232 kg m^{-1} s^{-1} shows that the AR lasted ~48 hours at the location of Mueller Hut.

In terms of heat flux, the vertical integral of heat flux during the November event was of similar value to that recorded in the June event reaching 10.55×10^9 W m^{-2} at 08-11-2018-12:00 (NZST) (Figure 5.14a). However, the November AR was a relatively warmer event where above freezing temperatures were observed at higher pressure levels (0.4 °C at 650 hPa, Figure 5.14b). This warm environment resulted in strong positive anomalies of temperature at 500 hPa (~10.2 °C), 850 hPa (~9.5 °C) and 1000 hPa (~5.6 °C) (Figure 5.14c).

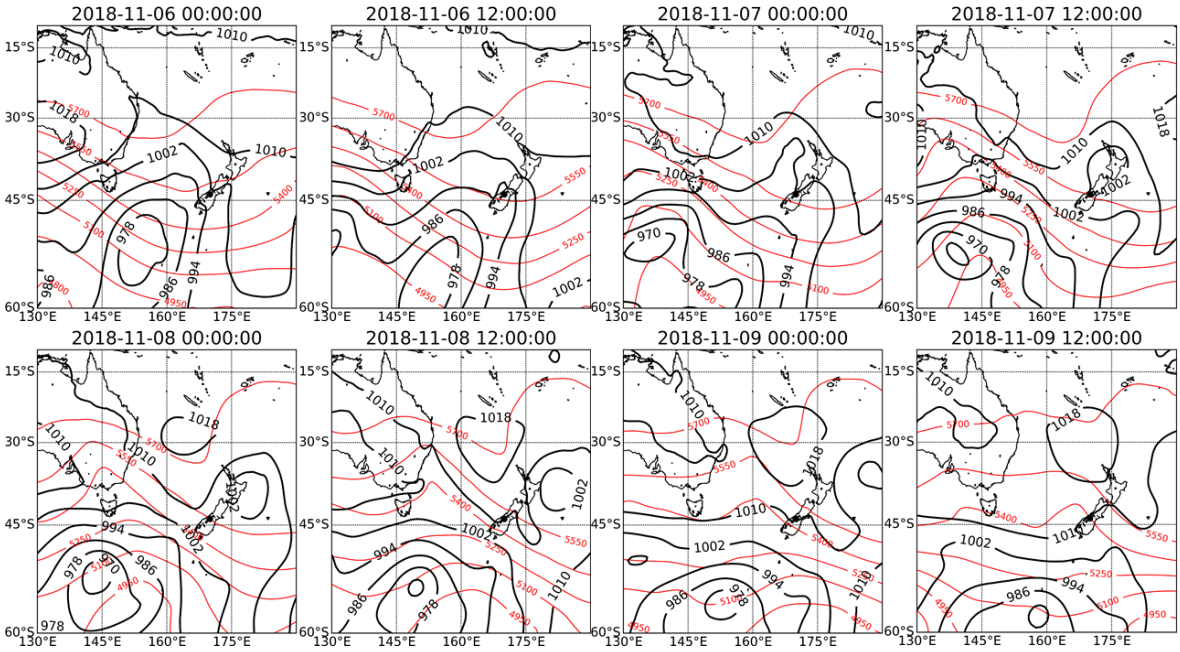

Figure 5.11 SLP (hPa) and Z500 (m) during November 2018 ROS event.

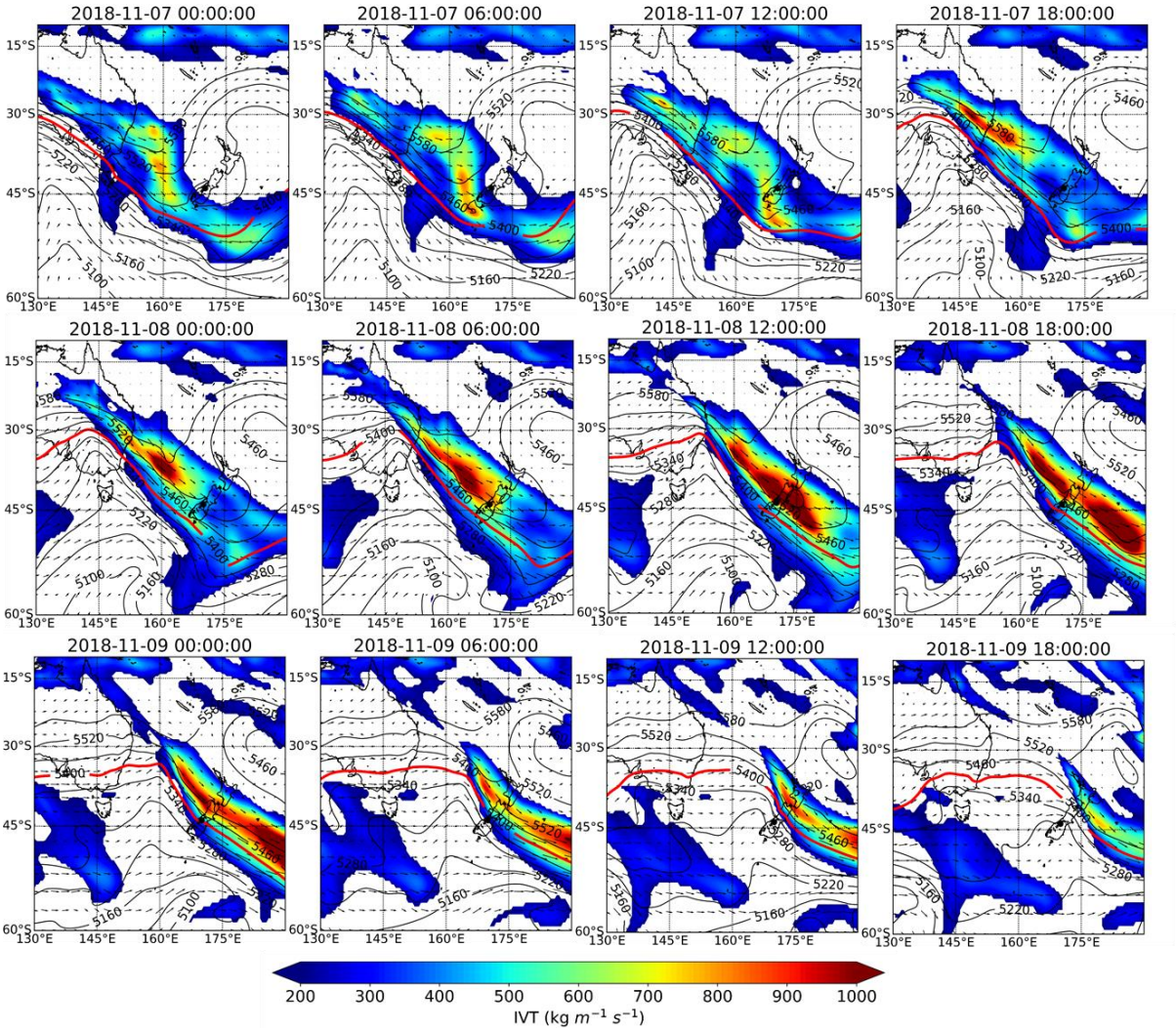

Figure 5.12 Six hourly IVT (kg m^{-1} s^{-1}) values during November 2018 ROS event. Red line is the 5400 m thickness line.

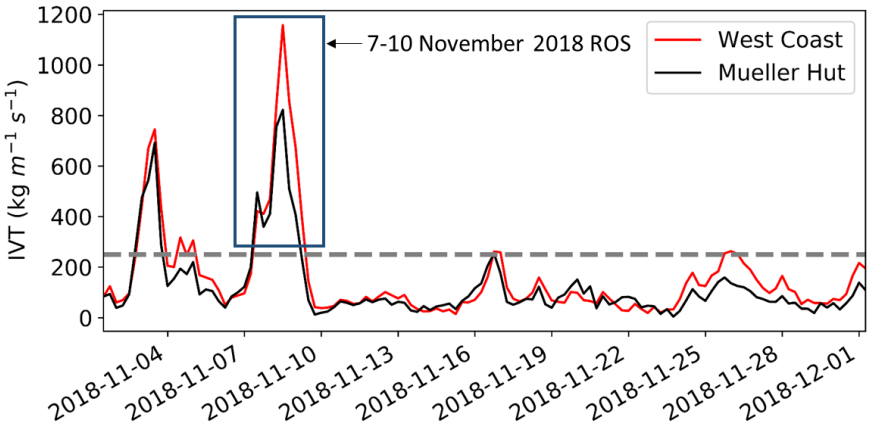

Figure 5.13 Six-hourly time series of IVT values (kg m^{-1} s^{-1}) during November 2018 alongside the West Coast of New Zealand and near the Main Divide (Mueller Hut). The dashed line indicates the 232 kg m^{-1} s^{-1} value.

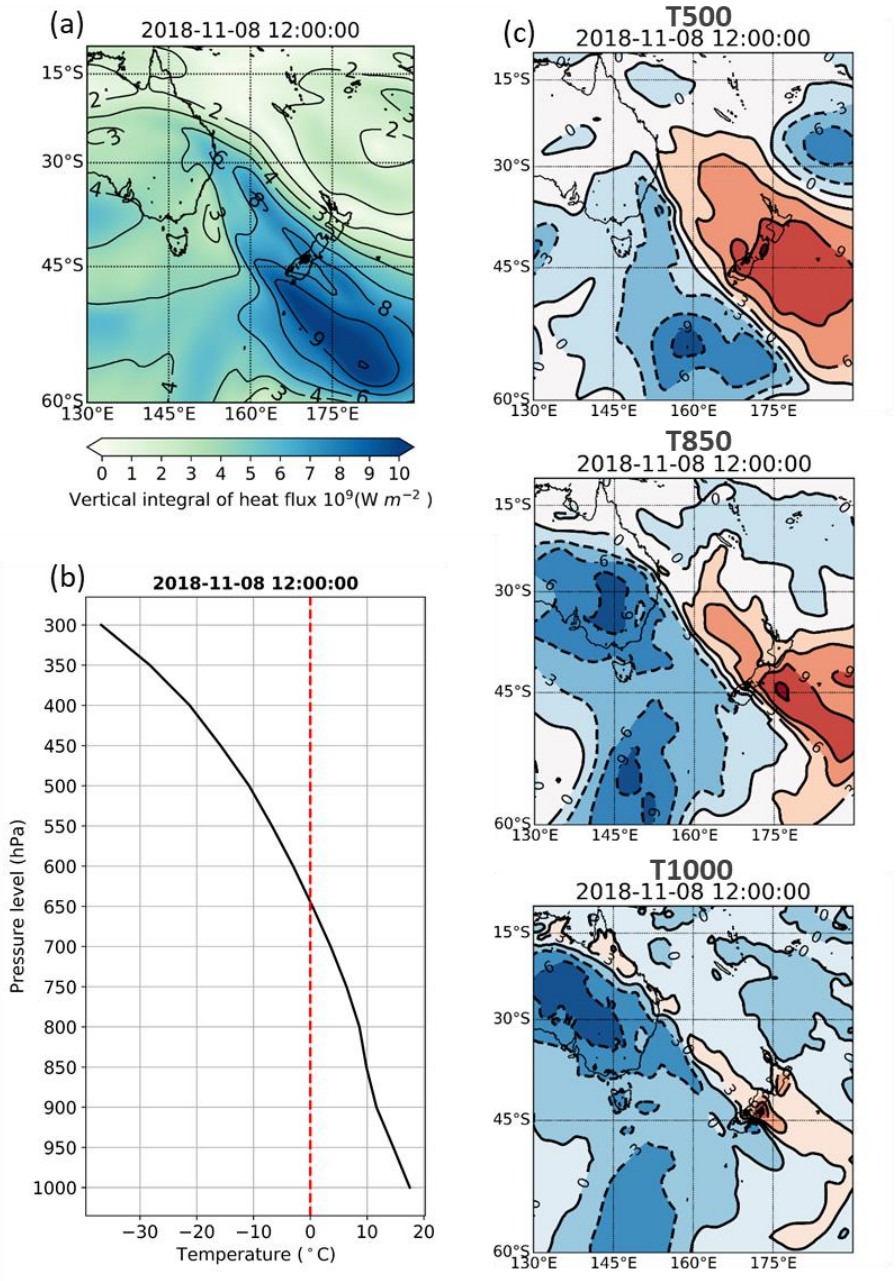

Figure 5.14 (a) The vertical integral of heat flux 08-08-2018 12:00 (NZST) (b) temperature profile at 08-11-2018 12:00 (NZST), the red dashed line defines the 0 °C line, and (c) anomalies of temperature during November 2018 ROS event at three pressure levels.

5.3.4 Hydrological characteristics of alpine rivers during rain-on-snow events

In order to assess the importance of AR-related ROS events in producing high flow rates in two alpine rivers studied here, the frequency of June 2016 and November 2018 flooding events were analysed by applying the flow duration curve. Figure 5.15 shows the flow duration curve of daily flow rates at Jollie River (1960-2018) and Hooker River (1965-2018). The analysis of flood peaks during the June 2016 ROS event the percentage

of exceedance was ≥5.34% (68.7 $m^3 s^1$) at Hooker River and ≥3% (21.4 $m^3 s^1$) at Jollie River. It is evident that warm ARs leading to heavy rain rather than snow at higher altitudes during winter can be a major deriver of winter flooding events in the Southern Alps. The analysis of flood peaks was repeated for November event. The percentage of exceedance during November 2018 ROS event provides more evidence of the significance of river flow rates during the passage of ARs and the consequent ROS event. During peak discharge rates at Hooker River (254 $m^3 s^{-1}$) and Jollie River (64 $m^3 s^{-1}$) the percentage of exceedance was 0.18 and 0.045%, respectively. The frequency analysis of flow rates during November event suggests that AR landfalls in spring months when snow is present on the ground can generate major flooding events in the mountain terrains of the South Island.

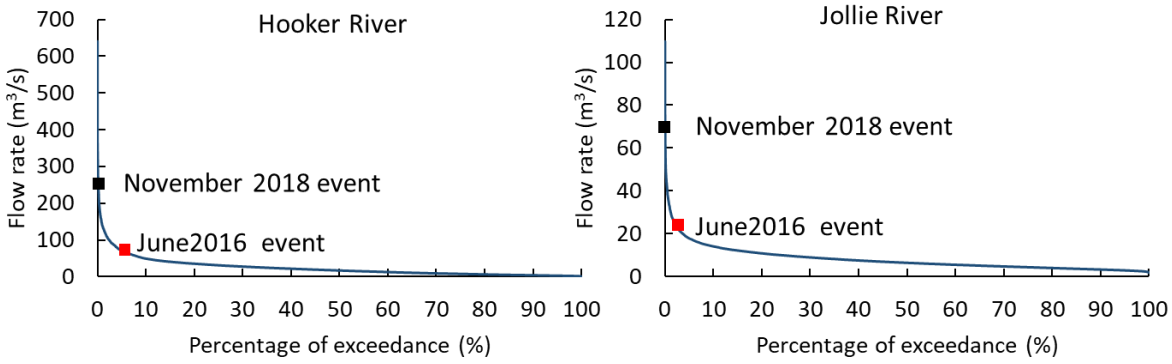

Figure 5.15 Flow duration curve at Hooker River and Jollie River.

5.4 Discussion and conclusions

Enhanced knowledge of atmospheric moisture transport during ROS events improves the understanding of their impacts on the hydrometeorology of alpine catchments. For the first time, the present study evaluated the hydrometeorological characteristics of ROS events in the Southern Alps. It was found that between 2010 and 2018 the 10 largest ROS events were associated with high fluxes of water vapour travelling over the Tasman Sea in a north-west to south-east direction towards the South Island of New Zealand (Table 5.1 and Figure 5.1). The results show a strong connection between major ROS events and ARs as the primary driver of water vapour transport resulting in heavy rain falling on

seasonal snowpacks in the Southern Alps. Out of 10 identified ROS events, nine were associated with ARs. While the role of ARs in different hydrological phenomena such as heavy precipitation and flooding events have been well documented in the mid-latitudes of the western North America, South America, the Norwegian coast and the British Isles (Neiman *et al.*, 2008a, 2013; Leung and Qian, 2009; Guan *et al.*, 2010; Dettinger *et al.*, 2011; Viale and Nuñez, 2011; Lavers *et al.*, 2012, 2013; Ralph *et al.*, 2016; Cordeira *et al.*, 2017), their role in generating ROS events has been largely unknown. Following recent studies in western United States (Neiman *et al.*, 2013; Guan *et al.*, 2016) and Swiss Alps (Rössler *et al.*, 2014), that reported links between ARs and ROS events, these findings in the Southern Alps highlighted the importance of further investigation of hydrometeorological characteristics during AR-related ROS in mountain regions.

The timing of large ROS events reported here shows that they are more frequent in spring months of October and November (8 out of 10). This is similar to the findings from California's Sierra Nevada where a frequent number of AR-related ROS events has been reported during spring month of March (Guan *et al.*, 2016). In terms of strength, spring ARs indicate higher IVT values compared to their winter counterparts. The IVT magnitudes during ROS events reported here for both winter and spring ARs are lower than those reported for intense summer-melt rates on Brewster Glacier by Little *et al.* (2019) (up to 1600 kg m^{-1} s^{-1}). The trend and timing of ARs in the Southern Alps seems to be different from those of AR-related storms reported in the western United States and South American Andes where a higher number of AR-related storms have been reported during cold months (Neiman *et al.*, 2008a; Guan *et al.*, 2010; Viale and Nuñez, 2011).

Detailed analysis of two AR-related ROS events in winter and spring provided a clear picture of hydrometeorological characteristics of ROS events. During the June 2016 ROS event, values of IVT reached a maximum of 467 kg m^{-1} s^{-1} near the Main Divide of the Sothern Alps, while the magnitude of IVT during November 2018 event rose up to 822 kg m^{-1} s^{-1}. Despite differences in timing and strength, both ARs contain several

similar hydrometeorological characteristics. Analysis of synoptic conditions showed that the events were associated with strong negative anomalies of sea level pressure with deep low pressures formed in the south and south west of the South Island (see Figure 5.5 and Figure 5.11). Another feature of these two AR-related ROS events is the distinctively high advection of warm airflows due to increases in vertical integral of heat flux up to more than 10.55×10^9 W m^{-2} over the Tasman Sea. As a result, anomalously high temperatures are evident at mid and lower troposphere during the passage of ARs. The 5400 m thickness line mainly located south of the South Island during the passage of ARs provided more evidence of warm environment during ROS. These conditions are comparable with anomalously high temperatures reported in other regions during AR-related ROS events. In California's Sierra Nevada, Guan *et al.* (2016) reported that ROS events associated with ARs are generally more than 2 °C warmer than melt events not associated with ARs. Likewise, in Switzerland's Bernese Alps a rise of 9 °C in air temperature has been found during a flood-generating ROS events associated with ARs (Rössler *et al.*, 2014). In the Southern Alps, the warm conditions associated with ARs resulted in enhanced temperatures at Mueller Hut with a maximum air temperature of 8.4 °C during June event and 10 °C during November event providing an environment favourable for rapid snowmelt. Records from temperature sensors inside the snowpack during the ROS events at Mueller Hut revealed a sudden increase in temperature due to anomalously warm rain percolating through snowpacks. Warm rain can induce faster snowmelt rates compared to non-ROS snowmelt events (Singh, et al., 1998). While the results of this study are mainly limited to large-scale atmospheric forcing rather than the energy flux over the snowpack, the illustration of vertical integral of heat flux implies a rapid increase of energy flux during AR-related ROS events leading to rapid significant snow loss (~10-12 cm during winter ROS event and ~20 cm during spring ROS event).

Similar to the characteristics of ROS events caused by ARs in European Alps and western United States (Neiman *et al.*, 2013; Rössler *et al.*, 2014; Guan *et al.*, 2016), the

analysis of flow rates during the passage of ARs over the Southern Alps showed that the combination of persistent heavy rainfall and intense snowmelt can generate significantly high peak flows in alpine rivers of the Southern Alps during both winter and spring. Numerous uncertainties especially related to snowpack conditions prior to ROS (e.g. the extent and thickness of the snow cover) and meteorological conditions during ROS events can create challenges to accurately predict flood events (McCabe *et al.*, 2007). While the primary focus of this study was the large-scale hydrometeorological characteristics of ROS events, further studies are required to comprehensively investigate flood-generating ROS events which are capable of causing disruptions in alpine catchments of the Southern Alps. To do so, specifically, it is important to determine the actual contribution of snowmelt and rainfall to runoff in order to better understand flood-generating processes associated with ROS. The use of hydrological models, with the ability to simulate snowmelt processes during ROS events, accompanied by field measurement of snowpack processes could provide a better understanding of streamflow generation during ROS floods in future studies.

The maritime snow-dominated regions have been found to be more vulnerable in a warming climate where even small increases in temperate can bring about significant changes in snow accumulation and snowmelt processes (Fitzharris *et al.*, 1999; Cullen and Conway, 2015; Fayad *et al.*, 2017). With a shift from snow-dominated patterns to rain-dominate patterns reported in many parts of the world (Barnett *et al.*, 2005; Nayak *et al.*, 2010; Krasting *et al.*, 2013), there is a higher likelihood of warm ARs during winter (Dettinger, 2011; Espinoza *et al.*, 2018). It is imperative that further research should emphasize on the impacts of climate change on the trend and variability of AR-related ROS events in the Southern Alps.

6 Thesis synthesis and conclusions

This chapter provides a synthesis of the main research findings, revisiting the initial objectives and demonstrating how these objectives have been met. With regard to the research questions, findings are summarised and general conclusions, the implications and the directions for future research are described (Figure 6.1 and Figure 6.2).

The primary aim of this thesis was to improve the knowledge of the atmospheric conditions influencing snow accumulation and snowmelt processes with a focus on large snowfall and snowmelt events in the maritime mountain environment of the Southern Alps. This aim was met by addressing four specific question:

1. What are the main characteristics of synoptic weather patterns during large snowfall events in the Southern Alps?
2. How does moisture flux change over the South Pacific Ocean across the Tasman Sea during large snowfall events in the Southern Alps
3. What are the main synoptic weather patterns that influence large snowmelt events?
4. What are the distinctive synoptic-scale characteristics of moisture transport during major rain-on-snow (ROS) events in the Southern Alps?

Previously, one of the barriers to improved understanding of the link between atmospheric patterns and large snowfall and snowmelt events was inadequate snow observations; particularly lack of spatial and temporal data at high altitudes. As highlighted in this research, data from the Snow and Ice Monitoring network provided a consistent observations of snow depth change at high altitudes of the Southern Alps. Coupling in-situ snow observations from three SIN stations and ERA-reanalysis dataset enabled the analysis of atmospheric forcing influencing hydrometeorology of snowfall and snowmelt in the Southern Alps of New Zealand.

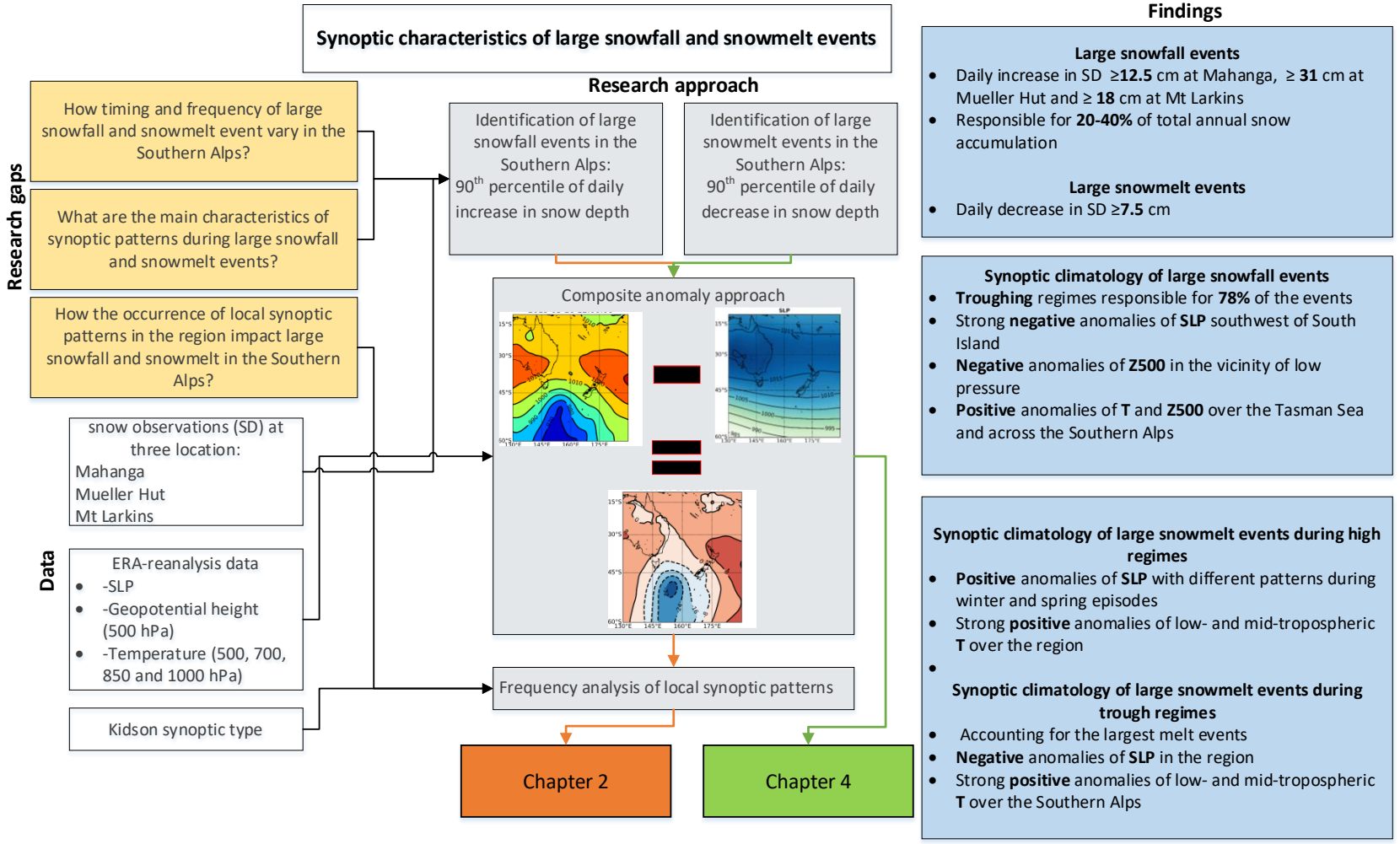

Figure 6.1 A summary of findings related to synoptic climatology of snowfall and snowmelt events (research questions 1 and 3).

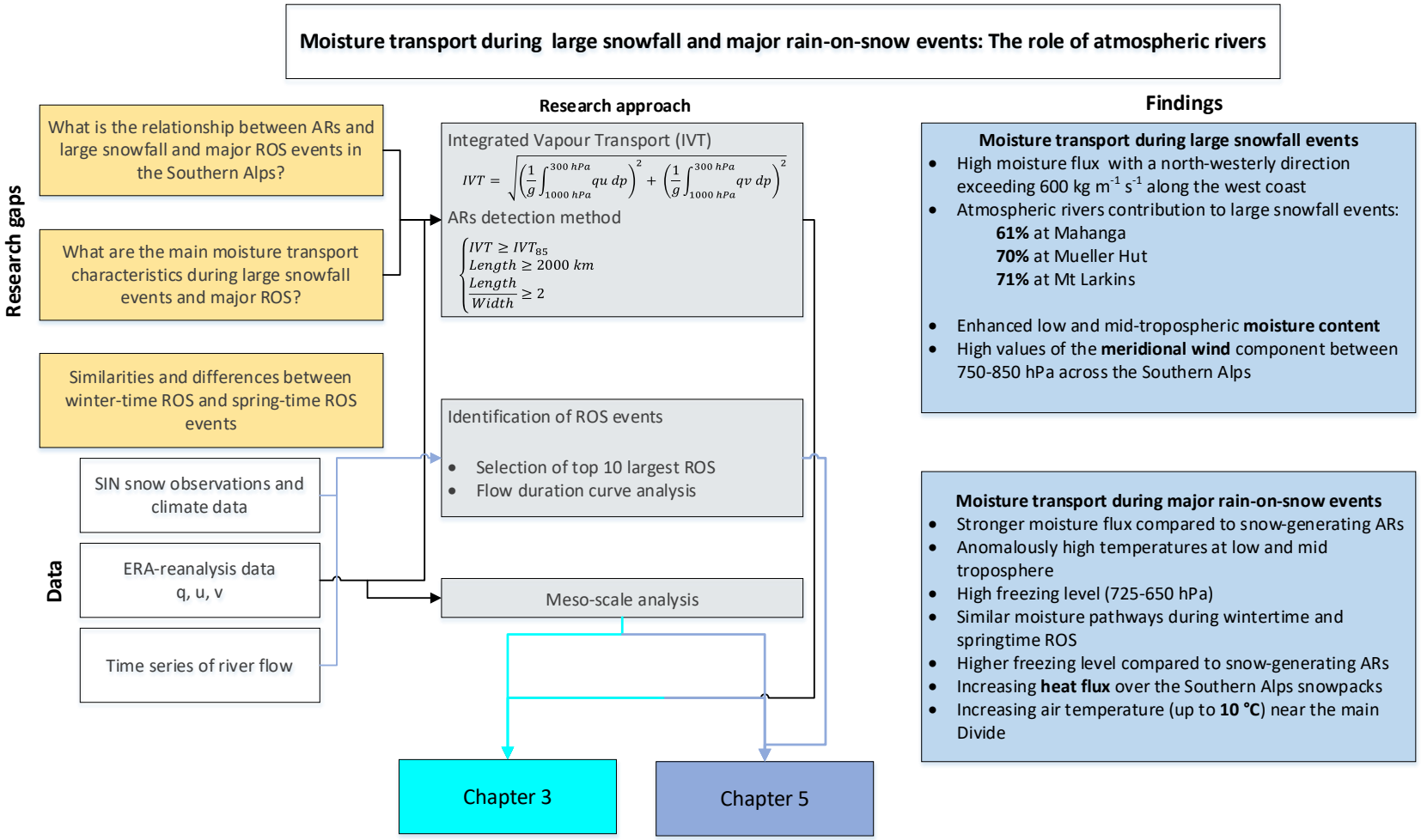

Figure 6.2 A summary of findings related to moisture transport during large snowfall and major ROS events (research questions 2 and 4).

6.1 Temporal variability of large snowfall and snowmelt events in the Southern Alps

An objective of this research was to improve the current understanding of large snowfall and snowmelt events in maritime mountain ranges. Examining the snow depth data recorded at three SIN locations (Mahanga, Mueller Hut and Mt Larkins) provided a clearer picture of snow accumulation and snowmelt patterns in the Southern Alps. Since the primary focus of this research was large snowfall and snowmelt events, the 90th percentile values of daily snow depth change (increase and decrease) were used to identify large snowfall and snowmelt events, respectively. This approach led to the selection of three thresholds for tagging days with large snowfall (i.e. 12.5 cm at Mahanga, 31 cm at Mueller Hut and 18 cm Mt Larkins). Regarding snowmelt events, a threshold of a snow depth decrease greater than 7.5 cm day^{-1} was selected using the snow observations at Mueller Hut near the Main Divide of the Southern Alps.

The contribution of large snowfall events relative to the total annual snow accumulation indicated that an average of 26% (Mahanga), 32% (Mueller Hut) and 28% (Mt Larkins) of the interannual variability in snow depth were associated with major events. Findings revealed that these large snowfall events alone can account for up to 40% of annual snow accumulation in some places over the Southern Alps. In the winter of 2016/17 at Mueller Hut for example, six snowstorms contributed to approximately 40% of annual snow accumulation. Based on timing of the occurrence, it was found that large snowfall events are not only limited to the typical snow accumulation months of June to September/October as such large events also occur during spring (October and November, Figure 2.7). Likewise, although spring (and summer) months are the primary time for large melt events, which account for ~80% of all events near the Main Divide, the snowpack can undergo periods of intense melt in the winter at Mueller Hut station (June, July, August and September) (see section 4.3 and Figure 4.4).

Previously, despite some work using short term data from limited locations across the Southern Alps (Prowse, 1981b; Moore and Owens, 1984; Neale and Fitzharris, 1997; Fitzharris *et al.*, 1999), the knowledge about annual variability of snow across this maritime mountain range was very limited. Observations of snow depth used in this study provided a better understanding of the general patterns of snow accumulation and snowmelt in the region. For the first time, this research documented the importance of large snowfall and snowmelt events in the Southern Alps in terms of both timing and magnitude. The SIN network (Hendrikx and Harper, 2013) used in this study has provided valuable measurements of snow at high altitudes. Even though the network is still in its infancy, as the dataset becomes longer its value will increase in the study of seasonal snow characters (the extent, duration, SWE etc.) in the Southern Alps. As the only systematic observations in the upper terrains of alpine catchments, SIN stations are an important source of information to help better understand the annual variability of snow cover required in managing water resources in alpine catchments. Additionally, because of limited ground-base observations of seasonal snow in many mid-latitude mountain regions especially in the Southern Hemisphere (Shaw *et al.*, 2020), the records of snow observations from New Zealand's Alps will provide important contributions to understanding snow accumulation in mid-latitude mountain regions of the Southern Hemisphere.

6.2 Synoptic characteristics of large snowfall and snowmelt events

Prior to this research being undertaken there was limited knowledge about the synoptic drivers of large snowfall and snowmelt events in the Southern Alps (Purdie *et al.*, 2011; Cullen *et al.*, 2019; Little *et al.*, 2019). In order to identify common atmospheric features of the days with large snowfall and snowmelt events, composite anomalies of the daily climate variables relative to the long-term climate normal were constructed. It was found that large snowfall events were usually associated with strong negative anomalies of sea level pressure (SLP) located over the southwest of New Zealand's South Island.

Such negative circulation anomalies generate strong westerly and north-westerly flows towards the Southern Alps. These conditions were concurrent with negative anomalies of geopotential heights at 500 (Z500) located in the centre of low pressure systems. However, across the Southern Alps, the Z500 anomalies were positive (Figure 2.10). Positive anomalies of Z500 accompanied by positive anomalies of temperature in the region suggest that warm tropical air flows are a primary driver of large snowfall events as they transport significant moisture towards the Southern Alps.

Additional information on synoptic conditions of snowfall events was achieved by calculating one-day difference maps for the day of snowfall and the day prior to the event. A common characteristic of the synoptic climatology during snowstorms was the rapid change in the atmospheric fields over a short time period (less than 24 hours). Investigation of the relationship between large snowfall events and local synoptic patterns as identified by Kidson (2000) agreed with previous findings (Purdie *et al.*, 2011) that troughing synoptic regimes dominate snowstorms. Indeed this research demonstrated that across the Southern Alps, troughing regimes were associated with approximately 78% of the snowstorms investigated. This highlighted the key role of moisture content transferred by such weather patterns through extratropical cyclones associated with jet streams. In addition to the fast moving weather types associated with troughing regimes, zonal regimes also contribute to large snowfall events to a lesser extent (16%). The Southern Alps can also receive large snowfall events during blocking regimes located to the east of the New Zealand region. These high pressure systems provide conditions favourable for solid precipitation by slowing down low pressure systems over the Tasman Sea moving towards the Southern Alps and resulting in snowfall on the edge of low pressure and high pressure systems.

By adopting a similar composite anomaly approach as that applied to the investigation of snow accumulation, this research documented the first synoptic-scale investigation of the climate variables associated with large snowmelt events at a site in the Southern Alps.

Observations from Mueller Hut showed that the Kidson synoptic patterns associated with high melt events were mostly high pressure patterns and troughing regimes. High pressure systems account for the majority of snowmelt events during winter-melt and spring-melt episodes. Rising temperatures in the mid- and lower troposphere, accompanied by positive anomalies of SLP were found to be the distinct synoptic features. Despite general similarities of weather patterns during winter- and spring-time melt episodes and noticeable temperature anomalies, different patterns of SLP were identified. While the centre of high pressure systems during the events occurring between June and September are located near the Main Divide and east of the New Zealand South Island, spring-time melt events are mainly coincident with high pressure systems with centres located on the west of New Zealand over Tasman Sea.

The presence of positive anomalies of temperature (2.5-4 °C) was also distinguishable during rapid snowmelt events associated with troughing regimes demonstrating that anomalously high temperatures are key drivers of these rapid melt episodes. Observations of daily snowmelt events during trough synoptic regimes showed that even though these events are less frequent compared to the ones associated with high systems, the largest winter-melt event (299 mm day^{-1}) and spring-melt event (330 mm day^{-1}) both occurred during troughing weather patterns.

These findings revealed the physical dynamics of weather patterns which control the timing and magnitude of major large snowfall and snowmelt events in a maritime climate. Providing a baseline for a better understanding of the current knowledge of atmospheric forcing influencing such events, these findings have important implications for investigating the possible future changes in frequencies of synoptic weather patterns in a warming climate. Since synoptic characteristics of weather patterns are more easily accessible compared to local in situ measurements of the energy flux (Esteban *et al.*, 2005; Romolo *et al.*, 2006a; Bednorz, 2012), they can be used to assess possible future

changes in large snowfall and rapid melt episodes in mountain regions which have a number of important implications in long-term watershed management.

6.3 Moisture transport during large snowfall events: The role of atmospheric rivers

An analysis of the synoptic characterization of snowfall events undertaken as part of this research recognized the important role of water vapour exports within a predominantly north-westerly airflow over the Tasman Sea as the main source of moisture during large snowfall events. While previous studies have provided basic knowledge about the key role of ARs in moisture flux transport towards the Southern Alps (Kingston *et al.*, 2016a; Little *et al.*, 2019; Prince, 2020), there was a lack of understanding of the hydrometeorological characteristics of ARs and their contribution to seasonal snowpacks across the Southern Alps.

To address this knowledge gap a detailed hydrometeorological analysis of snow-producing storms was obtained by computing the moisture flux over the Tasman Sea during the days leading to snowstorms in the Southern Alps. For the first time, the contribution of landfalling ARs to large snowfall events in the Southern Alps has been quantified by applying a commonly used AR detection method (e.g. Lavers and Villarini, 2013; Rutz *et al.*, 2014), which utilises IVT fields to identify ARs. The use of this method enabled the identification of long and narrow bands of intense water vapour transport (L ≥2000 km, L/W ≥2, and IVT ≥IVT^{85th} (232 kg m^{-1} s^{-1})) during large snowfall events. Strong fields of IVT responsible for moisture transport, accompanied by low pressure systems centred in west and southwest of the New Zealand's South Island was found to be the main driver of large snowfall events over the Southern Alps. Findings show that the magnitudes of maximum IVT during the snowstorms rarely exceed 600 kg m^{-1} s^{-1} along the west coast of the South Island, while the maximum IVT remains mainly just below 500 kg m^{-1} s^{-1} over the Southern Alps (see Table 3.2). By applying the above mentioned AR detection method, it was found ARs were responsible for approximately

61% of large snowfall events at Mahanga, while their contribution to the large snowfall events at Mueller Hut and Mt Larkins were 70 and 71%, respectively. Detailed analysis of individual landfalling ARs indicated that low and mid-level jet streams were the main drivers of moisture transfer across the South Pacific Ocean over Tasman Sea prior to large snowfall events in the Southern Alps. An enhanced presence of low and mid-level moisture between 700-850 hPa and pronounced increases of wind velocities with high values of the meridional component between 750-850 hPa were identified over the Southern Alps during AR-related snowfall events.

The contribution of ARs to snowfall events in the Southern Alps (41.5°-45.5° S) is in broad consistency with other work in Mount Shasta (Hansen *et al.*, 2013), California's Sierra Nevada (Guan *et al.*, 2010, 2012) and South American Andes (Viale *et al.*, 2018; Saavedra *et al.*, 2020) suggesting that ARs largely influence the winter precipitation at mid-latitudes especially during large snowfall events. The role of orography and its interaction with landfilling ARs in both Andes (Saavedra *et al.*, 2020) and western United States (Neiman *et al.*, 2013; Hecht and Cordeira, 2017) has proven to largely influence the local and regional precipitation distributions. Given the characteristics of the landfalling ARs in the Southern Alps shown in this research, it is important to further investigate the similar physical mechanisms controlled by orography such as windward orographic precipitation and the horizontal moisture convergence (Smith *et al.*, 2010) in the mountain regions of the Southern Alps.

6.4 The role of atmospheric rivers in major rain-on-snow events

Atmospheric rivers have been found to contain warmer temperatures compared to other winter storms due to the freezing level being at higher altitudes (Neiman *et al.*, 2013; Guan *et al.*, 2016). Therefore, there is a greater likelihood that some landfalling ARs result in ROS at high altitudes especially in maritime environments where ROS events are common phenomena (Guan *et al.*, 2016). Previously, only a few studies in the western United States (Guan *et al.*, 2016) and Swiss Alps (Rössler *et al.*, 2014) had documented

the connection between ARs and ROS. Considering the findings from composite anomaly maps (refer back to thesis section) that indicated warm temperatures associated with snow producing storms over the Southern Alps, the assumption was made that such storms could also lead to potential major ROS events in the region. Observations from Mueller Hut weather station were used to identify the ten topmost rainfall events between 2010 and 2018 while snow was present on the ground. Analysis of IVT showed that all ten events were associated with strong fluxes of tropical water vapour travelling over Tasman Sea in a north-west to south-east direction (see section 5.3 and Table 5.1). The position of the 5400m thickness lines during these events, mainly located far south of the New Zealand's South Island, is indicative of high temperatures associated with the moisture flux over the Tasman Sea. ARs were found to be responsible for nine out of ten identified ROS events. It should be noted that despite being more common during October and November (8 out of 10), ROS events also occurred during the colder months of June and September. Similar hydrometeorological characteristics such as duration and shape were identified during these rain-producing ARs compared to their snow-generating counterparts; however, in terms of strength, the former were found to contain higher IVT values. Exceptionally high values of IVT (up to 1500 kg m^{-1} s^{-1}) were observed over the ocean as the rain-producing ARs travelled over the Tasman Sea, while near the Main Divide the IVT values reached a maximum of ~822 kg m^{-1} s^{-1} (during 8th November storm).

A case study of two individual ROS-producing ARs which made landfall in winter (June 2016) and spring (November 2018) revealed further details about hydrometeorological characteristics and impacts of such events in the Southern Alps. The November AR (Figure 5.13) produced the largest ROS event during the study period with a total accumulated rainfall of 540 mm recorded in parts of the Southern Alps. The June event was regarded as the largest winter-time ROS with a total rainfall of 229.5 mm recorded near the Main Divide at Mueller Hut. Both rain-producing ARs had several

similar synoptic features including: a deep low pressure system, travelling from the southwest of South Island towards the Southern Alps; strong moisture fluxes containing anomalously high temperatures at lower levels of the troposphere; and high advection of warm airflows. Analysis of the vertical structure of the temperature revealed an increase in freezing level with the 0 °C line located between 725-650 hPa. These findings agree with observations in the western United States (Guan *et al.*, 2016) and Swiss Alps (Rössler *et al.*, 2014) that indicate similar anomalously high temperatures over the seasonal snowpacks during the passage of ARs. In the Southern Alps, these conditions brought about a rapid increase in air temperature with values up to 10 °C, and consequently high snowmelt rates (up to 20 cm day^{-1}) near the Main Divide.

This research expands the knowledge of the contribution of landfalling ARs to winter precipitation in both liquid and solid forms in the Southern Alps which can be useful for water management agencies in New Zealand. Following previous work in the Southern Alps that highlighted the key role of ARs in hydrological processes (Kingston et al., 2016; Little et al., 2019; Prince, 2020), this work has demonstrated the importance of ARs in snow hydrology of the Southern Alps. Since the position and strength of water vapour flux inside an AR impact the magnitude of incoming moisture available for precipitation, the findings of this study can be used to complement operational forecasting models for predicting large snow events and ROS flooding events in the maritime environments.

6.5 Future Work

This study found distinct characteristics of synoptic weather patterns associated with large snowfall and snowmelt events, but important research opportunities regarding hydrometeorology of seasonal snow in the Southern Alps remain. It is clear that interactions between large-scale and local-scale hydrometerological atmospheric conditions may impact the snow processes. Therefore, further research that takes the dominant synoptic weather patterns identified in this study, and explores the associated snow-surface energy exchange will improve knowledge of the connection between

large- scale weather systems and seasonal snow cover. Such information will be valuable when considering the potential impact of climate change in snow-dominated regions.

Findings of this thesis reveal that ARs are responsible for both intense rainfall and snowfall events at higher altitudes of the Southern Alps during spring and winter. In a changing climate, it is reasonable to surmise that a potential shift from snow to rain during the landfalling ARs. More frequent episodes of rain-generating ARs would largely impact the hydrological cycle by melting snow cover at higher melt rates resulting in the reduction water resources stored in the snowpacks and an increase in the risk of winter- and spring-time floods in the region. In addition, the sensitivity of AR-related snowfall events to small changes in temperature in the Southern Alps highlights the importance of determining the snow/rain transition line during winter and spring precipitation.

Analysis of AR-related ROS events in this research has improved the knowledge about hydrometeorlogical characteristics of such events and their impacts on snowpacks in a maritime snow-dominated region. Two case studies of rain-producing ARs provided evidence that they can lead to major flooding events in the upper terrains of alpine catchments. Additional research could be built on this study in order to accurately estimate the actual contribution of different components leading to the generation of total streamflow. Other factors such as excessive rainfall and antecedent soil moisture can be important contributions to ROS floods. Given the lack of information about hydrological processes in alpine catchments of the Southern Alps, next step could incorporate a distributed hydrological model with snowmelt modules capable of integrating catchment hydrological characteristics to explore snowmelt-runoff processes during ROS events.

7 References

Abermann J, Eckerstorfer M, Malnes E, Hansen BU. 2019. A large wet snow avalanche cycle in West Greenland quantified using remote sensing and in situ observations. *Natural Hazards*, 97(2): 517–534. https://doi.org/10.1007/s11069-019-03655-8.

Adnan M, Nabi G, Kang S, Zhang G, Adnan RM, Anjum MN, Iqbal M, Ali AF. 2017. Snowmelt Runoff Modelling under Projected Climate Change Patterns in the Gilgit River Basin of Northern Pakistan. *Polish Journal of Environmental Studies*, 26(2): 525–542. https://doi.org/10.15244/pjoes/66719.

Anderton PW, Chinn TJ. 1978. Ivory Glacier, New Zealand, an I.H.D. Representative Basin Study. *Journal of Glaciology*, 20(82): 67–84. https://doi.org/10.3189/S0022143000021225.

Backes TM, Kaplan ML, Schumer R, Mejia JF. 2015. A Climatology of the Vertical Structure of Water Vapor Transport to the Sierra Nevada in Cool Season Atmospheric River Precipitation Events. *Journal of Hydrometeorology*, 16(3): 1029–1047. https://doi.org/10.1175/JHM-D-14-0077.1.

Bales RC, Molotch NP, Painter TH, Dettinger MD, Rice R, Dozier J. 2006. Mountain hydrology of the western United States. *Water Resources Research*, 42(8): 1–13. https://doi.org/10.1029/2005WR004387.

Bao J-W, Michelson SA, Neiman PJ, Ralph FM, Wilczak JM. 2006. Interpretation of Enhanced Integrated Water Vapor Bands Associated with Extratropical Cyclones: Their Formation and Connection to Tropical Moisture. *Monthly Weather Review*, 134(4): 1063–1080. https://doi.org/10.1175/MWR3123.1.

Barnett TP, Adam JC, Lettenmaier DP. 2005. Potential impacts of a warming climate on water availability in snow-dominated regions. *Nature*, 438(7066): 303–309. https://doi.org/10.1038/nature04141.

Barry RG, Perry AH. 1973. *Synoptic climatology; methods and applications*. Methuen London.

Bednorz E. 2009. Synoptic conditions for rapid snowmelt in the Polish-German lowlands. *Theoretical and Applied Climatology*, 97(3–4): 279–286. https://doi.org/10.1007/s00704-008-0063-z.

Bednorz E. 2011. Synoptic conditions of the occurrence of snow cover in central European lowlands. *International Journal of Climatology*, 31(8): 1108–1118. https://doi.org/10.1002/joc.2130.

Bednorz E. 2012. Atmospheric conditions of intense thaws in the Polish lowlands. *Meteorologische Zeitschrift*, 21(1): 89–98. https://doi.org/10.1127/0941-2948/2012/0228.

Bednorz E. 2013. Heavy snow in Polish–German lowlands – Large-scale synoptic reasons and economic impacts. *Weather and Climate Extremes*. Elsevier, 2: 1–6. https://doi.org/10.1016/j.wace.2013.10.007.

Bednorz E, Wibig J. 2015. Spatial Distribution And Synoptic Conditions Of Snow

Accumulation And Snow Ablation In The West Siberian Plain. *Quaestiones Geographicae*, 34(3): 5–15. https://doi.org/10.1515/quageo-2015-0029.

Bednorz E, Wibig J. 2016. Spatial distribution and synoptic conditions of snow accumulation in the Russian Arctic. *Polar Research*, 35(1): 25916. https://doi.org/10.3402/polar.v35.25916.

Bednorz E, Wibig J. 2017. Circulation patterns governing October snowfalls in southern Siberia. *Theoretical and Applied Climatology*. Theoretical and Applied Climatology, 128(1–2): 129–139. https://doi.org/10.1007/s00704-015-1696-3.

Benedict I, Ødemark K, Nipen T, Moore R. 2019. Large-Scale Flow Patterns Associated with Extreme Precipitation and Atmospheric Rivers over Norway. *Monthly Weather Review*, 147(4): 1415–1428. https://doi.org/10.1175/MWR-D-18-0362.1.

Beniston M, Farinotti D, Stoffel M, Andreassen LM, Coppola E, Eckert N, Fantini A, Giacona F, Hauck C, Huss M, Huwald H, Lehning M, López-Moreno J-I, Magnusson J, Marty C, Morán-Tejéda E, Morin S, Naaim M, Provenzale A, Rabatel A, Six D, Stötter J, Strasser U, Terzago S, Vincent C. 2018. The European mountain cryosphere: a review of its current state, trends, and future challenges. *The Cryosphere*, 12(2): 759–794. https://doi.org/10.5194/tc-12-759-2018.

Beniston M, Keller F, Koffi B, Goyette S. 2003. Estimates of snow accumulation and volume in the Swiss Alps under changing climatic conditions. *Theoretical and Applied Climatology*, 76(3–4): 125–140. https://doi.org/10.1007/s00704-003-0016-5.

Berghuijs WR, Woods RA, Hrachowitz M. 2014. A precipitation shift from snow towards rain leads to a decrease in streamflow. *Nature Climate Change*, 4(7): 583–586. https://doi.org/10.1038/nclimate2246.

Bharati L, Gurung P, Jayakody P, Smakhtin V, Bhattarai U. 2014. The Projected Impact of Climate Change on Water Availability and Development in the Koshi Basin, Nepal. *Mountain Research and Development*, 34(2): 118–130. https://doi.org/10.1659/MRD-JOURNAL-D-13-00096.1.

Birkeland KW, Mock CJ. 1996. Atmospheric Circulation Patterns Associated with Heavy Snowfall Events, Bridger Bowl, Montana, U.S.A. *Mountain Research and Development*, 16(3): 281. https://doi.org/10.2307/3673951.

Cann MD, Friedrich K. 2020. The Role of Moisture Pathways on Snowfall Amount and Distribution in the Payette Mountains of Idaho. *Monthly Weather Review*, 148(5): 2033–2048. https://doi.org/10.1175/MWR-D-19-0350.1.

Clark M, Hreinsson EÖ, Martinez G, Tait A, Slater A, Hendrikx J, Owens I, Gupta H, Schmidt J, Woods R. 2009. Simulations of seasonal snow for the south Island, New Zealand. *Journal of Hydrology New Zealand*, 48(2): 41–58.

Clark MP, Hendrikx J, Slater AG, Kavetski D, Anderson B, Cullen NJ, Kerr T, Örn Hreinsson E, Woods RA. 2011. Representing spatial variability of snow water equivalent in hydrologic and land-surface models: A review. *Water Resources Research*, 47(7). https://doi.org/10.1029/2011WR010745.

Clow DW. 2010. Changes in the Timing of Snowmelt and Streamflow in Colorado: A Response to Recent Warming. *Journal of Climate*, 23(9): 2293–2306.

https://doi.org/10.1175/2009JCLI2951.1.

Cohen J, Ye H, Jones J. 2015. Trends and variability in rain-on-snow events. *Geophysical Research Letters*, 42(17): 7115–7122. https://doi.org/10.1002/2015GL065320.

Coles S. 2001. *An Introduction to Statistical Modeling of Extreme Values*. Springer London: London.

Conway H, Raymond CF. 1993. Snow stability during rain. *Journal of Glaciology*, 39(133): 635–642. https://doi.org/10.3189/S0022143000016531.

Cordeira JM, Ralph FM, Martin A, Gaggini N, Spackman JR, Neiman PJ, Rutz JJ, Pierce R. 2017. Forecasting Atmospheric Rivers during CalWater 2015. *Bulletin of the American Meteorological Society*, 98(3): 449–459. https://doi.org/10.1175/BAMS-D-15-00245.1.

Cullen NJ, Conway JP. 2015. A 22 month record of surface meteorology and energy balance from the ablation zone of Brewster Glacier, New Zealand. *Journal of Glaciology*, 61(229): 931–946. https://doi.org/10.3189/2015JoG15J004.

Cullen NJ, Gibson PB, Mölg T, Conway JP, Sirguey P, Kingston DG. 2019. The Influence of Weather Systems in Controlling Mass Balance in the Southern Alps of New Zealand. *Journal of Geophysical Research: Atmospheres*, 124(8): 4514–4529. https://doi.org/10.1029/2018JD030052.

Cutler ES, Fitzharris B. 2005. Observed surface snowmelt at high elevation in theSouthern Alps of New Zealand. *Annals of Glaciology*, 40: 163–168. https://doi.org/10.3189/172756405781813447.

Daniel JS, Solomon S, Portmann RW, Langford AO, Eubank CS, Dutton EG, Madsen W. 2002. Cloud liquid water and ice measurements from spectrally resolved near-infrared observations: A new technique. *Journal of Geophysical Research: Atmospheres*, 107(D21): AAC 21-1-AAC 21-16. https://doi.org/10.1029/2001JD000688.

Dayan U, Tubi A, Levy I. 2012. On the importance of synoptic classification methods with respect to environmental phenomena. *International Journal of Climatology*, 32(5): 681–694. https://doi.org/10.1002/joc.2297.

Dean S, Mullan BA, Renwick J. 2006. More shorts and gumboots? New Zealand climate at the end of this century as simulated by a regional climate model. *Joint conference of the New Zealand Hydrological Society, the New Zealand Association of ResourceManagement, and the Meteorological Society of New Zealand*. New Zealand, Christchurch, November 2006.

Dee DP, Uppala SM, Simmons AJ, Berrisford P, Poli P, Kobayashi S, Andrae U, Balmaseda MA, Balsamo G, Bauer P, Bechtold P, Beljaars ACM, van de Berg L, Bidlot J, Bormann N, Delsol C, Dragani R, Fuentes M, Geer AJ, Haimberger L, Healy SB, Hersbach H, Hólm E V., Isaksen L, Kållberg P, Köhler M, Matricardi M, McNally AP, Monge-Sanz BM, Morcrette J-J, Park B-K, Peubey C, de Rosnay P, Tavolato C, Thépaut J-N, Vitart F. 2011. The ERA-Interim reanalysis: configuration and performance of the data assimilation system. *Quarterly Journal of the Royal Meteorological Society*, 137(656): 553–597. https://doi.org/10.1002/qj.828.

Demaria EMCC, Dominguez F, Hu H, von Glinski G, Robles M, Skindlov J, Walter J.

2017. Observed Hydrologic Impacts of Landfalling Atmospheric Rivers in the Salt and Verde River Basins of Arizona, United States. *Water Resources Research*, 53(12): 10025–10042. https://doi.org/10.1002/2017WR020778.

Dettinger M. 2011. Climate Change, Atmospheric Rivers, and Floods in California - A Multimodel Analysis of Storm Frequency and Magnitude Changes1. *JAWRA Journal of the American Water Resources Association*, 47(3): 514–523. https://doi.org/10.1111/j.1752-1688.2011.00546.x.

Dettinger MD. 2013. Atmospheric Rivers as Drought Busters on the U.S. West Coast. *Journal of Hydrometeorology*, 14(6): 1721–1732. https://doi.org/10.1175/JHM-D-13-02.1.

Dettinger MD, Ralph FM, Das T, Neiman PJ, Cayan DR. 2011. Atmospheric Rivers, Floods and the Water Resources of California. *Water*, 3(2): 445–478. https://doi.org/10.3390/w3020445.

DeWalle DR, Rango A. 2008. *Principles of Snow Hydrology*. Cambridge University Press: Cambridge.

Dirmeyer PA, Kinter JL. 2009. The "Maya Express": Floods in the U.S. Midwest. *Eos, Transactions American Geophysical Union*, 90(12): 101–102. https://doi.org/10.1029/2009EO120001.

Eckhardt S, Stohl A, Wernli H, James P, Forster C, Spichtinger N. 2004. A 15-Year Climatology of Warm Conveyor Belts. *Journal of Climate*, 17(1): 218–237. https://doi.org/10.1175/1520-0442(2004)017<0218:AYCOWC>2.0.CO;2.

Espinoza V, Waliser DE, Guan B, Lavers DA, Ralph FM. 2018. Global Analysis of Climate Change Projection Effects on Atmospheric Rivers. *Geophysical Research Letters*, 45(9): 4299–4308. https://doi.org/10.1029/2017GL076968.

Esteban P, Jones PD, Martín-Vide J, Mases M. 2005. Atmospheric circulation patterns related to heavy snowfall days in Andorra, Pyrenees. *International Journal of Climatology*, 25(3): 319–329. https://doi.org/10.1002/joc.1103.

Farukh MA, Yamada TJ. 2014. Synoptic climatology associated with extreme snowfall events in Sapporo city of northern Japan. *Atmospheric Science Letters*, 15(4): n/a-n/a. https://doi.org/10.1002/asl2.497.

Fayad A, Gascoin S, Faour G, López-Moreno JI, Drapeau L, Page M Le, Escadafal R. 2017. Snow hydrology in Mediterranean mountain regions: A review. *Journal of Hydrology*, 551: 374–396. https://doi.org/10.1016/j.jhydrol.2017.05.063.

Fitzharris B, Lawson W, Owens I. 1999. Research on glaciers and snow in New Zealand. *Progress in Physical Geography: Earth and Environment*, 23(4): 469–500. https://doi.org/10.1177/030913339902300402.

Fitzharris BB, Chinn TJ, Lamont GN. 1997. Glacier balance fluctuations and atmospheric circulation patterns over the Southern Alps, New Zealand. *International Journal of Climatology*, 17(7): 745–763. https://doi.org/10.1002/(SICI)1097-0088(19970615)17:7<745::AID-JOC160>3.0.CO;2-Y.

Fitzharris BB, Garr CE. 1995. Simulation of past variability in seasonal snow in the Southern Alps, New Zealand. *Annals of Glaciology*, 21: 377–382.

https://doi.org/10.3189/S0260305500016098.

Fitzharris BB, Stewart D, Harrison W. 1980. CONTRIBUTION OF SNOWMELT TO THE OCTOBER 1978 FLOOD OF THE POMAHAKA AND FRASER RIVERS , OTAGO. *Journal of Hydrology (New Zealand)*, 19(2): 84–93.

García-Sellés C, Peña JC, Martí G, Oller P, Martínez P. 2010. WeMOI and NAOi influence on major avalanche activity in the Eastern Pyrenees. *Cold Regions Science and Technology*. Elsevier B.V., 64(2): 137–145. https://doi.org/10.1016/j.coldregions.2010.08.003.

Garreaud RD. 2009. The Andes climate and weather. *Advances in Geosciences*, 22(1): 3–11. https://doi.org/10.5194/adgeo-22-3-2009.

Gillies RR, Wang S-Y, Huang W-R. 2012. Observational and supportive modelling analyses of winter precipitation change in China over the last half century. *International Journal of Climatology*, 32(5): 747–758. https://doi.org/10.1002/joc.2303.

Gimeno L, Dominguez F, Nieto R, Trigo R, Drumond A, Reason CJC, Taschetto AS, Ramos AM, Kumar R, Marengo J. 2016. Major Mechanisms of Atmospheric Moisture Transport and Their Role in Extreme Precipitation Events. *Annual Review of Environment and Resources*, 41(1): 117–141. https://doi.org/10.1146/annurev-environ-110615-085558.

Gimeno L, Nieto R, VÃ¡zquez M, Lavers DA. 2014. Atmospheric rivers: a mini-review. *Frontiers in Earth Science*, 2(March): 1–6. https://doi.org/10.3389/feart.2014.00002.

Gorodetskaya I V., Tsukernik M, Claes K, Ralph MF, Neff WD, Van Lipzig NPM. 2014. The role of atmospheric rivers in anomalous snow accumulation in East Antarctica. *Geophysical Research Letters*, 41(17): 6199–6206. https://doi.org/10.1002/2014GL060881.

Griffiths. 2011. Drivers of extreme daily rainfalls in New Zealand. *Weather and Climate*, 31(2011): 24. https://doi.org/10.2307/26169716.

Griffiths GA, Mcsaveney MJ. 1983. Distribution of mean annual precipitation across some steepland regions of New Zealand. *New Zealand Journal of Science*, 26(2): 197–209.

Grundstein A. 2003. A synoptic-scale climate analysis of anomalous snow water equivalent over the Northern Great Plains of the USA. *International Journal of Climatology*, 23(8): 871–886. https://doi.org/10.1002/joc.908.

Grundstein AJ, Leathers DJ. 1998. A case study of the synoptic patterns influencing midwinter snowmelt across the northern Great Plains. *Hydrological Processes*, 12(15): 2293–2305. https://doi.org/10.1002/(SICI)1099-1085(199812)12:15<2293::AID-HYP797>3.0.CO;2-9.

Grundstein AJ, Leathers DJ. 1999. A spatial analysis of snow-surface energy exchanges over the northern Great Plains of the United States in relation to synoptic scale forcing mechanisms. *International Journal of Climatology*, 19(5): 489–511. https://doi.org/10.1002/(SICI)1097-0088(199904)19:5<489::AID-JOC373>3.0.CO;2-J.

Guan B, Molotch NP, Waliser DE, Fetzer EJ, Neiman PJ. 2010. Extreme snowfall events linked to atmospheric rivers and surface air temperature via satellite measurements.

Geophysical Research Letters, 37(20): n/a-n/a. https://doi.org/10.1029/2010GL044696.

Guan B, Molotch NP, Waliser DE, Fetzer EJ, Neiman PJ. 2013. The 2010/2011 snow season in California's Sierra Nevada: Role of atmospheric rivers and modes of large-scale variability. *Water Resources Research*, 49(10): 6731–6743. https://doi.org/10.1002/wrcr.20537.

Guan B, Waliser DE. 2015. Detection of atmospheric rivers: Evaluation and application of an algorithm for global studies. *Journal of Geophysical Research: Atmospheres*, 120(24): 12514–12535. https://doi.org/10.1002/2015JD024257.

Guan B, Waliser DE, Molotch NP, Fetzer EJ, Neiman PJ. 2012. Does the Madden–Julian Oscillation Influence Wintertime Atmospheric Rivers and Snowpack in the Sierra Nevada? *Monthly Weather Review*, 140(2): 325–342. https://doi.org/10.1175/mwr-d-11-00087.1.

Guan B, Waliser DE, Ralph FM, Fetzer EJ, Neiman PJ. 2016. Hydrometeorological characteristics of rain-on-snow events associated with atmospheric rivers. *Geophysical Research Letters*, 43(6): 2964–2973. https://doi.org/10.1002/2016GL067978.

Hansen C. 2016. Diagnosing the Role of Atmospheric Rivers, Past and Present, In Snowfall Events on Mt. Shasta, California. *University of Nevada, Reno*. University of Nevada, Reno.

Hansen C, Kaplan M, Mensing S, Underwood S, Lewis J, King K, Haugland J. 2013. They just don't make storms like this one anymore: Analyzing the anomalous record snowfall event of 1959. *Journal of Operational Meteorology*, 1(5): 52–65. https://doi.org/10.15191/nwajom.2013.0105.

Harman JR, Winkler JA. 1991. SYNOPTIC CLIMATOLOGY: THEMES, APPLICATIONS, AND PROSPECTS. *Physical Geography*, 12(3): 220–230. https://doi.org/10.1080/02723646.1991.10642429.

Harpold AA, Brooks PD. 2018. Humidity determines snowpack ablation under a warming climate. *Proceedings of the National Academy of Sciences*, 115(6): 1215–1220. https://doi.org/10.1073/pnas.1716789115.

Hay JE, Fitzharris BB. 1988. The synoptic climatology of ablation on a New Zealand glacier. *Journal of Climatology*, 8(2): 201–215. https://doi.org/10.1002/joc.3370080207.

Hecht CW, Cordeira JM. 2017. Characterizing the influence of atmospheric river orientation and intensity on precipitation distributions over North Coastal California. *Geophysical Research Letters*, 44(17): 9048–9058. https://doi.org/10.1002/2017GL074179.

Heine AJ. 1962. Snow structure at Mount Ruapehu. *New Zealand Journal of Geology and Geophysics*, 5(3): 375–383. https://doi.org/10.1080/00288306.1962.10420094.

Henderson RD, Thosmson SM. 1999. Extreme Rainfalls in the Southern Alps of New Zealand. *Journal of Hydrology (New Zealand)*, 38(2): 309–330.

Hendrikx J. 2005. AN EXAMINATION OF THE SNOW AND AVALANCHE HAZARD ON THE MILFORD ROAD, FIORDLAND, NEW ZEALAND. .

Hendrikx J. 2007. The June 2006 Canterbury snowstorm. *Journal of Hydrology (New Zealand)*, 46(1): 33–49.

Hendrikx J, Harper A. 2013. Development of a National Snow and Ice Monitoring Network for New Zealand. *Journal of Hydrology New Zealand*, 52(2): 83–95.

Hendrikx J, Hreinsson EÖ. 2012. The potential impact of climate change on seasonal snow in New Zealand: part II—industry vulnerability and future snowmaking potential. *Theoretical and Applied Climatology*, 110(4): 619–630. https://doi.org/10.1007/s00704-012-0713-z.

Hendrikx J, Hreinsson EÖ, Clark MP, Mullan AB. 2012. The potential impact of climate change on seasonal snow in New Zealand: part I—an analysis using 12 GCMs. *Theoretical and Applied Climatology*, 110(4): 607–618. https://doi.org/10.1007/s00704-012-0711-1.

Hendrikx J, Zammit C, Hreinsson EÖ, Becken S. 2013. A comparative assessment of the potential impact of climate change on the ski industry in New Zealand and Australia. *Climatic Change*, 119(3–4): 965–978. https://doi.org/10.1007/s10584-013-0741-4.

Hock R, Rasul G, Adler C, Cáceres B, Gruber S, Hirabayashi Y, Jackson M, Kääb A, Kang S, Kutuzov S, Milner A, Molau U, Morin S, Orlove B, Steltzer HI. 2019. Chapter 2: High Mountain Areas. IPCC Special Report on the Ocean and Cryosphere in a Changing Climate. *IPCC Special Report on the Ocean and Cryosphere in a Changing Climate*, 131–202.

Huning LS, Guan B, Waliser DE, Lettenmaier DP. 2019. Sensitivity of Seasonal Snowfall Attribution to Atmospheric Rivers and Their Reanalysis-Based Detection. *Geophysical Research Letters*, 46(2): 794–803. https://doi.org/10.1029/2018GL080783.

Huning LS, Margulis SA, Guan B, Waliser DE, Neiman PJ. 2017. Implications of Detection Methods on Characterizing Atmospheric River Contribution to Seasonal Snowfall Across Sierra Nevada, USA. *Geophysical Research Letters*, 44(20): 10,445-10,453. https://doi.org/10.1002/2017GL075201.

Ikeda S, Wakabayashi R, Izumi K, Kawashima K. 2009. Study of snow climate in the Japanese Alps: Comparison to snow climate in North America. *Cold Regions Science and Technology*. Elsevier B.V., 59(2–3): 119–125. https://doi.org/10.1016/j.coldregions.2009.09.004.

IPCC. 2013. Long-term Climate Change: Projections, Commitments and Irreversibility Pages 1029 to 1076. In: Intergovernmental Panel on Climate Change (ed) *Climate Change 2013 - The Physical Science Basis*. Cambridge University Press: Cambridge, 1029–1136.

Jeong D Il, Sushama L. 2018. Rain-on-snow events over North America based on two Canadian regional climate models. *Climate Dynamics*. Springer Berlin Heidelberg, 50(1–2): 303–316. https://doi.org/10.1007/s00382-017-3609-x.

Jeong D Il, Sushama L, Naveed Khaliq M. 2017. Attribution of spring snow water equivalent (SWE) changes over the northern hemisphere to anthropogenic effects. *Climate Dynamics*, 48(11–12): 3645–3658. https://doi.org/10.1007/s00382-016-3291-4.

Jobst AM. 2016. The Potential Impacts of Climate Change on the hydro-climate of the Clutha/Mata-Au catchment. *University of Otago*. University of Otago.

Jobst AM, Kingston DG, Cullen NJ, Schmid J. 2018. Intercomparison of different uncertainty sources in hydrological climate change projections for an alpine catchment (upper Clutha River, New Zealand). *Hydrology and Earth System Sciences*, 22(6): 3125–3142. https://doi.org/10.5194/hess-22-3125-2018.

Junker NW, Grumm RH, Hart R, Bosart LF, Bell KM, Pereira FJ. 2008. Use of Normalized Anomaly Fields to Anticipate Extreme Rainfall in the Mountains of Northern California. *Weather and Forecasting*, 23(3): 336–356. https://doi.org/10.1175/2007WAF2007013.1.

Kanada S, Nakano M, Kato T. 2010. Climatological Characteristics of Daily Precipitation over Japan in the Kakushin Regional Climate Experiments Using a Non-Hydrostatic 5-km-Mesh Model: Comparison with an Outer Global 20-km-Mesh Atmospheric Climate Model. *SOLA*, 6: 117–120. https://doi.org/10.2151/sola.2010-030.

Kerr T. 2011. The precipitation distribution in the Lake Pukaki Catchment. *Journal of Hydrology New Zealand*, 50(2): 361–382.

Kerr T. 2013. The contribution of snowmelt to the rivers of the South Island, New Zealand. *Journal of Hydrology New Zealand*, 52(2): 61–82.

Kerr T, Clark M, Hendrikx J, Anderson B. 2013. Snow distribution in a steep mid-latitude alpine catchment. *Advances in Water Resources*. Elsevier Ltd, 55: 17–24. https://doi.org/10.1016/j.advwatres.2012.12.010.

Khain AP, Pinsky M. 2018. *Physical Processes in Clouds and Cloud Modeling*. Cambridge University Press.

Kidson JW. 1994. Relationship of new zealand daily and monthly weather patterns to synoptic weather types. *International Journal of Climatology*, 14(7): 723–737. https://doi.org/10.1002/joc.3370140703.

Kidson JW. 2000. An analysis of New Zealand synoptic types and their use in defining weather regimes. *International Journal of Climatology*, 20(3): 299–316. https://doi.org/10.1002/(SICI)1097-0088(20000315)20:3<299::AID-JOC474>3.0.CO;2-B.

Kingston DG, Lavers DA, Hannah DM. 2016a. Floods in the Southern Alps of New Zealand: the importance of atmospheric rivers. *Hydrological Processes*, 30(26): 5063–5070. https://doi.org/10.1002/hyp.10982.

Kingston DG, McMecking J. 2015a. Precipitation delivery trajectories associated with extreme river flow for the Waitaki River, New Zealand. *Proceedings of the International Association of Hydrological Sciences*, 369: 19–24. https://doi.org/10.5194/piahs-369-19-2015.

Kingston DG, McMecking J. 2015b. Precipitation delivery trajectories associated with extreme river flow for the Waitaki River, New Zealand. *Proceedings of the International Association of Hydrological Sciences*, 369: 19–24. https://doi.org/10.5194/piahs-369-19-2015.

Kingston DG, Webster CS, Sirguey P. 2016b. Atmospheric circulation drivers of lake

inflow for the Waitaki River, New Zealand. *International Journal of Climatology*, 36(3): 1102–1113. https://doi.org/10.1002/joc.4405.

Knowles N, Dettinger MD, Cayan DR. 2006. Trends in Snowfall versus Rainfall in the Western United States. *Journal of Climate*, 19(18): 4545–4559. https://doi.org/10.1175/JCLI3850.1.

Krasting JP, Broccoli AJ, Dixon KW, Lanzante JR. 2013. Future Changes in Northern Hemisphere Snowfall. *Journal of Climate*, 26(20): 7813–7828. https://doi.org/10.1175/JCLI-D-12-00832.1.

Kumar M, Wang R, Link TE. 2012. Effects of more extreme precipitation regimes on maximum seasonal snow water equivalent. *Geophysical Research Letters*, 39(20): 2012GL052972. https://doi.org/10.1029/2012GL052972.

Lackmann GM, Gyakum JR. 1999. Heavy Cold-Season Precipitation in the Northwestern United States: Synoptic Climatology and an Analysis of the Flood of 17–18 January 1986. *Weather and Forecasting*, 14(5): 687–700. https://doi.org/10.1175/1520-0434(1999)014<0687:HCSPIT>2.0.CO;2.

Lavers DA, Allan RP, Villarini G, Lloyd-Hughes B, Brayshaw DJ, Wade AJ. 2013. Future changes in atmospheric rivers and their implications for winter flooding in Britain. *Environmental Research Letters*, 8(3). https://doi.org/10.1088/1748-9326/8/3/034010.

Lavers DA, Ralph FM, Waliser DE, Gershunov A, Dettinger MD. 2015. Climate change intensification of horizontal water vapor transport in CMIP5. *Geophysical Research Letters*, 42(13): 5617–5625. https://doi.org/10.1002/2015GL064672.

Lavers DA, Villarini G. 2013a. The nexus between atmospheric rivers and extreme precipitation across Europe. *Geophysical Research Letters*, 40(12): 3259–3264. https://doi.org/10.1002/grl.50636.

Lavers DA, Villarini G. 2013b. Atmospheric Rivers and Flooding over the Central United States. *Journal of Climate*, 26(20): 7829–7836. https://doi.org/10.1175/JCLI-D-13-00212.1.

Lavers DA, Villarini G, Allan RP, Wood EF, Wade AJ. 2012. The detection of atmospheric rivers in atmospheric reanalyses and their links to British winter floods and the large-scale climatic circulation. *Journal of Geophysical Research: Atmospheres*, 117(D20): 1–13. https://doi.org/10.1029/2012JD018027.

Leung LR, Qian Y. 2009. Atmospheric rivers induced heavy precipitation and flooding in the western U.S. simulated by the WRF regional climate model. *Geophysical Research Letters*, 36(3): n/a-n/a. https://doi.org/10.1029/2008GL036445.

Li D, Lettenmaier DP, Margulis SA, Andreadis K. 2019. The Role of Rain-on-Snow in Flooding Over the Conterminous United States. *Water Resources Research*, 55(11): 8492–8513. https://doi.org/10.1029/2019WR024950.

Li D, Wrzesien ML, Durand M, Adam J, Lettenmaier DP. 2017. How much runoff originates as snow in the western United States, and how will that change in the future? *Geophysical Research Letters*, 44(12): 6163–6172. https://doi.org/10.1002/2017GL073551.

Little K, Kingston DG, Cullen NJ, Gibson PB. 2019. The Role of Atmospheric Rivers for Extreme Ablation and Snowfall Events in the Southern Alps of New Zealand. *Geophysical Research Letters*, 46(5): 2761–2771. https://doi.org/10.1029/2018GL081669.

López-Moreno JI, Vicente-Serrano SM. 2007. Atmospheric circulation influence on the interannual variability of snow pack in the Spanish Pyrenees during the second half of the 20th century. *Hydrology Research*, 38(1): 33–44. https://doi.org/10.2166/nh.2007.030.

Loukas A, Vasiliades L, Dalezios N. 2000. Flood producing mechanisms identification in southern British Columbia, Canada. *Journal of Hydrology*, 227(1–4): 218–235. https://doi.org/10.1016/S0022-1694(99)00182-1.

Lu M, Lall U. 2016. Tropical Moisture Exports, Extreme Precipitation and Floods in Northeast US. *Hydrology and Earth System Sciences Discussions*, 1–40. https://doi.org/10.5194/hess-2016-403.

Lundquist JD, Neiman PJ, Martner B, White AB, Gottas DJ, Ralph FM. 2008. Rain versus Snow in the Sierra Nevada, California: Comparing Doppler Profiling Radar and Surface Observations of Melting Level. *Journal of Hydrometeorology*, 9(2): 194–211. https://doi.org/10.1175/2007JHM853.1.

Lute AC, Abatzoglou JT. 2014. Role of extreme snowfall events in interannual variability of snowfall accumulation in the western United States. *Water Resources Research*, 50(4): 2874–2888. https://doi.org/10.1002/2013WR014465.

Mahoney K, Jackson DL, Neiman P, Hughes M, Darby L, Wick G, White A, Sukovich E, Cifelli R. 2016. Understanding the Role of Atmospheric Rivers in Heavy Precipitation in the Southeast United States. *Monthly Weather Review*, 144(4): 1617–1632. https://doi.org/10.1175/MWR-D-15-0279.1.

Mankin JS, Viviroli D, Singh D, Hoekstra AY, Diffenbaugh NS. 2015. The potential for snow to supply human water demand in the present and future. *Environmental Research Letters*. IOP Publishing, 10(11): 114016. https://doi.org/10.1088/1748-9326/10/11/114016.

Marks D, Kimball J, Tingey D, Link T. 1998. The sensitivity of snowmelt processes to climate conditions ans forest during rain on snow (SNOBAL). *Hydrological Processes*, 1587(March): 1569–1587. https://doi.org/10.1002/(SICI)1099-1085(199808/09)12:10/11<1569::AID-HYP682>3.0.CO;2-L.

Masiokas MH, Villalba R, Luckman BH, Le Quesne C, Aravena JC. 2006. Snowpack Variations in the Central Andes of Argentina and Chile, 1951–2005: Large-Scale Atmospheric Influences and Implications for Water Resources in the Region. *Journal of Climate*, 19(24): 6334–6352. https://doi.org/10.1175/JCLI3969.1.

McCabe GJ, Clark MP, Hay LE. 2007. Rain-on-Snow Events in the Western United States. *Bulletin of the American Meteorological Society*, 88(3): 319–328. https://doi.org/10.1175/BAMS-88-3-319.

McGinnis DL. 2000. Synoptic controls on upper Colorado River basin snowfall. *International Journal of Climatology*, 20(2): 131–149. https://doi.org/10.1002/(SICI)1097-0088(200002)20:2<131::AID-JOC465>3.0.CO;2-H.

McKerchar AI, Pearson CP, Fitzharris BB. 1998. Dependency of summer lake inflows and precipitation on spring SOI. *Journal of Hydrology*, 205(1–2): 66–80. https://doi.org/10.1016/S0022-1694(97)00144-3.

Merino A, Fernández S, Hermida L, López L, Sánchez JL, García-Ortega E, Gascón E. 2014. Snowfall in the Northwest Iberian Peninsula: Synoptic Circulation Patterns and Their Influence on Snow Day Trends. *The Scientific World Journal*, 2014(January): 1–14. https://doi.org/10.1155/2014/480275.

Merz R, Blöschl G. 2003. A process typology of regional floods. *Water Resources Research*, 39(12). https://doi.org/10.1029/2002WR001952.

Ministry for the Environment. 2016. *Climate change projections for New Zealand: Atmosphere Projections based on simulations from the IPCC fifth assessment*. Wellington.

Moberg A, Jones PD, Lister D, Walther A, Brunet M, Jacobeit J, Alexander L V., Della-Marta PM, Luterbacher J, Yiou P, Chen D, Klein Tank AMG, Saladié O, Sigró J, Aguilar E, Alexandersson H, Almarza C, Auer I, Barriendos M, Begert M, Bergström H, Böhm R, Butler CJ, Caesar J, Drebs A, Founda D, Gerstengarbe F-W, Micela G, Maugeri M, Österle H, Pandzic K, Petrakis M, Srnec L, Tolasz R, Tuomenvirta H, Werner PC, Linderholm H, Philipp A, Wanner H, Xoplaki E. 2006. Indices for daily temperature and precipitation extremes in Europe analyzed for the period 1901–2000. *Journal of Geophysical Research*, 111(D22): D22106. https://doi.org/10.1029/2006JD007103.

Mock CJ. 1996. Climatic Controls and Spatial Variations of Precipitation in the Western United States. *Journal of Climate*, 9(5): 1111–1125. https://doi.org/10.1175/1520-0442(1996)009<1111:CCASVO>2.0.CO;2.

Mock CJ, Birkeland KW. 2000. Snow avalanche climatology of the western United States mountain ranges. *Bulletin of the American Meteorological Society*, 81(10): 2367–2392. https://doi.org/10.1175/1520-0477(2000)081<2367:SACOTW>2.3.CO;2.

Molero GC, Novelli YS. 2019. The role of atmospheric-tropospheric rivers in partitioning coastal habitats and limiting the poleward expansion of mangroves along the southeast coast of Brazil. *International Journal of Hydrology*, 3(2). https://doi.org/10.15406/ijh.2019.03.00168.

Moore RD, Owens IF. 1984. Controls on Advective Snowmelt in a Maritime Alpine Basin. *Journal of Climate and Applied Meteorology*, 23(1): 135–142. https://doi.org/10.1175/1520-0450(1984)023<0135:COASIA>2.0.CO;2.

Mora JÁN, Martín JR, García MM, de Pablo Davila F, Rivas Soriano L. 2016. Climatological characteristics and synoptic patterns of snowfall episodes in the central Spanish Mediterranean area. *International Journal of Climatology*, 36(14): 4488–4496. https://doi.org/10.1002/joc.4645.

Nayak A, Marks D, Chandler DG, Seyfried M. 2010. Long-term snow, climate, and streamflow trends at the Reynolds Creek Experimental Watershed, Owyhee Mountains, Idaho, United States. *Water Resources Research*, 46(6): 1–16. https://doi.org/10.1029/2008WR007525.

Neale SM, Fitzharris BB. 1997. Energy balance and synoptic climatology of a melting snowpack in the Southern Alps, New Zealand. *International Journal of Climatology*, 17(14): 1595–1609. https://doi.org/10.1002/(SICI)1097-

0088(19971130)17:14<1595::AID-JOC213>3.0.CO;2-7.

Neiman PJ, Ralph FM, Wick GA, Kuo Y-HH, Wee T-KK, Ma Z, Taylor GH, Dettinger MD. 2008a. Diagnosis of an intense atmospheric river impacting the pacific northwest: Storm summary and offshore vertical structure observed with COSMIC satellite retrievals. *Monthly Weather Review*, 136(11): 4398–4420. https://doi.org/10.1175/2008MWR2550.1.

Neiman PJ, Ralph FM, Wick GA, Lundquist JD, Dettinger MD. 2008b. Meteorological Characteristics and Overland Precipitation Impacts of Atmospheric Rivers Affecting the West Coast of North America Based on Eight Years of SSM/I Satellite Observations. *Journal of Hydrometeorology*, 9(1): 22–47. https://doi.org/10.1175/2007JHM855.1.

Neiman PJ, Ralph MF, Moore BJ, Hughes M, Mahoney KM, Cordeira JM, Dettinger MD, Ralph FM, Moore BJ, Hughes M, Mahoney KM, Cordeira JM, Dettinger MD, Ralph MF, Moore BJ, Hughes M, Mahoney KM, Cordeira JM, Dettinger MD. 2013. The Landfall and Inland Penetration of a Flood-Producing Atmospheric River in Arizona. Part I: Observed Synoptic-Scale, Orographic, and Hydrometeorological Characteristics. *Journal of Hydrometeorology*, 14(2): 460–484. https://doi.org/10.1175/JHM-D-12-0101.1.

Newell RE, Newell NE, Zhu Y, Scott C. 1992. Tropospheric rivers? - A pilot study. *Geophysical Research Letters*, 19(24): 2401–2404. https://doi.org/10.1029/92GL02916.

NZHERALD. 2018. *Wild weather sweeps away bridge near Arthur's Pass*. .

Orlowsky B, Seneviratne SI. 2012. Global changes in extreme events: regional and seasonal dimension. *Climatic Change*, 110(3–4): 669–696. https://doi.org/10.1007/s10584-011-0122-9.

Pall P, Tallaksen LM, Stordal F. 2019. A Climatology of Rain-on-Snow Events for Norway. *Journal of Climate*, 32(20): 6995–7016. https://doi.org/10.1175/JCLI-D-18-0529.1.

Paltan H, Waliser D, Lim WH, Guan B, Yamazaki D, Pant R, Dadson S. 2017. Global Floods and Water Availability Driven by Atmospheric Rivers. *Geophysical Research Letters*, 44(20): 10,387-10,395. https://doi.org/10.1002/2017GL074882.

Parsons S, McDonald AJ, Renwick JA. 2014. The use of synoptic climatology with general circulation model output over New Zealand. *International Journal of Climatology*, 34(12): 3426–3439. https://doi.org/10.1002/joc.3919.

Penna D, van Meerveld HJ, Zuecco G, Dalla Fontana G, Borga M. 2016. Hydrological response of an Alpine catchment to rainfall and snowmelt events. *Journal of Hydrology*, 537: 382–397. https://doi.org/10.1016/j.jhydrol.2016.03.040.

Pomeroy JW, Fang X, Marks DG. 2016. The cold rain-on-snow event of June 2013 in the Canadian Rockies - characteristics and diagnosis. *Hydrological Processes*, 30(17): 2899–2914. https://doi.org/10.1002/hyp.10905.

Poyck S, Hendrikx J, Mcmillan H, Hreinsson EÖ, Woods R, Poyck S, Hendrikx J, Mcmillan H, Örn E, Woods R. 2011. Combined snow and streamflow modelling to estimate impacts of climate change on water resources in the Clutha River, New Zealand. *Journal of Hydrology New Zealand*, 50(2): 293–311.

Prince H. 2020. A Climatology of New Zealand Atmospheric Rivers. University of

Otago.

Prowse TD. 1981a. THE SNOW ENVIRONMENT OF THE CRAIGIEBURN RANGE. Phd thesis, Department of Geography, University of Canterbury, Christchurch, New Zealand. 386 pp.

Prowse TD. 1981b. The snow environment of the Craigieburn range. University of Canterbury, Christchurch, New Zealand.

Purdie H, Mackintosh A, Lawson W, Anderson B. 2011. Synoptic Influences on Snow Accumulation on Glaciers East and West of a Topographic Divide: Southern Alps, New Zealand. *Arctic, Antarctic, and Alpine Research*, 43(1): 82–94. https://doi.org/10.1657/1938-4246-43.1.82.

Purdie H, Rack W, Anderson B, Kerr T, Chinn T, Owens I, Linton M. 2015. The impact of extreme summer melt on net accumulation of an avalanche fed glacier, as determined by ground-penetrating radar. *Geografiska Annaler: Series A, Physical Geography*, 97(4): 779–791. https://doi.org/10.1111/geoa.12117.

Purdie JM, Bardsley WE. 2010. Seasonal prediction of lake inflows and rainfall in a hydro-electricity catchment, Waitaki river, New Zealand. *International Journal of Climatology*, 30(3): 372–389. https://doi.org/10.1002/joc.1897.

Putniković S, Tošić I, Đurđević V. 2016. Circulation weather types and their influence on precipitation in Serbia. *Meteorology and Atmospheric Physics*, 128(5): 649–662. https://doi.org/10.1007/s00703-016-0432-6.

Ralph FM, Dettinger M, Lavers D, Gorodetskaya I V., Martin A, Viale M, White AB, Oakley N, Rutz J, Spackman JR, Wernli H, Cordeira J. 2017. Atmospheric Rivers Emerge as a Global Science and Applications Focus. *Bulletin of the American Meteorological Society*, 98(9): 1969–1973. https://doi.org/10.1175/BAMS-D-16-0262.1.

Ralph FM, Neiman PJ, Wick GA. 2004. Satellite and CALJET Aircraft Observations of Atmospheric Rivers over the Eastern North Pacific Ocean during the Winter of 1997/98. *Monthly Weather Review*, 132(7): 1721–1745. https://doi.org/10.1175/1520-0493(2004)132<1721:SACAOO>2.0.CO;2.

Ralph FM, Prather KA, Cayan D, Spackman JR, DeMott P, Dettinger M, Fairall C, Leung R, Rosenfeld D, Rutledge S, Waliser D, White AB, Cordeira J, Martin A, Helly J, Intrieri J. 2016. CalWater Field Studies Designed to Quantify the Roles of Atmospheric Rivers and Aerosols in Modulating U.S. West Coast Precipitation in a Changing Climate. *Bulletin of the American Meteorological Society*, 97(7): 1209–1228. https://doi.org/10.1175/BAMS-D-14-00043.1.

Ralph FM, Rutz JJ, Cordeira JM, Dettinger M, Anderson M, Reynolds D, Schick LJ, Smallcomb C. 2019. A Scale to Characterize the Strength and Impacts of Atmospheric Rivers. *Bulletin of the American Meteorological Society*, 100(2): 269–289. https://doi.org/10.1175/BAMS-D-18-0023.1.

Renwick JA. 2011. Kidson's synoptic weather types and surface climate variability over New Zealand. *Weather and Climate*, 31: 3–23.

Romolo L, Prowse TD, Blair D, Bonsal BR, Marsh P, Martz LW. 2006a. The synoptic climate controls on hydrology in the upper reaches of the Peace River Basin. Part II:

Snow ablation. *Hydrological Processes*, 20(19): 4113–4129. https://doi.org/10.1002/hyp.6422.

Romolo L, Prowse TD, Blair D, Bonsal BR, Martz LW. 2006b. The synoptic climate controls on hydrology in the upper reaches of the Peace River Basin. Part I: snow accumulation. *Hydrological Processes*, 20(19): 4097–4111. https://doi.org/10.1002/hyp.6421.

Rössler O, Froidevaux P, Börst U, Rickli R, Martius O, Weingartner R. 2014. Retrospective analysis of a nonforecasted rain-on-snow flood in the Alps – a matter of model limitations or unpredictable nature? *Hydrology and Earth System Sciences*, 18(6): 2265–2285. https://doi.org/10.5194/hess-18-2265-2014.

Rutz JJ, Shields CA, Lora JM, Payne AE, Guan B, Ullrich P, O'Brien T, Leung LR, Ralph FM, Wehner M, Brands S, Collow A, Goldenson N, Gorodetskaya I, Griffith H, Kashinath K, Kawzenuk B, Krishnan H, Kurlin V, Lavers D, Magnusdottir G, Mahoney K, McClenny E, Muszynski G, Nguyen PD, Prabhat M, Qian Y, Ramos AM, Sarangi C, Sellars S, Shulgina T, Tome R, Waliser D, Walton D, Wick G, Wilson AM, Viale M. 2019. The Atmospheric River Tracking Method Intercomparison Project (ARTMIP): Quantifying Uncertainties in Atmospheric River Climatology. *Journal of Geophysical Research: Atmospheres*, 124(24): 13777–13802. https://doi.org/10.1029/2019JD030936.

Rutz JJ, Steenburgh WJ, Ralph FM. 2014a. Climatological Characteristics of Atmospheric Rivers and Their Inland Penetration over the Western United States. *Monthly Weather Review*, 142(2): 905–921. https://doi.org/10.1175/MWR-D-13-00168.1.

Rutz JJ, Steenburgh WJ, Ralph FM, James Steenburgh W, Martin Ralph F, Steenburgh WJ, Ralph FM, James Steenburgh W, Martin Ralph F. 2014b. Climatological Characteristics of Atmospheric Rivers and Their Inland Penetration over the Western United States. *Monthly Weather Review*, 142(2): 905–921. https://doi.org/10.1175/MWR-D-13-00168.1.

Saavedra F, Cortés G, Viale M, Margulis S, McPhee J. 2020. Atmospheric Rivers Contribution to the Snow Accumulation Over the Southern Andes (26.5° S–37.5° S). *Frontiers in Earth Science*, 8. https://doi.org/10.3389/feart.2020.00261.

Safeeq M, Shukla S, Arismendi I, Grant GE, Lewis SL, Nolin A. 2016. Influence of winter season climate variability on snow-precipitation ratio in the western United States. *International Journal of Climatology*, 36(9): 3175–3190. https://doi.org/10.1002/joc.4545.

Sailor DJ, Li X. 1999. A Semiempirical Downscaling Approach for Predicting Regional Temperature Impacts Associated with Climatic Change. *Journal of Climate*, 12(1): 103–114. https://doi.org/10.1175/1520-0442-12.1.103.

Salinger MJ, Mullan AB. 1999. New Zealand climate: temperature and precipitation variations and their links with atmospheric circulation 1930-1994. *International Journal of Climatology*, 19(10): 1049–1071. https://doi.org/10.1002/(SICI)1097-0088(199908)19:10<1049::AID-JOC417>3.0.CO;2-Z.

Scherrer SC, Appenzeller C, Laternser M. 2004. Trends in Swiss Alpine snow days: The role of local- and large-scale climate variability. *Geophysical Research Letters*,

31(13): n/a-n/a. https://doi.org/10.1029/2004GL020255.

Schoof JT. 2013. Atmospheric Sciences. *Reference Module in Earth Systems and Environmental Sciences*. Elsevier.

Schumacher B, Katurji M, Meyer H, Appelhans T, Otte I, Nauss T. 2020. Atmospheric moisture pathways of East Africa and implications for water recycling at Mount Kilimanjaro. *International Journal of Climatology*, joc.6468. https://doi.org/10.1002/joc.6468.

Semmens KA, Ramage J, Bartsch A, Liston GE. 2013. Early snowmelt events: detection, distribution, and significance in a major sub-arctic watershed. *Environmental Research Letters*, 8(1): 014020. https://doi.org/10.1088/1748-9326/8/1/014020.

Serreze MC, Clark MP, Frei A. 2001. Characteristics of large snowfall events in the montane western United States as examined using snowpack telemetry (SNOTEL) data. *Water Resources Research*, 37(3): 675–688. https://doi.org/10.1029/2000WR900307.

Shaw TE, Gascoin S, Mendoza PA, Pellicciotti F, McPhee J. 2020. Snow Depth Patterns in a High Mountain Andean Catchment from Satellite Optical Tristereoscopic Remote Sensing. *Water Resources Research*, 56(2). https://doi.org/10.1029/2019WR024880.

Shields CA, Rutz JJ, Leung L-Y, Ralph FM, Wehner M, Kawzenuk B, Lora JM, McClenny E, Osborne T, Payne AE, Ullrich P, Gershunov A, Goldenson N, Guan B, Qian Y, Ramos AM, Sarangi C, Sellars S, Gorodetskaya I, Kashinath K, Kurlin V, Mahoney K, Muszynski G, Pierce R, Subramanian AC, Tome R, Waliser D, Walton D, Wick G, Wilson A, Lavers D, Collow A, Krishnan H, Magnusdottir G, Nguyen P. 2018. Atmospheric River Tracking Method Intercomparison Project (ARTMIP): project goals and experimental design. *Geoscientific Model Development*, 11(6): 2455–2474. https://doi.org/10.5194/gmd-11-2455-2018.

Siderius C, Biemans H, Wiltshire A, Rao S, Franssen WHP, Kumar P, Gosain AK, van Vliet MTH, Collins DN. 2013. Snowmelt contributions to discharge of the Ganges. *Science of The Total Environment*, 468–469: S93–S101. https://doi.org/10.1016/j.scitotenv.2013.05.084.

Simon Wang S-Y, Gillies RR, Fosu B, Singh PM. 2015. The Deadly Himalayan Snowstorm of October 2014: Synoptic Conditions and Associated Trends. *Bulletin of the American Meteorological Society*, 96(12): S89–S94. https://doi.org/10.1175/BAMS-D-15-00113.1.

Sirguey P. 2009. Monitoring Snow Cover and Modelling Catchment Discharge With Remote Sensing in the Upper Waitaki Basin , New Zealand. Ph. D. thesis, School of Surveying, University of Otago, Dunedin, New Zealand. 436 pp.

Ski Areas Association of New Zealand (SAANZ). 2018. *Records smashed with 1.6m visitors to NZ slopes in 2017*. *https://info.scoop.co.nz/Ski_Area_Association*.

Smart GM, McKerchar AI. 2010. More flood disasters in New Zealand. *Journal of Hydrology New Zealand*, 49(2): 69–78.

Smith BL, Yuter SE, Neiman PJ, Kingsmill DE. 2010. Water Vapor Fluxes and Orographic Precipitation over Northern California Associated with a Landfalling Atmospheric River. *Monthly Weather Review*, 138(1): 74–100.

https://doi.org/10.1175/2009MWR2939.1.

Smithson PA. 1986. Synoptic and dynamic climatology. *Progress in Physical Geography: Earth and Environment*, 10(1): 100–110. https://doi.org/10.1177/030913338601000106.

Sodemann H, Stohl A. 2013. Moisture Origin and Meridional Transport in Atmospheric Rivers and Their Association with Multiple Cyclones. *Monthly Weather Review*, 141(8): 2850–2868. https://doi.org/10.1175/MWR-D-12-00256.1.

Spreitzhofer G. 1999. Spatial, temporal and intensity characteristics of heavy snowfall events over Austria. *Theoretical and Applied Climatology*, 62(3–4): 209–219. https://doi.org/10.1007/s00704005085.

Stehr A, Aguayo M. 2017. Snow cover dynamics in Andean watersheds of Chile (32.0–39.5° S) during the years 2000–2016. *Hydrology and Earth System Sciences*, 21(10): 5111–5126. https://doi.org/10.5194/hess-21-5111-2017.

Stimberis J, Rubin CM. 2011. Glide avalanche response to an extreme rain-on-snow event, Snoqualmie Pass, Washington, USA. *Journal of Glaciology*, 57(203): 468–474. https://doi.org/10.3189/002214311796905686.

Stohl A, Forster C, Sodemann H. 2008. Remote sources of water vapor forming precipitation on the Norwegian west coast at 60°N-a tale of hurricanes and an atmospheric river. *Journal of Geophysical Research: Atmospheres*, 113(D5): n/a-n/a. https://doi.org/10.1029/2007JD009006.

Stone RS, Dutton EG, Harris JM, Longenecker D. 2002. Earlier spring snowmelt in northern Alaska as an indicator of climate change. *Journal of Geophysical Research: Atmospheres*, 107(D10): ACL 10-1-ACL 10-13. https://doi.org/10.1029/2000JD000286.

Sturman AP, Tapper NJ. 2006. *The Weather and Climate of Australia and New Zealand*. Oxford University Press: Melbourne VIC Australia.

Sturman, Trewinnard, Gorman. 1984. A STUDY OF ATMOSPHERIC CIRCULATION OVER THE SOUTH ISLAND OF NEW ZEALAND (1961-1980). *Weather and Climate*, 4(2): 53. https://doi.org/10.2307/44279622.

Surfleet CG, Tullos D. 2013. Variability in effect of climate change on rain-on-snow peak flow events in a temperate climate. *Journal of Hydrology*, 479: 24–34. https://doi.org/10.1016/j.jhydrol.2012.11.021.

Suriano ZJ. 2019. On the role of snow cover ablation variability and synoptic-scale atmospheric forcings at the sub-basin scale within the Great Lakes watershed. *Theoretical and Applied Climatology*. Theoretical and Applied Climatology, 135(1–2): 607–621. https://doi.org/10.1007/s00704-018-2414-8.

Suriano ZJ, Leathers DJ. 2017. Spatio-temporal variability of Great Lakes basin snow cover ablation events. *Hydrological Processes*, 31(23): 4229–4237. https://doi.org/10.1002/hyp.11364.

Tachibana Y. 1995. A Statistical Study of the Snowfall Distribution on the Japan Sea Side of Hokkaido and Its Relation to Synoptic-Scale and Meso-Scale Environments. *Journal of the Meteorological Society of Japan. Ser. II*, 73(3): 697–715. https://doi.org/10.2151/jmsj1965.73.3_697.

Tait A, Henderson R, Turner R, Zheng X. 2006. Thin plate smoothing spline interpolation of daily rainfall for New Zealand using a climatological rainfall surface. *International Journal of Climatology*, 26(14): 2097–2115. https://doi.org/10.1002/joc.1350.

Thompson SM. 2002. River discharge from mountains with frequent rain. *Journal of Hydrology New Zealand*, 41(2): 125–144.

Trenberth KE. 1976. Fluctuations and trends in indices of the southern hemispheric circulation. *Quarterly Journal of the Royal Meteorological Society*, 102(431): 65–75. https://doi.org/10.1002/qj.49710243106.

Trenberth KE, Mo KC. 1985. Blocking in the Southern Hemisphere. *Monthly Weather Review*, 113(1): 3–21. https://doi.org/10.1175/1520-0493(1985)113<0003:BITSH>2.0.CO;2.

Trubilowicz JW, Moore RD. 2017. Quantifying the role of the snowpack in generating water available for run-off during rain-on-snow events from snow pillow records. *Hydrological Processes*, 31(23): 4136–4150. https://doi.org/10.1002/hyp.11310.

Turner J, Phillips T, Thamban M, Rahaman W, Marshall GJ, Wille JD, Favier V, Winton VHL, Thomas E, Wang Z, Broeke M, Hosking JS, Lachlan-Cope T. 2019. The Dominant Role of Extreme Precipitation Events in Antarctic Snowfall Variability. *Geophysical Research Letters*, 46(6): 3502–3511. https://doi.org/10.1029/2018GL081517.

Ummenhofer CC, England MH. 2007. Interannual Extremes in New Zealand Precipitation Linked to Modes of Southern Hemisphere Climate Variability. *Journal of Climate*, 20(21): 5418–5440. https://doi.org/10.1175/2007JCLI1430.1.

Viale M, Nuñez MN. 2011. Climatology of Winter Orographic Precipitation over the Subtropical Central Andes and Associated Synoptic and Regional Characteristics. *Journal of Hydrometeorology*, 12(4): 481–507. https://doi.org/10.1175/2010JHM1284.1.

Viale M, Valenzuela R, Garreaud RD, Ralph FM. 2018. Impacts of Atmospheric Rivers on Precipitation in Southern South America. *Journal of Hydrometeorology*, 19(10): 1671–1687. https://doi.org/10.1175/JHM-D-18-0006.1.

Vicente-Serrano SM, Zabalza-Martínez J, Borràs G, López-Moreno JI, Pla E, Pascual D, Savé R, Biel C, Funes I, Azorin-Molina C, Sanchez-Lorenzo A, Martín-Hernández N, Peña-Gallardo M, Alonso-González E, Tomas-Burguera M, El Kenawy A. 2017. Extreme hydrological events and the influence of reservoirs in a highly regulated river basin of northeastern Spain. *Journal of Hydrology: Regional Studies*, 12: 13–32. https://doi.org/10.1016/j.ejrh.2017.01.004.

Vogel RM, Fennessey NM. 1995. FLOW DURATION CURVES II: A REVIEW OF APPLICATIONS IN WATER RESOURCES PLANNING. *Journal of the American Water Resources Association*, 31(6): 1029–1039. https://doi.org/10.1111/j.1752-1688.1995.tb03419.x.

Waliser D, Guan B. 2017. Extreme winds and precipitation during landfall of atmospheric rivers. *Nature Geoscience*, 10(3): 179–183. https://doi.org/10.1038/ngeo2894.

Webster CS, Kingston DG, Kerr T. 2015. Inter-annual variation in the topographic

controls on catchment-scale snow distribution in a maritime alpine catchment, New Zealand. *Hydrological Processes*, 29(6): 1096–1109. https://doi.org/10.1002/hyp.10224.

Whan K, Sillmann J, Schaller N, Haarsma R. 2020. Future changes in atmospheric rivers and extreme precipitation in Norway. *Climate Dynamics*, 54(3–4): 2071–2084. https://doi.org/10.1007/s00382-019-05099-z.

Wratt DS, Ridley RN, Sinclair MR, Larsen H, Thompson SM, Henderson R, Austin GL, Bradley SG, Auer A, Sturman AP, Owens I, Fitzharris B, Ryan BF, Gayet J-F. 1996. The New Zealand Southern Alps Experiment. *Bulletin of the American Meteorological Society*, 77(4): 683–692. https://doi.org/10.1175/1520-0477(1996)077<0683:TNZSAE>2.0.CO;2.

Würzer S, Jonas T. 2018. Spatio-temporal aspects of snowpack runoff formation during rain on snow. *Hydrological Processes*, 32(23): 3434–3445. https://doi.org/10.1002/hyp.13240.

Yarnal B. 1993. *Synoptic climatology in environmental analysis: A primer*. Belhaven Press. London, UK.

Yarnal B, Comrie AC, Frakes B, Brown DP. 2001. Developments and prospects in synoptic climatology. *International Journal of Climatology*, 21(15): 1923–1950. https://doi.org/10.1002/joc.675.

Yarnell SM, Viers JH, Mount JF. 2010. Ecology and Management of the Spring Snowmelt Recession. *BioScience*, 60(2): 114–127. https://doi.org/10.1525/bio.2010.60.2.6.

Young AM, Skelly KT, Cordeira JM. 2017. High-impact hydrologic events and atmospheric rivers in California: An investigation using the NCEI Storm Events Database. *Geophysical Research Letters*, 44(7): 3393–3401. https://doi.org/10.1002/2017GL073077.

Zheng X, Wang Q, Zhou L, Sun Q, Li Q. 2018. Predictive Contributions of Snowmelt and Rainfall to Streamflow Variations in the Western United States. *Advances in Meteorology*, 2018: 1–14. https://doi.org/10.1155/2018/3765098.

Zhu Y, Newell RE. 1998. A Proposed Algorithm for Moisture Fluxes from Atmospheric Rivers. *Monthly Weather Review*, 126(3): 725–735. https://doi.org/10.1175/1520-0493(1998)126<0725:APAFMF>2.0.CO;2.